



# The Role of Lysine Acetylation in Photosynthesis

Kumulative Dissertation der Fakultät Biologie  
der Ludwig-Maximilians Universität München

zur Erlangung des akademischen Grades

Doktor der Naturwissenschaften  
(Dr. rer. nat.)

vorgelegt von

Magdalena Sophie Füßl  
Juni, 2022

Erstgutachter: Prof. Dr. Dario Leister

Zweitgutachterin: Prof. Dr. Iris Finkemeier

Tag der Abgabe: 01.06.2022

Tag der mündlichen Prüfung: 07.11.2022



**Table of Contents**

I. Abbreviations.....	4
II. List of Publications.....	7
III. Declaration of contribution as a co-author.....	8
IV. Summary.....	9
V. Zusammenfassung.....	11
VI. List of Figures and Tables.....	14
1. Introduction.....	15
1.1 General introduction into photosynthesis.....	16
1.2 Posttranslational modifications in the chloroplast and the regulation of photosynthetic enzymes.....	18
1.2.1 Phosphorylation.....	18
1.2.2 Redox modification, protein thiol regulation, nitration, and tryptophan oxidation.....	19
1.2.3 Methylation.....	23
1.2.4 Sumoylation.....	23
1.2.5 Glycosylation.....	23
1.2.6 N-terminal acetylation.....	24
1.2.7 Lysine acetylation.....	24
1.3 Lysine acetyltransferases and -deacetylases.....	28
1.3.1 Lysine acetyltransferases.....	29
1.3.2 Lysine deacetylases.....	30
1.4 Acetyl-CoA metabolism in plants.....	33
1.5 Mass spectrometry-based proteomics to study lysine acetylation in plants.....	37
2. Aim of the thesis.....	41

---

3. Summarising Discussion.....	43
3.1 Lysine acetylation occurs as a reversible and dynamic modification on histone and non-histone proteins of diverse function in photosynthetic organisms.....	43
3.2 Lysine acetylation is a dynamic PTM in <i>Chlamydomonas reinhardtii</i> .....	47
3.3 Lysine acetylation of enzymes involved in photosynthesis in <i>Arabidopsis thaliana</i> ....	49
3.3.1 <i>Arabidopsis</i> KDACs have many non-histone substrate proteins.....	49
3.3.2 KDACs are localized outside the nucleus and deacetylate non-histone proteins in <i>Arabidopsis</i> .....	50
3.3.3 Acetylome analyses revealed the plastidial substrate proteins of HDA14....	54
3.3.4 HDA14 regulates Rubisco activase activity under low light conditions.....	57
4. Conclusion and Outlook.....	61
5. References.....	65
VII. Statutory declaration and statement (Eidesstattliche Versicherung und Erklärung).....	77
VIII. Acknowledgements.....	78
IX. Publications.....	1-3



**I. Abbreviations**

AK	Acetate kinase
ACP	Malonyl-acyl-carrier protein
APX	Ascorbate peroxidase
Acetyl-CoA	Acetyl-Coenzyme A
ACL	ATP-citrate lyase
ACN	Acetate non-utilizing
ACS	Acetyl-CoA synthetase
ADP	Adenosine diphosphate
ATP	Adenosine triphosphate
<i>A. thaliana</i>	<i>Arabidopsis thaliana</i>
CTE	C-terminal extension
CBP/p300	CREB-binding protein
CA	Carbonic anhydrase
CA1P	2-Carboxyarabinitol-1-Phosphate
CES	Controlled by epistasy of synthesis
C (Cys)	Cysteine
<i>C. reinhardtii</i>	<i>Chlamydomonas reinhardtii</i>
CO <sub>2</sub>	Carbon dioxide
D (Asp)	Aspartic acid
DDA	Data-dependent acquisition
DAC	Defective accumulation of cytochrome B6/f complex
ENR	Enoyl-ACP reductase
ESI	Electrospray ionization
<i>E. coli</i>	<i>Escherichia coli</i>
ER	Endoplasmic reticulum
ELP3	Elongator protein 3
EX1	Executer1
E (Glu)	Glutamic acid
FBPase	Fructose bisphosphatase
FBA	Fructose-1,6-bisphosphate aldolase
FTR	Ferredoxin/thioredoxin reductase
GAPDH	Glyceraldehyde 3-phosphate dehydrogenase
GA	Golgi apparatus
GFP	Green fluorescence protein
GCN5	General control nonrepressible 5

---

HPLC	High pressure liquid chromatography
HCD	Higher-energy collisional dissociation
Hyl	Hydroxylysine
Hyp	Hydroxyproline
H <sub>2</sub> O <sub>2</sub>	Hydrogen peroxide
ICL	Isocitrate lyase
KAS	β-Ketoacyl-acyl carrier protein synthase
kDa	Kilo Dalton
K (Lys)	Lysine
KAc	Lysine acetylation
KAT	Lysine acetyltransferase
KDAC	Lysine deacetylase
LHCII	Light harvesting complexes II
L (Leu)	Leucin
LC-MS/MS	Liquid chromatography-mass spectrometry
LFQ	Label-free quantification
LSU	Large subunit
MS; MS/MS	Mass spectrometry; Tandem mass spectrometry
M (Met)	Methionine
mRNA	Messenger RNA
NAT	N-terminal acetyltransferase
NADP <sup>+</sup> /NADPH	Oxidized/reduced nicotinamide adenine dinucleotide phosphate
NTR	NADPH-dependent thioredoxin reductase
NTA	N-terminal acetylation
NAD <sup>+</sup>	Adenine dinucleotide
N (Asn)	Asparagine
<sup>1</sup> O <sub>2</sub>	Singlet oxygen
ONOO <sup>-</sup>	Peroxynitrite
PDC	Pyruvate dehydrogenase complex
PTA	Phosphotransacetylase
pI	Isoelectric point
PCAF	p300/CBP associated factor
PGK	Phosphoglycerate kinase
PPE	Phosphopentose epimerase
PRK	Phosphoribulokinase
PDH	Pyruvate dehydrogenase
PSI	Photosystem I

---

PSII	Photosystem II
P (Pro)	Proline
PTM	Posttranslational modification
RCA	RuBisCO activase
RuBisCO	Ribulose-1,5-bisphosphate carboxylase/oxygenase
RuBP	Ribulose-1,5-bisphosphate
RBCL	RuBisCO large subunit
RBCS	RuBisCO small subunit
RPD	Reduced potassium dependency
ROS	Reactive oxygen species
Rtt109	Regulator of Ty1 transposition gene product 109
RPD	Reduced potassium dependency
R (Arg)	Arginine
SBP	Sedoheptulose-1,7-bisphosphate
SBPase	Seduheptulose-1,7-bisphosphatase
STN7	State transition 7
S-nitrosylation	Nitrosylation of cysteines
SUMO	Small ubiquitin-like modifier
S (Ser)	Serine
Sir2	Silent information regulator 2
SUBA	Subcellular location of proteins in <i>Arabidopsis</i> database
TAF1	TATA-binding protein associated factor
TPI	Triosephosphate isomerase
TK	Transketolase
Trx	Thioredoxin
T (Thr)	Threonine
TSA	Trichostatin A
TCA cycle	Tricarboxylic acid cycle
WT	Wild type
W (Trp)	Tryptophan
Y (Tyr)	Tyrosine
ZIC-HILIC	Zwitterionic hydrophilic interaction liquid chromatography

## II. List of Publications

- [1] **Füßl M\***, König AC\*, Eirich J, Hartl M, Kleinknecht L, Bohne AV, Harzen A, Kramer K, Leister D, Nickelsen J, Finkemeier I. Dynamic light- and acetate-dependent regulation of the proteome and lysine acetylome of *Chlamydomonas*. *The Plant Journal* 2022 (109, 261-277)
- [2] **Füßl M**, Lassowskat I, Née G, Koskela M, Brünje A, Tilak P, Giese J, Leister D, Mulo P, Schwarzer D, Finkemeier I. Beyond Histones: New Substrate Proteins of Lysine Deacetylases in *Arabidopsis* Nuclei. *Frontiers in Plant Science* 2018 (10;9:461)
- [3] Hartl M\*, **Füßl M\***, Boersema PJ, Jost JO, Kramer K, Bakirbas A, Sindlinger J, Plöschinger M, Leister D, Uhrig G, Moorhead GB, Cox J, Salvucci ME, Schwarzer D, Mann M, Finkemeier I. Lysine acetylome profiling uncovers novel histone deacetylase substrate proteins in *Arabidopsis*. *Molecular Systems Biology* 2017 (13:949)

### Collaborative work not included in this thesis:

- [4] Wagner S, Behera S, De Bortoli S, Logan DC, Fuchs P, Carraretto L, Teardo E, Cendron L, Nietzel T, **Füßl M**, Doccula FG, Navazio L, Fricker MD, Van Aken O, Finkemeier I, Meyer AJ, Szabò I, Costa A, Schwarzländer M. The EF-Hand Ca<sup>2+</sup> Binding Protein MICU Choreographs Mitochondrial Ca<sup>2+</sup> Dynamics in *Arabidopsis*. *Plant Cell* 2015 (27(11):3190-212)

\* These authors contributed equally to this work.

**III. Declaration of contribution as a co-author**

- [1] **Füßl M\***, König AC\*, Eirich J, Hartl M, Kleinknecht L, Bohne AV, Harzen A, Kramer K, Leister D, Nickelsen J, Finkemeier I. Dynamic light- and acetate-dependent regulation of the proteome and lysine acetylome of *Chlamydomonas*. *The Plant Journal* 2022 (109, 261-277)

**Füßl M performed the acetylome and proteome sample preparations, including extraction, digestion of proteins, dimethyl-labelling and fractionation and enrichment of peptides. Füßl M contributed equally to the data analyses, writing of the manuscript, and literature research together with König AC.**

- [2] **Füßl M**, Lassowskat I, Née G, Koskela M, Brünje A, Tilak P, Giese J, Leister D, Mulo P, Schwarzer D, Finkemeier I. Beyond Histones: New Substrate Proteins of Lysine Deacetylases in *Arabidopsis* Nuclei. *Frontiers in Plant Science* 2018 (10;9:461)

**Füßl M performed the literature research and wrote the part on HAC1 and HAC5. Füßl M contributed to the finalization of the text and the figures.**

- [3] Hartl M\*, **Füßl M\***, Boersema PJ, Jost JO, Kramer K, Bakirbas A, Sindlinger J, Plöchinger M, Leister D, Uhrig G, Moorhead GB, Cox J, Salvucci ME, Schwarzer D, Mann M, Finkemeier I. Lysine acetylome profiling uncovers novel histone deacetylase substrate proteins in *Arabidopsis*. *Molecular Systems Biology* 2017 (13:949)

**Füßl M performed and designed the acetylome experiments of *hda14* and TSA with the help of Hartl M and Finkemeier I. Füßl M also performed the data analyses for these experiments. Füßl M performed the pulldown experiments and the protoplast isolation of the HDA14-GFP overexpression line and did the microscopy analyses. Füßl M performed the RuBisCO and RCA activity measurements with the help of Salvucci ME. Füßl M contributed equally to the literature research, the writing and the figure design of the manuscript.**

- [4] Wagner S, Behera S, De Bortoli S, Logan DC, Fuchs P, Carraretto L, Teardo E, Cendron L, Nietzel T, **Füßl M**, Doccula FG, Navazio L, Fricker MD, Van Aken O, Finkemeier I, Meyer AJ, Szabò I, Costa A, Schwarzländer M. The EF-Hand Ca<sup>2+</sup> Binding Protein MICU Choreographs Mitochondrial Ca<sup>2+</sup> Dynamics in *Arabidopsis*. *Plant Cell* 2015 (27(11):3190-212)

**Füßl M performed the sample preparation for the proteomic analyses.**

\* These authors contributed equally to this work.

#### IV. Summary

Plants are sessile organisms, which face constantly changing environmental conditions such as changes in light intensity, wind, temperature, water and nutrient status. They have to acclimate their metabolism to the changing environmental conditions to regulate growth and protection against harmful conditions. For example, plants can turn their leaves to absorb the maximum of the sun light or close their stomata to protect themselves against water loss. On the molecular level, acclimation can happen as long-term responses with the change of gene expression and a resulting change in protein composition of the cell. As short-term responses, plants use inter alia post-translational modifications to swiftly modulate enzyme activities and on occasion. A great variety of post-translational modifications are known to date. These include phosphorylation, redox modifications, protein thiol regulation, and lysine acetylation among many others. It is already known that the properties of proteins in the thylakoid membrane are changed by phosphorylation. Thus, upon excessive stimulation of photosystem II, the light harvesting antenna LHCII get phosphorylated and associate with photosystem I. This process is called state transition. Hence, the plant can adjust the electron flow through the thylakoid membrane using phosphorylation.

Lysine acetylation is another reversible modification and is known to occur in all organisms. In this thesis, lysine-acetylated proteins in *Arabidopsis thaliana* and *Chlamydomonas reinhardtii* were detected and quantified using a novel mass spectrometry-based approach. A huge number of lysine-acetylated proteins was found acting in a variety of metabolic processes such as photosynthesis, fatty acid synthesis, TCA cycle, and acetate metabolism. Lysine acetylation is mediated by lysine acetyltransferases and the removal of the acetyl group is catalysed by lysine deacetylases. To prove that lysine acetylation is a dynamic post-translational modification, we performed acetylome studies using leaves of *Arabidopsis* plants treated with either trichostatin A or apicidin as deacetylase inhibitors. These inhibitors act on different deacetylases. We were able to show that the treatment with these inhibitors led to a different acetylation pattern. Thus, we could conclude that the deacetylases fulfil a very specialized function in the cells and act on their own substrate proteins. Since we found a great number of lysine-acetylated proteins which are localized in the chloroplast in *Arabidopsis*, enzymes mediating this post-translational modification have to occur in this organelle. Thus, another part of this thesis was to identify and to investigate deacetylases localized in the chloroplast. Using *in silico* analyses we found HDA14 (At4g33470) to have a predicted localization in chloroplasts and mitochondria. Deacetylase activity assays confirmed the deacetylase function of HDA14, and the inhibition of HDA14 by the classical deacetylase inhibitor trichostatin A but not apicidin. In protoplasts of mutant plants overexpressing GFP-tagged HDA14, we were able to confirm the predicted dual localization of HDA14 in chloroplast and mitochondria. In order to find possible

interaction partners of HDA14 we performed acetylome studies of normal light and low light treated plants using a knockout mutant *hda14* and wildtype. Since we found photosynthetic proteins differing in their lysine acetylation pattern between wildtype and mutant, we concluded that HDA14 deacetylates inter alia enzymes involved in photosynthesis. RuBisCO and its activating chaperone (RuBisCO activase) were significantly changed in their acetylation level. Strikingly, RuBisCO activity assays showed that its total and initial activity was significantly higher in *hda14* mutant plants under low-light conditions. Since RuBisCO activase is responsible for the reactivation of RuBisCO under low light conditions and the acetylation state of lysine 438 of RuBisCO activase was significantly higher in *hda14* mutants after low light treatment and after treatment with trichostatin A, we isolated recombinant RuBisCO activase proteins with lysine 438 changed either to glutamine or arginine to mimic or abolish the lysine acetylation status and performed activity assays using these proteins and wildtype. Interestingly, the mimic of the acetylated RuBisCO activase was less sensitive to rising ADP levels, while the arginine exchange led to an increased sensitivity. Taken together, these results indicate that HDA14 deacetylates photosynthetic proteins and plays a role in the regulation of RuBisCO activity by the deacetylation of RuBisCO and RuBisCO activase. In another project, I studied the unicellular algae *Chlamydomonas*, which can grow with different carbon sources. *Chlamydomonas* can either grow heterotrophically in the dark on acetate-containing medium, mixotrophically in the light on acetate-containing medium, or photoautotrophically using light and carbon dioxide for growth. To determine whether lysine acetylation is used to acclimate the metabolism of *Chlamydomonas* to the different growth conditions, we performed acetylome and proteome studies comparing the three growth conditions. Strikingly, we found enzymes involved in the Calvin-Benson Cycle to be significantly increased in their acetylation level under heterotrophic growth conditions including lysine 175 of the large subunit of RuBisCO, when RuBisCO is inactive in the dark. This finding indicates that also in *Chlamydomonas* RuBisCO activity is changed through lysine acetylation. Enzymes involved in the acetate metabolism including the glyoxysomal citrate synthase were also significantly changed in their acetylation status and in their activity level.

In summary, these results lead us to conclude that lysine acetylation is a widespread protein modification in photosynthetic organisms and is used as a molecular switch to acclimate their metabolism to changing environmental conditions.

## V. Zusammenfassung

Pflanzen sind sessile Organismen, die ständig wechselnden Umweltbedingungen, wie Veränderungen in der Lichtintensität, Windstärke, Temperatur und die Zugänglichkeit zu Nährstoffen, ausgesetzt sind. Wenn sich die Umweltbedingungen verändern, müssen Pflanzen ihren Stoffwechsel anpassen, um Wachstum und Abwehrmechanismen zu regulieren. So können Pflanzen beispielsweise die Stellung ihrer Blätter dahingehend verändern, dass das Sonnenlicht im besten Winkel auftrifft und somit ein Maximum an Licht absorbiert werden kann oder sie können die Stomata schließen, um Wasserverlust zu verhindern. Auf molekularer Ebene kann die Anpassung über längerfristige Veränderungen vorgenommen werden. Zu diesen gehören Veränderungen in der Genexpression, die zu einer Änderung in der Proteinzusammensetzung der Zellen führt. Kurzfristige Akklimatisierungen können unter anderem auch über posttranslationale Modifikationen geschehen. Es sind verschiedene posttranslationale Modifikationen bekannt, die dabei eine Rolle spielen. Zu diesen gehören neben vielen anderen Phosphorylierung, Redox-Modifikationen, Thiol Regulierung von Proteinen und Lysin Acetylierung. Es ist bereits bekannt, dass Phosphorylierung die Eigenschaften von Proteinen in der Thylakoidmembran verändert. Wenn beispielsweise das Photosystem II (PSII) übermäßig belichtet wird, führt dies zu einer Phosphorylierung der Lichtsammelkomplexe von PSII (LHCII). Dies führt zu einer Verschiebung der mobilen LHCII hin zum Photosystem I. Diesen Prozess nennt man „state transition“. Somit kann der Elektronenfluss durch die Thylakoidmembran mit Hilfe von Phosphorylierung angepasst werden. Die Acetylierung von Lysinen ist eine weitere reversible Modifikation. Es können Lysin-Reste einer großen Anzahl von Proteinen acetyliert werden. Mit Hilfe von neuartigen massenspektrometrischen Methoden wurden in dieser Arbeit Lysin-acetylierte Proteine in *Arabidopsis thaliana* und *Chlamydomonas reinhardtii* detektiert und quantifiziert. Es wurde eine große Anzahl Lysin-acetylierter Proteine entdeckt, die an einer Vielzahl von Stoffwechselfvorgängen, wie Photosynthese, Fettsäure Metabolismus, TCA Zyklus und Acetat Stoffwechsel, beteiligt sind. Die Lysin Acetylierung wird durch Lysin-Acetyltransferasen und die Umkehrreaktion von Lysin-Deacetylasen katalysiert. Um zu belegen, dass die Lysin Acetylierung eine dynamische posttranslationale Modifikation ist, wurden Acetylomdaten aus Blättern von *Arabidopsis* Pflanzen, die mit einem der Deacetylase Inhibitoren Trichostatin-A oder Apicidin behandelt wurden, generiert. Hierbei konnte gezeigt werden, dass sich die Acetylierung veränderte, je nachdem, welcher der Inhibitoren verwendet wurde. Da diese Inhibitoren verschiedene Deacetylasen beeinträchtigen, konnten wir daraus schließen, dass jede der Deacetylasen spezielle Proteinsubstrate besitzt. Wir fanden eine große Anzahl von acetylierten Proteinen im Chloroplasten und schlossen daraus, dass es in diesem Organell Enzyme geben muss, die diese Modifikation regulieren. Deswegen sollten in einem weiteren Teil dieser Arbeit Deacetylasen charakterisiert werden, welche im Chloroplasten lokalisiert

sind. Mit Hilfe von *in silico* Analysen, konnten wir die Deacetylase HDA14 (At4g33470) identifizieren, der eine chloroplastidäre Lokalisation prognostiziert wurde. Wir führten Analysen durch, in welchen wir die Deacetylaseaktivität bestätigen konnten. Außerdem konnten wir in diesem Ansatz zeigen, dass HDA14 von Trichostatin-A gehemmt wird, nicht aber von Apicidin. Protoplasten wurden aus Linien isoliert, die GFP-fusionierte HDA14 überexprimierten. Das GFP Signal zeigte eine duale Lokalisation von HDA14 in Chloroplasten und Mitochondrien. Um Interaktionspartner von HDA14 zu finden, wurden vergleichende Acetylom Studien mit der Knockout Mutante *hda14* und dem Wildtyp durchgeführt. Die Pflanzen wurden zuvor normalen Lichtintensitäten oder Schwachlicht ausgesetzt. Diese Analysen zeigten, dass HDA14 in der Deacetylierung von photosynthetischen Enzymen eine Rolle spielt. So waren RuBisCO und ihr aktivierendes Chaperon RuBisCO Aktivase signifikant in ihrer Acetylierung verändert. Aktivitätsmessungen von RuBisCO zeigten, dass die gesamte und die initiale Aktivität unter Schwachlichtbedingungen in *hda14* Mutanten signifikant höher waren als in Wildtyp Pflanzen. RuBisCO Aktivase ist für die Reaktivierung von RuBisCO unter Schwachlichtbedingungen verantwortlich und die Acetylierung des Lysins 438 war in *hda14* Mutanten unter Schwachlicht und nach der Behandlung mit Trichostatin A im Wildtyp signifikant erhöht. Daher wurde rekombinantes RuBisCO Aktivase Protein produziert, in welchem das Lysin 438 entweder zu Glutamin oder zu Arginin getauscht wurde. Ersteres imitiert das acetylierte Lysin, während Zweiteres diese Modifikation verhindert. Interessanterweise zeigten die Aktivitätsmessungen, dass der Austausch gegen Glutamin zu einer niedrigeren ADP Inhibierung im Vergleich zum Wildtyp Protein führte. Im Gegensatz dazu führte der Austausch zu Arginin zu einer höheren Sensitivität gegenüber ADP. Diese Ergebnisse weisen eindeutig darauf hin, dass HDA14 photosynthetische Proteine deacetyliert und eine Rolle in der Regulation der Aktivitäten von RuBisCO und RuBisCO Aktivase spielt. In einem weiteren Projekt wurde die einzellige Alge *Chlamydomonas* untersucht, die verschiedene Kohlenstoffquellen für ihr Wachstum verwenden kann. Die Alge *Chlamydomonas* kann heterotroph wachsen, indem sie im Dunkeln Acetat-haltiges Medium verstoffwechselt. *Chlamydomonas* kann auch mixotroph im Licht mit Acetat wachsen und sie ist auch in der Lage nur mit Licht und Kohlenstoffdioxid photoautotroph zu leben. Um herauszufinden, ob die Alge Lysin Acetylierung zu Regulation des Metabolismus nutzt, wurden vergleichende Acetylomstudien von Zellen der drei Wachstumsbedingungen durchgeführt. Auffallend war, dass die Acetylierung von Enzymen des Calvin-Benson Zyklus unter heterotrophen Wachstumsbedingungen signifikant erhöht war. Zu diesen gehörte auch das Lysin 175 der großen Untereinheit von RuBisCO, dessen Acetylierungs-Niveau anstieg, wenn RuBisCO im Dunkeln inaktiv war. Dies deutet darauf hin, dass auch in *Chlamydomonas* die RuBisCO Aktivität über Acetylierung reguliert werden kann. Auch Enzyme, die im Acetatmetabolismus involviert sind, so wie die glyoxysomale Citratsynthase, waren signifikant in ihrer Acetylierung und in ihrer Aktivität unter den verschiedenen

Wachstumsbedingungen verändert. Daraus lässt sich schließen, dass die Acetylierung eine häufig verwendete Proteinmodifikation des Metabolismus ist, um Enzymaktivitäten zu modulieren.

## VI. List of Figures and Tables

### List of figures

1. Simplified scheme of the gas exchange during photosynthesis and environmental stimuli a plant is facing.....	15
2. Overview of photosynthetic light reactions and the Calvin-Benson Cycle including RuBisCO activation by RCA in higher plants in the chloroplast.....	16
3. Enzymatically catalysed acetylation and deacetylation of the $\epsilon$ -aminogroup of a lysine side chain.....	25
4. Overview of the possible posttranslational modifications occurring in the chloroplast.....	28
5. Simplified scheme of acetyl-CoA metabolism in the different organelles of a plant cell.....	34
6. Possible sources of acetyl-CoA from pyruvate and acetate metabolism in plants.....	36
7. Simplified schematic of a Q-Exactive mass spectrometer without the optical components (Thermo Scientific).....	38
8. Scheme of chemical dimethyl labelling of peptides.....	40
9. Alignment of <i>Chlamydomonas</i> and <i>Arabidopsis</i> RBCL using <i>Clustal omega</i> .....	46
10. Gene expression pattern of <i>HDA14</i> in different tissues of <i>Arabidopsis</i> .....	52
11. Gene expression pattern of <i>HDA14</i> in different developmental stages of <i>Arabidopsis</i> .....	53
12. Lysine acetylation on photosynthetic protein complexes in <i>Chlamydomonas</i> and <i>Arabidopsis</i> .....	61
13. Alignment of <i>Arabidopsis</i> HDA14 and HDA5.....	62

### List of tables

1. Subcellular localization of <i>Arabidopsis</i> KDACs.....	31
2. Regulated KAc sites on proteins involved in photosynthesis found in <i>Chlamydomonas</i> and <i>Arabidopsis</i> .....	45

## 1. Introduction

Higher plants are sessile organisms. Thus, they have developed the ability to rapidly adapt their metabolism to changes in local environmental conditions during the day and during seasons. Plants have to deal with changes in water and nutrient status, differing light intensities, temperature, and wind, for example [1] (Figure 1). These changes occur constantly and force the plant to adapt its metabolism rapidly on occasion. The acclimation of a plants` metabolism can happen inter alia through changes in gene expression or by modulation of metabolic enzyme activities by the usage of posttranslational modifications (PTMs) [2, 3]. PTMs can alter protein function, localisation, and turnover, as well as gene expression through addition of a chemical group to an amino acid side chain of proteins. Often these chemical modifications are reversible and therefore highly flexible [4]. There are several hundred types of PTMs known like for example phosphorylation, ubiquitination, nitration, glycosylation, sumoylation, methylation, redox modifications, carbamylation, and acetylation [5]. Hence, these manifold chemical modifications will result in different chemical properties and proteoforms of the proteins and offer mechanisms to fine-tune protein functions such as enzyme activity to alter metabolism. Especially photosynthesis has to be acclimated fast and frequently, because the light conditions are changing often during the day [6] (Figure 1).

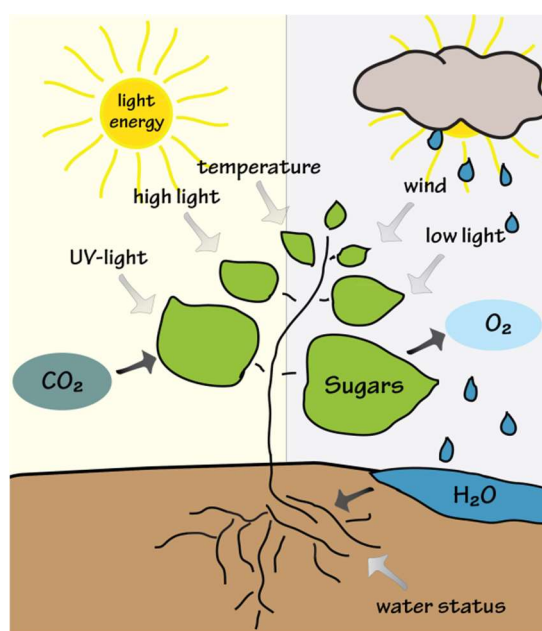


Figure 1: **Simplified scheme of the gas exchange during photosynthesis and environmental stimuli a plant is facing.** To guarantee optimized performance of photosynthesis, plants have to adapt their metabolism to changing parameters like water, nutrient status, temperature, light conditions, and wind.

## 1.1 General introduction into photosynthesis

Most plants are photoautotroph living organisms since they can use light energy to produce sugars using photosynthesis. These reactions are fundamental metabolic processes in plants and cyanobacteria. Photosynthesis consists of two distinct pathways: the light-dependent reactions at the thylakoid membranes and the Calvin-Benson Cycle in the stroma. In the light reactions, light energy is converted to ATP and NADPH, which can be used in the Calvin-Benson Cycle to fix atmospheric carbon dioxide for sugar production (Figure 2).

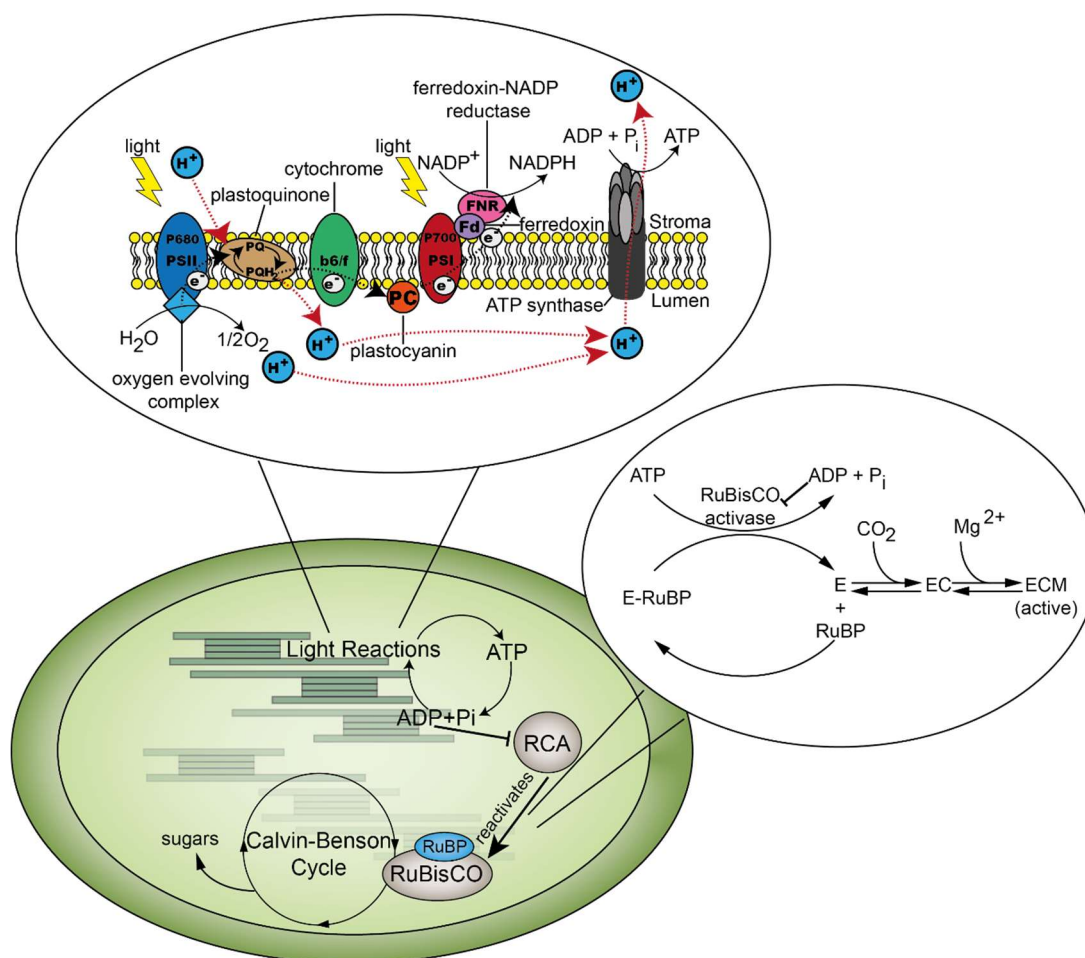


Figure 2: **Overview of photosynthetic light reactions and the Calvin-Benson Cycle including Ribulose-Bisphosphate Carboxylase/Oxygenase (RuBisCO) activation by RuBisCO activase (RCA) in higher plants in the chloroplast.** In this picture the red dashed arrows depict the transfer of protons over the thylakoid membrane during the light reactions and the black arrows depict the electron transfer from water to NADP<sup>+</sup>. Uncarbamylated, inactive RuBisCO with a RuBP bound is reactivated by RCA in an ATP-dependent reaction. Thereby RuBP is released and RuBisCO is then carbamylated and activated. In the activation scheme the following abbreviations are used: E: RuBisCO; EC: Carbamylated RuBisCO; ECM: carbamylated RubisCO with a bound magnesium ion (right) (modified from [3]). PQ: plastoquinone; PQH<sub>2</sub>: plastoquinol; PC: plastocyanin (top). Light reaction scheme was modified from [http://chemwiki.ucdavis.edu/Biological\\_Chemistry/Photosynthesis/Photosynthesis\\_overview/The\\_Light\\_Reactions](http://chemwiki.ucdavis.edu/Biological_Chemistry/Photosynthesis/Photosynthesis_overview/The_Light_Reactions).

The light reactions take place in the thylakoid membrane and enable the transfer of electrons from water to  $\text{NADP}^+$ , which thereby is reduced to NADPH. The initiating enzyme complex is photosystem II (PSII, P680) with its chlorophyll containing light harvesting complexes (LHCII). It uses the energy of light to split two molecules of water into one molecule of oxygen, four protons, and electrons at the luminal located water splitting complex. The electrons are transferred to plastoquinone, which shuttles them to the cytochrome  $b_6/f$  complex. Through reduction and oxidation of plastoquinone protons are transferred over the membrane inside the lumen and a proton gradient is build up over the thylakoid membrane. This gradient can be used by the ATP synthase to phosphorylate ADP to ATP. The electrons are further transferred from the cytochrome  $b_6/f$  complex to plastocyanin and subsequently to photosystem I (PSI, P700). This protein complex reduces ferredoxin which is finally used by the ferredoxin-NADP-reductase to reduce  $\text{NADP}^+$  (Figure 2) (reviewed in [7]).

The carbon reactions of the Calvin-Benson Cycle are initiated by the enzyme Ribulose-1,5-bisphosphate carboxylase/oxygenase (RuBisCO). RuBisCO catalyses the fixation of inorganic  $\text{CO}_2$  onto the organic acceptor molecule ribulose-1,5-bisphosphate (RuBP). Thereby two molecules of 3-phosphoglycerate (3-PGA) are generated which are then reduced to triose phosphates. Five out of six of these molecules are used to recycle the organic acceptor RuBP and only one is used to produce sugars. Because RuBisCO can be inhibited by compounds which bind to its active site, plants express an enzyme, which releases these inhibitors and induces a conformational change at RuBisCO active site to allow the release of the tightly bound inhibitory sugar phosphates. The release of inhibitors from the active site is followed by a carbamylation reaction of RuBisCO to ensure the carboxylation reaction. This helper protein is a catalytic  $\text{AAA}^+$ -ATPase chaperone, which is called RuBisCO activase (RCA). RCA uses the energy in form of ATP to remove tightly bound RuBP and other sugar phosphates from uncarbamyated RuBisCO and thereby activates it [8-10]. Since RCA is inhibited by ADP it links the activity of the light reactions to the activity of RuBisCO. In the dark, the ADP/ATP ratio is high enough to largely inactivate RCA, but also the RuBP levels are very low and thus the activation state of RuBisCO depends on the stromal  $\text{CO}_2$  concentration and its carbamylation state. During light when the ADP/ATP ratio decreases and RuBP concentrations increase, RuBisCO activation is dependent on RCA activity (Figure 2) [11-13]. It appears that Xylulose-1,5-bisphosphate is also inhibiting RuBisCO competitively with RuBP [14]. In some plant species such as *Phaseolus vulgaris* (beans), *Beta vulgaris* (sugar beet), and *Glycine max* (soybean) there is another inhibitory sugar phosphate present, which is also removed by RCA. It is called 2-Carboxyarabinitol-1-Phosphate (CA1P) and its synthesis is light regulated. It is synthesised when the plants are transferred to lower light intensities or darkness, which results in a decline in RuBisCO activity. Hence it seems that CA1P production is also connecting RuBisCO activity and its activation state to the light intensity [15].

## **1.2 Posttranslational modifications in the chloroplast and the regulation of photosynthetic enzymes**

Plant cells are using a variety of PTMs to adjust the activities of photosynthetic enzymes to changing environmental conditions. In the following chapter an overview of PTMs occurring in the chloroplast and their impact on the proteins especially those involved in photosynthesis is described (Figure 4).

### **1.2.1 Phosphorylation**

A prominent example for the regulation of photosynthesis by PTMs is the phosphorylation of thylakoid proteins. In the model organism *Arabidopsis thaliana* (*Arabidopsis*) and the green algae *Chlamydomonas reinhardtii* (*Chlamydomonas*) it was shown that phosphorylation is required for acclimation to changing light conditions. To balance the light absorption capacity between both photosystems the mobile antenna of LHCII of PSII can reversibly associate with PSI and PSII, respectively. If PSII gets excessively stimulated relative to PSI, and thereby the plastoquinone pool gets reduced, a kinase is activated, which phosphorylates LHCII. This leads to a displacement of the antenna complex from PSII to PSI, and this process is called state transition [16, 17]. In *Arabidopsis*, the thylakoid protein kinase STN7 (state transition 7) phosphorylates LHCII after illumination of leaves with blue light to excite PSII. This leads to an increase in relative PSI fluorescence at 730 nm, which indicates a displacement of the light excitation energy from PSII to PSI [17, 18]. Similarly, phosphorylation of thylakoid proteins leads to an enhanced cyclic flow of electrons around PSII to protect the plant against photo-inhibitory effects of excessive light intensities [19]. The phosphorylation-dependent changes in LHCII occur within minutes and are thus called short term responses [20]. In a long-term response, imbalances in the energy distribution are antagonized by changing the protein composition of PSII and PSI through regulation of gene expression over hours and days [21]. The redox state of the plastoquinone pool initiates a signal to regulate the expression of genes in chloroplasts and the nucleus. The plant can coordinate the expression in both organelles and adapt it to its needs depending on the light conditions. Environmentally induced changes in the redox state of chloroplast proteins and through generation of various types of reactive oxygen species (ROS), are known to be involved in many retrograde signalling pathways to regulate protein expression of the photosynthetic machinery [18, 22, 23]. Phosphorylation is not just important in acclimation of the light reactions, but also plays a role in regulating enzymes of the Calvin Benson Cycle and the photorespiratory pathway. RuBisCO, the enzyme which produces the first metabolite of both pathways carries at least 10 phosphorylation sites in *Arabidopsis*. These sites are distributed all over the protein in the small and the large subunits. Some of them are highly conserved, in close proximity to the substrate binding site, and their modification is therefore believed to have an influence on the catalytic activity [24]. Likewise, the RCA

is also known to be phosphorylated at least on two residues in *Arabidopsis*: Threonine (Thr)-78 and serine (Ser)-172. These residues are located in the N-domain of the Walker A motif of the protein facing the ATPase  $\beta$ -region [25]. This domain is believed to take part in RuBisCO-RCA interactions [26]. Thr-78 is more phosphorylated in the dark and under low light conditions. Exchange of this residue to Ser in *Arabidopsis* led to a hyperphosphorylation of the residue relative to the  $\beta$ -RCA Wildtype (WT) form. Additionally, these mutants showed a reduced quantum efficiency of PSII and reduced growth rates compared to plants expressing  $\beta$ -RCA WT. Strikingly, the Thr-78 to alanine exchange, which is the phosphorylation null mutant showed faster photosynthetic induction kinetics and increased quantum efficiency of PSII. Therefore, it seems that phosphorylation of Thr-78 plays an important role in the negative regulation of RCA activity [27]. Additionally, the large RCA isoform ( $\alpha$ -RCA) is redox regulated by two C-terminal cysteine (Cys) residues and its activity can thus be adapted to the redox state of the chloroplast which is dependent on changing light conditions [28].

There are a variety of PTMs occurring in both, the large and the small subunits of RuBisCO [29] but the most prominent and well-studied example is the carbamylation of lysine (Lys)-201 of the large subunit in spinach (Figure 2). The carbamate has been proposed to be the essential base for proton abstraction of the C3 of RuBP [30, 31].

### **1.2.2 Redox modification, protein thiol regulation, nitration and tryptophan oxidation**

#### Redox

In chloroplasts of oxygenic photosynthetic organisms, the ferredoxin/thioredoxin system links the light to the regulation of enzymes in photosynthesis. It is composed of ferredoxin, ferredoxin/thioredoxin reductase (FTR) and thioredoxin (Trx). When ferredoxin gets reduced in the light by PSI it can reduce Trx through FTR by transferring electrons and protons to its disulfide bond. Trx itself can further reduce target enzymes and activate them. In chloroplasts two Trx are known *f* and *m* [32-34]. 35 thioredoxin linked proteins were found functioning in 18 different processes in chloroplasts [32]. In the membrane fraction of chloroplasts 14 potential Trx target proteins were found including seven which are associated with photosynthetic electron flow, ATP synthesis, and PSII/PSI state transitions [35].

In the stroma, many enzymes involved in the Calvin-Benson Cycle are known to be regulated by Trx mediated reduction and oxidation. The large  $\alpha$ -isoform of RCA is containing two redox regulated Cys residues at its C-terminal extension (CTE). After oxidation of these residues to a disulfide, the affinity for ATP decreases and RCA is more sensitive to inhibition by ADP. Interestingly, the ADP inhibition is less if RCA has been reduced by Trx and in the shorter  $\beta$ -isoform which lacks the CTE including the Cys residues [36]. Furthermore, Transketolase (TK), Triose Phosphate Isomerase (TPI), Ribulose Phosphate

3-Epimerase (PPE), Fructose biphosphatase (FBPase), SBPase, as well as phosphoribulokinase (PRK) are known to be linked to Trx [32, 37]. Concerning the carbon reactions, it seems that Trx *f* and *m* specifically bind their target proteins and that the reduction by Trx *f* functions in enzyme activation, while reduced Trx *m* deactivates its target enzymes [37]. Recent studies in Cyanobacteria show that PRK and glyceraldehyde 3-phosphate dehydrogenase (GAPDH) are redox-regulated by CP12. Strikingly, CP12 binding to GAPDH influences substrate accessibility of all GAPDH active sites [38].

However, besides the Calvin cycle and starch synthesis redox regulation occurs also in plant mitochondria. In these organelles, Trx get reduced by the NADPH-dependent thioredoxin reductases (NTR), which process is called the TRX/NTR system [34]. *In vitro* analysis in different species revealed that mitochondria host more than 100 target proteins of Trx including enzymes of the Tricarboxylic acid cycle (TCA cycle). In *Arabidopsis*, citrate synthase was found as target enzyme of Trx [39, 40]. Citrate synthase plays an important role in the TCA since it catalyzes the fusion of the carbon-carbon bond between oxaloacetate and acetyl-Coenzyme A (acetyl-CoA). *In vitro* studies showed that the activity of citrate synthase in whole leaf extracts of *Arabidopsis* decreased by 25% upon oxidation, while reduction increased the enzyme activity [41]. Similarly, the recombinant citrate synthase 4 protein showed sensitivity to oxidation by hydrogen peroxide (H<sub>2</sub>O<sub>2</sub>), since the activity decreased by 54% [42]. Nevertheless, *in vivo* studies in *Arabidopsis* mutants lacking Trx o1 and NADP-Trx-reductase revealed that the mitochondrial fumarase and the succinate dehydrogenase to be deactivated and the ATP-citrate lyase (ACL) to be upregulated by Trx. The data suggest citrate synthase not to be upregulated in its activity *in vivo* [43]. Recent studies revealed the role of Cys redox regulation in mitochondria during germination. To germinate the seedling relies on its energy resources which can be used by a transition of the thiol redox state of mitochondrial metabolic activity taking place with seed hydration. Before gene expression is altered hundreds of redox switches provide direct metabolic regulation. Strikingly, mutant seeds lacking the mitochondrial thiol redox machinery could not use their energy resources as efficient as WT which suggests that the redox switch is needed for an adequate use of the resources [44]. Furthermore, the redox potential of the matrix redox pairs in the mitochondria is linked to divers PTMs. If NADPH or NADH is high and thus the redox potential is very negative, the reduction of disulfide bonds of Cys residues is promoted. Under the same conditions with additional high ROS/NO or ROS levels S-nitrosylation (Nitrosylation of cysteines), tyrosine (Tyr) nitration and carbonylation, Cys and methionine (Met) oxidation take place. A very negative redox potential combined with high ATP levels lead to phosphorylation of proteins. Protein acetylation takes place under a moderate redox potential because pyruvate dehydrogenase (PDH) can resume Acetyl-CoA production. Sirtuins deacetylate their partner proteins depending on the binding of NAD<sup>+</sup>

irrespective from the redox potential. Consequently, the mitochondrial redox potential could control the metabolism of the organelle through PTMs [45].

### Protein thiol regulation

Thiol redox modifications are transmitted by enzymes and occur reversibly and selectively. Thus, the chemistry of sulfur is used for a variety of modifications and for regulatory systems by multiple switching steps and allows flexible fine-tuning of target protein activities. The thiol group can be reversibly switched into a thiolate, followed by the oxidation by  $\text{H}_2\text{O}_2$  into sulfenic acid. In the next step this group can be glutathionylated and further oxidized into disulfide bonds [46]. Since mitochondria host a lot of protein thiols, it is likely that the redox regulation of thiol groups is essential for the function of mitochondria [46]. In the mitochondrial matrix as well as in the intermembrane space separate redox environments were found [47-49]. The differences arise from the specific reduction by NADPH and oxidation by molecular oxygen as the final electron acceptor [46].

In the chloroplast the photosynthetic metabolism seems to rely on the thiol-based redox regulation of Cys residues since it controls ATP and NADPH consumption in the Calvin cycle as well as other metabolic activities in the chloroplast [50]. The regulation of chloroplast enzymes by dithiol-disulfide transitions is mediated by reduction and oxidation of these groups which enables the fine tuning of target protein activities [51]. Thiols in proteins can be oxidized either by molecular dioxygen, by ROS, especially  $\text{H}_2\text{O}_2$  or by dithiol-disulfide exchange. In chloroplasts  $\text{H}_2\text{O}_2$  serves as the final electron acceptor molecule in the redox regulatory network which reacts with thiol peroxidases [52]. Within this network there are redox elements which functions as electron donors and in the redox regulation pathways. The electrons are transmitted to the redox regulated proteins and thiol peroxidases react subsequently with peroxides. They become oxidized and get re-reduced by electrons from redox transmitters like Trx *f* and *m* [53].

### Nitration

During protein nitration, which can happen enzymatically or spontaneously, a nitro group ( $-\text{NO}_2$ ) is added to either Tyr, tryptophan (Trp), Cys or Met. Tyr is nitrated by the covalent addition of a nitro group to an *ortho*-carbon of the aromatic ring of the Tyr residue. This changes the Tyr into a negatively charged hydrophilic moiety and is mediated by peroxynitrite ( $\text{ONOO}^-$ ) which has strong nitration activity because of the rapid reaction between superoxide radicals. It is shown that Tyr nitration affects the activity, the conformation and the turnover of the modified protein [54]. The most Tyr nitrated proteins were found to be localized in the chloroplasts and the mitochondria where  $\text{ONOO}^-$  is produced [55]. In *Arabidopsis*, 126 Tyr-nitrated and 12 Trp-nitrated proteins were found in the thylakoid

membrane. The Tyr-nitration inhibits the activity of FNR (ferredoxin-NADP<sup>+</sup> oxidoreductase) and the chloroplast superoxide dismutase 3 [56]. The activities of the GAPDH and the carbonic anhydrase (CA) were significantly decreased upon Tyr-nitration. Furthermore, it was found that Tyr-nitration could disturb the electron transfer chain since the Tyr-nitration of the D1 protein led to the release of the secondary electron-accepting plastoquinone from PSII, and the double nitration of the PSI subunit D disturbs the electron transfer from PSI to ferredoxin. However, it was shown that the extent of the phosphorylation and the nitration level of proteins involved in the light reaction is dependent on the light conditions and can be reversed [55, 57-60]. S-nitrosylation also occurs in the chloroplast enzymatically or enzyme independent and can affect protein activities, interactions, and localization [61]. The chloroplastidic proteins such as RuBisCO, GAPDH and the dehydroascorbate reductase showed a significant decrease in their activities upon S-nitrosylation [62]. Hess and Stamler reviewed (2012) [63] that many kinases and phosphatases in eukaryotic cells are S-nitrosylated and the authors proposed a signaling crosstalk between the two PTMs since the S-nitrosylation of kinases is in most cases inhibiting the enzyme which can lead to changes in the protein phosphorylation status.

#### Trp oxidation

Extensive light conditions lead to the formation of ROS in the chloroplast, especially singlet oxygen (<sup>1</sup>O<sub>2</sub>) is produced in LHC and in the reaction centre of PSII, since chlorophyll molecules provide light energy to produce <sup>1</sup>O<sub>2</sub> [64, 65]. Because <sup>1</sup>O<sub>2</sub> is highly reactive and has an extremely short lifespan it was believed to be toxic for a long time [64]. However, the *Arabidopsis* mutants *chlorina 1 (ch1)* and *fluorescent (flu)* gave insights into the role of <sup>1</sup>O<sub>2</sub> in acclimation, growth inhibition and cell death by the regulation of retrograde signalling. In the *ch1* mutant the inhibition of chlorophyll a oxidase leads to a loss of the PSII antenna complex and photoinhibition in the reaction centre of PSII under excess of light [66, 67]. In the *flu* mutant, <sup>1</sup>O<sub>2</sub> is generated upon a shift from dark to light which causes retrograde signalling independent from photoinhibition [68]. β-carotene and EXECUTER1 (EX1), two <sup>1</sup>O<sub>2</sub> sensors were found in these mutants [67, 69-71]. One part of the PSII repair machinery, so called FtsH proteases promotes the degradation of EX1 dependent on <sup>1</sup>O<sub>2</sub>. Thus EX1 could play a role in <sup>1</sup>O<sub>2</sub> sensing during PSII repair [72]. Strikingly, EX1 was found to accumulate in the dark, whereas it is degraded upon a shift to light. The residue Trp643 of EX1 showed oxidation in a light-dependent manner and FtsH protease was co-immunoprecipitated with EX1-GFP (green fluorescence protein) in the etioplasts. Consequently, the thylakoid membrane-anchored EX1 is oxidized when <sup>1</sup>O<sub>2</sub> is produced during photosynthesis followed by a rapid proteolysis by FtsH serving as a <sup>1</sup>O<sub>2</sub> sensor in the thylakoid margin. The authors also found PSII core proteins to be Trp oxidated in a light-dependent manner suggesting a special role of this PTM in sensing of <sup>1</sup>O<sub>2</sub> [73].

### **1.2.3 Methylation**

Another PTM occurring in the chloroplast is the methylation of Lys (K) or arginine (Arg) residues. One to three methyl groups can be added to the  $\epsilon$ -amine of a Lys residue by Lys-methyltransferases whereas only one or two can be added to the distal nitrogen atoms of an Arg residue catalyzed by Arg-methyltransferases [74, 75]. The addition of methyl group(s) lead(s) to an increased hydrophobicity of the altered residue without altering the charge. This could result in changes in the stability, localization, activity or interaction properties of the modified protein [76]. In *Arabidopsis*, the large subunit of RuBisCO (RBCL) and ATP synthase  $\beta$ -subunit are both, Lys and Arg methylated. RBCL is trimethylated at K14 [77]. Five proteins functioning in the Calvin-Benson Cycle were found to be methylated, like for example Fructose-1,6-Bisphosphate aldolase (FBA) [78]. Strikingly, it seems that the methylation of chloroplast proteins is at least partly induced by light since both the labelling of the thylakoid and the stroma fraction increased significantly more upon incubation in the light than in the dark in pea (*Pisum sativum*) [79]. Even if no functional differences between the methylated and the unmethylated proteins have been demonstrated to date, it is likely that this PTM plays a role in sensing and signaling in the carbon metabolism of the chloroplast [79, 80].

### **1.2.4 Sumoylation**

Sumoylation is the covalent binding of the small ubiquitin-like modifier (SUMO) protein which consists out of approximately 100 amino acids and affects cellular processes such as the regulation of transcription or stress responses [81]. This modification requires three enzymes: the SUMO-activation, the SUMO-conjugating enzyme, and the SUMO ligase. Herein, an isopeptide bond is formed between a C-terminal glycine (Gly) of the SUMO and the  $\epsilon$ -amino group of a K of the target protein. The removal is catalyzed by SUMO proteases. Sumoylation occurs in the cytosol and the modified proteins are subsequently imported into the chloroplast. SUMO attachment can influence the interaction between proteins, the activity, and the localization of the modified protein [82, 83].

### **1.2.5 Glycosylation**

During protein glycosylation carbohydrates are added to proteins. Two different forms of glycosylation do exist: (i) *N*-glycosylation which is the addition of carbohydrates to asparagine (Asn), and (ii) *O*-glycosylation which is the modification of Ser, Thr, hydroxylysine (Hyl) or hydroxyproline (Hyp) residues. Both modifications can happen in the endoplasmic reticulum (ER) and the Golgi apparatus (GA). Following *N*-glycosylation the protein is transported into the chloroplast via the vesicular golgi-to-plastid transport pathway [84, 85]. In *Arabidopsis*, about 3500 proteins were predicted to contain a N-terminal signal peptide with at least one consensus motif for *N*-glycosylation which is Asn-X-Ser/Thr

(with X as any amino acid except proline (Pro)) [86]. About 2200 N-glycosylation sites have been identified by Zielinska et al (2012) [87]. CA is N-glycosylated at five predicted sites and the modification is required for proper folding and catalytic activity [88]. O-glycosylated proteins are mainly found to be involved in cell wall formation and plant immunity [89]. Overall, it seems that glycosylation reflects the overall energy status of the cell and is therefore ideal to regulate the carbon metabolism [80].

### 1.2.6 N-terminal acetylation

Acetylation can happen irreversibly on the N-terminal amino group of a protein and is a frequently occurring PTM in eukaryotes [90, 91]. The positive charge of the N-terminus gets neutralized upon its acetylation and thus the isoelectric point (pI) of the modified protein shifts into more acidic direction. Defects in the N<sup>α</sup>-acetylation result in severe growth abnormalities since this modification is directly linked to protein translation in the cytosol and the transit peptides of many nuclear-encoded proteins have to be acetylated, because this modification plays an important role in the protein import into organelles [92-94]. In *Arabidopsis*, human (*Homo sapiens*), fruit fly (*Drosophila melanogaster*) and yeast (*Saccharomyces cerevisiae*) the core N-terminal acetyltransferase A (NatA) complex is formed by NAA10 and NAA15. By interaction with NAA50 the NatE complex is formed which co-translationally N-acetylates proteins [95]. In *Arabidopsis*, the loss of NAA10 and NAA15 resulted in an embryo lethal phenotype, whereas the loss of NAA50 led to severe growth abnormalities. These could be rescued by complementation with either AtNAA50 or HsNAA50, but not with ScNAA50 which is consistent with previous results indicating ScNAA50 has no NAT activity. AtNAA50 has a broad substrate specificity spectrum and acts as NAT as well as lysine acetyltransferase (KAT) to autoacetylate internal Lys residues [94, 96]. Nuclear-encoded chloroplast proteins can also be modified at their N-terminus after the cleavage of the transit peptide in the chloroplast, such as in the FNR [56]. Hence, chloroplast-encoded proteins are targets of either co- or posttranslational N<sup>α</sup>-acetylation in the chloroplast, and at least seven plastidial acetyltransferase enzymes have been identified recently [91, 97]. It has been shown that N<sup>α</sup>-acetylation in the chloroplast is dynamic and light responsive and thus could play a role in the acclimation to environmental conditions [56].

### 1.2.7 Lysine acetylation

Acetylation of the ε-aminogroup of the K side chains is a reversible and highly dynamic PTM of proteins (Figure 3). It is known to occur in both pro- and eukaryotic organisms. Lysine acetylation (KAc) was first discovered on histone proteins in the nucleus [98] where gene expression and chromatin structure is regulated by the acetylation and deacetylation of the DNA-binding histone proteins [99-101]. Positively charged Lys residues within histone proteins provoke a tight binding to the negative charged DNA, whereas acetylation of these Lys residues causes losing of the binding to the DNA. Hence histone

acetylation leads to more accessible chromatin and promotes transcription with increased mRNA (Messenger RNA) synthesis [102]. This is additionally achieved by recruiting transcriptional regulators which contain bromodomains to the acetylated histones, since bromodomains have a high affinity towards acetyl-lysine [103].

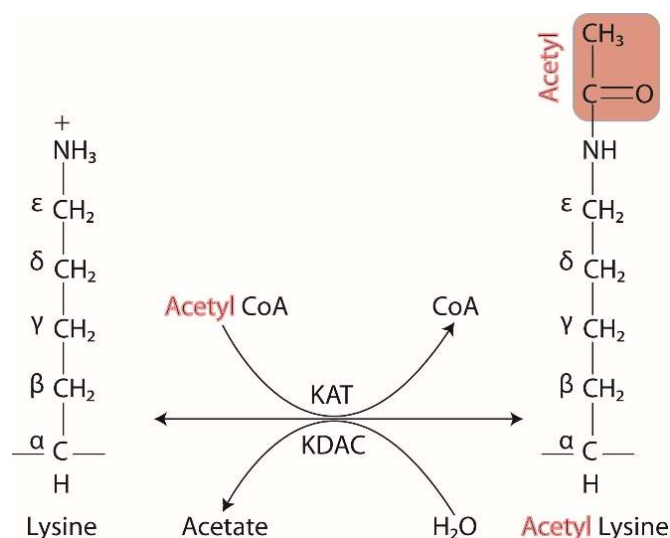


Figure 3: **Enzymatically catalysed acetylation and deacetylation of the ε-aminogroup of a lysine side chain.** Acetylation is catalysed by lysine acetyltransferases (KAT) and the reverse reaction by lysine deacetylases (KDAC). The substrate for acetylation is acetyl-CoA and the product of the deacetylation reaction is acetate which both links the PTM to the primary metabolism of the cell.

Nowadays, in addition to its occurrence on nuclear proteins, KAc has been recently found to occur on a large number of proteins with diverse biological functions and subcellular localisations in bacteria, yeast, animal cells and plants [104-107],[108-115]. The enzyme-dependent KAc is catalysed by KATs and lysine deacetylases (KDACs) and can have a strong impact on the function of modified proteins (Figure 3). Since acetylation neutralizes the positive charge of the Lys residue, and thus prevents the formation of hydrogen bonds and blocks the Lys from other modifications, KAc can influence protein-protein, protein-DNA, and protein-RNA interactions. In addition, KAc can affect the structural properties of proteins and their stability [116]. KAc appears to be important for cytoskeleton dynamics, energy metabolism, and autophagy [117, 118], and is dependent on the availability of acetyl-CoA, which is an important metabolic intermediate in the cell. In plants, acetyl-CoA is at the interface of many metabolic pathways and thus it is ideal to link the energy status of the cell to the regulation of gene expression and of the activity of many key enzymes controlling metabolic pathways [119]. Acetyl-CoA itself is not known to be transported over membranes so far, and thus each organelle has an own pool which connects acetylation to the local carbon status [120]. These properties qualify KAc as an important PTM for short term acclimations by rapid regulation of enzyme activities and for long term acclimations by regulating changes in gene expressions.

This hypothesis is also supported by the fact that KAc sites are more conserved than the unmodified K residues, e.g. in *Drosophila melanogaster* (fruit fly). In contrast phosphorylated Ser and Thr residues were identified as only marginally higher conserved than the corresponding unmodified residues [113]. Moreover, it turned out that the conservation of acetylated Lys residues of *Drosophila melanogaster* and humans compared to those in nematodes and zebrafish is significantly higher than the conservation of the unmodified residues [113]. This conservation gives a hint for the importance of KAc in regulating gene expression and several key enzyme activities acting in metabolic pathways.

Next to the enzyme catalysed KAc, this modification can also occur chemically in mammalian mitochondria. With an increased pH and a high acetyl-CoA concentration soluble liver proteins were acetylated in a dose- and time-dependent manner [121]. In plant mitochondria it was also shown that soluble proteins can be acetylated in a non-enzymatic reaction when the pH is slightly increased [122]. The acetylation was even more increased by denaturing the sample with heat, since the Lys residues are exposed to the medium upon the unfolding of the proteins. The non-enzymatic KAc does not exclude the regulation by KATs, although until now there is no known KAT to be localized in plant mitochondria. A combined operation of enzymatic and enzyme-independent acetylation is known to occur in mammalian mitochondria [122]. Hence, due to the non-catalysed KAc taking place in respiring mitochondria, deacetylases act as important regulators and cleaners in these organelles.

Similarly, in the chloroplast stroma the pH is slightly basic during photosynthesis with an optimum for the Calvin Benson Cycle reaction at 8.1 [123]. Hence, it is conceivable that with an increased concentration of acetyl-CoA the same scenario as in mitochondria could happen. A high acetyl-CoA concentration would thereby lead to the spontaneous, non-enzymatic acetylation of stromal enzymes. At the start of this thesis, it was unknown whether KATs and KDACs occur in the chloroplast, and thus these enzymes are described in more detail in the following chapter.

In *Arabidopsis*, many proteins involved in the central metabolism were found N<sup>ε</sup>-acetylated. These include proteins from the TCA cycle and the respiratory chain in mitochondria, and in photosynthesis, such as PSI-H, the β-subunit of the plastidial ATP synthase as well as key enzymes of the Calvin-Benson Cycle like RuBisCO and RCA in the chloroplast [104, 105]. The peripheral LHCII was found to be significantly more acetylated than the one which is tightly bound to PSII [105]. This finding suggested KAc might have similar roles like phosphorylation in controlling the state transitions. However, the extent of acetylation was not altered by changes in light [105]. Interestingly, a novel KAT has recently been identified in chloroplasts, which is required for *Arabidopsis* to perform state transitions, and is independent on the phosphorylation state of the LHCII proteins [124]. Also in the cyanobacterium *Synechocystis sp. PCC 6803*, about 50 % of the proteins involved in metabolic processes are acetylated

and about 15 % of those are involved in photosynthesis [125]. In both organisms, RBCL contains multiple KAc sites and its acetylation status increases under heterotrophic conditions in *Synechocystis* [104, 105, 125]. In *Arabidopsis*, at least nine acetylation sites (K14, 18, 21, 146, 175, 252, 316, 356, 463) were found in the chloroplast encoded RBCL [104]. Strikingly, K175 is a catalytically active residue which accepts protons after enolization of RuBP and protonates the carboxylate in the last reaction step [31]. K252 and K356 are known to interfere on a dimer-dimer interface of two large subunits and K146 builds a salt bridge with Glutamic acid (Glu)-110. K252 interacts with Aspartic acid (Asp)-286 on the border of two large subunits and is important for the stability of the hexadimeric RuBisCO complex [126]. If this residue gets acetylated and thereby neutralized it is probably prevented from the formation of a salt bond with Asp-286. This might lead to a lowered stability of the holoenzyme. Removal of Alanine-9 to K14 [77, 127] from the N-terminus of RBCL from *Spinacia oleracea* resulted in a dramatic loss of activity whereas the removal of the first eight amino acids had no effect. K316 is strictly conserved in all RuBisCO isoforms of different species and interacts also with the highly conserved Asp-137 [126]. Since the acetylated Lys residues are on delicate areas within the enzyme, it is conceivable that this PTM can regulate activity, stability, and holoenzyme assembly and disassembly. It has been shown that the deacetylation of the RBCL with recombinant human sirtuin 3 resulted in a 40 % increase of RuBisCO activity *in vitro* [104], and that KAc correlated with lower enzyme activity in a light-dependent manner [128], while another study was not able to observe this effect in 6-week old rosettes, which indicates that the acetylation occurs condition or development dependent [129]. Finkemeier and co-workers (2011) additionally identified a KAc site in RCA: K167. This residue lies near the ATP binding site and could play an important role for the regulation of the ATPase activity [104, 130]. Also another Calvin-Benson Cycle enzyme, phosphoglycerate kinase (PGK) and the TCA cycle enzyme malate dehydrogenase were found to be altered in activity by KAc *in vitro* [104].

In summary, there is a variety of PTMs occurring in the chloroplast. The function of most of these PTMs still remains unclear since this field of research is ongoing. The improvements of techniques to study PTMs in the last years have paved the way for the determination of regulatory pathways and functions of PTMs. Figure 4 gives an overview of the described PTMs in the chloroplast.

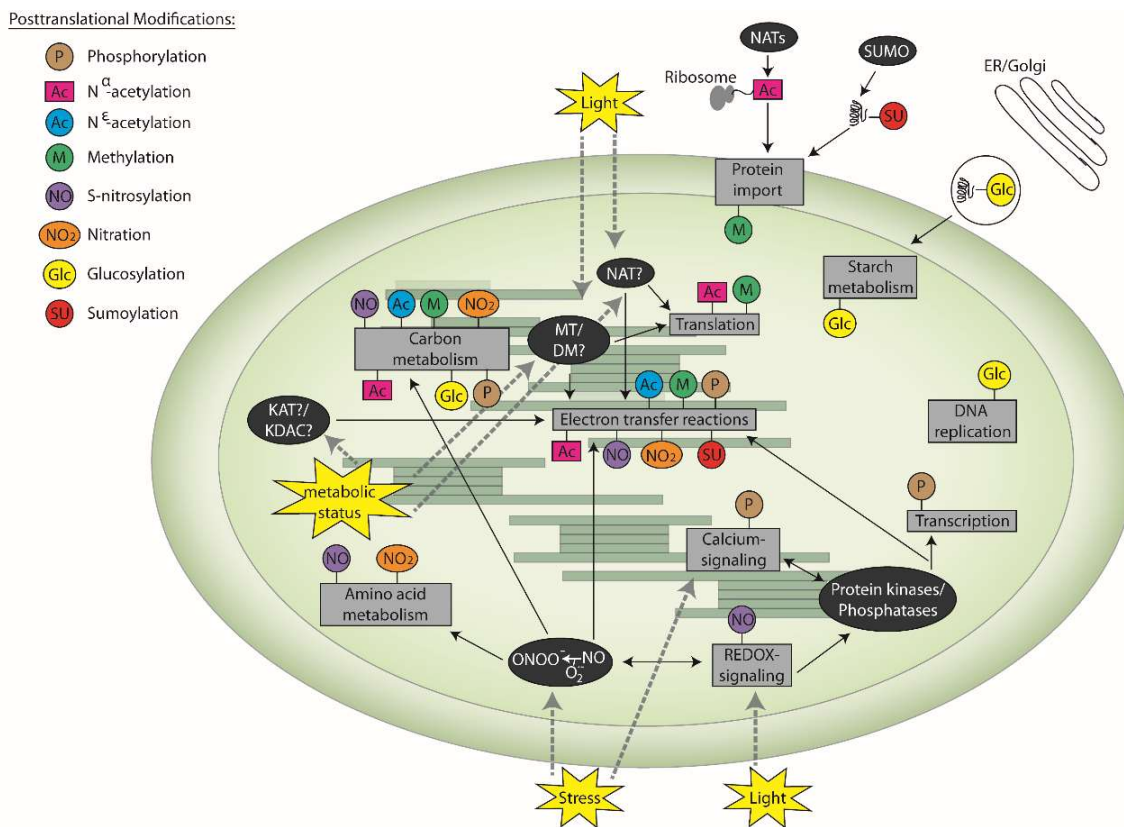


Figure 4: **Overview of the possible posttranslational modifications occurring in the chloroplast.** In order to acclimate to environmental changes and external stress (yellow stars), the plastid has to adapt its metabolism. This can be mediated by PTMs which are depicted with coloured pins. The main pathways regulated by PTMs are shown in light grey boxes and the enzymes which catalyse the modifications in dark grey boxes. So far uncharacterized enzymes are highlighted with question marks. KAT: Lysine acetyltransferase, KDAC: Lysine Deacetylase; NAT: N<sup>α</sup>- acetyltransferase; MT: methyltransferase, DM: demethylase; SUMO: sumoylation machinery. Modified from [80].

Since the reversible acetylation of the  $\epsilon$ -amino group of a Lys residue has a great potential to regulate activities of enzymes involved in photosynthesis, and in response to environmental changes the responsible writer and eraser enzymes are described in more detail in the next chapters.

### 1.3 Lysine acetyltransferases and -deacetylases

Lysine deacetylases and acetyltransferases were first discovered in the nucleus, where they modify histone proteins. Hence, they were named histone deacetylases (HDACs) and histone acetyltransferases (HATs), respectively. As more and more non-histone targets were discovered, it was suggested to change their names into lysine deacetylases (KDACs) and lysine acetyltransferase (KATs) [131]. Since the majority of identified KAc proteins reside outside the nucleus, it can be expected that several KATs and KDACs can also be found in other cellular compartments. In the next paragraph, KATs and KDACs existing in *Arabidopsis* are briefly introduced.

### 1.3.1 Lysine acetyltransferases

In *Arabidopsis*, 12 classical histone acetyltransferases were originally identified based on sequence homologies, which can be divided into two different groups depending on their subcellular localization [132-134]. Type B KATs localise in the cytoplasm while Type A KATs are localised exclusively in the nucleus [135]. Generally, type A KATs include the GCN5-related (general control nonrepressible 5) acetyltransferases, the MYST-related (named for its members MOZ, yeast Ybf2/Sas3, yeast Sas2 and human Tip60) KATs and the CBP/p300 (CREB-binding protein/p300) KATs [135]. In addition, KATs can be grouped into five families based on sequence divergence in the KAT domain. These families include KAT1, Gcn5/PCAF (p300/CBP associated factor), MYST, p300/CBP and Rtt109 (regulator of Ty1 transposition gene product 109) and the TATA-binding protein associated factor 1 (TAF1). Gcn5/PCAF, HAT1 and MYST have family homologs from yeast to man while p300/CBP is found in metazoa and Rtt109 is fungal-specific [136]. However, in *Arabidopsis* orthologs of the p300 and CBP were reported and named p300/CBP acetyltransferase-related protein 1-4 (PCAT1-4) [137]. In *Arabidopsis*, the 12 KAT genes are divided into four groups: The GNAT/MYST superfamily contains five members which are named *HAG*. The GNAT family can be further subgrouped into GCN5, ELP3 (elongator protein 3), HAT1 and HPA1, all containing a single member (HAG1, HAG2, HAG3), whereas HAG4 and HAG5 belong to the MYST family [132]. Five KATs belong to the CBP family and are named with the symbol *HAC* (HAC1, HAC2, HAC4, HAC5, HAC12) [137]. The CBP family of KATs contains large, multidomain proteins and its histone acetylation domain is unrelated to that of the GNAT and the MYST family [132]. The fourth group, the TAF<sub>II</sub>250 consists of two members, symbolled *HAF* (HAF1 and HAF2) [138].

Generally, KATs harbour a structurally conserved acetyl-CoA binding region containing a three-stranded  $\beta$ -sheet with a long  $\alpha$ -helix parallel [139]. KATs were first discovered to acetylate histone proteins but it turned out that they are also acting on non-histone proteins like transcription factors, cytoskeletal proteins, molecular chaperones, and nuclear import factors for example [140]. Furthermore, Gu and Roeder demonstrated that the tumour suppressor protein p53 gets activated by acetylation mediated by its coactivator p300. The acetylation of p53 stimulates its DNA-binding capacity by a conformational change which is induced by acetylation [141].

In plants the GCN5-related KATs are involved in stress-induced changes of gene expression and developmental changes by interacting with the *Arabidopsis* homologs of the yeast transcriptional adaptor proteins ADA2a and ADA2b. [142]. In maize, the protein level of ZmGCN5 decreased after treatment with the deacetylase inhibitor trichostatin-A (TSA) which corresponded with an increase in the acetylation levels of histone H4. Vice versa the reduction of ZmGCN5 in antisense lines of *Zmgn5* led to a decrease in the abundance of the deacetylase ZmRpd3. Strikingly the results in gene expression changes of the KDAC partly overlapped with the TSA treatment [143]. These findings suggest that the

expression of KATs and KDACs is dependent on the acetylation status of histone proteins [135, 143, 144]. Since KATs acetylate not only histone proteins but also other KATs they also have an autoregulatory role. Thus KATs play an important role in regulating gene expression and are important for the plant to switch to developmental stages and to adapt to environmental changes [115, 135]. Strikingly, a recent study showed that seven out of ten predicted GNATs in *Arabidopsis* are localized in the chloroplast. It was also shown that recombinant GNAT2 and GNAT10 protein harbour not only KAT but also NAT activity demonstrating that GNAT proteins have both acetylation activities without an additional regulatory subunit. *In vivo*, the knockout of GNAT2 (NSI) led to defects in the state transition and acetylome studies of the mutant revealed a unique substrate specificity which could not be compensated by the other GNAT members [97, 124]. The N-terminal acetylation (NTA) in the cytosol was not affected in this mutant while there was a decrease in NTA of plastid-localized proteins. Interestingly all of them are nuclear encoded and thus GNAT2 post-translationally acetylates plastid-imported proteins [97]. Acetylation is not just regulated by KATs but also by their antagonists, the KDACs which are the erasers of the acetyl moiety and are described in the following chapter.

### 1.3.2 Lysine deacetylases

KDACs remove the acetyl moiety from N<sup>ε</sup>-acetylated Lys residues. Thereby an acetate molecule is released in case of the classical class I and class II KDAC family (Figure 3). The first deacetylases were discovered in yeast, where it was shown that RPD1 (reduced potassium dependency) and RPD3 regulate gene expression [145]. The first class (class I) of isolated human deacetylases has a high homology to the yeast RPD3. Three other families have been isolated since then, the Hda1 family (class II), the Sir2 (Silent information regulator 2) family (class III), and the class IV KDACs [146].

In total 18 genes encode for putative KDACs in the *Arabidopsis* genome, and they belong to three different types of KDACs. The first type of KDACs are the classical histone deacetylases, which are homologous to the yeast RPD3 family and HDA1-like proteins. In *Arabidopsis*, this group contains 12 putative members from class I, class II and Class IV [132]. Class I consists of six members: HDA6, HDA7, HDA9, HDA10, HDA17 and HDA19. Class II has five members: HDA5, HDA8, HDA14, HDA15, and HDA18, and class IV contains a single member HDA2 [147]. HDA10 and HDA17 are almost duplicates of the C-terminal sequence of HDA9 and lack a catalytic domain. Thus, it is likely that they are no functional KDACs [148].

Table 1: Subcellular localization of *Arabidopsis* KDACs (modified from [149]).

<b>KDAC family</b>	<b>Enzymes</b>	<b>Localization</b>	<b>References</b>
RPD3/HDA1-like	AtHDA5	Cytoplasm (ER)	Alinsug et al. (2012) [150]
	AtHDA6	Nucleolus	Chen and Tian (2007) [135], Earley et al. (2006) [151]
	AtHDA7	Nucleus	Cigliano et al (2013) [152]
	AtHDA8	Cytoplasm	Alinsug et al. (2012) [150]
	AtHDA9	Nucleus	Yu et al (2011) [153]
	AtHDA10		Alinsug et al (2009) [147]
	AtHDA14	Chloroplasts, Mitochondria, Cytoplasm	Alinsug et al. (2012) [150] Tran et al. (2012) [161] Hartl et al 2017 [106] (Publication [3])
	AtHDA15	Cytoplasm, Nucleus	Alinsug et al. (2012) [150]
	AtHDA17		Alinsug et al (2009) [147]
	AtHDA18	Cytoplasm, Nucleus	Alinsug et al. (2012) [150] Liu et al (2013a) [154]
	AtHDA19	Nucleus	Fong et al. (2006) [155]
HD2	AtHD2A	Nucleolus	Zhou et al. (2004) [156]
	AtHD2B	Nucleolus	Zhou et al. (2004) [156]
	AtHD2C	Nucleolus	Zhou et al. (2004) [156]
	AtHD2D	Nucleus	Han et al,2016 [157]
SIR2-like	AtSRT1		
	AtSRT2	Mitochondria	König et al. (2014) [158]

The members of the RPD3-like superfamily are structural distinct from each other. While HDA6, 7, and 9 contain polyglycine regions HDA15, 10, and 17 have aspartate-rich regions, and HDA15 contains a zinc-finger domain [159]. However, they all require a  $Zn^{2+}$  for catalytic activity and the active site consists of a curved-tubular shape where the  $Zn^{2+}$  ion locates at the bottom of the pocket. The  $Zn^{2+}$  ion and the adjacent residues (two histidine, two Asp, one Tyr) are required for the removal of the acetyl group [160]. The members of this protein family are inhibited by TSA and sodium butyrate which both bind to the  $Zn^{2+}$  ion in the active site [159]. RPD3-like KDACs are highly expressed in inflorescences and young floral tissues but are low expressed in vegetative tissues. In *Arabidopsis*, HDA6, 9, 19 show similar expression profiles and only HDA14 is expressed differently from all other family

members [159]. This could result in a distinct function of HDA14 in the plant cell [159]. HDA14 was found recently to deacetylate tubulin, and associated with  $\alpha/\beta$ -tubulin and the phosphatase PP2-A. These proteins are localised in the cytosol and the nucleus. The association of a phosphatase and a deacetylase suggests a direct link between acetylation and phosphorylation [161]. Luo and co-workers demonstrated that HDA5 and HDA6 are part of a multiple protein complex which controls the expression of flowering repressor genes in *Arabidopsis*. They also showed that HDA5 and HDA6 co-regulate gene expression of various pathways belonging to developmental changes [162]. However, HDA9 was found to repress seedling traits like RuBisCO and RCA in dry seeds in *Arabidopsis* and thereby has a negative influence on germination. The knockout of HDA9 led to a faster germination compared to wild type plants [163]. Furthermore, it was shown recently, that the class I HDA19 and the class II HDA5/14/15/18 have different roles in the salt stress response. The *hda19* mutant showed more tolerance to salinity stress, while *hda5/14/15/18* mutants were hypersensitive to salt stress [164].

The second type, the HD-tuins are unique in plants and were first discovered in maize [165]. This family consists of four members HDT1-4 in *Arabidopsis* and is structurally distinct from the RPD3-like superfamily but shows sequence similarities with peptidyl-prolyl cis-transisomerases [166]. The members of the HD-tuins all contain three domains: the N-terminal domain containing a conserved pentapeptide motif (ME-FWG), a high charged central acidic domain and a variant C-terminal domain [166]. Six out of eight analysed HD-tuin proteins contain a single putative zinc-finger motif which is possibly involved in protein-protein interactions [149]. The conserved N-terminal ME-FWG domain is required for repression. In HDT1 this region is essential for its catalytic activity [132, 167, 168]. The HD-tuins are expressed similarly as the members of the RPD3 superfamily and thus show a higher expression in floral than in vegetative tissues [159].

The third type of KDACs, the sirtuins, contains two genes in *Arabidopsis*: SRT1 and SRT2, of which SRT2 has at least seven spliceforms [158]. Hence, in contrast to fungi and animals, all higher plants contain a reduced number of SIR2 genes. Yeast, for example has five Sir2 genes and mammalian cells even seven [169]. SIR-like KDACs are nicotinamide adenine dinucleotide (NAD<sup>+</sup>)-dependent and do not share any sequence or structural homology with other KDAC family members. Their activity can be inhibited by nicotinamide as a competitive inhibitor, but not by TSA or sodium butyrate [159]. SIR2-like proteins are conserved from bacteria to humans and control basic cellular processes [170, 171]. It has been shown that SIRT2 is localized in the mitochondria of *Arabidopsis* and that it deacetylates the ADP/ATP carrier and thus controls the ADP uptake in mitochondria [158]. The expression pattern of the SIR2-like family members is distinct from the enzymes belonging to the RPD3-like superfamily or the HD-tuins.

#### **1.4 Acetyl-CoA metabolism in plants**

Acetyl-Coenzyme A (acetyl-CoA) is the substrate molecule for chemical and enzymatically catalysed KAc in the cell. Furthermore, it is a key intermediate in various metabolic pathways and is produced and consumed in the plastids, the mitochondria, the peroxisomes, the nucleus, and the cytosol in plant cells. Acetyl-CoA is produced by the catabolism of organic acids, carbohydrates, lipids, and amino acids and at the same time it is the precursor for many important cell components (Figure 5). Hence, the flux that controls the metabolism of this intermediate is the rate of conversion of carbon reserves into important metabolites [120]. Acetyl-CoA and other CoA derivatives are not known to be directly transported over membranes so each organelle has its own metabolite pool. Thus, the acetyl-CoA concentration is a local indicator for the carbon and energy status and may be tightly regulated in response to developmental and environmental conditions [172]. In the cytosol acetyl-CoA is produced by the ACL by converting citrate and ATP into acetyl-CoA and oxaloacetate. This enzyme was first discovered in vertebrates as a homotetramer and as a lipogenic enzyme it is highly regulated by transcriptional and posttranslational mechanisms [173]. In plants ACL is a heterooctamer which consists of ACLA and ACLB subunits [172]. Fatland and coworkers [174] reported that the cytosolic acetyl-CoA pool generated by ACL is essential for normal plant growth and development and that no other source can compensate deficiencies of this pool. The precursor of cytosolic acetyl-CoA is mainly derived from mitochondrial citrate synthesized by the citrate synthase from oxaloacetate and acetyl-CoA, and is then exported via the citrate/oxaloacetate shuttle into the cytosol. Hence, acetate-equivalents are moved from the mitochondrial matrix to the cytosol and vice versa [120]. In the peroxisomes, acetyl-CoA is mainly derived from fatty acid breakdown and feeds into the glyoxylate shunt which is especially important during seed germination because it is essential for the conversion of fatty acids into sucrose. The enzyme which was identified to be responsible for the conversion of fatty acids that are not longer than C-4 into acetyl-CoA in peroxisomes is an acyl-CoA synthetase, the acetate non-utilizing 1 (ACN1). It was found to be more active with acetate than with butyrate and is especially important during seed germination and seedling establishment since the  $\beta$ -oxidation of fatty acids produces large quantities of acetate [175].

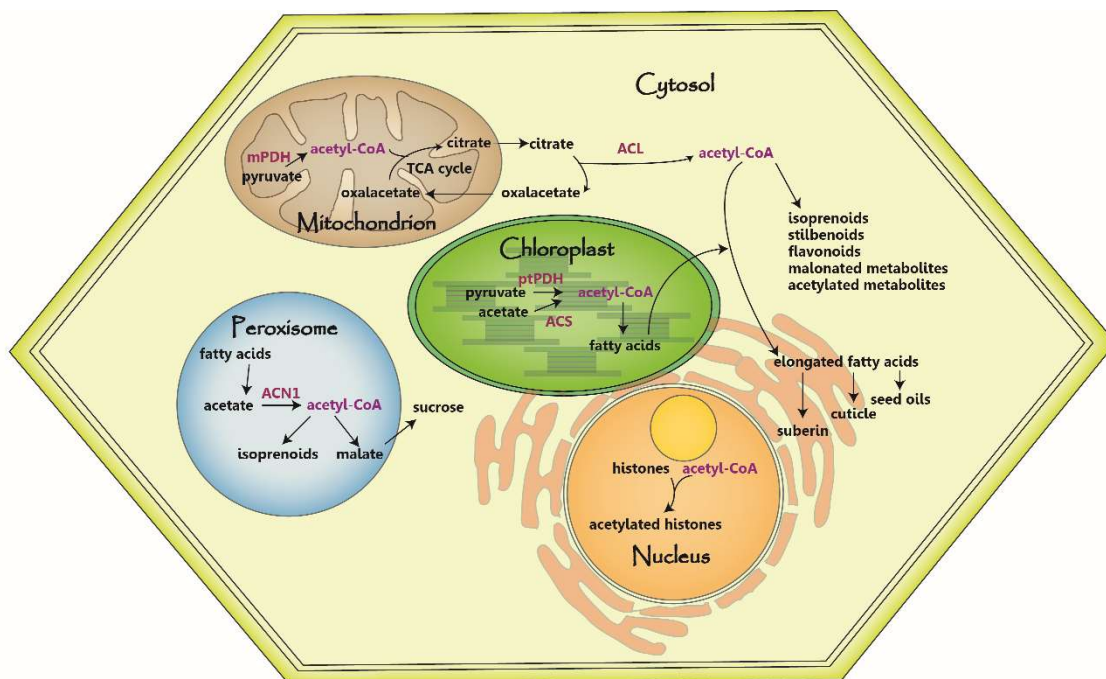


Figure 5: **Simplified scheme of acetyl-CoA metabolism in the different organelles of a plant cell.** Acetyl-CoA is produced in the mitochondrion by the mitochondrial pyruvate dehydrogenase (mPDH) and converted to citrate by the citrate synthase. Citrate exported from the mitochondria is used by the ATP-citrate lyase (ACL) in the cytosol to generate acetyl-CoA, which is used for the formation of isoprenoids, stilbenoids, flavonoids, malonated and acetylated metabolites or the elongation of fatty acids derived from the chloroplast. In plastids acetyl-CoA can be produced by the plastidal PDH (ptPDH) from pyruvate or by the acetyl-CoA synthetase (ACS) using acetate. In the peroxisomes, acetyl-CoA is synthesized from acetate, which is derived from the  $\beta$ -oxidation of fatty acids. The conversion of acetate to acetyl-CoA is catalysed by the acetate non-utilizing 1 (ACN1) enzyme. In the nucleus, acetyl-CoA is derived from the cytosol and is used as substrate molecule to acetylate histones and thus for the regulation of gene expression. After [120].

In mitochondria and plastids, the main source of acetyl-CoA is the PDH complex (PDC). This complex consists of three central enzymes: the E1 subunit is a specific  $\alpha$ -ketoacid dehydrogenase, the E2 subunit is a dihydrolipoyl acyltransferase, and the E3 subunit is a dihydrolipoyl dehydrogenase and catalyses the formation of acetyl-CoA from pyruvate [176]. The mitochondrial PDH (mPDH) E1 component consists of two subunits, the  $\alpha$  and the  $\beta$  subunit, which form a heterotetramer, whereas the E2 is a multidomain protein composed of one or two lipoyl acid-binding domains, an E1-binding domain and a C-terminal catalytic and assembly domain. The E2 component forms the core of the PDH. The E3 subunit consists of an FAD- and an NAD-binding domain, a central domain, and an interface domain, which is responsible for the dimerization [176, 177]. The mPDH links glycolysis to the TCA cycle since the produced acetyl-CoA is used by the citrate synthase to produce citrate as initial step of the TCA cycle. Hence the carbon flux through this enzyme controls the TCA cycle activity [176]. The plastidal PDC (ptPDC) catalyses the same reaction as the mitochondrial PDH and its organization is similar. PtPDC not just supplies the plastid with acetyl-CoA which is used for *de novo* fatty acid

synthesis and the formation of amino acids and glucosinolates in the stroma but the ptPDC is also the primary source of stromal NADH which is necessary for fatty acid biosynthesis [176, 178, 179]. These fatty acids produced in the chloroplast are subsequently elongated in the cytosol using the acetyl-CoA derived from citrate cleavage via ATP-citrate lyase and are converted into various chemicals, which are further condensed into polyketides [120]. The second source of plastidial acetyl-CoA is from acetate, which is converted into acetyl-CoA by the acetyl-CoA synthetase (ACS) (Figure 5). ACS is a monomeric protein which seems to be dependent on the presence of the reducing agent and  $K^+$  ions for maximum activity. This reduction is not related to the classical Trx system, because the activation of ACS is not light-dependent [180]. Since the fatty acid composition is not altered in ACS deficient mutants the major source of acetyl-CoA used for fatty acid biosynthesis comes from the ptPDH, and the role of ACS in the plastid is still unclear. Furthermore, the mutants with in- or decreased ACS levels do not show any obvious morphological phenotype such as growth rate, rosette, final or root or leaf size, seed number and weight, the time of flowering, or the germination date or rate [180]. The knockout mutant of ACS is more sensitive to exogenous acetate, ethanol and acetaldehyde suggesting that ACS plays an important role in detoxifying these fermentation intermediates [120, 181]. It is still unknown what the source of acetate is, which is detoxified by ACS. One explanation could be a role in a PDH-bypass reaction in plants. In this “aerobic fermentation” pathway pyruvate, which is generated by glycolysis is first oxidized to acetaldehyde by the cytosolic pyruvate decarboxylase and then to acetate by the acetaldehyde dehydrogenase. ACS could then convert acetate to acetyl-CoA which is then used for the fatty acid biosynthesis (Figure 6). This bypass pathway is suggested to be essential for providing high metabolic rates in tissues, which may be under hypoxic conditions such as growing pollen tubes [120, 182].

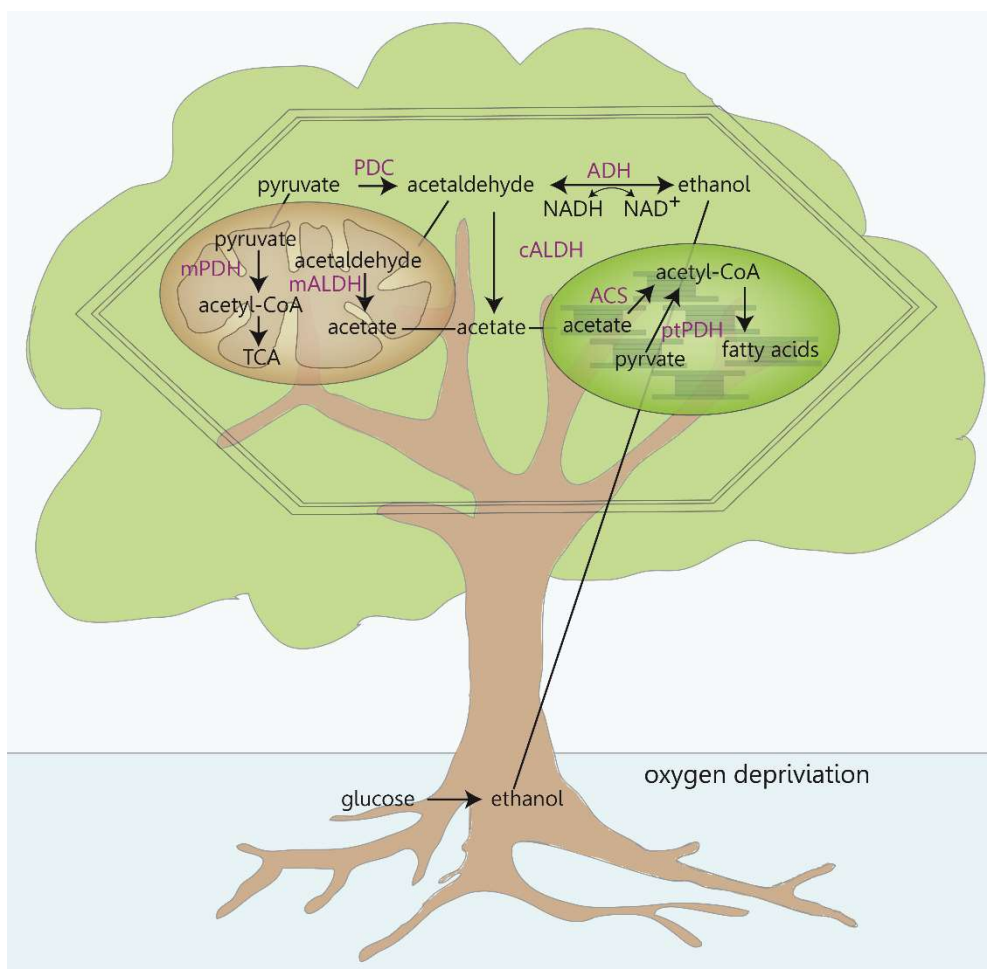


Figure 6: **Possible sources of acetyl-CoA from pyruvate and acetate metabolism in plants.** In the PDH bypass pathway acetyl-CoA can be formed under conditions where PDH activity is limited using the pyruvate decarboxylase (PDC), which forms acetaldehyde from pyruvate. Acetaldehyde is converted to acetate by the cytosolic (cALDH) or the mitochondrial aldehyde dehydrogenase (mALDH), which can be converted to acetyl-CoA by ACS in the plastid. Ethanol is supposed to be generated in roots under oxygen ( $O_2$ ) limited conditions and is transported to the leaves where it is either lost as organic compound or oxidized to acetaldehyde by the alcohol dehydrogenase (ADH) and can be used to build fatty acids. mPDH: mitochondrial pyruvate dehydrogenase; ptPDH: plastidal pyruvate dehydrogenase. After [120, 183].

Acetate or its precursors can be formed in organs that are exposed to low oxygen stress. The C-2 fermentation intermediates, ethanol and acetaldehyde, can be either emitted to the environment or transported to the leaves (reviewed in [120]). Precursor feeding experiments suggest that they are formed in the roots and are subsequently transported to the leaves (reviewed in [120]). Hence, it is likely that the ethanol produced in the roots is transported to the leaves where it gets oxidized to acetaldehyde and acetate. Acetate is then activated by ACS using ATP to form acetyl-CoA which can be further metabolised to fatty acids. Therefore it is suggested that ACS has a role in keeping the levels of fermentation products below toxic levels while some of the lost carbon gets recaptured (reviewed in [120]).

The plastidial ACS and the peroxisomal ACN1 are related members of the acyl-activating enzymes family (the AAE superfamily) [184]. These two enzymes provide redundant function in different organelles to protect the cell against hyperaccumulation of acetate [185]. The T-DNA insertion lines of ACS or ACN1 in *Arabidopsis* did not show severe phenotypical changes. However, the double knockout mutants *acs x acn1* showed highly pleiotropic defects with delayed growth rates and sterility. The mutant plants were infertile and showed a slower root growth, and truncated leaves compared to WT or the single mutants [185]. Metabolome studies showed a reduction in nearly all metabolites measured in the double mutant compared to WT. However, acetate levels were strongly increased in the double mutant compared to the single mutant or WT plants. The shoot weight and the root length were significantly lower in plants expressing neither ACS nor ACN1. Growth on acetate containing medium enhanced the phenotypic deficiencies [185]. However, there are many unanswered questions in the acetate metabolism of higher plants which have to be clarified in the future.

### **1.5 Mass spectrometry-based proteomics to study lysine acetylation in plants**

In the last decades mass spectrometric techniques have been developed and improved to analyse various PTMs on proteins. To analyse PTMs in a complex sample is challenging since the modified proteins are usually underrepresented in a proteome. Hence, for the analyses there are high amounts of freshweight plant material necessary, often in the milligram range. This makes the analysis of PTMs in a complex sample time intensive and the reagents for the analyses are expensive. Since reversible PTMs can change within seconds in the plants, the biological variance between samples can be high, and hence the statistics can be challenging. The PTM abundance in biological replicates has to be similar and therefore biological replicates harvested at the exact time points and growth condition are necessary for a meaningful data analysis. Since PTMs are underrepresented in a complex proteome sample they need to be enriched prior analysis. For this, different techniques can be used but they can introduce a certain sampling bias, due to different affinities of PTM sites to the affinity matrix. Hence, sample preparation needs to be performed very carefully and biological replicates are indispensable [186].

To analyse KAc in complex mixtures of proteins bottom-up mass-spectrometric approaches are commonly performed. As a part of sample preparation, proteins get digested with a protease (e.g., trypsin) before MS-analyses. Due to the cleavage site after Lys and Arg residues positively charged peptides are generated, with a charge state of at least +2. This is an important feature for ionisation in the mass spectrometer, which is run in the positive mode and peptides get protonated during MS analysis. In addition, only peptides in the range of about 7 to 35 amino acid residues are suitable for the assignment of peptides to proteins [187]. Desalted peptides are then separated in a liquid

chromatography (LC) according to their hydrophobicity before they are ionised in the electrospray ionisation (ESI) and subjected to mass spectrometry. Tandem Mass spectrometry, also named MS/MS is nowadays a commonly used method. It consists of two stages: (1) the determination of the mass of the intact precursor ion and (2) the isolation and the fragmentation of the precursor ion. For fragmentation of the precursor ions higher-energy collisional dissociation (HCD) is the mostly used fragmentation mode. For this the precursor ions collide with an inert gas such as nitrogen. Normally, the MS/MS analyses are carried out using data-dependent acquisition (DDA) in the mass spectrometer. Therein, first a full scan (MS1) is recorded by the instrument whereby the masses over charge states ( $m/z$ ) and the masses of the precursor ions that elute at the same time from the LC are recorded.

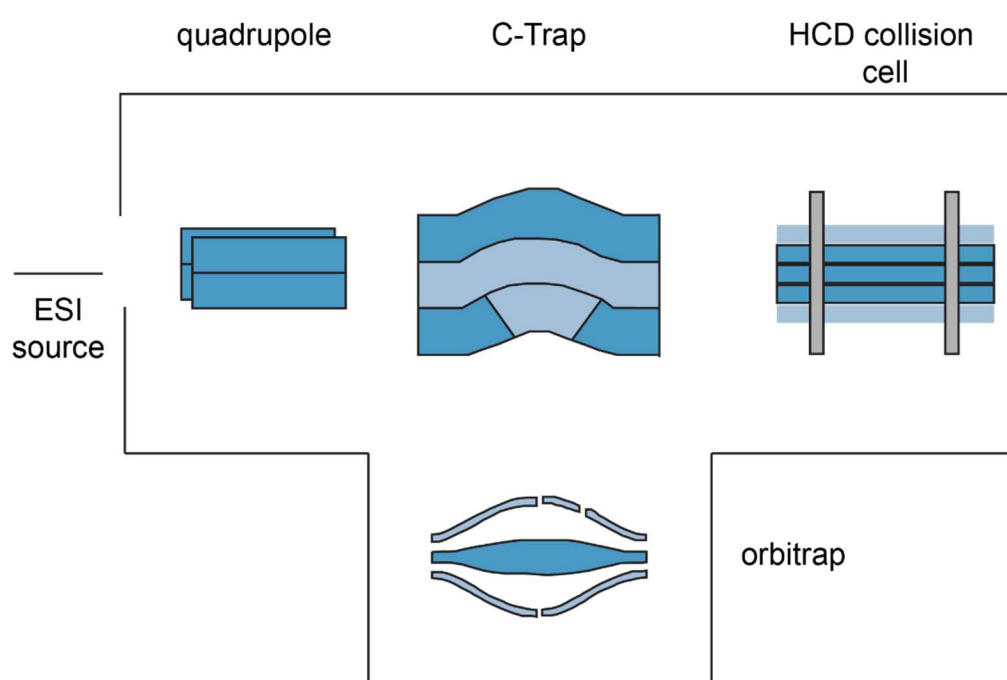


Figure 7: **Simplified schematic of a Q-Exactive mass spectrometer without the optical components (Thermo Scientific).** Peptides are ionized at the ESI source (electrospray ionization source) and are flying through the quadrupole before they are collected in the C-Trap. The MS1 spectra are recorded in the orbitrap and the most intense peptides are guided to the HCD (Higher-energy collisional dissociation) collision cell, where they collide with  $N_2$  as and are thereby fragmented. Accordingly, the fragments are guided back to the C-Trap before the Orbitrap where the MS2 spectra are recorded.

During DDA, the molecules which show the most intense signals are selected for fragmentation and a second scan is performed (MS2). Accordingly, a set of MS1 and MS2 spectra is reported by the instrument. This method is repeated over the whole duration of the liquid chromatography and electrospray ionisation. Since the less abundant peptides are not chosen for fragmentation and usually most PTMs are underrepresented in complex samples, peptides carrying a PTM have to be enriched before the MS analyses (see below). The instrument used for the analyses of KAc was a hybrid Quadrupole Orbitrap type mass spectrometer (Q Exactive; Thermo scientific; Figure 7).

Mass spectrometry is not absolutely quantitative since the ion intensities are dependent on the ionization properties of the molecule. Hence, one option is a relative quantification, such as used in label-free quantification (LFQ), where the ion intensities of the same precursor molecules are compared between the samples. To avoid variations during sample preparations and between runs, methods have been developed which allow the direct comparison of precursor ion abundances. These methods include the stable labelling of proteins or peptides, which can be pooled and analysed together in one single run and thus allow a direct comparison of ion intensities. The ionization and chromatographic properties of the labelled peptides are nearly identical, but they can be distinguished by their mass shift [188]. There are various techniques for the stable labelling of proteins or peptides available. For *in vivo* labelling of proteins  $^{15}\text{N}$  metabolic labelling can be used. Thereby the isotopic label can be introduced as an amino acid or by adding a  $^{15}\text{N}$  source to the medium. For stable isotopic labelling by amino acids in cell culture (SILAC) stable isotope labelled amino acids are added to the medium. In *Arabidopsis*, it has been shown that [ $^{13}\text{C}_6$ ]-Arg is working best with an efficiency of 80 % [189]. However, a higher efficiency is nearly impossible in plants, because they can synthesise all amino acids from nitrate or ammonium and are thus not dependent on the feeding of exogenous amino acids [188].  $^{15}\text{N}$  metabolic labelling via nitrate and ammonium overcomes this limitation by adding the stable isotope to a liquid culture medium, which is then incorporated in all amino acids synthesised by the plant [190]. The disadvantage is that the label is present in all amino acids so the mass difference of labelled and unlabelled peptides will vary depending on their protein sequence, and this makes the data analysis challenging [188]. Another approach is the stable isotopic labelling of tryptic peptides *in vitro*. In dimethyl-labeling, all primary amines (N-terminus and Lys) in the peptides are converted to dimethylamines (Figure 8). The chemical labelling is advantageous because it is inexpensive and can be applied to microgram of peptides up to several milligrams. The labelled peptides are mixed and are subsequently analysed by LC-MS/MS [191].

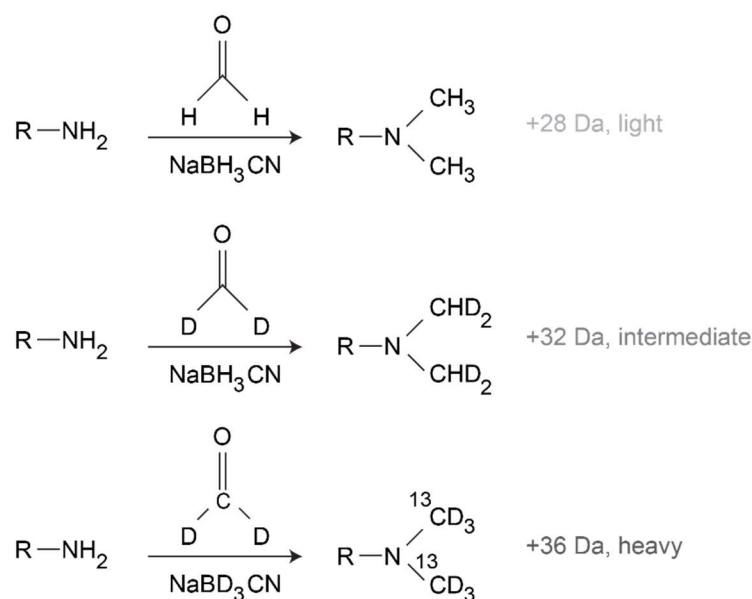


Figure 8: **Scheme of chemical dimethyl labelling of peptides.** The primary amines (N-terminus and lysine residues) are converted to dimethylamines upon labelling. Three conditions/genotypes can be compared by using the stable isotopes and adding either “light”, “intermediate” or “heavy” dimethyl groups.

Modified from [191].

Up to three different conditions or genotypes can be compared using the stable isotope dimethyl labelling technique for quantifications of protein abundances or changes in PTMs levels. Due to their low abundance, modified peptides have to be enriched from complex proteome samples prior analyses. There are several enrichment strategies depending on the PTM of interest. Peptides carrying one or more KAc sites can be enriched using an Anti-KAc antibody which is coupled to agarose beads [108]. Before the enrichment, the complexity of the proteome can be further reduced by fractionating the tryptic peptides using high pressure liquid chromatographic (HPLC) techniques [192]. Zwitterionic hydrophilic interaction liquid chromatography (ZIC-HILIC) can be used for this approach. It has been shown that reducing the complexity of a peptide mixture with ZIC-HILIC resulted in a significantly higher identification number of peptides [193]. Using these techniques together with the dimethyl labelling strategy it is possible to study changes in KAc between samples from different treatments or genotypes.

## **2. Aim of the thesis**

As outlined above, the acetylation of the  $\epsilon$ -amino group of Lys residues can have major impact on the properties and functions of the protein, since acetylation leads to an uncharged and more hydrophobic amino acid side chain. This can impact on the formation of hydrogen bonds and the structural properties within proteins in dependence on the exact location of the Lys residue within the protein structure. In addition, KAc can also affect the stability of the protein and the interactions with other proteins or DNA and RNA [116]. Likewise, the acetylated Lys residue is blocked for other modifications such as methylation or ubiquitination. KAc can therefore affect changes in enzyme activity, marks for cargo transport, and it acts as a recognition site for bromodomain-containing proteins [117, 118].

In the last decade, the identification of non-histone KAc proteins increased considerably. Advances and affinity enrichment techniques led to the identification from a few acetylation sites to thousands of sites [108]. Hence, mass spectrometry is nowadays a frequently used tool to study different PTMs. The modified proteins are of various functions and subcellular localizations. In several plant species more than 1000 KAc sites on several hundred proteins were identified in the last years since the technical equipment is improving continuously. Especially acetylated enzymes which are localized in the plastid and are involved in photosynthesis including the light reactions and the Calvin-Benson Cycle were identified. However, the simple occurrence of a KAc site on a protein does not necessarily indicate that this site is important for the regulation of protein function.

Hence, the major aim of this thesis was to identify KAc sites on proteins, which are regulated by modifying enzymes and in dependence on environmental conditions.

Since the reversible KAc of proteins is dependent on KATs and KDACs, the first objective of this thesis was to identify substrate proteins of KDACs using general KDAC inhibitors in *Arabidopsis* leaves and to quantify the KAc sites by mass spectrometry-based proteomics. In a next step, members of these enzyme families, which are localized in the plastids and therefore have a potential role in the control of KAc of enzymes involved in photosynthesis had to be identified. For this, TargetP bioinformatic prediction of candidate KDAC proteins combined with confocal laser scanning microscopy of GFP-tagged KDAC proteins was used, as well using a KDAC-trap on isolated chloroplast proteins. With this combination of methods, the first plastidial KDAC was identified and characterized.

Another part of this thesis was to investigate the KAc in the green alga *Chlamydomonas reinhardtii* in dependence of light and nutrient source. This unicellular alga has a short life cycle and can grow hetero-, mixo- or photoautotrophically. Under hetero- and mixotrophic growth conditions it can use acetate as a carbon source, which converted to acetyl-CoA, which is the substrate molecule for KAc.

The aim of this study was to reveal if the growth conditions have an impact on the KAc state of *Chlamydomonas* and if key metabolic enzymes are regulated by this PTM to adjust to these growth conditions.

### **3. Summarising discussion**

#### **3.1 Lysine acetylation occurs as a reversible and dynamic modification on histone and non-histone proteins of diverse function in photosynthetic organisms**

The work in this thesis focussed on the investigation of KAc proteins in *Arabidopsis thaliana* and *Chlamydomonas reinhardtii* with a special emphasis on the KAc of proteins involved in photosynthesis and those involved in acetate metabolism. Overall, the optimization of the method, advances in mass spectrometry and sample preparation led to a tremendous increase in the number of identified KAc sites compared to previous studies. Around 100 KAc sites were reported in *Arabidopsis* in the first reports [104, 105]. With the improved method, which was developed during this thesis, the number of identified KAc sites increased to 2152 on 1022 protein groups in *Arabidopsis* leaves. This corresponds to 2057 novel acetylation sites and 959 novel acetylated proteins compared to the data published before [104-106, 122] (Publication [3]). Proteins belonging to the functional categories of photosynthesis, tetrapyrrole synthesis, gluconeogenesis, redox, TCA cycle, and DNA and RNA regulation of transcription were the most prominent. Strikingly, the plastid and nucleus localized proteins (based on the SUBA (Subcellular location of proteins in *Arabidopsis* database) consensus [194]) were clearly overrepresented among the acetylated proteins [106] (Publication [3]). Hence, almost half of the identified KAc proteins (43%) were putatively localized in plastids. Interestingly, about one fourth of the enzymes involved in the photosynthetic light reactions carried at least four acetylation sites. The high number of KAc proteins in the plastid and in photosynthesis indicates that this PTM bears a special function to provide an additional layer of regulation for photosynthetic enzymes as it is already known for phosphorylation and a variety of other PTMs, which occur in chloroplasts (Figure 4). Each type of modification fulfils a special function, and the complexity of the proteome increases massively due to the PTMs of proteins, which therefore provide further levels of regulation and adaption of enzymes to changing environmental conditions. Thus, plant growth and development can be optimized through the fine-regulation of the metabolism by KAc and other PTMs in response to environmental conditions [6]. Our work showed that many enzymes outside the nucleus are K-acetylated in *Arabidopsis* and that they are involved in a variety of cellular functions and that KAc is a dynamic PTM and changes within hours depending on the treatment or light conditions. The regulation of enzyme activities by PTMs is acting fast, and they are fine-tuning enzyme activities. Thus, it is likely that KAc is not just used by the plant to adapt gene expression by the modification of histone proteins in the nucleus, but also provides an additional layer of regulation by the acetylation of metabolic key enzyme activities. KAc could therefore be used to adjust enzyme activities in short term responses and alter gene expression in long term responses. Since KAc is dependent on the acetyl-CoA level in the cell it is directly connected to the carbon and energy status of the cell. Acetyl-

CoA is not known to be transported over membranes so far and thus reflects the local carbon status of each organelle where it is produced (Figure 5) [120]. KAc is found predominantly on proteins involved in metabolic processes, photosynthesis, and stress response [107] and is changing within the diurnal cycle [107]. In seedlings KAc of the photosynthetic machinery is highly increased at the end of the night while in roots in general KAc is elevated at the end of the day. On Calvin-Benson Cycle enzymes KAc also showed diurnal changes. It is likely that KAc regulates enzymes involved in the Calvin-Benson Cycle because of the large carbon pools in the chloroplast stroma which are used for the generation of acetyl-CoA. Using acetyl-CoA for KAc mediated regulation instead of phosphorylating the target enzyme is reserving ATP pools for carbon assimilation [107].

We found the enzyme complexes in the thylakoid membrane involved in the photosynthetic light reactions acetylated at several Lys residues. About 24 % of the proteins were acetylated on at least four Lys residues. In PSII overall, 56 KAc sites were found whereas the total number of KAc sites in the Cytb<sub>6</sub>f complex was seven. Strikingly, in the PSI complex there were 100 KAc sites found and in the plastidial ATP synthase, the last enzyme complex in the light reactions, 34 KAc sites could be detected. The light harvesting complexes of PSII and PSI are heavily acetylated in *Arabidopsis* with 45 KAc sites: 29 were found in the LHCs of PSII and 16 in the LHCs of PSI. All enzymes involved in the carbon fixing reactions, the Calvin-Benson Cycle, contain four or more acetylated Lys residues. In the plastidial GAPDH, which reduces 3-PGA to GAP with the help of NADPH, 20 KAc sites were found, and the TPI, the enzyme, which catalyses the following reaction in the Calvin-Benson Cycle, carried three KAc sites. All enzymes which are involved in the regeneration of the organic acceptor molecule for CO<sub>2</sub>, RuBP, were found acetylated, such as the aldolase with 13 KAc sites, the FBPase with two, and the TK with 18 sites. In the PGK and in the seduheptulose-1,7-bisphosphatase (SBPase) seven, in the phosphopentose isomerase four, and in the PRK six KAc sites were detected. The enzyme which carried most acetylation sites is RuBisCO with RBCL carrying 18 KAc sites. In RBCL the following Lys residues were found to be acetylated inter alia: K14, K21, K32, K146, K164, K175, K183, K201, K236, K252, K316, K334, K356, K450, K474. In the small subunit RBCS2B (At5g38420) five KAc sites appeared and in RBCS1A (At1g67090) eight, for example: K66, K83, K92, K126, K140, K146, K147. In all three isoforms of RCA in total 11 KAc sites were detected. Since the isoforms only differ in the length of the C-terminus, it was not possible to distinguish between them except for the Lys residues on the very C-terminus of one of the isoforms. The KAc sites which could not be referred to a special isoform are inter alia K204, K218, K221, K302, K317, K359, and K368. The Lys residue 438 was found to be acetylated in all three isoforms and in RCA2 acetylated K442 was additionally detected.

Mass spectrometry-based profiling of the proteome and K-acetylome was also performed in the unicellular green algae *Chlamydomonas reinhardtii* under varying growth conditions. *Chlamydomonas*

can grow either heterotrophically in acetate supplied medium in the dark, mixotrophically in acetate supplied medium and light, or photoautotrophically with light as the only energy source. Overall, 1376 KAc sites on 625 protein groups were identified. The KAc proteins belonged to the functional categories fatty acid and propanoate metabolism, pentose phosphate pathway, peroxisomal microbodies, photosynthesis, and antenna proteins. Using a binary comparison of the three growth conditions we found in each approach at least 250 quantified KAc sites. Proteins belonging to central metabolic pathways were significantly changed in their KAc status.

In both *Arabidopsis* and *Chlamydomonas* enzymes involved in photosynthesis were found to be heavily acetylated. The presence of KAc is not a proof of the regulatory function of KAc. Thus, variations in KAc under differing environmental conditions give a hint at the regulatory function of modification of Lys residues within a protein. In table 2 regulated KAc sites on proteins involved in photosynthesis which were found in *Chlamydomonas* and *Arabidopsis* are shown. Since these proteins were found in both organisms to be regulated in their KAc it is likely, that this PTM plays a pivotal role in the regulation of their activities.

Table 2: Regulated KAc sites on proteins involved in photosynthesis found in *Chlamydomonas* and *Arabidopsis* (data used from [195] (Publication [1]) and [106] (Publication [3]))

<u>Protein</u>	<u>KAc site in</u> <i>Arabidopsis</i>	<u>mean</u> <u>logFC</u>	<u>experiment</u>	<u>KAc site in</u> <i>Chlamydomonas</i>	<u>Corrected</u> <u>logFC</u>	<u>experiment</u>
RBCL	14	1.153	<i>hda14</i> LL	14	1.62	Mixo/Photo
RBCL	334	-2.816	<i>hda14</i>	450	-1.74; -1.90	Mixo/Photo; Hetero/Photo
RBCL	164	-4.666	<i>hda14</i> LL	175	1.61; 1.77; 3.26	Hetero/Mixo, Mixo/Photo; Hetero/Photo
RBCL	474	1.967	<i>hda14</i> LL			
FBA	377	-1.981	<i>hda14</i> LL	331	3.62	Hetero/Mixo
FBA	202	-1.438	<i>hda14</i> LL	246	-2.21; 5.44	Hetero/Mixo; Mixo/Photo
FBA				36	-3.16; 4.32	Hetero/Mixo; Mixo/Photo
ATPB	495	2.321; 3.524	<i>hda14</i> thyl.; <i>hda14</i> LL	225	-1.97; 3.90	Hetero/Mixo; Mixo/Photo
PSBR	79	2.331	<i>hda14</i> LL	38	3.02	Mixo/Photo



### **3.2 Lysine acetylation is a dynamic PTM in *Chlamydomonas reinhardtii***

The unicellular alga *Chlamydomonas reinhardtii* is an ideal model organism to study metabolic regulation by gene expression and by acetylation because it can adjust its metabolism to different energy sources. It can, unlike most higher plants and animals, not just use light or reduced carbon as energy source but grow photoautotrophic with light as energy source, use acetate as carbon source under heterotrophic conditions or it can grow mixotrophic by the usage of both sources [197]. The supplementation of the medium with acetate leads to increased acetyl-CoA levels since it is converted by acetate activating enzymes [198, 199]. At the start of this study, we speculated that the increased acetyl-CoA levels could likely have an effect on the acetylation state in the cell, in particular of the acetyl-CoA synthesizing enzymes ACS and the PDH, the ATP-citrate lyase (ACL), and the acetate kinase (AK) [172, 176, 181]. Hence, we performed a proteome wide acetylation study to determine differences in the acetylation state depending on the different growth conditions. As material, a *Chlamydomonas* preculture was inoculated and grown under mixotrophic conditions using medium light intensity (30  $\mu$ E). The derived main culture was washed with minimal medium and split into three parts so that the three resulting samples are derived from one preculture, to avoid changes due to differing cultures. To get photoautotroph growth the algae were transferred to minimal medium without acetate and grown under high light intensities, whereas for heterotrophic growth the culture grew on acetate containing medium in the dark and the mixotrophic samples were subjected to high light intensities and acetate medium.

Under hetero- and mixotrophic growth conditions acetate is entering the metabolism through the glyoxylate cycle in *Chlamydomonas* and thereby acetyl-CoA is converted and metabolised to citrate, isocitrate, glycolate, malate and finally to oxalacetate. These C2 compounds can be further metabolised to amino acids or soluble carbohydrates [200]. Five enzymes associated with the glyoxylate cycle are localised within the peroxisomal microbodies. It could be shown in other algae and in *Chlamydomonas* that the number of these organelles and the transcript levels of enzymes involved in the glyoxylate cycle increased with the acetate concentration in the medium [201, 202]. Furthermore, a regulation system of enzymes can be the usage of PTMs. We were able to show that KAc of enzymes involved in the glyoxylate cycle is depending on acetate and light, which is discussed in the next chapter.

The comparison of hetero- and mixotrophic growth conditions showed that 42 acK sites on 31 unique protein groups were significantly regulated. Peroxisomal proteins involved in the glyoxylate cycle, such as malate synthase and citrate synthase were found upregulated under heterotrophic conditions. Additionally, the peroxin 11A, the acetyl-synthase 3, and the multifunctional protein 2 which is

involved in fatty acid beta oxidation were increased in their acetylation level under the presence of acetate in the growth medium. Strikingly, some chloroplastic enzymes involved in the light reactions (AtpB and E, PsaB, PSAD, PSBO1, and LHCA1) were downregulated in acetylation under heterotrophic conditions while enzymes involved in the Calvin-Benson Cycle including RbcL K175 were highly upregulated, which indicates enzymatic regulation of the acetylation status also in *Chlamydomonas*. The changes in acetylation levels between hetero- and photoautotrophic conditions were similar but much more pronounced with a up to 16-fold increase in acetylation. Among the regulated enzymes, we found that K205 and K218 of the ACS were increased in their acetylation when the growth medium was supplied with acetate [195] (Publication [1]). It is known in several organisms that ACS is regulated by KAc [203-205]. Strikingly, K340 of the peroxisomal citrate synthase also showed an increase in acetylation with acetate in the growth medium which correlated with an increase in activity of the cellular citrate synthase. In *E.coli* it is known that acetylation of the citrate synthase II is regulating its activity [206]. Unfortunately, the corresponding K338 in *Chlamydomonas* citrate synthase was not detected in your experiments. Interestingly, also four KAc sites of malate synthase were strongly increased under heterotrophic compared to photoautotrophic conditions. It is already known in *Chlamydomonas* that acetate and light are the main regulatory effectors of malate synthase gene expression and thus PTMs like KAc could play an additional role to acclimate the metabolism to light and acetate availability through the regulation of malate synthase activity [207]. Another enzyme involved in the glyoxylate cycle is the isocitrate lyase (ICL2) which contains two regulated KAc sites (K295, K318). Strikingly, ICL and malate synthase are transcriptionally controlled in *Corynebacterium glutamicum* depending on the acetate concentration in the growth medium [208].

K516 of the phosphoenolpyruvate carboxykinase (A8J7NO) were also found to be increased in their acetylation level under heterotrophic growth conditions. This enzyme plays an important role in the gluconeogenesis pathway where it is converting oxaloacetate and ATP into phosphoenolpyruvate and carbon dioxide [209]. Strikingly, under heterotrophic and mixotrophic compared to photoautotrophic growth conditions, the acetyl-CoA synthesizing enzyme ACS3 (A8JFR9) was strongly increased in acetylation of the Lys residues 205 and 218. ACS converts acetate to acetyl-CoA and could thus be an ideal target for the activity regulation by acetylation (Figure 5) [181]. The malate synthase (Q6X898) which converts acetyl-CoA and glyoxylate into malate and CoA [210] showed a higher acetylation of K54 and K422 under heterotrophic growth conditions. One of the main outcomes of this study was that peroxisomal citrate synthase (A8J2S0) showed an increase in the acetylation of the Lys residues 99, 340, and 446 especially under heterotrophic conditions. Citrate synthase is converting oxaloacetate and acetyl-CoA to citrate and thus is essential for all eukaryotes [211]. Consequently, the acetylation state of the glyoxysomal citrate synthase increases with either acetate in the medium or the change

to a non-photosynthetic metabolism and this could play a regulatory role for the enzyme function. Strikingly, the enzyme activity correlated with the increase in acetylation under mixotrophic and heterotrophic growth conditions. Citrate synthase is the target of a variety of PTMs in different organisms. Not just in *E.coli* it is known that citrate synthase activity is regulated by KAc [206], but the mitochondrial citrate synthase was found to be redox-regulated in *Arabidopsis*. [42]. Interestingly, knockdown of the citrate synthase in *Caenorhabditis elegans* leads to a hyperacetylation of mitochondrial proteins and to an early embryonic arrest, which could be rescued by the prevention of hyperacetylation. Thus, it is feasible that citrate synthase of *Caenorhabditis elegans* acts as sink for elevated acetyl-CoA levels by metabolising it [212]. Furthermore, hypersuccinylation of Lys residues reduces enzymatic activity and suppresses colon cancer cell proliferation [213]. In human cells, citrate synthase was found to be methylated by a mitochondrial methyltransferase and thereby citrate synthase activity was inhibited [214].

In summary, the work in this thesis revealed that KAc in *Chlamydomonas* is dependent on the growth conditions, and that KAc of enzymes involved in glyoxysomal acetate metabolism increased when acetate was added to the medium under hetero- and mixotrophic growth conditions. In plastids, opposite changes in acetylation of proteins from the light and carbon reactions was observed upon addition of acetate. Hence, it is highly likely that the activities of the enzymes in these metabolic pathways are controlled by KAc, which could allow this unicellular alga to adjust its metabolism in dependence on light and acetate.

### **3.3 Lysine acetylation of enzymes involved in photosynthesis in *Arabidopsis thaliana***

#### **3.3.1 *Arabidopsis* KDACs have many non-histone substrate proteins**

KAc can be found on thousands of proteins in various organisms [104-114, 215, 216]. However, the sheer presence of an acetylation site does not indicate whether this site is regulated by modifying enzymes. The main aim of this work was to identify the proteins, which are dynamically regulated by K-acetylation to reveal novel mechanisms, which plants use to regulate their metabolism. Here we used, two histone deacetylase inhibitors, which led to an increase in K-acetylation of proteins, which are putative substrates of the *Arabidopsis* KDACs. One of the inhibitors we used was apicidin [cyclo(*N*-*O*-methyl-L-tryptophanyl-Lisoleucinyl-D-pipecolinyl-L2-amino-8-oxodecynoyl)], which is a class I-specific KDAC inhibitor. Apicidin is a fungal metabolite that exhibits antiprotozoal activity *in vitro* and was found to be active *in vivo* against malaria in mice [217]. The antiparasitic activity results from an inhibition of class I KDACs, which induces hyperacetylation of histones in treated parasites [217]. Upon treatment of *Arabidopsis* leaves with apicidin, 832 KAc sites could be quantified of which 182 were significantly up-regulated. The majority of the up-regulated sites were found on proteins which are

exclusively localized in the nucleus and three were found on plastidial proteins involved in photosynthesis (PSAH-1, PSAH-2) and the Calvin-Benson Cycle (SBPase). Another inhibitor we used was TSA, which is able to inhibit both class I and class II KDACs, by binding to the Zn<sup>2+</sup> ion in the active site [159]. TSA is a metabolite of *Streptomyces*, which inhibits specifically the cell growth and the cell cycle of normal rat fibroblasts by causing an accumulation of highly acetylated histones *in vivo* in extremely low concentrations [144]. The hyperacetylation of histones caused by TSA is due to the potent inhibition of class I and class II KDACs, and it could be shown that TSA had no effect on other enzyme activities such as kinases, phosphatases, DNA topoisomerases, and calmodulin *in vitro* [144]. In our study a total of 385 KAc sites could be quantified upon TSA treatment, of which 72 were up-regulated, and of which three were found on plastid localized proteins involved in photosynthesis (Defective accumulation of cytochrome B6/f complex (DAC, At3g17930), RCA β1-isoform, and PSAD1/2). Upon apicidin treatment, 77 potential new substrates of the RPD3-like KDACs were found up-regulated in *Arabidopsis* [106] (Publication [3]). In general, the effect of 5 μM TSA was much stronger than that of 5 μM apicidin, since the log<sub>2</sub>FC of the acetylation sites was much higher after TSA treatment. The up-regulated KAc sites upon TSA treatment were mostly found on nuclear proteins, which fits to the predicted localization of several class I KDACs. However, TSA also inhibits the class II KDACs, to which in *Arabidopsis* HDA5, 8, 14, and 15 belong to. The specific targets of this group were up-regulated after TSA treatment, but not after treatment with apicidin. Those included the RCA β1-isoform, DAC, and PSAD-2 [106] (Publication [3]). The comparison of both inhibitor treatments revealed an overlap of 25 protein groups and showed that most of the protein substrates of the RPD3/HDA1 family are localized in the nucleus, while some selected targets are localised in the plastids. Hence, our study revealed that both class I and class II KDACs of *Arabidopsis* possess many more target proteins other than histones. Furthermore, the class II KDACs HDA5, 14, and 15 could be detected in *Arabidopsis* leaves using a KDAC-trap [106] (Publication [3]). This indicates that these three KDACs are active in *Arabidopsis* leaves, and that at least one of them is active on plastid proteins.

### **3.3.2 KDACs are localized outside the nucleus and deacetylate non-histone proteins in *Arabidopsis***

Proteins from various subcellular localisations outside the nucleus are K-acetylated in plants [104-106, 158]. Hence, to reversibly regulate this PTM, KAc modifying enzymes are required in different organelles of the cell to fulfil their function. To reveal organellar KDACs, we performed a TargetP prediction [218] on all *Arabidopsis* KDACS and found that HDA14 (At4g33470) might localize in the chloroplast, and SRT2 (At5g09230) in the mitochondrion. König and coworkers [158] tagged SRT2 with a GFP at the C-terminus and verified the predicted mitochondrial localization in *Arabidopsis* protoplasts. SRT2 resides predominantly at the inner membrane of mitochondria and interacts there with several proteins involved in energy metabolism and metabolite transport. The ATP synthase and

the ADP/ATP carrier showed an increase in acetylation in the *srt2* mutant in *Arabidopsis* [158]. In another study, HDA5, HDA8, HDA15, and HDA18 showed a cytoplasmic localization when YFP was fused to the C-terminus of each protein of interest. HDA5 regulates flowering time in *Arabidopsis*. Hence, *hda5* mutants displayed a late flowering phenotype with an up-regulated expression of the flowering repressor genes *FLC* and *MAF1* [162]. Strikingly, HDA15 shuttles between the nucleus and the cytoplasm depending on the absence or presence of light [150]. In 2012, Alinsug and co-workers predicted HDA14 to be dual localized in the mitochondrion and the chloroplast in *Arabidopsis* [150]. Controversially at the same time HDA14 was found to localize in the nucleus and the cytosol in *Arabidopsis* [161]. However, in the latter work, HDA14 was N-terminally tagged with GFP and expressed in epidermal leaf cells of fava bean (*Vicia faba*). Hence, the N-terminal GFP tag masked the targeting peptide sequence for chloroplast import [219]. In that study, HDA14 was found to deacetylate and associate with  $\alpha/\beta$ -tubulin, by direct interaction with the phosphatase PP2A-A2 subunit [161]. It has been stated that the PTMs of tubulin, such as phosphorylation and acetylation and probably others, are important for the cargo transport and that the modifying enzymes PP2A and HDA14 play an important role [161]. In this thesis, this statement could not be proven but the dual localization prediction of HDA14 into mitochondria and chloroplasts could be confirmed. Here, HDA14 was C-terminally tagged with GFP and protoplasts of stable transformed overexpression lines were analysed using a confocal microscope. The dual chloroplast and mitochondrial localisation could be verified by Western blot analyses using isolated mitochondria and chloroplasts of *hda14* mutants and WT and an antibody against HDA14 [106] (Publication [3]). A putative role of HDA14 (At4g33470) in photosynthesis is further supported by gene expression data found in the Genevestigator tool, which provides full genome gene expression data based on various microarray studies ([https://genevestigator.com/gv/doc/intro\\_plant.jsz](https://genevestigator.com/gv/doc/intro_plant.jsz), [220]). The data from the Genevestigator database showed that *HDA14* is mainly expressed in the shoot apex and the cotyledon of seedlings and in the leaves and shoots of adult plants. In roots, calli and primary cells/cell culture there is almost no expression detectable

(Figure 10 and 11). Hence, *HDA14* is mainly expressed in green tissue and thus it could play an important role in the regulation of photosynthetic enzymes.

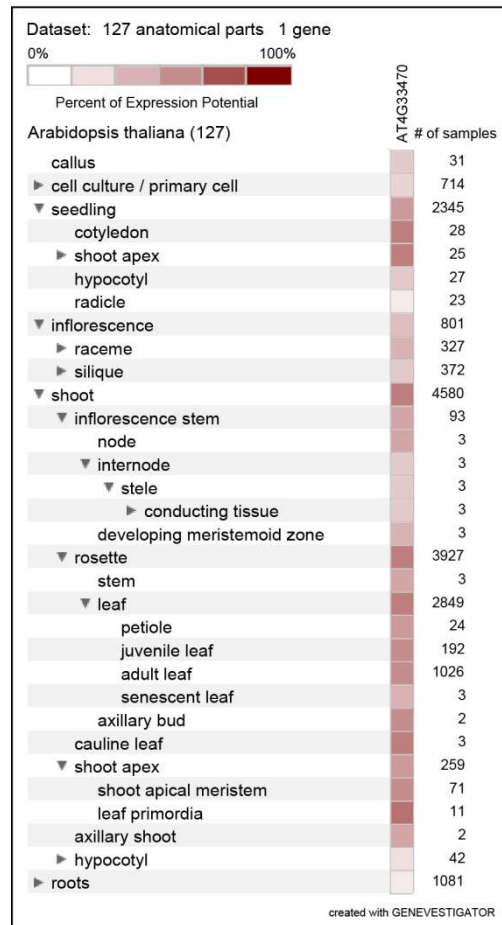


Figure 10: **Gene expression pattern of *HDA14* in different tissues of *Arabidopsis*.** The heat map shows  $\log_2$  expression values and was generated using Genevestigator [220].

In addition, *HDA14* is expressed throughout the whole life cycle of *Arabidopsis* (Figure 11).

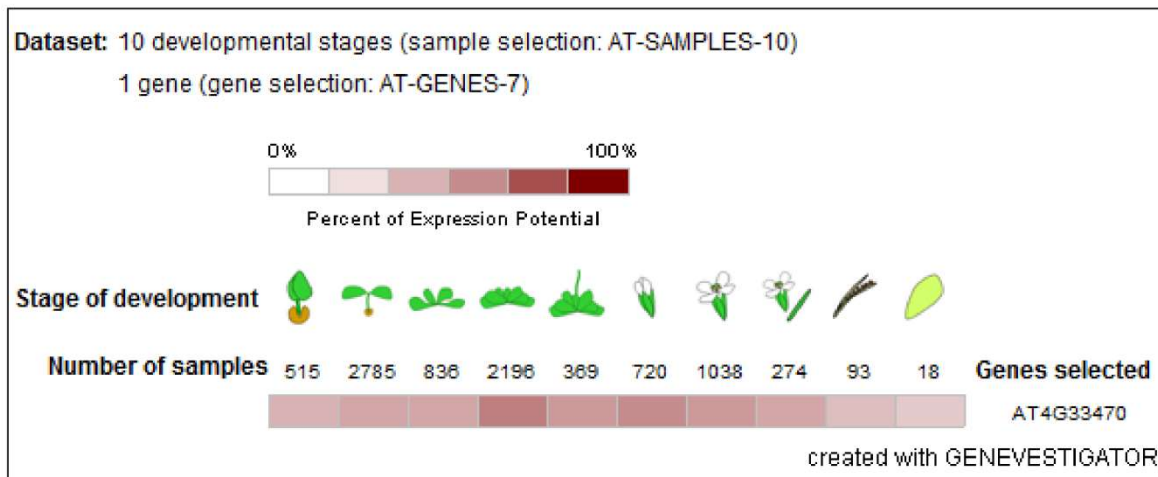


Figure 11: **Gene expression pattern of *HDA14* in different developmental stages of *Arabidopsis*.** The heat map shows  $\log_2$  expression values and was generated using Genevestigator [220]. Developmental stages (left to right): germinated seed - seedling - young rosette - developed rosette - bolting - young flower - developed flower - flowers and siliques - mature siliques – senescence.

At the start of this thesis, HDA14 was only predicted to have deacetylase activity since it contains a conserved histone deacetylase domain. Therefore, it had to be experimentally proven that HDA14 possesses deacetylase activity. The function of HDA14 was confirmed *in vitro* using a recombinant His-tagged HDA14 protein. For this purpose, a colorimetric assay was performed which is based on the deacetylation of a synthetic acetylated p53 peptide coupled to 5-amoni-2-nitro-benzonic acid a fluorophore. If the p53 peptide gets deacetylated it is accessible for trypsin digestion and the fluorophore is cleaved off and can be measured at 405 nm. Thus the increase in fluorescence is proportional to the deacetylase activity [221]. Using this assay, the deacetylase activity of HDA14 could be verified. Instead of  $Zn^{2+}$ , the cofactor  $Co^{2+}$  is used by some members of the RPD3-like superfamily, e.g. the human HDAC8 [222], which shares about 28 % protein sequence homology to HDA14. For HDA14 activity no differences could be determined between these cofactors indicating that both bivalent cations might be used *in vivo*. Additionally, the influence of TSA and apicidin on HDA14 deacetylase activity was tested, which are two known deacetylase inhibitors as described in the first experiment [144, 217]. Strikingly, TSA and apicidin both inhibited the activity of HDA14 to some extent. TSA inhibited HDA14 at a concentration of 5  $\mu M$  to a remaining activity of about 20 %. In contrast using 100  $\mu M$  apicidin about 80 % of the activity remained [106] (Publication [3]). To reveal the protein targets and function of HDA14, a *hda14* knockout (At4g33470.1, SALK\_097005C) plant line was used. The disruption of the gene by the T-DNA insertion was verified with PCR. In addition, the relative abundance of *HDA14* transcript was determined by RT-PCR analyses and indicated that only 10 % of a

truncated transcript was present in the *hda14* mutants line compared to WT Col-0. The absence of the HDA14 protein in the *hda14* mutant line was additionally verified by Western blot analyses.

To learn more about the possible function and the interaction partners of HDA14 in *Arabidopsis* proteome wide acetylation studies were performed. Therefore, the abundance of acetylated proteins was compared between *hda14* mutants and WT. Three experiments were performed: one under normal light conditions, one after low light treatment, and to get a better insight in the acetylation of photosynthetic membrane proteins enriched thylakoid fractions were used. Under normal light conditions, 832 KAc sites could be identified and quantified. Additionally, 425 KAc sites were identified from isolated thylakoids. Taken together, 137 sites on 122 protein groups were significantly increased in their acetylation state in the mutant. More than 90 % of these regulated sites were detected on plastid localized proteins, of which 24 % are predicted to be involved in photosynthesis.

### **3.3.3 Acetylome analyses revealed the plastidial substrate proteins of HDA14**

In all three experiments DAC (At3g17930) showed a highly up-regulated acetylation level in *hda14* mutants compared to WT with a  $\log_2FC$  of at least five. This highly significant up-regulation in the three independent experiments gives a strong hint that HDA14 is deacetylating DAC in *Arabidopsis in vivo*. DAC is a thylakoid membrane protein with two predicted transmembrane domains and is conserved from cyanobacteria to vascular plants [223]. The *dac* mutant shows a severe defect in the accumulation of the Cytb<sub>6</sub>f complex since the efficiency of the complex assembly is affected in the mutant. Yeast 2 hybrid screens revealed that DAC is specifically interacting with PetD which is a subunit of the Cytb<sub>6</sub>f complex [223]. Hence, DAC is no intrinsic component of the Cytb<sub>6</sub>f complex but a factor for stabilization/assembly of the complex probably through the interaction with PetD [223]. Cytb<sub>6</sub>f itself is a multiprotein complex in the thylakoid membrane which functions in the linear and the cyclic electron transport. The complex consists of at least eight subunit in higher plants: Cytf, Cytb<sub>6</sub> and PetC/D/M/L/G/N. [224]. During assembly Cytb<sub>6</sub> and PetD form a mildly protease resistant subcomplex which serves as a template for the assembly of Cytf and PetG forming a protease resistant cytochrome moiety [224]. PetC and PetL then participate in the assembly of the functional dimer [225]. PetD itself is more unstable if Cytb<sub>6</sub> is absent and the synthesis of Cytf is greatly reduced if Cytb<sub>6</sub> or PetD are inactivated. Hence, both are prerequisite for the synthesis of Cytf which is called CES mechanism [226]. DAC interacts with PetD during assembly and has thus a function in the assembly and stabilization of PetD. After assembly DAC is released from the cytochrome subcomplex. In the *dac* mutant a considerable amount of newly synthesized PetD, Cytf, Cytb<sub>6</sub> is degraded since they are not efficiently assembled. Hence, the *dac* mutant plants are unable to grow photoautotrophically and to produce fertile flowers [223]. It is likely that the acetylation and deacetylation of DAC has an impact on the

interaction with PetD since the positive charge of the Lys residue gets neutralized upon acetylation and thus changes the properties of the modified enzyme. The transmembrane domains are in between the amino acids 92-110 and 122-142. K165 lies outside these domains and is thus likely involved in protein-protein interactions. The acetylated residue is conserved in higher plants, mosses and algae and could be important for the functionality for the enzyme. Hence, it is likely that HDA14 affects the assembly of the Cytb<sub>6</sub>f complex by the deacetylation of DAC K165. However, *hda14* mutant has no strong growth phenotype compared to the *dac* mutant, which might indicate that the deacetylation of DAC could be compensated by another mechanism, such as increased protein turnover of DAC.

The water-cycle of chloroplasts is a significant source of ROS (reactive oxygen species) in light exposed green tissues. Through the photoreduction of molecular oxygen via PSI superoxide ( $O_2^-$ ) is produced and rapidly dismutated to  $H_2O_2$  [227]. There are two detoxification systems for  $H_2O_2$  in plants (i) the Ascorbate peroxidase (APX)-dependent ascorbate glutathione cycle [227] and (ii) the PRX-dependent (peroxiredoxins-dependent) scavenging system [228, 229]. Generally, APXs reduce  $H_2O_2$  to water, thereby playing an important role in the antioxidant system of plants. They are heme-binding enzymes which use ascorbate as electron donor for the reduction of  $H_2O_2$  [227]. Chloroplasts harbour three APXs: the stromal APX (sAPX, 33 kDa [kilo-Dalton]), the thylakoidal APX (tAPX, 38 kDa) and a putative luminal APX. sAPX shows a dual localization in mitochondria and chloroplasts. All three APXs are encoded by a single nuclear gene. tAPX is anchored in the thylakoid membrane via a C-terminal transmembrane domain and its catalytic site is facing the stroma [230]. This catalytic peroxidase domain is located between amino acids 78 and 344 [231]. In wheat the mutant (reduction of enzyme activity of about 40 %) showed lowered photosynthetic carbon assimilation and a reduced growth rate [232]. In *Arabidopsis*, WT, *tapx*, *sapx* and *tapx x sapx* mutants were germinated under photooxidative stress with the use of methyl viologen. This chemical component extracts electrons from PSI to produce  $O_2^-$  ( $H_2O_2$ ) in chloroplasts. WT and the *tapx* mutant showed a hindered greening of the seedlings, while the double mutant showed no greening at all. The *sapx* mutant had an intermediate phenotype and produced pale green seedlings [233]. The authors proposed a function in the oxidative stress tolerance of sAPX during the early greening phase of the seedling. In *Arabidopsis* and tobacco, tAPX overexpression lines were found to have an enhanced tolerance to methyl-viologen-induced photooxidative stress [234, 235]. In this thesis, the tAPX (At1g77490) was found to be significantly increased in its acetylation level in the *hda14* mutant at K362. It was found to be significantly increased by a  $\log_2FC$  of four to five in all three experiments. Furthermore, we found the overall APX activity slightly increased in *hda14* mutant plants (unpublished data, not shown). Although the regulated K362 lies outside the catalytic peroxidase domain it is likely that the acetylation state affects the activity of the enzyme since intermolecular interactions such as hydrogen bonds are affected by the

neutralization of the positive charge. Furthermore, K362 is conserved from mosses to higher plants, which gives a hint of the importance of the residue and the high functional relevance since it has not been exchanged during evolution.

The biosynthesis of fatty acids in plants starts with the formation of the direct substrate malonyl-CoA which is produced by the acetyl-CoA carboxylase [236, 237]. The second step is the fatty acid chain elongation which is catalysed by KasIII ( $\beta$ -ketoacyl-acyl carrier protein synthase III). It is a condensation reaction of the malonyl-acyl-carrier protein (ACP) and acetyl-ACP [238, 239]. The elongation of the carbon chain C4 to C18 is catalysed by the condensing enzymes KasI and KasII. While KasI has a high activity for the butyryl- to myristyl-ACP (C4:0-C14:0 ACP) as substrates to produce hexanoyl- to palmitoyl-ACP (C6:0-C16:0 ACP), KasII mainly uses palmitoyl-ACP as substrate to produce stearyl-ACP [240]. After the condensation reaction the 3-ketoacyl-ACP is reduced at the carbonyl-group by the 3-ketoacyl-ACP reductase, dehydrated by the hydroxyacyl-ACP dehydratase, and completed by enoyl-ACP reductase (ENR). ENR reduces the trans-2 double bond to form a saturated fatty acid [241]. In the acetylome of the *hda14* mutant, KasI (At5g46290) acetylation at K123 was significantly up-regulated and showed a log<sub>2</sub>FC of almost three under normal light conditions. The *kasI* mutant shows multiple morphological defects. It is chlorotic and has curly leaves and shows a reduced fertility, and semi dwarfism. The mesophyll cells in young rosettes contain one to five enlarged chloroplasts in their chlorotic sectors. This indicates a suppressed chloroplast division. The significant change in the polar lipid composition of *kasI* mutant plants leads to a suppressed expression of FtsZ and Min system genes and therefore to a disordered Z-ring placement of oversized chloroplasts and an inhibited polymerization of FtsZ protein at mid-site of the chloroplasts [242]. The mutants have a disrupted embryo development before the globular stage since they show a dramatic reduction of fatty acids (33.6 % of WT levels) in seeds. The authors propose that polar lipid supply is important for chloroplast division and development, since they constitute for the skeleton of the membrane system. *KASI* is expressed in seedlings, roots, flowers, young siliques and highly expressed in embryos at the cotyledon stage and in very young leaves. Its expression reduces along with the leaf development [242]. *HDA14* was found to be expressed in the shoot apex and the cotyledon of young seedlings, and in leaves and shoots of adult plants. It is mainly expressed in green tissue, but its expression declined during senescence. Hence, it seems that both *HDA14* and *KASI* are expressed in photosynthetic active tissues and therefore could interact with each other. Analyses of the fatty acid composition in WT and *hda14* mutant plants revealed that the content of  $\alpha$ -Linolic acid (C18:3 (9Z, 12Z, 15Z)) was significantly increased in the mutant plants. Therefore, the C16/C18 ratio was significantly decreased (unpublished data, not shown).

Similarly in *Arabidopsis kasl* mutant plants, the content of  $\alpha$ -Linolic acid was significantly increased in seeds compared to WT seeds. The same phenomenon was observed in rice *kasl* mutant plants where the  $\alpha$ -Linolic acid content was significantly higher in roots. In tobacco silencing of the two *KasI*-genes *KasI-1* and *-2* led to fewer chloroplasts and a significant decrease in chlorophyll a and b content. Furthermore, the overall fatty acid content decreased. Controversially, there was a significant increase in medium chain fatty acids (C10-C14) and a decrease in long chain fatty acids (C16-C18) found. Since in *Arabidopsis* and rice the knockout of *KasI* led to an increase in  $\alpha$ -Linolic acid it is likely that in *hda14* mutants *KasI* activity is decreased due to the increase in acetylation.

#### **3.3.4 HDA14 regulates Rubisco activase activity under low light conditions**

To get a better insight into the role of acetylation in the regulation of photosynthesis under low light conditions; i.e. when the Calvin-Benson Cycle gets partially inactivated [9, 243], proteome wide acetylation studies were performed with plants of WT and *hda14* mutants exposed to low light (20 $\mu$ E) for 2 hours. Compared to the WT, 36 KAc sites on 32 protein groups showed a significant increase under low light conditions without a change in protein abundance in the *hda14* mutant.

Under low light conditions, the AtRCA2 (At2g39730.2) acetylation level was significant up-regulated on two sites (K368 and K438). Hence, we can conclude that HDA14 is deacetylating RCA2 to adjust its activity to the light conditions. The hypothesis that HDA14 could interact with different proteins depending on the light conditions is supported by the finding that under low light conditions the targets of HDA14 seem to differ from those found under normal light conditions. Interestingly, K368 of RCA is located in the N-domain of the protein, which is believed to be important for the interaction of RCA and RuBisCO [25, 26, 244]. So far it is not known that the N-domain is involved in ATP hydrolysis. In another AAA+ protein, the N-ethyl maleimide sensitive factor, which is involved in the assembly and disassembly of membrane-associated proteins, the interaction with the target protein is conferred by the N-domain [245]. However, the N-domain of AAA+ ATPases is not well conserved and contains no typical motif and could therefore have different functions in the different AAA+ proteins of several species. The N-domain of RCA for example forms a loop with a little helical structure [25]. The Lys residue 368 of RCA is located in the Walker A motif. This domain is important for various properties of the enzyme such as nucleotide binding and hydrolysis, inter- and intramolecular interactions and movements since it forms a loop [130]. K438 is on the C-terminus of RCA. This region is the only one which differs between the three isoforms of *Arabidopsis*. The longest isoform AtRCA1 confers redox-regulation via two Cys residues in the C-terminus and has the longest C-terminus which is believed to result in an enhanced inhibition by ADP and less thermostability. AtRCA2 and AtRCA3 differ only in 5 amino acids in size, but the expression level of AtRCA2 is higher under normal conditions. However,

the expression of AtRCA3 increases upon heat stress and the C-terminus of the protein is therefore believed to be crucial for thermostability. The shorter it is the more thermostable RCA is believed to be [246]. In summary, the up-regulated K-acetylation sites are within delicate areas of RCA that are essential for the interaction with RuBisCO, confer ATP binding and, hydrolysis, and change the properties of the enzyme.

Strikingly, K438 of the RCA  $\beta$ -isoform was found to be significantly increased under low light conditions in the *hda14* mutants as well as after TSA treatment. Since HDA14 is specifically inhibited by TSA, it is likely that HDA14 is the only KDAC responsible for the deacetylation of this K438 *in vivo*. To gain insight on the impact of the acetylation of RCA K438, RuBisCO initial and total activity and its activation state was determined in whole leaf extracts [247] of low light treated WT and *hda14* mutant plants. The total activity of RuBisCO was increased by 30 %, while the initial activity was more than doubled in *hda14* mutants. This leads to a 90 % increased activation state (initial/total activity) of RuBisCO under low light conditions in *hda14* mutants. RCA is responsible for the reactivation of RuBisCO by the ATP-dependent induction of conformational changes to remove inhibitory sugar molecules from the active site. RCA itself inhibited by rising ADP levels in the low light [9, 248], hence it is likely that its change in acetylation state in *hda14* mutants alters the RuBisCO activity under low light conditions. To prove this hypothesis, site directed mutagenesis was performed on this site with an N-terminally His-tagged recombinant RCA- $\beta$ 1 (RCA2) protein. The K438 was either changed to glutamine (Q) to mimic the acetylated Lys residue and block acetylation or to Arg (R), which mimics the unmodified Lys due to its positive charge. ATPase activity measurements showed that K438Q behaved more like WT RCA, but the activity of K438R was strongly decreased. To mimic low light conditions, the ADP concentration was increased to an ADP/ATP ratio of 0.11. Strikingly, the K438R exchange showed a significantly higher downregulation of ATPase activity, while K438Q was less inhibited than the WT. Hence, we can conclude that acetylation decreased the ADP sensitivity of RCA2.

K438 of RCA in *Arabidopsis* is conserved in wheat (*Triticum aestivum*) TaRCA2- $\alpha$  as K428. It is already known that the CTE of the  $\alpha$ -isoform is modulated by Trx-f by the reduction of a disulfide bond in the CTE domain. In addition, the sensitivity towards ADP inhibition of RCA activity is also dependent on the CTE. In wheat, K428 was exchanged to R and Q to determine whether this Lys residue is influencing the ADP sensitivity [249]. A reduction in ADP inhibition was found in the K428R but this was not due to a change in ADP affinity, but ATP substrate affinity was significantly increased in the mutant. In the  $\beta$ -isoform of TaRca2 no changes in ATP affinity and ADP inhibitions were found in the R and Q variants of the corresponding Lys residue K432 [249]. Interestingly, the activity of TaRca2-  $\beta$  isoform was found to be unaffected by increasing ADP levels. Exchanges of two residues in the C-terminus of TaRca2- $\beta$  to the corresponding in TaRca1- $\beta$  (T358K & Q362E) resulted in an intermediate ADP inhibition sensitivity

between the isoforms, suggesting that these residues could be responsible for ADP inhibition [250]. In *Arabidopsis*, it is already known that the redox state of the CTE of the  $\alpha$ -isoform has an effect on the binding affinity to ATP. Thus, the binding of ATP in the nucleotide binding pocket is selectively impaired when the Cys residues in the CTE can form a disulfide bridge and when negatively charged residues are present in a sufficient number around the nucleotide binding pocket [248]. It is likely that the  $\alpha$ -isoform reacts different to the substitutions than the  $\beta$ -isoform. In future experiments, it has to be determined if a substitution of the K438 in the AtRCA1 isoform would lead to the same results as in wheat. All these results indicate that KAc has a regulatory function in RCA.

Since Calvin-Benson Cycle enzymes were differentially acetylated in *hda14* mutants, the effect of the acetylation level on RuBisCO and metabolites of this pathway was determined. RuBP, the organic acceptor molecule of atmospheric CO<sub>2</sub>, as well as Sedoheptulose-1,7-biphosphate (SBP) which is an intermediate of the regeneration process of RuBP, were significantly increased in abundance in *hda14* mutants (unpublished data, not shown). SBP is dephosphorylated by the SBPase to sedoheptulose-7-phosphate which is the first committed step of the regeneration of RuBP. Thus, the activity of SBPase controls RuBP regeneration [251]. It was shown that overexpressing the cyanobacterial FBP/SBPase in tobacco plants led to an increase in photosynthetic capacity, carbohydrates, and growth rate. The initial activity of RuBisCO was about 1.2 times higher in the *hda14* mutant plants compared to WT, which resulted in an increased activation state. Levels of RuBP were found to be 1.8 times increased in the mutants [252]. It is conceivable that the increased levels of RuBP result from a higher RCA activity since RCA binds exclusively inactive RuBisCO when the active site is occupied with RuBP [253]. When RCA is sufficiently active, the rate of carbamylated RuBisCO responses positively to increased concentration of RuBP. Thus, the carbamylation depends both on RuBP levels and RCA activity. The adaptation of RuBisCO activity follows the levels of RuBP [254]. It is possible that the elevated RuBP levels in *hda14* mutants are due to a metabolic adaptation to an increase in RCA and thus RuBisCO activity.

In the *hda14* mutant, KAc sites are not only regulated in RCA, but also in RuBisCO itself. The regulated KAc sites in RBCL are also in important areas within the enzyme. K14 on the N-terminus seems to be important since the removal resulted in a dramatic loss of RuBisCO activity in previous studies. Furthermore this site was also found to be trimethylated [77, 127]. The region between A9 and K14 seems to be important although it does not directly participate in catalysis but is believed to involve a catalytic-dependent conformational change. Hence, the N-Terminus is of interest because of its requirement for catalytic competence and because it contains several sites for PTMs [127]. K334 of the RBCL is in close proximity to the active site and its acetylation is significantly decreased three times ( $\log_2FC$ ) in *hda14* mutants under normal light conditions but there is no change in acetylation of K334

under low light conditions in *hda14* mutants. This Lys residue is within the C-Terminus of a large subunit (LSU), which forms three salt-bridges with the N-Terminus of another LSU and builds a dimer. Four of these dimers form the ring like structure of RuBisCO which is coated by two groups of four small subunits (L<sub>8</sub>S<sub>8</sub>) [126, 255]. However, the three salt-bridges are formed between E60, E109 and E110 of the N-domain of one LSU and R213, R253 and K334 of the C-domain of the other LSU. E60 is strictly conserved and builds the only deep buried ion-pair between two LSUs with K334 in the active site loop number 6 of the  $\alpha/\beta$ -barrel domain [126]. KAc of the K334 would prevent it from the formation of the salt-bridge since the positive charge gets neutralized upon acetylation and thus has a great impact on the activity of the holoenzyme since the properties change significantly. Furthermore, K334 is folded over and is an extension into the active site which interacts with gaseous substrates during catalysis [256]. KAc of K201, K252, K175, K177 and K334 was found to increase during dark treatment of *Arabidopsis* plants. Contrary, the RuBisCO activity declined with the increasing KAc level. Thus, KAc of K334 which is important for the proper closure of the active site could affect the catalytic properties of the enzyme [128]. In total we detected 10 KAc sites in RBCL under normal light conditions, and 13 KAc sites under low light conditions, which is consistent with the results of Gao and Co-workers [128]. Dark treatment of *Arabidopsis* plants increased KAc ratio of K201 [128]. We found no differences in KAc of K201 between WT and *hda14* mutants under normal light or low light conditions. We neither found K175 to be acetylated under normal light. Strikingly, K175 was found acetylated in low light treated plants independent of the genotype. In *Chlamydomonas* we found this highly conserved residue to be increased in acetylation in heterotrophic grown cells. It seems that KAc of K175 is crucial for the downregulation of RuBisCO activity as indicated by previous *in vitro* enzyme activity studies [104], and it should be further investigated if KAc is increasing under low light conditions in *Arabidopsis* WT and other species. Due to the set-up of the dimethyl-labelling experiment, a direct quantitative comparison between normal and low light conditions was not possible with our dataset, unfortunately. Still our results indicate that HDA14 plays a role in the acclimation of photosynthesis to different light conditions since RuBisCO activity is *inter alia* controlled by KAc.

Taken together, the chloroplast localized deacetylase HDA14 acts on several target enzymes of various functions in this organelle. It is likely that the deacetylation of photosynthetic enzymes by HDA14 is used by the plant to fine tune activity to differing light conditions when required. The regulation of the *in vivo* HDA14 activity needs to be investigated in more detail in future research. Currently, it is not clear why some targets only appear under low light conditions and some in all light conditions. The regulatory mechanism needs to be discovered, which enables HDA14 to select between its substrate proteins.

#### 4. Conclusion and Outlook

In summary, this work shows that KAc is found in many metabolic processes in the photosynthetic cell. Enzymes which are localized in the chloroplast were found to be heavily acetylated in *Arabidopsis* and *Chlamydomonas*. In the green alga KAc differed between growth conditions with either light or acetate as carbon source. In *Arabidopsis*, the deacetylase HDA14 was found to be localized in plastids and to regulate KAc in this organelle. Hence, KAc is not merely present in the plastid due to the presence of Acetyl-CoA in this organelle, but it is also used as a regulatory PTM in differing environmental conditions in both *Arabidopsis* and *Chlamydomonas*. KAc sites were detected on proteins acting in the photosynthetic light reactions and were found in *Arabidopsis* and *Chlamydomonas* (Figure 12). Several of the proteins were found to be acetylated in both species (green), but some of them were specific to either species (blue and orange). Although, in *Arabidopsis* more KAc sites involved in photosynthesis were found, it does not necessarily mean, that there are less acetylated proteins in *Chlamydomonas* since this difference could be due to the growth conditions and the higher number of acetylome studies in *Arabidopsis*.

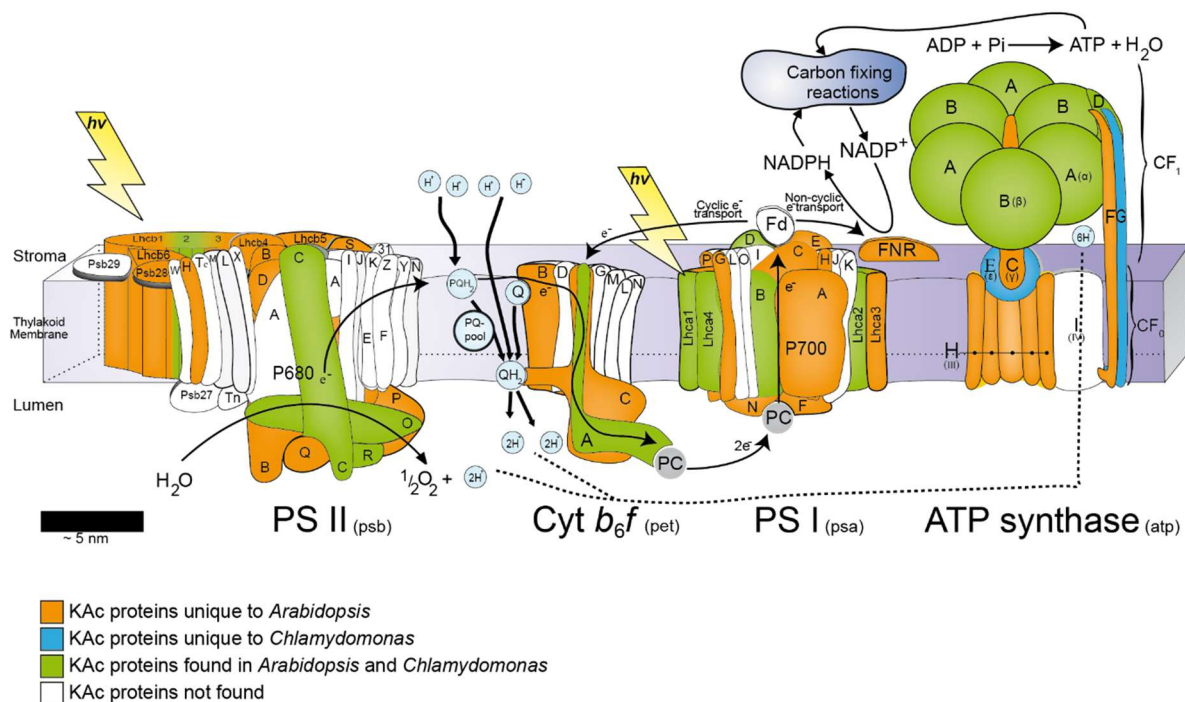


Figure 12: Lysine acetylation on photosynthetic protein complexes in *Chlamydomonas* and *Arabidopsis*. Proteins of *Chlamydomonas* were mapped to the corresponding *Arabidopsis* proteins. KAc proteins, which were found only in *Arabidopsis* [106] (Publication [3]) are highlighted in orange. Unique KAc proteins in *Chlamydomonas* [195] (Publication [1]) are depicted in blue and those sites, which were found in both organisms are marked in green. Proteins without any KAc sites or which were not identified at all are shown in white. Data based on [106] (Publication [3]) and [195] (Publication [1]). Genes were matched with the MapMan database [257].



was found to promote its stability by preventing the poly-ubiquitination. Furthermore, a broad range of HDACs were found to be phosphorylated but the exact regulation mechanism needs to be elucidated for each context since deacetylases act in a variety of cellular processes and each fulfils a very specialized function (reviewed in [260]).

In the soil-dwelling alga *Chlamydomonas*, enzymes regulating the acetate metabolism and photosynthesis were found to be differentially acetylated depending on the carbon source. It needs to be further investigated if KAc is fine-tuning enzyme activities in metabolic processes in *Chlamydomonas*. Therefore, detailed enzyme activity measurements of regulated enzymes need to be implemented in future studies. Since RuBisCO acetylation is conserved in rice, spinach, maize, and some cyanobacteria, it is likely that KAc of the large subunit is a regulation mechanism to acclimate carboxylase activity to differing light conditions [128]. After three hours exposure to the dark the KAc of the RBCL was increased compared to KAc of RBCL in the light in *Arabidopsis*. The carboxylase activity of RuBisCO purified from light treated plants was three-fold higher than that in the dark. This was not due to bound inhibitory phosphates, since they were removed during RuBisCO purification [128]. RuBisCO deacetylation was found to increase its relative activity [104]. K175 of RBCL is a catalytically active residue since it is a proton acceptor after enolization of RUBP and protonates the aci-carboxylate in the last step [31]. Hence, it is likely that KAc of RBCL K175 is used for the regulation of RuBisCO activity. In future studies RuBisCO total and initial activities should be measured using RuBisCO with acetylated K175 and unmodified K175. Since in *Chlamydomonas* the KAc of this residue is found highly upregulated under heterotrophic growth conditions when RuBisCO is mostly inactive, it is likely that the activity of the key enzyme of the Calvin-Benson Cycle is downregulated by KAc of K175 of the large subunit. In *Arabidopsis* K175 of RuBisCO was only found in low light-treated plants, hence it is likely that KAc of this residue is acting on the downregulation of enzyme activity. When plants were grown with a light intensity of  $80 \mu\text{E m}^{-2}\text{s}^{-1}$  K175 was also found to be acetylated in *Arabidopsis* [104]. The comparison on acetylation level of wild type *Arabidopsis* plants treated with normal, intermediate, and low light conditions could give answer to the rising question of the regulation of KAc of this important residue and the impact on enzyme activity. The same study should be carried out with *Chlamydomonas* to investigate if the regulation mechanism of RuBisCO is conserved.

Nevertheless, it is also important to find the KAc regulating enzymes in *Chlamydomonas*. Future studies should focus on the identification and characterization of KATs and KDACs with special emphasis on the chloroplast-localized enzymes. The *Chlamydomonas* genome contains 17 genes which are predicted KDACs. Three of those belong to the Sir2-type KDACs. HDA1-HDA14 are homologous to the *Arabidopsis* RPD3/HDA1 type ones [132, 148, 261]. Strikingly, in *Chlamydomonas* no member of the plant specific HD2-family was found [261]. TSA acts as a KDAC inhibitor and led to enhanced acetylation

of histone 3 after incubation of cells with TSA for 20 h [261]. It is feasible that in *Chlamydomonas* TSA treatment increases the acetylation of non-histone proteins and thus acetylome studies of treated cells could rise new knowledge on the substrate proteins of KDACs outside the nucleus in *Chlamydomonas*. A predicted deacetylase is Cre06.g290400 which shares almost 37% identity in its protein sequence with HDA14 of *Arabidopsis*. With a C-terminal GFP-tag localization studies could be carried out to investigate if this predicted KDAC is also localized in the plastids. Furthermore, a knockout mutant should be designed for the use in acetylome studies in comparison to wild type to reveal its substrate proteins.

Additionally, there are proteins related to human  $\alpha$ -tubulin acetyltransferase and N $\alpha$ -acetyltransferase found in *Chlamydomonas* [262]. These related proteins should be further characterized to gain insight into their function on substrate protein which could also be non-histone proteins. Besides the classical KATs, *Chlamydomonas* harbours an AK and a phosphotransacetylase (PTA) which together form a pathway for the generation of acetyl-CoA from acetate. If the acetyl-CoA rises *Chlamydomonas* could generate ATP from it using these enzymes [263]. Since high acetyl-CoA levels can lead to non-enzymatic acetylation at high pH, it is possible that KAc is indirectly controlled by AK and PTA activities [121, 263]. In addition, AK and PTA form the highly reactive intermediate acetyl-phosphate, which is known to increase KAc in *E.coli* drastically [264, 265]. Hence, KAc in *Chlamydomonas* could also be driven by via acetyl-phosphate, and it needs to be further investigated whether KAc of non-histone proteins is mediated chemically, enzymatically or if there is a combination of both, and why higher plant do not possess these enzymes.

## 5. References

1. **Calfapietra, C., Penuelas, J., and Niinemets, U.** *Urban plant physiology: adaptation-mitigation strategies under permanent stress.* Trends Plant Sci, 2015, **20**(2): p. 72-5.
2. **Hartl, M., and Finkemeier I.** *Plant mitochondrial retrograde signaling: post-translational modifications enter the stage.* Front Plant Sci, 2012, **3**: p. 253.
3. **Johnova, P., et al.** *Plant responses to ambient temperature fluctuations and water-limiting conditions: A proteome-wide perspective.* Biochim Biophys Acta, 2016, **1864**(8): p. 916-31.
4. **Deribe, Y.L., Pawson, T., and Dikic, I.** *Post-translational modifications in signal integration.* Nat Struct Mol Biol, 2010, **17**(6): p. 666-72.
5. **Wold, F.** *In vivo chemical modification of proteins (post-translational modification).* Annu Rev Biochem, 1981, **50**: p. 783-814.
6. **Nunes-Nesi, A., Fernie, A.R., and M. Stitt, M.** *Metabolic and signaling aspects underpinning the regulation of plant carbon nitrogen interactions.* Mol Plant, 2010, **3**(6): p. 973-96.
7. **Vernon, L.P., and Avron, M.** *Photosynthesis.* Annu Rev Biochem, 1965, **34**: p. 269-96.
8. **Henderson, J.N., et al.** *Biophysical characterization of higher plant Rubisco activase.* Biochim Biophys Acta, 2013, **1834**(1): p. 87-97.
9. **Carmo-Silva, A.E., and Salvucci, M.E.** *The regulatory properties of Rubisco activase differ among species and affect photosynthetic induction during light transitions.* Plant Physiol, 2013, **161**(4): p. 1645-55.
10. **Hauser, T., et al.** *Role of auxiliary proteins in Rubisco biogenesis and function.* Nat Plants, 2015, **1**: p. 15065.
11. **Salvucci, M.E., Portis, A.R., and Ogren, W.L.** *Light and CO<sub>2</sub> Response of Ribulose-1,5-Bisphosphate Carboxylase/Oxygenase Activation in Arabidopsis Leaves.* Plant Physiol, 1986, **80**(3): p. 655-9.
12. **Robinson, S.P., et al.** *Purification and assay of rubisco activase from leaves.* Plant Physiol, 1988, **88**(4): p. 1008-14.
13. **Schnyder, H., Mächler, F., and Nösberger, J.** *Influence of Temperature and O<sub>2</sub> concentration on Photosynthesis and Light Activation of Ribulose-1,5-Bisphosphate Carboxylase Oxygenase in Intact Leaves of White Clover (Trifolium repense L.).* Journal of Experimental Botany, 1984, **35**: p. 10.
14. **McCurry, S.D., and Tolbert, N.E.** *Inhibition of Ribulose-1,5-Bisphosphate Carboxylase/Oxygenase by Xylulose 1,5-Bisphosphate.* Journal of Biological Chemistry, 1977, **252**: p. 4.
15. **Kobza, J., and Seemann, J.R.** *Light-Dependent Kinetics of 2-Carboxyarabinitol 1-Phosphate Metabolism and Ribulose-1,5-Bisphosphate Carboxylase Activity in Vivo.* Plant Physiol, 1988, **89**: p. 6.
16. **Allen, J.F.** *Protein phosphorylation in regulation of photosynthesis.* Biochim Biophys Acta, 1992, **1098**(3): p. 275-335.
17. **Bellafore, S., et al.** *State transitions and light adaptation require chloroplast thylakoid protein kinase STN7.* Nature, 2005, **433**(7028): p. 892-5.
18. **Pesaresi, P., et al.** *Optimizing photosynthesis under fluctuating light: the role of the Arabidopsis STN7 kinase.* Plant Signal Behav, 2010, **5**(1): p. 21-5.
19. **Horton, P., and Lee, P.** *Stimulation of a cyclic electron-transfer pathway around photosystem II by phosphorylation of chloroplast thylakoid proteins.* FEBS Lett, 1983, **162**: p. 4.
20. **Nilsson, A., et al.** *Phosphorylation controls the three-dimensional structure of plant light harvesting complex II.* J Biol Chem, 1997, **272**(29): p. 18350-7.
21. **Dal Bosco, C., et al.** *Inactivation of the chloroplast ATP synthase gamma subunit results in high non-photochemical fluorescence quenching and altered nuclear gene expression in Arabidopsis thaliana.* J Biol Chem, 2004, **279**(2): p. 1060-9.
22. **Wang, L., et al.** *The Arabidopsis SAFEGUARD1 suppresses singlet oxygen-induced stress responses by protecting grana margins.* Proc Natl Acad Sci USA, 2020, **117**(12): p. 6918-6927.

23. **Kleine, T., and Leister, D.** *Retrograde signaling: Organelles go networking.* *Biochim Biophys Acta*, 2016, **1857**(8): p. 1313-1325.
24. **Hodges, M., et al.** *Protein phosphorylation and photorespiration.* *Plant Biol (Stuttg)*, 2013, **15**(4): p. 694-706.
25. **Boex-Fontvieille, E., et al.** *Phosphorylation pattern of Rubisco activase in Arabidopsis leaves.* *Plant Biol (Stuttg)*, 2014, **16**(3): p. 550-7.
26. **Salvucci, M.E., et al.** *Photoaffinity labeling of the ATP binding domain of Rubisco activase and a separate domain involved in the activation of ribulose-1,5-bisphosphate carboxylase/oxygenase.* *Biochemistry*, 1994, **33**(49): p. 14879-86.
27. **Kim, S.Y., et al.** *In vivo evidence for a regulatory role of phosphorylation of Arabidopsis Rubisco activase at the Thr78 site.* *Proc Natl Acad Sci USA*, 2019, **116**(37): p. 18723-18731.
28. **Zhang, N., et al.** *Light modulation of Rubisco in Arabidopsis requires a capacity for redox regulation of the larger Rubisco activase isoform.* *Proc Natl Acad Sci USA*, 2002, **99**(5): p. 3330-4.
29. **Houtz, R.L., and Portis, Jr. A.R.** *The life of ribulose 1,5-bisphosphate carboxylase/oxygenase--posttranslational facts and mysteries.* *Arch Biochem Biophys*, 2003, **414**(2): p. 150-8.
30. **Lorimer, G.H.** *Ribulosebiphosphate carboxylase: amino acid sequence of a peptide bearing the activator carbon dioxide.* *Biochemistry*, 1981, **20**(5): p. 1236-40.
31. **Cleland, W.W., et al.** *Mechanism of Rubisco: The Carbamate as General Base.* *Chem Rev*, 1998, **98**(2): p. 549-562.
32. **Balmer, Y., et al.** *Proteomics gives insight into the regulatory function of chloroplast thioredoxins.* *Proc Natl Acad Sci USA*, 2003, **100**(1): p. 370-5.
33. **Schurmann, P., and Buchanan, B.B.** *The ferredoxin/thioredoxin system of oxygenic photosynthesis.* *Antioxid Redox Signal*, 2008, **10**(7): p. 1235-74.
34. **Buchanan, B.B.** *The ferredoxin/thioredoxin system: a key element in the regulatory function of light in photosynthesis.* *Bioscience*, 1984, **34**(6): p. 378-83.
35. **Balmer, Y., et al.** *Thioredoxin target proteins in chloroplast thylakoid membranes.* *Antioxid Redox Signal*, 2006, **8**(9-10): p. 1829-34.
36. **Zhang, N., and Portis, A.R. Jr.** *Mechanism of light regulation of Rubisco: a specific role for the larger Rubisco activase isoform involving reductive activation by thioredoxin-f.* *Proc Natl Acad Sci USA*, 1999, **96**(16): p. 9438-43.
37. **Schurmann, P., and Jacquot, J.P.** *Plant Thioredoxin Systems Revisited.* *Annu Rev Plant Physiol Plant Mol Biol*, 2000, **51**: p. 371-400.
38. **McFarlane, C.R., et al.** *Structural basis of light-induced redox regulation in the Calvin-Benson cycle in cyanobacteria.* *Proc Natl Acad Sci USA*, 2019, **116**(42): p. 20984-20990.
39. **Yoshida, K., et al.** *Systematic exploration of thioredoxin target proteins in plant mitochondria.* *Plant Cell Physiol*, 2013, **54**(6): p. 875-92.
40. **Balmer, Y., et al.** *Thioredoxin links redox to the regulation of fundamental processes of plant mitochondria.* *Proc Natl Acad Sci USA*, 2004, **101**(8): p. 2642-7.
41. **Stevens F.J., et al.** *Identification of potential inter-domain disulfides in three higher plant mitochondrial citrate synthases: paradoxical differences in redox-sensitivity as compared with the animal enzyme.* *Photosynthesis Research*, 1997, **54**: p. 185-197.
42. **Schmidtman, E., et al.** *Redox regulation of Arabidopsis mitochondrial citrate synthase.* *Mol Plant*, 2014, **7**(1): p. 156-69.
43. **Daloso, D.M., et al.** *Thioredoxin, a master regulator of the tricarboxylic acid cycle in plant mitochondria.* *Proc Natl Acad Sci USA*, 2015, **112**(11): p. E1392-400.
44. **Nietzel, T., et al.** *Redox-mediated kick-start of mitochondrial energy metabolism drives resource-efficient seed germination.* *Proc Natl Acad Sci USA*, 2020, **117**(1): p. 741-751.
45. **Moller, I.M., et al.** *Matrix Redox Physiology Governs the Regulation of Plant Mitochondrial Metabolism through Posttranslational Protein Modifications.* *Plant Cell*, 2020, **32**(3): p. 573-594.

46. **Nietzel, T., et al.** *Redox regulation of mitochondrial proteins and proteomes by cysteine thiol switches.* Mitochondrion, 2017, **33**: p. 72-83.
47. **Kojer, K., et al.** *Kinetic control by limiting glutaredoxin amounts enables thiol oxidation in the reducing mitochondrial intermembrane space.* Mol Biol Cell, 2015, **26**(2): p. 195-204.
48. **Riemer, J., et al.** *Thiol switches in mitochondria: operation and physiological relevance.* Biol Chem, 2015, **396**(5): p. 465-82.
49. **Kojer, K., et al.** *Glutathione redox potential in the mitochondrial intermembrane space is linked to the cytosol and impacts the Mia40 redox state.* EMBO J, 2012, **31**(14): p. 3169-82.
50. **Buchanan, B.B. and Balmer, Y.** *Redox regulation: a broadening horizon.* Annu Rev Plant Biol, 2005, **56**: p. 187-220.
51. **Scheibe, R. and Dietz, K.J.** *Reduction-oxidation network for flexible adjustment of cellular metabolism in photoautotrophic cells.* Plant Cell Environ, 2012, **35**(2): p. 202-16.
52. **Dietz, K.J.** *Thiol-Based Peroxidases and Ascorbate Peroxidases: Why Plants Rely on Multiple Peroxidase Systems in the Photosynthesizing Chloroplast?* Mol Cells, 2016, **39**(1): p. 20-5.
53. **Vogelsang, L. and Dietz, K.J.** *Regulatory thiol oxidation in chloroplast metabolism, oxidative stress response and environmental signaling in plants.* Biochem J, 2020, **477**(10): p. 1865-1878.
54. **Corpas, F.J., et al.** *Protein tyrosine nitration: a new challenge in plants.* Plant Signal Behav, 2009, **4**(10): p. 920-3.
55. **Lozano-Juste, J., Colom-Moreno, R., and Leon, J.** *In vivo protein tyrosine nitration in Arabidopsis thaliana.* J Exp Bot, 2011, **62**(10): p. 3501-17.
56. **Lehtimäki, N., et al.** *Posttranslational modifications of FERREDOXIN-NADP+ OXIDOREDUCTASE in Arabidopsis chloroplasts.* Plant Physiol, 2014, **166**(4): p. 1764-76.
57. **Galetskiy, D., et al.** *Mass spectrometric characterization of photooxidative protein modifications in Arabidopsis thaliana thylakoid membranes.* Rapid Commun Mass Spectrom, 2011, **25**(1): p. 184-90.
58. **Chaki, M., et al.** *High temperature triggers the metabolism of S-nitrosothiols in sunflower mediating a process of nitrosative stress which provokes the inhibition of ferredoxin-NADP reductase by tyrosine nitration.* Plant Cell Environ, 2011, **34**(11): p. 1803-18.
59. **Holzmeister, C., et al.** *Differential inhibition of Arabidopsis superoxide dismutases by peroxy-nitrite-mediated tyrosine nitration.* J Exp Bot, 2015, **66**(3): p. 989-99.
60. **Galetskiy, D., et al.** *Phosphorylation and nitration levels of photosynthetic proteins are conversely regulated by light stress.* Plant Mol Biol, 2011, **77**(4-5): p. 461-73.
61. **Benhar, M., Forrester, M.T., and Stamler, J.S.** *Protein denitrosylation: enzymatic mechanisms and cellular functions.* Nat Rev Mol Cell Biol, 2009, **10**(10): p. 721-32.
62. **Lindermayr, C., Saalbach, G., and Durner, J.** *Proteomic identification of S-nitrosylated proteins in Arabidopsis.* Plant Physiol, 2005, **137**(3): p. 921-30.
63. **Hess, D.T., and Stamler, J.S.** *Regulation by S-nitrosylation of protein post-translational modification.* J Biol Chem, 2011, **287**(7): p. 4411-8.
64. **Apel, K., and Hirt, H.** *Reactive oxygen species: metabolism, oxidative stress, and signal transduction.* Annu Rev Plant Biol, 2004, **55**: p. 373-99.
65. **Asada, K.** *Production and scavenging of reactive oxygen species in chloroplasts and their functions.* Plant Physiol, 2006, **141**(2): p. 391-6.
66. **Ramel, F., et al.** *Light-induced acclimation of the Arabidopsis chlorina1 mutant to singlet oxygen.* Plant Cell, 2013, **25**(4): p. 1445-62.
67. **Ramel, F., Mialoundama, A.S., and Havaux, M.** *Nonenzymic carotenoid oxidation and photooxidative stress signalling in plants.* J Exp Bot, 2013, **64**(3): p. 799-805.
68. **Meskauskiene, R., et al.** *FLU: a negative regulator of chlorophyll biosynthesis in Arabidopsis thaliana.* Proc Natl Acad Sci USA, 2001, **98**(22): p. 12826-31.
69. **Kim, C., and Apel, K.** *Singlet oxygen-mediated signaling in plants: moving from flu to wild type reveals an increasing complexity.* Photosynth Res, 2013, **116**(2-3): p. 455-64.
70. **Havaux, M.** *Carotenoid oxidation products as stress signals in plants.* Plant J, 2014, **79**(4): p. 597-606.

71. **Lee, K.P., et al.** EXECUTER1- and EXECUTER2-dependent transfer of stress-related signals from the plastid to the nucleus of *Arabidopsis thaliana*. *Proc Natl Acad Sci USA*, 2007, **104**(24): p. 10270-5.
72. **Dogra, V., et al.** FtsH2-Dependent Proteolysis of EXECUTER1 Is Essential in Mediating Singlet Oxygen-Triggered Retrograde Signaling in *Arabidopsis thaliana*. *Front Plant Sci*, 2017, **8**: p. 1145.
73. **Dogra, V., et al.** Oxidative post-translational modification of EXECUTER1 is required for singlet oxygen sensing in plastids. *Nat Commun*, 2019, **10**(1): p. 2834.
74. **Schubert, H.L., Blumenthal, R.M., and Cheng, X.** Many paths to methyltransfer: a chronicle of convergence. *Trends Biochem Sci*, 2003, **28**(6): p. 329-35.
75. **Bedford, M.T., and Clarke, S.G.** Protein arginine methylation in mammals: who, what, and why. *Mol Cell*, 2009, **33**(1): p. 1-13.
76. **Rice, J.C., and Allis, C.D.** Histone methylation versus histone acetylation: new insights into epigenetic regulation. *Curr Opin Cell Biol*, 2001, **13**(3): p. 263-73.
77. **Houtz, R.L., et al.** Posttranslational modifications in the amino-terminal region of the large subunit of ribulose- 1,5-bisphosphate carboxylase/oxygenase from several plant species. *Plant Physiol*, 1992, **98**(3): p. 1170-4.
78. **Alban, C., et al.** Uncovering the protein lysine and arginine methylation network in *Arabidopsis chloroplasts*. *PLoS One*, 2014, **9**(4): p. e95512.
79. **Niemi, K.J., Adler, J., and Selman, B.R.** Protein methylation in pea chloroplasts. *Plant Physiol*, 1990, **93**(3): p. 1235-40.
80. **Lehtimäki, N., Koskela, M.M., and Mulo, P.** Posttranslational Modifications of Chloroplast Proteins: An Emerging Field. *Plant Physiol*, 2015, **168**(3): p. 768-75.
81. **Miura, K., Jin, J.B., and Hasegawa, P.M.** Sumoylation, a post-translational regulatory process in plants. *Curr Opin Plant Biol*, 2007, **10**(5): p. 495-502.
82. **Vierstra, R.D.** The expanding universe of ubiquitin and ubiquitin-like modifiers. *Plant Physiol*, 2012, **160**(1): p. 2-14.
83. **Rodriguez, M.S., Dargemont, C., and R.T. Hay, R.T.** SUMO-1 conjugation in vivo requires both a consensus modification motif and nuclear targeting. *J Biol Chem*, 2001, **276**(16): p. 12654-9.
84. **Villarejo, A., et al.** Evidence for a protein transported through the secretory pathway en route to the higher plant chloroplast. *Nat Cell Biol*, 2005, **7**(12): p. 1224-31.
85. **Kitajima, A., et al.** The rice alpha-amylase glycoprotein is targeted from the Golgi apparatus through the secretory pathway to the plastids. *Plant Cell*, 2009, **21**(9): p. 2844-58.
86. **Song, W., et al.** N-glycoproteomics in plants: perspectives and challenges. *J Proteomics*, 2011, **74**(8): p. 1463-74.
87. **Zielinska, D.F., et al.** Mapping N-glycosylation sites across seven evolutionarily distant species reveals a divergent substrate proteome despite a common core machinery. *Mol Cell*, 2012, **46**(4): p. 542-8.
88. **Buren, S., et al.** Importance of post-translational modifications for functionality of a chloroplast-localized carbonic anhydrase (CAH1) in *Arabidopsis thaliana*. *PLoS One*, 2011, **6**(6): p. e21021.
89. **Velasquez, M., et al.** Recent Advances on the Posttranslational Modifications of EXTs and Their Roles in Plant Cell Walls. *Front Plant Sci*, 2012, **3**: p. 93.
90. **Baerenfaller, K., et al.** Genome-scale proteomics reveals *Arabidopsis thaliana* gene models and proteome dynamics. *Science*, 2008, **320**(5878): p. 938-41.
91. **Bienvenut, W.V., et al.** Comparative large scale characterization of plant versus mammal proteins reveals similar and idiosyncratic N-alpha-acetylation features. *Mol Cell Proteomics*, 2012, **11**(6): p. M111 015131.
92. **Van Damme, P., Arnesen, T., and Gevaert, K.** Protein alpha-N-acetylation studied by N-terminomics. *FEBS J*, 2011, **278**(20): p. 3822-34.
93. **Pesaresi, P., et al.** Cytoplasmic N-terminal protein acetylation is required for efficient photosynthesis in *Arabidopsis*. *Plant Cell*, 2003, **15**(8): p. 1817-32.

94. **Armbruster, L., et al.** *NAA50 Is an Enzymatically Active N (alpha)-Acetyltransferase That Is Crucial for Development and Regulation of Stress Responses.* *Plant Physiol*, 2020, **183**(4): p. 1502-1516.
95. **Aksnes, H., Ree, R., and Arnesen, T.** *Co-translational, Post-translational, and Non-catalytic Roles of N-Terminal Acetyltransferases.* *Mol Cell*, 2019, **73**(6): p. 1097-1114.
96. **Weidenhausen, J., et al.** *Structural and functional characterization of the N-terminal acetyltransferase Naa50.* *Structure*, 2021, **29**(5): p. 413-425
97. **Bienvetut, W.V., et al.** *Dual lysine and N-terminal acetyltransferases reveal the complexity underpinning protein acetylation.* *Mol Syst Biol*, 2020, **16**(7): p. e9464.
98. **Gershey, E.L., Vidali, G., and Allfrey, V.G.** *Chemical studies of histone acetylation. The occurrence of epsilon-N-acetyllysine in the f2a1 histone.* *J Biol Chem*, 1968, **243**(19): p. 5018-22.
99. **Lusser, A., Kolle, D., and Loidl, P.** *Histone acetylation: lessons from the plant kingdom.* *Trends Plant Sci*, 2001, **6**(2): p. 59-65.
100. **Kurdistani, S.K., and Grunstein, M.** *Histone acetylation and deacetylation in yeast.* *Nat Rev Mol Cell Biol*, 2003, **4**(4): p. 276-84.
101. **Martin, C. and Zhang, Y.** *The diverse functions of histone lysine methylation.* *Nat Rev Mol Cell Biol*, 2005, **6**(11): p. 838-49.
102. **Allfrey, V.G., Faulkner, R., and Mirsky, A.E.** *Acetylation and Methylation of Histones and Their Possible Role in the Regulation of Rna Synthesis.* *Proc Natl Acad Sci USA*, 1964, **51**: p. 786-94.
103. **Raisner, R., et al.** *Enhancer Activity Requires CBP/P300 Bromodomain-Dependent Histone H3K27 Acetylation.* *Cell Rep*, 2018, **24**(7): p. 1722-1729.
104. **Finkemeier, I., et al.** *Proteins of diverse function and subcellular location are lysine acetylated in Arabidopsis.* *Plant Physiol*, 2011, **155**(4): p. 1779-90.
105. **Wu, X., et al.** *Lysine acetylation is a widespread protein modification for diverse proteins in Arabidopsis.* *Plant Physiol*, 2011, **155**(4): p. 1769-78.
106. **Hartl, M., et al.** *Lysine acetylome profiling uncovers novel histone deacetylase substrate proteins in Arabidopsis.* *Mol Syst Biol*, 2017, **13**(10): p. 949.
107. **Uhrig, R.G., et al.** *Diurnal changes in concerted plant protein phosphorylation and acetylation in Arabidopsis organs and seedlings.* *Plant J*, 2019, **99**(1): p. 176-194.
108. **Choudhary, C., et al.** *Lysine acetylation targets protein complexes and co-regulates major cellular functions.* *Science*, 2009, **325**(5942): p. 834-40.
109. **Henriksen, P., et al.** *Proteome-wide analysis of lysine acetylation suggests its broad regulatory scope in Saccharomyces cerevisiae.* *Mol Cell Proteomics*, 2012, **11**(11): p. 1510-22.
110. **Lundby, A., et al.** *Proteomic analysis of lysine acetylation sites in rat tissues reveals organ specificity and subcellular patterns.* *Cell Rep*, 2012, **2**(2): p. 419-31.
111. **Melo-Braga, M.N., et al.** *Modulation of protein phosphorylation, N-glycosylation and Lys-acetylation in grape (Vitis vinifera) mesocarp and exocarp owing to Lobesia botrana infection.* *Mol Cell Proteomics*, 2012, **11**(10): p. 945-56.
112. **Smith-Hammond, C.L., et al.** *Initial description of the developing soybean seed protein Lys-N(epsilon)-acetylome.* *J Proteomics*, 2014, **96**: p. 56-66.
113. **Weinert, B.T., et al.** *Proteome-wide mapping of the Drosophila acetylome demonstrates a high degree of conservation of lysine acetylation.* *Sci Signal*, 2011, **4**(183): p. ra48.
114. **Weinert, B.T., et al.** *Acetyl-phosphate is a critical determinant of lysine acetylation in E. coli.* *Mol Cell*, 2013, **51**(2): p. 265-72.
115. **Nallamilli, B.R., et al.** *Global Analysis of Lysine Acetylation suggests the Involvement of Protein Acetylation in Divers Biological Processes in Rice (Oryza sativa).* *Plos One*, 2014. **9**(2): p. 12.
116. **Yang, X.J., and Seto, E.** *The Rpd3/Hda1 family of lysine deacetylases: from bacteria and yeast to mice and men.* *Nat Rev Mol Cell Biol*, 2008, **9**(3): p. 206-18.
117. **Yang, X.J., and Seto, E.** *Lysine acetylation: codified crosstalk with other posttranslational modifications.* *Mol Cell*, 2008, **31**(4): p. 449-61.

118. **Matthias, P., Yoshida, M., and S. Khochbin, S.** *HDAC6 a new cellular stress surveillance factor.* Cell Cycle, 2008, **7**(1): p. 7-10.
119. **Xing, S., and Poirier, Y.** *The protein acetylome and the regulation of metabolism.* Trends Plant Sci, 2012, **17**(7): p. 423-30.
120. **Oliver, D.J., Nikolau, B.J., and Wurtele, E.S.** *Acetyl-CoA--Life at the metabolic nexus.* Plant Science, 2009, **176**: p. 5.
121. **Wagner, G.R., and Payne, R.M.** *Widespread and enzyme-independent Nepsilon-acetylation and Nepsilon-succinylation of proteins in the chemical conditions of the mitochondrial matrix.* J Biol Chem, 2013, **288**(40): p. 29036-45.
122. **König, A.C., et al.** *The mitochondrial lysine acetylome of Arabidopsis.* Mitochondrion, 2014, **19 Pt B**: p. 252-60.
123. **Hauser, M., et al.** *Stimulation by Light of Rapid pH Regulation in the Chloroplast Stroma in Vivo as Indicated by CO<sub>2</sub> Solubilization in Leaves.* Plant Physiol, 1995, **108**(3): p. 1059-1066.
124. **Koskela, M.M., et al.** *Chloroplast Acetyltransferase NSI Is Required for State Transitions in Arabidopsis thaliana.* Plant Cell, 2018, **30**(8): p. 1695-1709.
125. **Mo, R., et al.** *Acetylome analysis reveals the involvement of lysine acetylation in photosynthesis and carbon metabolism in the model cyanobacterium Synechocystis sp. PCC 6803.* J Proteome Res, 2015, **14**(2): p. 1275-86.
126. **Knight, S., Andersson, I., and Branden, C.I.** *Crystallographic analysis of ribulose 1,5-bisphosphate carboxylase from spinach at 2.4 Å resolution. Subunit interactions and active site.* J Mol Biol, 1990, **215**(1): p. 113-60.
127. **Houtz, R.L., et al.** *Post-translational modifications in the large subunit of ribulose bisphosphate carboxylase/oxygenase.* Proc Natl Acad Sci USA, 1989, **86**(6): p. 1855-9.
128. **Gao, X., et al.** *Downregulation of Rubisco Activity by Non-enzymatic Acetylation of RbcL.* Mol Plant, 2016, **9**(7): p. 1018-27.
129. **O'Leary, B.M., et al.** *Rubisco lysine acetylation occurs at very low stoichiometry in mature Arabidopsis leaves: implications for regulation of enzyme function.* Biochem J, 2020, **477**(19): p. 3885-3896.
130. **Hasse, D., Larsson, A.M., and Andersson, I.** *Structure of Arabidopsis thaliana Rubisco activase.* Acta Crystallogr D Biol Crystallogr, 2015, **71**(Pt 4): p. 800-8.
131. **Allis, C.D., et al.** *New nomenclature for chromatin-modifying enzymes.* Cell, 2007, **131**(4): p. 633-6.
132. **Pandey, R., et al.** *Analysis of histone acetyltransferase and histone deacetylase families of Arabidopsis thaliana suggests functional diversification of chromatin modification among multicellular eukaryotes.* Nucleic Acids Res, 2002, **30**(23): p. 5036-55.
133. **Earley, K.W., et al.** *In vitro specificities of Arabidopsis co-activator histone acetyltransferases: implications for histone hyperacetylation in gene activation.* Plant J, 2007, **52**(4): p. 615-26.
134. **Servet, C., Conde e Silva, N., and Zhou, D.X.** *Histone acetyltransferase AtGCN5/HAG1 is a versatile regulator of developmental and inducible gene expression in Arabidopsis.* Mol Plant, 2010, **3**(4): p. 670-7.
135. **Chen, Z.J., and Tian, L.** *Roles of dynamic and reversible histone acetylation in plant development and polyploidy.* Biochim Biophys Acta, 2007, **1769**(5-6): p. 295-307.
136. **Yuan, H., Marmorstein, R.** *Histone acetyltransferases: Rising ancient counterparts to protein kinases.* Biopolymers, 2013, **99**(2): p. 98-111.
137. **Bordoli, L., et al.** *Plant orthologs of p300/CBP: conservation of a core domain in metazoan p300/CBP acetyltransferase-related proteins.* Nucleic Acids Res, 2001. **29**(3): p. 589-97.
138. **Chen, W.Q., et al.** *One additional histone deacetylase and 2 histone acetyltransferases are involved in cellular patterning of Arabidopsis root epidermis.* Plant Signal Behav, 2016, **11**(2): p. e1131373.
139. **Neuwald, A.F., and Landsman, D.** *GCN5-related histone N-acetyltransferases belong to a diverse superfamily that includes the yeast SPT10 protein.* Trends Biochem Sci, 1997, **22**(5): p. 154-5.

140. **Glozak, M.A., et al.** *Acetylation and deacetylation of non-histone proteins.* Gene, 2005, **363**: p. 15-23.
141. **Gu, W. and Roeder, R.G.** *Activation of p53 sequence-specific DNA binding by acetylation of the p53 C-terminal domain.* Cell, 1997, **90**(4): p. 595-606.
142. **Stockinger, E.J., et al.** *Transcriptional adaptor and histone acetyltransferase proteins in Arabidopsis and their interactions with CBF1, a transcriptional activator involved in cold-regulated gene expression.* Nucleic Acids Res, 2001, **29**(7): p. 1524-33.
143. **Bhat, R.A., et al.** *Alteration of GCN5 levels in maize reveals dynamic responses to manipulating histone acetylation.* Plant J, 2003, **33**(3): p. 455-69.
144. **Yoshida, M., et al.** *Potent and specific inhibition of mammalian histone deacetylase both in vivo and in vitro by trichostatin A.* J Biol Chem, 1990, **265**(28): p. 17174-9.
145. **Vidal, M. and Gaber, R.F.** *RPD3 encodes a second factor required to achieve maximum positive and negative transcriptional states in Saccharomyces cerevisiae.* Mol Cell Biol, 1991, **11**(12): p. 6317-27.
146. **Gray, S.G., and Ekstrom, T.J.** *The human histone deacetylase family.* Exp Cell Res, 2001, **262**(2): p. 75-83.
147. **Alinsug, M.V., Yu, C.W., and Wu, K.** *Phylogenetic analysis, subcellular localization, and expression patterns of RPD3/HDA1 family histone deacetylases in plants.* BMC Plant Biol, 2009, **9**: p. 37.
148. **Chen, X., Ding, A.B. and Zhong, X.** *Functions and mechanisms of plant histone deacetylases.* Sci China Life Sci, 2020, **63**(2): p. 206-216.
149. **Ma, X., et al.** *Histone deacetylases and their functions in plants.* Plant Cell Rep, 2013, **32**(4): p. 465-78.
150. **Alinsug, M.V., et al.** *Subcellular localization of class II HDAs in Arabidopsis thaliana: nucleocytoplasmic shuttling of HDA15 is driven by light.* PLoS One, 2012, **7**(2): p. e30846.
151. **Earley, K., et al.** *Erasure of histone acetylation by Arabidopsis HDA6 mediates large-scale gene silencing in nucleolar dominance.* Genes Dev, 2006, **20**(10): p. 1283-93.
152. **Cigliano, R.A., et al.** *Histone deacetylase AtHDA7 is required for female gametophyte and embryo development in Arabidopsis.* Plant Physiol, 2013, **163**(1): p. 431-40.
153. **Yu, C.W., et al.** *HISTONE DEACETYLASE6 interacts with FLOWERING LOCUS D and regulates flowering in Arabidopsis.* Plant Physiol, 2011, **156**(1): p. 173-84.
154. **Liu, C., et al.** *HDA18 affects cell fate in Arabidopsis root epidermis via histone acetylation at four kinase genes.* Plant Cell, 2013, **25**(1): p. 257-69.
155. **Fong, P.M., Tian, L., and Chen, Z.J.** *Arabidopsis thaliana histone deacetylase 1 (AtHD1) is localized in euchromatic regions and demonstrates histone deacetylase activity in vitro.* Cell Res, 2006, **16**(5): p. 479-88.
156. **Zhou, C., et al.** *Expression and function of HD2-type histone deacetylases in Arabidopsis development.* Plant J, 2004, **38**(5): p. 715-24.
157. **Han, Z., et al.** *AtHD2D Gene Plays a Role in Plant Growth, Development, and Response to Abiotic Stresses in Arabidopsis thaliana.* Front Plant Sci, 2016, **7**: p. 310.
158. **König, A.C., et al.** *The Arabidopsis class II sirtuin is a lysine deacetylase and interacts with mitochondrial energy metabolism.* Plant Physiol, 2014, **164**(3): p. 1401-14.
159. **Hollender, C., and Liu, Z.** *Histone deacetylase genes in Arabidopsis development.* J Integr Plant Biol, 2008, **50**(7): p. 875-85.
160. **de Ruijter, A.J., et al.** *Histone deacetylases (HDACs): characterization of the classical HDAC family.* Biochem J, 2003, **370**(Pt 3): p. 737-49.
161. **Tran, H.T., et al.** *Arabidopsis thaliana histone deacetylase 14 (HDA14) is an alpha-tubulin deacetylase that associates with PP2A and enriches in the microtubule fraction with the putative histone acetyltransferase ELP3.* Plant J, 2012, **71**(2): p. 263-72.
162. **Luo, M., et al.** *Regulation of flowering time by the histone deacetylase HDA5 in Arabidopsis.* Plant J, 2015, **82**(6): p. 925-36.

163. **van Zanten, M., et al.** *HISTONE DEACETYLASE 9 represses seedling traits in Arabidopsis thaliana dry seeds.* Plant J, 2014, **80**(3): p. 475-88.
164. **Ueda, M., et al.** *The Distinct Roles of Class I and II RPD3-Like Histone Deacetylases in Salinity Stress Response.* Plant Physiol, 2017, **175**(4): p. 1760-1773.
165. **Lusser, A., et al.** *Identification of maize histone deacetylase HD2 as an acidic nucleolar phosphoprotein.* Science, 1997, **277**(5322): p. 88-91.
166. **Dangl, M., et al.** *Comparative analysis of HD2 type histone deacetylases in higher plants.* Planta, 2001, **213**(2): p. 280-5.
167. **Wu, K., et al.** *Functional analysis of HD2 histone deacetylase homologues in Arabidopsis thaliana.* Plant J, 2000, **22**(1): p. 19-27.
168. **Brosch, G., et al.** *An inhibitor-resistant histone deacetylase in the plant pathogenic fungus Cochliobolus carbonum.* Biochemistry, 2001, **40**(43): p. 12855-63.
169. **Frye, R.A.** *Phylogenetic classification of prokaryotic and eukaryotic Sir2-like proteins.* Biochem Biophys Res Commun, 2000, **273**(2): p. 793-8.
170. **Denu, J.M.** *The Sir 2 family of protein deacetylases.* Curr Opin Chem Biol, 2005, **9**(5): p. 431-40.
171. **Grubisha, O., Smith, B.C., and Denu, J.M.** *Small molecule regulation of Sir2 protein deacetylases.* FEBS J, 2005, **272**(18): p. 4607-16.
172. **Fatland, B.L., et al.** *Molecular characterization of a heteromeric ATP-citrate lyase that generates cytosolic acetyl-coenzyme A in Arabidopsis.* Plant Physiol, 2002, **130**(2): p. 740-56.
173. **Sato, R., et al.** *Transcriptional regulation of the ATP citrate-lyase gene by sterol regulatory element-binding proteins.* J Biol Chem, 2000, **275**(17): p. 12497-502.
174. **Fatland, B.L., Nikolau, B.J., and Wurtele, E.S.** *Reverse genetic characterization of cytosolic acetyl-CoA generation by ATP-citrate lyase in Arabidopsis.* Plant Cell, 2005, **17**(1): p. 182-203.
175. **Turner, J.E., et al.** *Characterization of Arabidopsis fluoroacetate-resistant mutants reveals the principal mechanism of acetate activation for entry into the glyoxylate cycle.* J Biol Chem, 2005, **280**(4): p. 2780-7.
176. **Mooney, B.P., Miernyk, J.A., and D.D. Randall, D.D.** *The complex fate of alpha-ketoacids.* Annu Rev Plant Biol, 2002, **53**: p. 357-75.
177. **Faure, M., et al.** *Interaction between the lipoamide-containing H-protein and the lipoamide dehydrogenase (L-protein) of the glycine decarboxylase multienzyme system 2. Crystal structures of H- and L-proteins.* Eur J Biochem, 2000, **267**(10): p. 2890-8.
178. **Camp, P.J., and Randall, D.D.** *Purification and Characterization of the Pea Chloroplast Pyruvate Dehydrogenase Complex : A Source of Acetyl-CoA and NADH for Fatty Acid Biosynthesis.* Plant Physiol, 1985, **77**(3): p. 571-7.
179. **DeBrosse, S., and Kerr, S.D.** *Pyruvate Dehydrogenase Complex Deficiency.* Mitochondrial case Studies, 2016.
180. **Behal, R.H., et al.** *Role of acetyl-coenzyme A synthetase in leaves of Arabidopsis thaliana.* Arch Biochem Biophys, 2002, **402**(2): p. 259-67.
181. **Lin, M., and Oliver, D.J.** *The role of acetyl-coenzyme a synthetase in Arabidopsis.* Plant Physiol, 2008, **147**(4): p. 1822-9.
182. **Gass, N., et al.** *Pyruvate decarboxylase provides growing pollen tubes with a competitive advantage in petunia.* Plant Cell, 2005, **17**(8): p. 2355-68.
183. **Wei, Y., et al.** *The roles of aldehyde dehydrogenases (ALDHs) in the PDH bypass of Arabidopsis.* BMC Biochem, 2009, **10**: p. 7.
184. **Shockey, J.M., Fulda, M.S., and Browse, J.** *Arabidopsis contains a large superfamily of acyl-activating enzymes. Phylogenetic and biochemical analysis reveals a new class of acyl-coenzyme a synthetases.* Plant Physiol, 2003, **132**(2): p. 1065-76.
185. **Fu, X., et al.** *Failure to Maintain Acetate Homeostasis by Acetate-Activating Enzymes Impacts Plant Development.* Plant Physiol, 2020, **182**(3): p. 1256-1271.
186. **Pagel, O., et al.** *Current strategies and findings in clinically relevant post-translational modification-specific proteomics.* Expert Rev Proteomics, 2015, **12**(3): p. 235-53.

187. **Thelen, J.J., and Miernyk, J.A.** *The proteomic future: where mass spectrometry should be taking us.* *Biochem J*, 2012, **444**(2): p. 169-81.
188. **Thelen, J.J., and Peck, S.C.** *Quantitative proteomics in plants: choices in abundance.* *Plant Cell*, 2007, **19**(11): p. 3339-46.
189. **Gruhler, A., et al.** *Stable isotope labeling of Arabidopsis thaliana cells and quantitative proteomics by mass spectrometry.* *Mol Cell Proteomics*, 2005, **4**(11): p. 1697-709.
190. **Whitelegge, J.P.** *Mass spectrometry for high throughput quantitative proteomics in plant research: lessons from thylakoid membranes.* *Plant Physiol Biochem*, 2004, **42**(12): p. 919-27.
191. **Boersema, P.J., et al.** *Multiplex peptide stable isotope dimethyl labeling for quantitative proteomics.* *Nat Protoc*, 2009, **4**(4): p. 484-94.
192. **Giese, J., Lassowskat, I., and Finkemeier, I.** *High-Resolution Lysine Acetylome Profiling by Offline Fractionation and Immunoprecipitation.* *Methods Mol Biol*, 2020, **2139**: p. 241-256.
193. **Di Palma, S., et al.** *Zwitterionic hydrophilic interaction liquid chromatography (ZIC-HILIC and ZIC-chILIC) provide high resolution separation and increase sensitivity in proteome analysis.* *Anal Chem*, 2011, **83**(9): p. 3440-7.
194. **Heazlewood, J.L., et al.** *SUBA: the Arabidopsis Subcellular Database.* *Nucleic Acids Res*, 2007, **35**(Database issue): p. D213-8.
195. **Füssl, M., et al.** *Dynamic light- and acetate-dependent regulation of the proteome and lysine acetylome of Chlamydomonas.* *Plant J*, 2022, **109**(1): p. 261-277.
196. **Mininno, M., et al.** *Characterization of chloroplastic fructose 1,6-bisphosphate aldolases as lysine-methylated proteins in plants.* *J Biol Chem*, 2012, **287**(25): p. 21034-44.
197. **Bohne, A.V., et al.** *Reciprocal regulation of protein synthesis and carbon metabolism for thylakoid membrane biogenesis.* *PLoS Biol*, 2013, **11**(2): p. e1001482.
198. **Chou, T.C., and Lipmann, F.** *Separation of acetyl transfer enzymes in pigeon liver extract.* *J Biol Chem*, 1952, **196**(1): p. 89-103.
199. **Beinert, H., et al.** *The acetate activating enzyme system of heart muscle.* *J Biol Chem*, 1953, **203**(1): p. 35-45.
200. **Lauersen, K.J., et al.** *Efficient phototrophic production of a high-value sesquiterpenoid from the eukaryotic microalga Chlamydomonas reinhardtii.* *Metab Eng*, 2016, **38**: p. 331-343.
201. **Graves, L.B., Jr., Hanzely, L., and, Trelease, R.N.** *The occurrence and fine structural characterization of microbodies in Euglena gracilis.* *Protoplasma*, 1971, **72**(2): p. 141-52.
202. **Hayashi, Y., et al.** *Increase in peroxisome number and the gene expression of putative glyoxysomal enzymes in Chlamydomonas cells supplemented with acetate.* *J Plant Res*, 2015, **128**(1): p. 177-85.
203. **Starai, V.J., et al.** *Sir2-dependent activation of acetyl-CoA synthetase by deacetylation of active lysine.* *Science*, 2002, **298**(5602): p. 2390-2.
204. **Gardner, J.G., et al.** *Control of acetyl-coenzyme A synthetase (AcsA) activity by acetylation/deacetylation without NAD(+) involvement in Bacillus subtilis.* *J Bacteriol*, 2006, **188**(15): p. 5460-8.
205. **Crosby, H.A., et al.** *Reversible N epsilon-lysine acetylation regulates the activity of acyl-CoA synthetases involved in anaerobic benzoate catabolism in Rhodospseudomonas palustris.* *Mol Microbiol*, 2010, **76**(4): p. 874-88.
206. **Venkat, S., et al.** *Characterizing lysine acetylation of Escherichia coli type II citrate synthase.* *FEBS J*, 2019, **286**(14): p. 2799-2808.
207. **Nogales, J., et al.** *Functional analysis and regulation of the malate synthase from Chlamydomonas reinhardtii.* *Planta*, 2004, **219**(2): p. 325-31.
208. **Wendisch, V.F., et al.** *Regulation of acetate metabolism in Corynebacterium glutamicum: transcriptional control of the isocitrate lyase and malate synthase genes.* *Arch Microbiol*, 1997, **168**(4): p. 262-9.
209. **Leegood, R.C., and Walker, R.P.** *Regulation and roles of phosphoenolpyruvate carboxykinase in plants.* *Arch Biochem Biophys*, 2003, **414**(2): p. 204-10.

210. **Eggerer, H., and Klette, A.** *On the catalysis principle of malate synthase.* Eur J Biochem, 1967, **1**(4): p. 447-75.
211. **Wiegand, G., and Remington, S.J.** *Citrate synthase: structure, control, and mechanism.* Annu Rev Biophys Biophys Chem, 1986, **15**: p. 97-117.
212. **Hada, K., et al.** *Tricarboxylic acid cycle activity suppresses acetylation of mitochondrial proteins during early embryonic development in *Caenorhabditis elegans*.* J Biol Chem, 2019, **294**(9): p. 3091-3099.
213. **Ren, M., et al.** *Citrate synthase desuccinylation by SIRT5 promotes colon cancer cell proliferation and migration.* Biol Chem, 2020, **401**(9): p. 1031-1039.
214. **Malecki, J., et al.** *Uncovering human METTL12 as a mitochondrial methyltransferase that modulates citrate synthase activity through metabolite-sensitive lysine methylation.* J Biol Chem, 2017, **292**(43): p. 17950-17962.
215. **Nallamilli, B.R., et al.** *Global analysis of lysine acetylation suggests the involvement of protein acetylation in diverse biological processes in rice (*Oryza sativa*).* PLoS One, 2014, **9**(2): p. e89283.
216. **Smith-Hammond, C.L., Hoyos, E., and Miernyk, J.A.** *The pea seedling mitochondrial Nepsilon-lysine acetylome.* Mitochondrion, 2014, **19 Pt B**: p. 154-65.
217. **Darkin-Rattray, S.J., et al.** *Apicidin: a novel antiprotozoal agent that inhibits parasite histone deacetylase.* Proc Natl Acad Sci USA, 1996, **93**(23): p. 13143-7.
218. **Emanuelsson, O., et al.** *Predicting subcellular localization of proteins based on their N-terminal amino acid sequence.* J Mol Biol, 2000, **300**(4): p. 1005-16.
219. **Soll, J., and Schleiff, E.** *Protein import into chloroplasts.* Nat Rev Mol Cell Biol, 2004. **5**(3): p. 198-208.
220. **Hruz, T., et al.** *Genevestigator v3: a reference expression database for the meta-analysis of transcriptomes.* Adv Bioinformatics, 2008, **2008**: p. 420747.
221. **Dose, A., et al.** *Facile synthesis of colorimetric histone deacetylase substrates.* Chem Commun (Camb), 2012, **48**(76): p. 9525-7.
222. **Dowling, D.P., et al.** *Structures of metal-substituted human histone deacetylase 8 provide mechanistic inferences on biological function.* Biochemistry, 2010, **49**(24): p. 5048-56.
223. **Xiao, J., et al.** *DAC is involved in the accumulation of the cytochrome b6/f complex in *Arabidopsis*.* Plant Physiol, 2012, **160**(4): p. 1911-22.
224. **Wollman, F.A.** *The structure, function and biogenesis of cytochrome b6f complexes.* Advanced Photosynthesis Research, 2004. **7**: p. 459-476.
225. **Schwenkert, S., et al.** *Role of the low-molecular-weight subunits PetL, PetG, and PetN in assembly, stability, and dimerization of the cytochrome b6f complex in tobacco.* Plant Physiol, 2007, **144**(4): p. 1924-35.
226. **Kuras, R., and Wollman, F.A.** *The assembly of cytochrome b6/f complexes: an approach using genetic transformation of the green alga *Chlamydomonas reinhardtii*.* EMBO J, 1994, **13**(5): p. 1019-27.
227. **Asada, K.** *THE WATER-WATER CYCLE IN CHLOROPLASTS: Scavenging of Active Oxygens and Dissipation of Excess Photons.* Annu Rev Plant Physiol Plant Mol Biol, 1999, **50**: p. 601-639.
228. **Dietz, K.J., et al.** *The function of peroxiredoxins in plant organelle redox metabolism.* J Exp Bot, 2006, **57**(8): p. 1697-709.
229. **Rouhier, N., and Jacquot, J.P.** *Plant peroxiredoxins: alternative hydroperoxide scavenging enzymes.* Photosynth Res, 2002, **74**(3): p. 259-68.
230. **Maruta, T., et al.** **Arabidopsis* chloroplastic ascorbate peroxidase isoenzymes play a dual role in photoprotection and gene regulation under photooxidative stress.* Plant Cell Physiol, 2010, **51**(2): p. 190-200.
231. **Marchler-Bauer, A., et al.** *CDD: NCBI's conserved domain database.* Nucleic Acids Res, 2015, **43**(Database issue): p. D222-6.
232. **Danna, C.H., et al.** *Thylakoid-bound ascorbate peroxidase mutant exhibits impaired electron transport and photosynthetic activity.* Plant Physiol, 2003, **132**(4): p. 2116-25.

233. **Kangasjarvi, S., et al.** *Diverse roles for chloroplast stromal and thylakoid-bound ascorbate peroxidases in plant stress responses.* Biochem J, 2008, **412**(2): p. 275-85.
234. **Yabuta, Y., et al.** *Thylakoid membrane-bound ascorbate peroxidase is a limiting factor of antioxidative systems under photo-oxidative stress.* Plant J, 2002, **32**(6): p. 915-25.
235. **Murgia, I., et al.** *Arabidopsis thaliana plants overexpressing thylakoidal ascorbate peroxidase show increased resistance to Paraquat-induced photooxidative stress and to nitric oxide-induced cell death.* Plant J, 2004, **38**(6): p. 940-53.
236. **Guchhait, R.B., et al.** *Acetyl coenzyme A carboxylase system of Escherichia coli. Purification and properties of the biotin carboxylase, carboxyltransferase, and carboxyl carrier protein components.* J Biol Chem, 1974, **249**(20): p. 6633-45.
237. **Gornicki, P., and Haselkorn, R.** *Wheat acetyl-CoA carboxylase.* Plant Mol Biol, 1993, **22**(3): p. 547-52.
238. **Jackowski, S., and Rock, C.O.** *Acetoacetyl-acyl carrier protein synthase, a potential regulator of fatty acid biosynthesis in bacteria.* J Biol Chem, 1987, **262**(16): p. 7927-31.
239. **Clough, R.C., et al.** *Purification and characterization of 3-ketoacyl-acyl carrier protein synthase III from spinach. A condensing enzyme utilizing acetyl-coenzyme A to initiate fatty acid synthesis.* J Biol Chem, 1992, **267**(29): p. 20992-8.
240. **Shimakata, T., and Stumpf, P.K.** *Isolation and function of spinach leaf beta-ketoacyl-[acyl-carrier-protein] synthases.* Proc Natl Acad Sci USA, 1982, **79**(19): p. 5808-12.
241. **Mou, Z., et al.** *Deficiency in fatty acid synthase leads to premature cell death and dramatic alterations in plant morphology.* Plant Cell, 2000, **12**(3): p. 405-18.
242. **Wu, G.Z., and Xue, H.W.** *Arabidopsis beta-ketoacyl-[acyl carrier protein] synthase i is crucial for fatty acid synthesis and plays a role in chloroplast division and embryo development.* Plant Cell, 2010, **22**(11): p. 3726-44.
243. **Buchanan, B.B.** *The carbon (formerly dark) reactions of photosynthesis.* Photosynth Res, 2016, **128**(2): p. 215-7.
244. **Stotz, M., et al.** *Structure of green-type Rubisco activase from tobacco.* Nat Struct Mol Biol, 2011, **18**(12): p. 1366-70.
245. **Ogura, T., and Wilkinson, A.J.** *AAA+ superfamily ATPases: common structure--diverse function.* Genes Cells, 2001, **6**(7): p. 575-97.
246. **DeRidder, B.P., et al.** *Changes at the 3'-untranslated region stabilize Rubisco activase transcript levels during heat stress in Arabidopsis.* Planta, 2012, **236**(2): p. 463-76.
247. **Carmo-Silva, A.E., and M.E. Salvucci, M.E.** *The temperature response of CO<sub>2</sub> assimilation, photochemical activities and Rubisco activation in Camelina sativa, a potential bioenergy crop with limited capacity for acclimation to heat stress.* Planta, 2012, **236**(5): p. 1433-45.
248. **Portis, A.R., Jr., et al.** *Regulation of Rubisco activase and its interaction with Rubisco.* J Exp Bot, 2008, **59**(7): p. 1597-604.
249. **Scafaro, A.P., et al.** *A single point mutation in the C-terminal extension of wheat Rubisco activase dramatically reduces ADP inhibition via enhanced ATP binding affinity.* J Biol Chem, 2019, **294**(47): p. 17931-17940.
250. **Perdomo, J.A., et al.** *Rubisco activation by wheat Rubisco activase isoform 2beta is insensitive to inhibition by ADP.* Biochem J, 2019, **476**(18): p. 2595-2606.
251. **Andralojc, P.J., et al.** *Increasing metabolic potential: C-fixation.* Essays Biochem, 2018, **62**(1): p. 109-118.
252. **Miyagawa, Y., Tamoi, M., and Shigeoka, S.** *Overexpression of a cyanobacterial fructose-1,6-/sedoheptulose-1,7-bisphosphatase in tobacco enhances photosynthesis and growth.* Nat Biotechnol, 2001, **19**(10): p. 965-9.
253. **Salvucci, M.E., and Ogren, W.L.** *The mechanism of Rubisco activase: Insights from studies of the properties and structure of the enzyme.* Photosynth Res, 1996, **47**(1): p. 1-11.

254. **Portis, A.R., Jr., Lilley, R.M., and Andrews, T.J.** *Subsaturating Ribulose-1,5-Bisphosphate Concentration Promotes Inactivation of Ribulose-1,5-Bisphosphate Carboxylase/Oxygenase (Rubisco) (Studies Using Continuous Substrate Addition in the Presence and Absence of Rubisco Activase)*. *Plant Physiol*, 1995, **109**(4): p. 1441-1451.
255. **van Lun, M., van der Spoel, D., and Andersson, I.** *Subunit interface dynamics in hexadecameric rubisco*. *J Mol Biol*, 2011, **411**(5): p. 1083-98.
256. **Andersson, I.** *Catalysis and regulation in Rubisco*. *J Exp Bot*, 2008, **59**(7): p. 1555-68.
257. **Thimm, O., et al.** *MAPMAN: a user-driven tool to display genomics data sets onto diagrams of metabolic pathways and other biological processes*. *Plant J*, 2004, **37**(6): p. 914-39.
258. **Willems, P., et al.** *The Plant PTM Viewer, a central resource for exploring plant protein modifications*. *Plant J*, 2019, **99**(4): p. 752-762.
259. **Okuda, K., Ito, A., and Uehara, T.** *Regulation of Histone Deacetylase 6 Activity via S-Nitrosylation*. *Biol Pharm Bull*, 2015, **38**(9): p. 1434-7.
260. **Bahl, S., and Seto, E.** *Regulation of histone deacetylase activities and functions by phosphorylation and its physiological relevance*. *Cell Mol Life Sci*, 2021, **78**(2): p. 427-445.
261. **Neupert, J., et al.** *An epigenetic gene silencing pathway selectively acting on transgenic DNA in the green alga Chlamydomonas*. *Nat Commun*, 2020, **11**(1): p. 6269.
262. **Gardiner, J.** *Posttranslational modification of plant microtubules*. *Plant Signal Behav*, 2019, **14**(10): p. e1654818.
263. **Ingram-Smith, C., Martin, S.R., and Smith, K.S.** *Acetate kinase: not just a bacterial enzyme*. *Trends Microbiol*, 2006, **14**(6): p. 249-53.
264. **Weinert, B.T., et al.** *Accurate Quantification of Site-specific Acetylation Stoichiometry Reveals the Impact of Sirtuin Deacetylase CobB on the E. coli Acetylome*. *Mol Cell Proteomics*, 2017, **16**(5): p. 759-769.
265. **Castano-Cerezo, S., et al.** *Protein acetylation affects acetate metabolism, motility and acid stress response in Escherichia coli*. *Mol Syst Biol*, 2014, **10**: p. 762.

**VII. Statutory declaration and statement (Eidesstattliche Versicherung und Erklärung)**

Vor- und Nachname	Magdalena Sophie Füßl
Geburtsdatum	06.07.1987
Geburtsort	München

Ich versichere hiemit an Eides statt, dass die eingereichte Dissertation von mir selbstständig und ohne unerlaubte Hilfe angefertigt wurde. Keine Anderen, als die angegeben Quellen und Hilfsmittel wurden von mir benutzt. Außerdem versichere ich, dass diese Dissertation nicht ganz und nicht in wesentlichen Teilen einer anderen Prüfungskommission als dieser vorgelegt worden ist. Ich habe mich nicht anderweitig einer Prüfung zur Erlangung eines Doktorgrades ohne Erfolg unterzogen und auch nicht ohne Erfolg versucht eine Dissertation einzureichen.

München, den 15.01.2023.....

Magdalena Füßl

## VIII. Acknowledgements

Ich möchte mich hiermit bei allen bedanken, die mich während der Zeit meiner Promotion auf meinem Weg begleitet und mich in meinen Vorhaben unterstützt haben.

Zuallererst möchte ich mich bei Hrn. Prof. Dr. Dario Leister für die Bereitschaft zur Betreuung meiner Promotionsarbeit und die freundliche Aufnahme in seine Arbeitsgruppe am Biozentrum in Martinsried herzlich bedanken.

Einen besonders großen Dank möchte ich Fr. Prof. Dr. Iris Finkemeier aussprechen für die tagtägliche Betreuung meines Promotionsprojektes aussprechen. Vielen Dank für die großartige Unterstützung und Hilfestellung, die ich während der gesamten Promotionszeit erfahren durfte. Vielen Dank auch für die Geduld, die mir entgegengebracht wurde und die Nachsicht über eine so lange Baby-Pause. Ich möchte mich außerdem bei Fr. Prof. Dr. Iris Finkemeier dafür bedanken, dass sie mir jegliche Art der wissenschaftlichen Weiterbildung ermöglicht hat und ich mich während der Promotion sehr weiterentwickeln konnte. Danke auch für die wundervolle Zeit in Köln und in Münster, in der ich sehr viel gelernt habe und meinen Horizont erweitern konnte.

Ein weiterer großer Dank gebührt Hrn. Dr. Markus Hartl für die lehrreiche Unterstützung und die nicht endende Geduld beim Beantworten aller Fragen und das Korrekturlesen meiner Arbeit. Ich möchte mich auch für die wissenschaftlichen Diskussionen, für das Praktikum in Wien und die außerordentlich gute Zusammenarbeit bedanken.

Des Weiteren danke ich Fr. Dr. Ann-Christine König für die tolle Freundschaft, die sehr gute Zusammenarbeit, das wundervolle Zusammenleben in Köln und die zahlreichen Diskussionen über HDAF und andere Themen.

Ich danke außerdem Hrn. Prof. em. Dr. Ulrich Koop für die Vorbereitung auf die Promotion während meiner Arbeit in seiner Gruppe, für die lehrreichen Jahre der Zusammenarbeit und die Unterstützung auch nach dieser.

I want to thank Michael E. Salvucci for the lab exchange in his group at the USDA. I learned a lot, not just about RuBisCO and its activase but also about Arizona. Thank you, Mike, for showing us all the awesome places, the great time in the US, and the good contact resulted from this time.

Bei allen Mitarbeitern der AG Finkemeier möchte ich mich auf diesem Wege für die gute Zusammenarbeit und die Unterstützung bedanken.

Auch meiner und Dominiks gesamten Familie danke ich für die Geduld, das Verständnis und die Unterstützung auf meinem Weg durch die Promotion.

Besonders bedanke ich mich bei meinem Mann Dominik Klaassen Federspiel für seine Geduld und seinen Glauben in mich und dafür, dass er mir die notwendige Unterstützung gab, die Dissertation schließlich fertig zu schreiben. Auch danke ich ihm, Merle und Jans dafür, mein Leben bereichert zu haben und mir so viel Liebe zu schenken.

## IX. Publications

- [1] **Füßl M\***, König AC\*, Eirich J, Hartl M, Kleinknecht L, Bohne AV, Harzen A, Kramer K, Leister D, Nickelsen J, Finkemeier I. Dynamic light- and acetate-dependent regulation of the proteome and lysine acetylome of *Chlamydomonas*. *The Plant Journal* 2022 (109, 261-277)
- [2] **Füßl M**, Lassowskat I, Née G, Koskela M, Brünje A, Tilak P, Giese J, Leister D, Mulo P, Schwarzer D, Finkemeier I. Beyond Histones: New Substrate Proteins of Lysine Deacetylases in *Arabidopsis* Nuclei. *Frontiers in Plant Science* 2018 (10;9:461)
- [3] Hartl M\*, **Füßl M\***, Boersema PJ, Jost JO, Kramer K, Bakirbas A, Sindlinger J, Plöchinger M, Leister D, Uhrig G, Moorhead GB, Cox J, Salvucci ME, Schwarzer D, Mann M, Finkemeier I. Lysine acetylome profiling uncovers novel histone deacetylase substrate proteins in *Arabidopsis*. *Molecular Systems Biology* 2017 (13:949)

\* These authors contributed equally to this work.

Publication 1

**Dynamic light- and acetate-dependent regulation of the proteome and lysine acetylome of *Chlamydomonas*.**

**Füßl M**, König AC, Eirich J, Kleinknecht L, Bohne AV, Harzen A, Kramer K, Leister D, Nickelsen J, Finkemeier I.

(2022)

*The Plant Journal* (109,261-277)

## RESOURCE

# Dynamic light- and acetate-dependent regulation of the proteome and lysine acetylome of *Chlamydomonas*

Magdalena Füßl<sup>1,2,3,†</sup>, Ann-Christine König<sup>1,2,4,†</sup>, Jürgen Eirich<sup>3</sup> , Markus Hartl<sup>1,2,5</sup> , Laura Kleinknecht<sup>2</sup>, Alexandra-Viola Bohne<sup>2</sup> , Anne Harzen<sup>1</sup>, Katharina Kramer<sup>1</sup>, Dario Leister<sup>2</sup> , Jörg Nickelsen<sup>2</sup>  and Iris Finkemeier<sup>1,2,3,\*</sup> 

<sup>1</sup>Plant Proteomics, Max Planck Institute for Plant Breeding Research, Carl von Linné Weg 10, Cologne DE-50829, Germany,

<sup>2</sup>Faculty of Biology, Ludwig-Maximilians-University, Grosshaderner Strasse 2-4, Munich DE-82152, Germany,

<sup>3</sup>Plant Physiology, Institute of Plant Biology and Biotechnology, University of Muenster, Schlossplatz 7, Muenster DE-48149, Germany,

<sup>4</sup>Helmholtz Zentrum München, German Research Center for Environmental Health, Research Unit Protein Science, Heidemannstr. 1, Munich DE-80939, Germany, and

<sup>5</sup>Mass Spectrometry Facility, Max Perutz Labs, University of Vienna, Vienna Biocenter (VBC), Dr. Bohr-Gasse 7, Vienna AT-1030, Austria

Received 26 July 2021; revised 19 October 2021; accepted 22 October 2021; published online 28 October 2021.

\*For correspondence (e-mail iris.finkemeier@uni-muenster.de).

†These authors contributed equally to this work.

## SUMMARY

The green alga *Chlamydomonas reinhardtii* is one of the most studied microorganisms in photosynthesis research and for biofuel production. A detailed understanding of the dynamic regulation of its carbon metabolism is therefore crucial for metabolic engineering. Post-translational modifications can act as molecular switches for the control of protein function. Acetylation of the  $\epsilon$ -amino group of lysine residues is a dynamic modification on proteins across organisms from all kingdoms. Here, we performed mass spectrometry-based profiling of proteome and lysine acetylome dynamics in *Chlamydomonas* under varying growth conditions. *Chlamydomonas* liquid cultures were transferred from mixotrophic (light and acetate as carbon source) to heterotrophic (dark and acetate) or photoautotrophic (light only) growth conditions for 30 h before harvest. In total, 5863 protein groups and 1376 lysine acetylation sites were identified with a false discovery rate of <1%. As a major result of this study, our data show that dynamic changes in the abundance of lysine acetylation on various enzymes involved in photosynthesis, fatty acid metabolism, and the glyoxylate cycle are dependent on acetate and light. Exemplary determination of acetylation site stoichiometries revealed particularly high occupancy levels on K175 of the large subunit of RuBisCO and K99 and K340 of peroxisomal citrate synthase under heterotrophic conditions. The lysine acetylation stoichiometries correlated with increased activities of cellular citrate synthase and the known inactivation of the Calvin–Benson cycle under heterotrophic conditions. In conclusion, the newly identified dynamic lysine acetylation sites may be of great value for genetic engineering of metabolic pathways in *Chlamydomonas*.

**Keywords:** *Chlamydomonas*, lysine acetylation, acetate, proteome, citrate synthase, glyoxylate cycle, RuBisCO.

## INTRODUCTION

The soil-dwelling green alga *Chlamydomonas reinhardtii* (hereafter *Chlamydomonas*) is one of the most studied microorganisms in photosynthesis research and for biofuel production, because of its ability to use different carbon sources for its growth (Leite et al., 2013; Merchant et al., 2012). *Chlamydomonas* can grow photoautotrophically with

just light as an energy source for carbon dioxide fixation, as well as heterotrophically with acetate as carbon source for respiration. In addition, *Chlamydomonas* is often grown in a mixture between both conditions (acetate and light), which is named mixotrophic growth (Hooper, 1989). Using chloroplast and nuclear genome engineering, enhancing *Chlamydomonas* characteristics for biofuel production has

been achieved over the last years (Scranton et al., 2015). Still there is a huge gap of knowledge about the underlying biochemistry and regulation of metabolic processes in *Chlamydomonas*. Hence, to further develop the usage of *Chlamydomonas* as an alternative source for biofuel production, the main challenge is to understand the regulatory mechanisms of its metabolic pathways. Metabolic flux balance analyses have revealed the different metabolic pathways that *Chlamydomonas* uses depending on different growth conditions (Boyle and Morgan, 2009). However, the underlying mechanisms which enable fast regulation of protein activity under variable growth conditions are still not fully uncovered. An acclimation to growth conditions can occur on several levels, which include transcriptional and translational control, as well as protein stability, product inhibition, and allosteric effects on enzyme activities (Erickson et al., 2015; Hooper, 1989; Ledford et al., 2007). The effects of acetate on photosynthesis, gene expression, and metabolite pools have already been largely established in *Chlamydomonas* and other green algae (Bogaert et al., 2019; Boyle and Morgan, 2009; Boyle et al., 2017; Hayashi et al., 2015; Lauersen et al., 2016; Rai et al., 2013; Roach et al., 2013; Smith et al., 2015). To utilize C<sub>2</sub> compounds, such as acetate, *Chlamydomonas* uses the glyoxylate cycle to form C<sub>4</sub> compounds, which can be further metabolized to amino acids or soluble carbohydrates (Lauersen et al., 2016). Five out of six enzymes associated with the glyoxylate cycle are localized in the peroxisomal microbodies. Peroxisomes in algae are referred to as peroxisomal microbodies since they contain fewer proteins than those in higher plants (Kato et al., 1997; Stabenau, 1974; Stabenau et al., 1993).

Another mechanism for a fast metabolic acclimation to acetate-containing medium might be mediated by post-translational protein modifications (PTMs) (Kaur et al., 2021). Such modifications can act as reversible molecular switches, which enable proteins to change their activities, functions, or even localizations in the cell (Castano-Cerezo et al., 2014; Jing et al., 2013). Nearly nothing is known about PTM-dependent regulation of metabolic pathways in *Chlamydomonas*. Next to protein phosphorylation, lysine acetylation (acK) is one of the most prominent PTMs and occurs on the ε-amino group of the lysine side chain. In eukaryotes, lysine acetylation was discovered in the context of histones and gene expression, where it is linked to transcriptional regulation by changing the interaction of transcription factors with the chromatin (Sterner and Berger, 2000). In *Chlamydomonas*, alpha-tubulin in axonemal microtubules was discovered as the first non-nuclear lysine-acetylated protein more than 30 years ago (L'Hernault and Rosenbaum, 1983, 1985). Lysine acetylation is nowadays known to occur in all kingdoms of life on proteins from various subcellular localizations, and is particularly important for the regulation of metabolism, as well as photosynthesis in plants (Finkemeier et al., 2011; Hartl et al., 2017; Hosp et al., 2017; Koskela et al., 2020; Liu et al., 2021; Narita

et al., 2019; Wu et al., 2011). Recently, it was shown that lysine acetylation is directly connected to acetate metabolism in *Escherichia coli* (Weinert et al., 2017). In bacteria and eukaryotes, acetate can be used for acetyl-CoA production by the enzyme acetyl-CoA synthetase (ACS). Acetyl-CoA is the substrate for enzymatic as well as non-enzymatic acetylation of the amino group of lysine residues (König et al., 2014; Wagner and Payne, 2013). Lysine acetylation was even found to regulate the activity of ACS in *Salmonella enterica* (Starai et al., 2002). In addition, bacteria as well as green algae can produce acetyl-CoA from acetate by the two enzymes acetate kinase and phosphotransacetylase, which form a highly reactive acetyl-phosphate intermediate able to trigger lysine acetylation. In *E. coli*, the addition of acetate to the growth medium caused a strong increase in protein acetylation in the absence of the protein lysine deacetylase cobB, and was dependent on acetyl phosphate availability (Castano-Cerezo et al., 2014; Weinert et al., 2017). To reveal whether protein acetylation is affected by the carbon source availability in *Chlamydomonas*, we investigated the proteome and lysine acetylome dynamics of *Chlamydomonas* grown under phototrophic, mixotrophic, and heterotrophic growth conditions by using a stable isotope dimethyl-labeling technique followed by quantitative liquid chromatography mass spectrometry (LC-MS) analyses.

## RESULTS

### Lysine acetylation dynamics in *Chlamydomonas* is dependent on light and acetate

In order to analyze the impact of different growth conditions on the lysine acetylation status of *Chlamydomonas* proteins, a pre-culture of CC-3491 cells was grown under mixotrophic conditions with a medium light intensity (30 μmol m<sup>-2</sup>sec<sup>-1</sup>). The cells were then washed with acetate-free medium and used to inoculate the main cultures, which were grown under either heterotrophic, photoautotrophic, or mixotrophic conditions for 30 h (Figure 1a). The light intensity of the photoautotrophic and mixotrophic growth conditions was increased to 100 μmol m<sup>-2</sup>sec<sup>-1</sup> to support photosynthesis (Gorman and Levine, 1965; Harris, 1989). After 30 h of growth under the respective condition, the cells were harvested by centrifugation, shock-frozen in liquid nitrogen, and stored at -80°C until further analysis. We selected a 30-h cultivation time, since there was a visible difference in the acetylation status of a putative histone protein band (below 29 kDa) detectable on the Western blot between the light- and dark-grown cultures (Figure 1b). In addition, a prominent band between 45 and 66 kDa was visible, especially under heterotrophic conditions. This band most likely represents the large subunit (RbcL) of ribulose-1,5-bisphosphate carboxylase/oxygenase (RuBisCO), since it has previously been shown that RbcL is highly acetylated in Arabidopsis, especially during the night (Finkemeier et al., 2011; Gao et al., 2016).

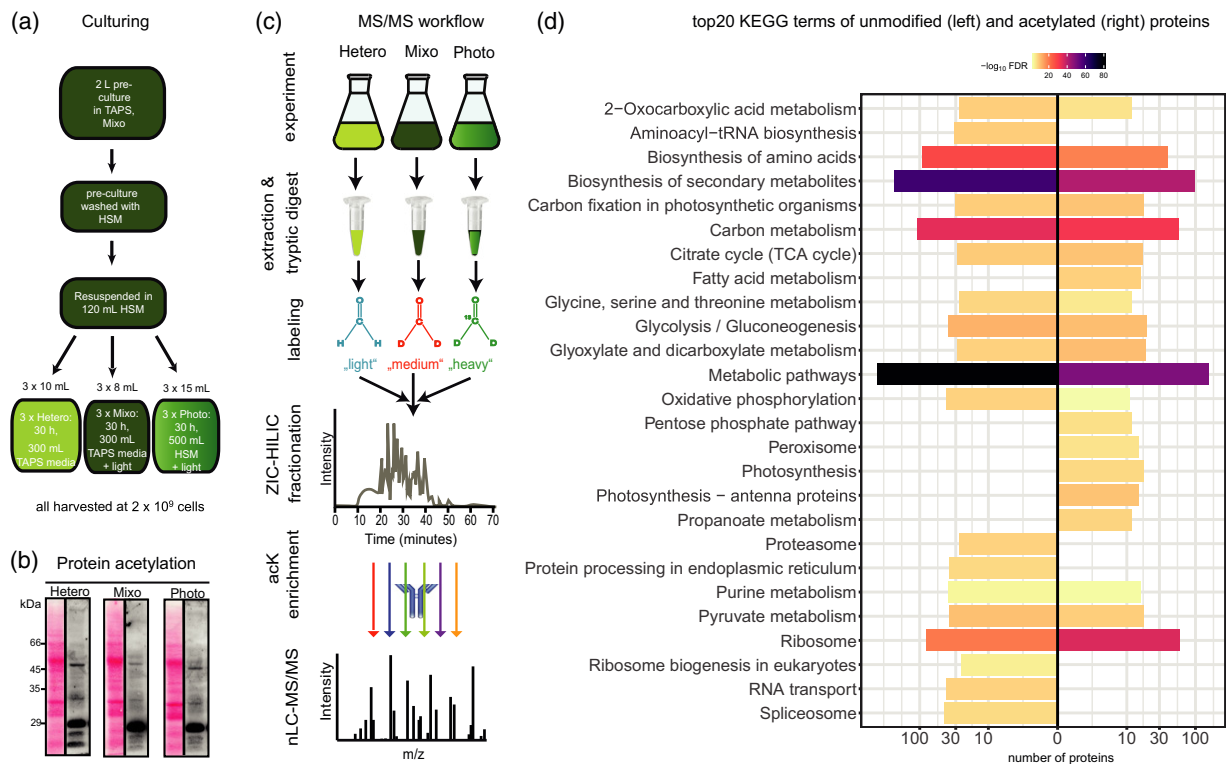


**Figure 1.** General overview of the experimental setup and proteomic analyses of *Chlamydomonas* cells from different growth conditions. (a) Culturing conditions. A common pre-culture was split into three specific growth conditions (hetero-, mixo-, and autotrophic, experiments performed in three biological replicates). Initial cell density was adjusted to compensate for different growth under the respective conditions and yield  $2 \times 10^9$  cells at harvest. (b) Anti-acK Western blot of *Chlamydomonas* cell extracts (the Ponceau S stain is presented next to the blots as loading control). (c) LC-MS/MS workflow. After harvest, proteins were digested and isotopically labeled. Pooled peptide samples were pre-fractionated, enriched by immunoprecipitation of acK peptides, and analyzed by LC-MS/MS in addition to full proteome samples (in biological triplicates). (d) Overview of the top 20 KEGG pathways containing unmodified proteins identified in total extracts (bars to the left) and with an acK site (bars to the right). No bar is shown when the respective KEGG term was not among the top 20 terms ranked according to protein number per term and protein condition.  $-\log_{10}(\text{FDR})$  from the functional enrichment analysis via StringDB are used as fill color.

### Mass spectrometry-based profiling of the *Chlamydomonas* proteome and acetylome

The variety of lysine-acetylated proteins detected on the Western blot prompted us to quantify total proteome and acetylome changes under the different growth conditions in a large-scale MS-based shotgun proteomic approach combined with a stable isotope dimethyl-labeling strategy (Lassowskat et al., 2017). An overview of the MS-based workflow is shown in Figure 1(c). Samples from the three different growth conditions were analyzed in three biological replicates. Proteins from each replicate were extracted and digested with trypsin, and free amino groups of peptides were labeled with light, medium, and heavy stable isotope dimethyl forms, respectively. To prevent any labeling bias, a swap of the light, medium, and heavy dimethyl labels was performed on the third replicate. Equal amounts of the labeled peptides from the three growth conditions were combined and subjected to ZIC-HILIC fractionation to reduce the sample complexity (Giese et al., 2020). After fractionation, the samples were

enriched for lysine-acetylated peptides by immunoaffinity purification. All fractions were analyzed on a Q-Exactive Plus (Thermo Fisher Scientific, Bremen, Germany) mass spectrometer and proteins and acetylation sites were identified and quantified using MaxQuant (Tyanova et al., 2016). In total, more than 5000 protein groups were identified with a protein false discovery rate (FDR) of  $<1\%$ . The detected proteins have various functions in a broad variety of metabolic pathways according to the top 20 KEGG terms (Figure 1d, left). In addition, we identified almost 1400 lysine acetylation sites (acK sites) in total. Out of the top 20 KEGG terms, fatty acid and propanoate metabolism, the pentose phosphate pathway, peroxisomal microbodies, photosynthesis, and antenna proteins are exclusively enriched as functional terms within the acetylated proteins (Figure 1d, right).

### Proteome changes depending on light and acetate

We first evaluated the protein abundance changes depending on the different growth conditions in a pairwise manner. For each condition, more than 4700 protein groups

were quantified in at least two replicates (Table S1). The different growth conditions affected the abundance of up to 30% of the protein groups in between treatments (regulated with a  $p$ -value of  $<0.05$ , Table 1, Figure 2a). The protein groups with an absolute value for the  $\log_2(\text{fold change [FC]})$  of  $\geq 1$  and a corresponding  $p$ -value of  $<0.05$ , quantified in at least two replicates by their respective dimethyl ratios, were analyzed using StringDB for functional enrichment (Figure 2b,c).

In the comparison of heterotrophic to mixotrophic conditions (Figure 2b, left column), mainly proteins involved in photosynthesis are downregulated, while (motor) proteins associated with cell projection located in cilia and flagella are upregulated under heterotrophic conditions. A similar picture emerged when comparing the heterotrophic to photoautotrophic growth conditions (Figure 2b, middle column).

In the comparison of mixo- and phototrophic conditions (Figure 2b, right column), the StringDB analysis indicates that the photosynthetic machinery seems to vary to a lesser extent between those two states than in the comparisons of heterotrophic conditions to either one of them. It is mainly ribosomal proteins that are more strongly

expressed under (purely) phototrophic conditions, whereas proteins associated with oxidative phosphorylation are upregulated under mixotrophic conditions accounting for the adaptations specific to these conditions (Figure 2b, right column).

Due to our experimental setup, we are not only able to make binary comparisons as just described, but also to evaluate protein changes that are specific to overlapping features, namely light and dark acclimation or  $\text{CO}_2$  and acetate as carbon sources (Figure 2c). We first turned to proteins specific for the comparison of growth in the dark and the light by comparing the heterotrophically grown cells to those grown under the two other conditions. Acclimation to growth in the light (Figure 2c, top left) is accompanied by upregulation of proteins associated with photosynthesis, while in the dark, proteins associated with fatty acid degradation, peroxisomal microbodies, and the TCA cycle are higher in abundance. Pherophorins are upregulated (Figure 2c, bottom right), indicating a switch to sexual reproduction, which is typical for algae when grown under unfavorable conditions (Hallmann, 2011).

When comparing the phototrophic state to the two other growth conditions, one can gain insights into the proteome adjustments under fully autotrophic conditions compared to acclimation to an external carbon source. Acclimation to growth in the absence of an organic carbon source (Figure 2c, top right) is accompanied by upregulation of proteins associated with photosynthesis, including clusters that are associated with carbonic anhydrase, which is important to provide adequate  $\text{CO}_2$  supply for photosynthesis (Tirumani et al., 2014; Ynalvez et al., 2008). In the presence of acetate as an external carbon source in the growth medium, proteins associated with the degradation of fatty acids and other organic compounds are significantly enriched (Figure 2c, bottom left).

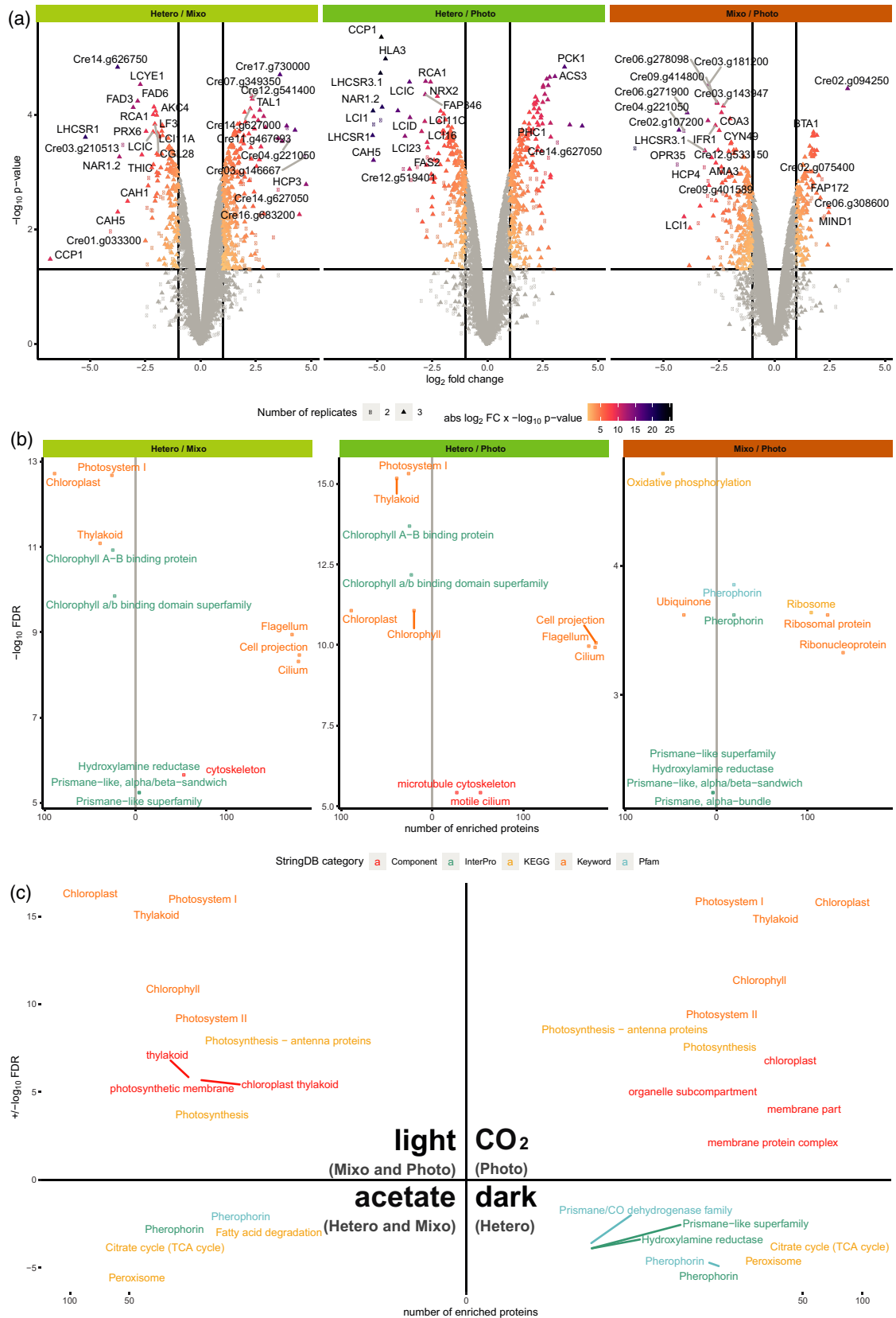
We found 79 proteins to be significantly upregulated in both mixo- and heterotrophic conditions when compared to phototrophic conditions. These proteins are mainly related to acetate metabolism. An analysis of the best matching loci of *Arabidopsis thaliana* homologs via Stitch DB revealed that 18 of those are known to interact with acetate directly (Figure S1) (Szkarczyk et al., 2016).

There are 68 proteins downregulated under both conditions, whereof 14 are reported to be directly associated with  $\text{CO}_2$  metabolism (Figure S2). In summary, under

**Table 1** Summary of identified and quantified protein groups and lysine acetylation (acK) sites. For quantification of protein levels and acK sites, a ternary comparison between heterotrophic (Hetero), mixotrophic (Mixo), and photoautotrophic (Photo) growth conditions was made by pooling light, medium, and heavy dimethyl-labeled peptides from the respective growth condition in biological triplicates. Between biological replicates labels were swapped between conditions to prevent any labeling bias. Filters applied: 1% false discovery rate (FDR) at peptide-to-spectrum match (PSM), peptide, and protein levels. Filters applied for up- and downregulated features: values in minimum two out of the three biological replicates, LIMMA  $p$ -value  $<0.05$

	Hetero/Mixo	Mixo/Photo	Hetero/Photo
Protein groups			
Quantified	5346	5340	5355
Up	1072	409	835
Down	552	705	670
5863 identified			
AcK sites			
Quantified	280	278	289
Up	32	40	55
Down	10	5	9
1376 identified			

**Figure 2.** Differential protein expression analysis of *Chlamydomonas* under different growth conditions. (a) Volcano plots correlating the  $\log_2(\text{FC})$  values of protein groups and the respective  $-\log_{10}(p\text{-values})$  from LIMMA statistical analyses. Only proteins quantified in at least two biological replicates are shown. The color gradient indicates the absolute value of the product of the  $\log_2(\text{FC})$  and  $-\log_{10}(p\text{-values})$ . (b) Volcano plots for functional enrichment analysis performed with StringDB on either up- or downregulated proteins in the respective binary comparison using the website's 'Proteins with Values/Ranks - Functional Enrichment Analysis' function. Plots are shown correlating the number of proteins in specific functional terms enriched in either growth condition and the respective  $-\log_{10}(\text{FDR})$  given by StringDB when testing for enrichment. (c) Scatter plot for functional enrichment for StringDB features that are shared or unique between different growth conditions: light (Mixo and Photo) versus dark (Hetero) (top left versus bottom right) and  $\text{CO}_2$  (Photo) versus acetate (Hetero and Mixo) (top right versus bottom left). The respective number of proteins enriched in a term is shown on the x-axis and the  $-\log_{10}(\text{FDR})$  resulting from the functional enrichment analysis by StringDB are given on the y-axis.



heterotrophic growth conditions, most photosynthesis- and chloroplast-related processes were downregulated. Upregulated proteins include those involved in fatty acid oxidation and the TCA cycle. By comparing the up- and downregulated proteins from the different growth conditions, novel protein regulations responding to either acetate and inorganic carbon or light and dark acclimation could be identified, such as the perophorins.

#### Identification and functional annotation of lysine-acetylated proteins in *Chlamydomonas*

In total, 1376 acK sites were detected on 625 protein groups of *Chlamydomonas* (Table 1). For each of the binary comparisons between different growth conditions, more than 250 sites were quantified and more than half of those in at least two replicates (Table S2). We found about 15% of those sites to be significantly changed in their abundance. Under all three growth conditions, about 25% of the detected acK sites are found on proteins that were not detected and quantified as unmodified proteins under those conditions (Figure 3a,b). To investigate whether specific sequence motifs can be found surrounding the acK sites, the iceLogo tool was used to generate a sequence logo using the 15 amino acids on each site surrounding the acetylated lysine residue (Colaert et al., 2009). The sequence on top gives an overview of the sequence context for all detected acK sites. Amongst others, mainly glycine residues were generally overrepresented from -4 to +6 adjacent to the acetylated lysine residues (Figure 3c), as well as lysine at +4 and proline at -3 and +1. The sequence motifs surrounding the significantly differentially regulated acetylation sites also differ between the different growth conditions, probably indicating that different lysine deacetylases and acetyltransferases are active in *Chlamydomonas* depending on the available carbon sources (Figure 3c). Interestingly, the enrichment of glycine residues near the acetylation site disappears in the comparison of heterotrophic and mixotrophic growth conditions.

#### Lysine acetylation dynamics between heterotrophic, photoautotrophic, and mixotrophic growth conditions

To investigate the regulation of differential lysine acetylation between heterotrophic, photoautotrophic, and mixotrophic conditions a LIMMA statistical analysis was performed on the acetylated peptide ratios derived from the three biological replicates (Figure 4a, Table S2). The volcano plots in Figure 4(a) visualize changes in lysine acetylation between the different growth conditions. In addition, to distinguish the regulation at the level of the acetylated peptide from regulation of the total protein abundance, the protein ratios are plotted against the peptide ratios (Figure 4b). We focused our downstream analysis on the main metabolic pathways influenced by light and carbon source acclimations. Many proteins from central metabolic pathways were significantly changed in

lysine acetylation levels as briefly outlined in the following (Figures 1e, 4c, and 5).

*Heterotrophic versus mixotrophic growth conditions.* In the comparison of heterotrophically and mixotrophically grown cells, light is the main difference between these two conditions, as both media contained acetate as carbon source. In total, 42 acK sites belonging to 31 unique protein groups were significantly differentially regulated in their abundance in heterotrophic compared to mixotrophic conditions (Figure 4a, left column). Under heterotrophic conditions several peroxisomal proteins such as enzymes of the glyoxylate cycle (malate synthase and citrate synthase), peroxin 11A, acetyl-CoA synthetase 3, and the multifunctional protein 2 involved in fatty acid beta-oxidation were increased in acetylation at several sites. In addition, acetylation of several chloroplastic proteins was affected. While proteins from the light reactions (AtpB and E, PsaB, PSAD, PSBO1, and LHCA1) showed a significant downregulation in their acetylation level under heterotrophic compared to mixotrophic conditions, enzymes of the Calvin-Benson cycle, such as glyceraldehyd-3-phosphate dehydrogenase, phosphoglycerate kinase, and RbcL (K175), showed a significant upregulation in their acetylation level. Among nuclear proteins, increased acetylation of a NuA4-domain acetyltransferase, a homeodomain-like/winged-helix DNA-binding family protein, the nuclear matrix protein THO1, and histone H2A was observed.

*Heterotrophic versus photoautotrophic growth conditions.* The comparison of heterotrophic versus photoautotrophic growth (Figure 4, middle column, Figure 5) showed the most distinct changes in lysine acetylation deriving from the diverging conditions with either an organic or inorganic carbon source. Photoautotrophically grown cells produce their energy by the fixation of inorganic CO<sub>2</sub> via the Calvin-Benson cycle. On this account, a total of 64 acK sites, belonging to 48 unique proteins, were significantly differentially regulated between heterotrophic and photoautotrophic conditions. The changes in lysine acetylation between heterotrophic and photoautotrophic conditions occurred on similar acK sites as the changes between heterotrophic and mixotrophic conditions, but were much more pronounced (up to 16-fold increase in lysine acetylation). The most affected pathways with several highly significantly differentially regulated acK sites are related to carbon metabolism, in particular those from fatty acid beta-oxidation and the glyoxylate cycle in peroxisomal microbodies, as well as from photosynthesis metabolism in chloroplasts. In Figure 5, an overview map of metabolism is presented depicting the relative changes in lysine acetylation normalized to protein abundance of the respective proteins. Although some of the peroxisomal enzymes were also strongly upregulated at the protein

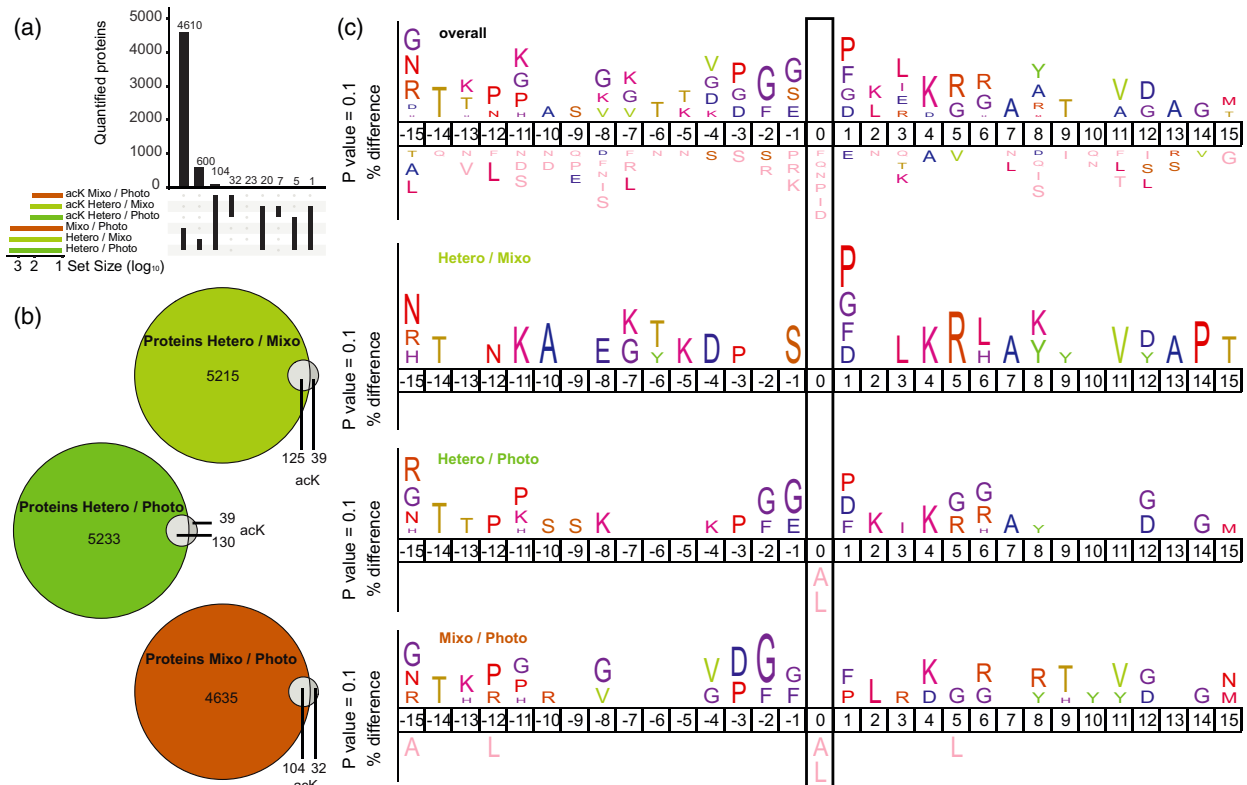


**Figure 3.** Comparison of the overlap of the unmodified, quantified proteins and proteins carrying a lysine acetylation site (a, b), and acetylation site motif analyses globally and per growth condition (c). (a) Upset plot for the overlap of unmodified, quantified proteins and proteins carrying an acK site under different growth conditions. Bars in the lower right panel indicate which binary comparisons overlap. (b) Venn diagrams presenting the overlap of unmodified proteins (colored) and proteins with acK sites (gray) per binary comparison between growth conditions. (c) Sequence context of all detected acK sites (top) and sequence windows found specifically differentially regulated in the respective binary comparison of growth conditions, comparing the frequency percentage of an amino acid at a certain location when acetylated. All motives are centered around the acK site, indicated by a box. The sequence logos were generated with the ic-Logo tool (Colaert et al., 2009).

level, the change in lysine acetylation levels for several of these proteins at multiple sites was considerably higher, indicating that a unique increase in lysine acetylation occurred for these proteins (Figure 4b, middle). For example, acetyl-CoA synthase 3 (ACS3) provides one of the entry points into the glyoxylate cycle pathway by producing acetyl-CoA from acetate in peroxisomal microbodies (Lauersen et al., 2016) (Figure 5). We identified two acK sites (K205 and K218) on ACS3, which were more than 16-fold increased under heterotrophic compared to photoautotrophic conditions. In the glyoxylate cycle, acetyl-CoA is then converted to citrate by the citrate synthase CIS2, which carried three strongly upregulated acK sites (K99, K340, and K446). While several acetylation sites were detected on the peroxisomal aconitase (ACH1) and isocitrate dehydrogenase (ICL1), none of them were quantifiable due to their low abundance (Table S1). A strong increase in lysine acetylation was observed under heterotrophic conditions on two out of 10 detected acK sites (K54 and K422) of malate synthase 1 (MAS1), which is the enzyme that converts succinate to malate in the glyoxylate

cycle (Figures 4a,b and 5). Several additional peroxisomal and peroxisome-related proteins showed a strong increase in lysine acetylation, while the total protein level was only slightly increased. Interestingly, acetyl-CoA acyltransferase 1 (ATO1), which is related to beta-oxidation (Atteia et al., 2009; Goodenough et al., 2014), possesses three acetylation sites (K230, K274, and K232), which showed an up to 16-fold increase under heterotrophic conditions. In addition to proteins from the glyoxylate cycle, also other enzymes related to acetyl-CoA metabolism in different sub-cellular compartments showed an increase in acetylation under heterotrophic conditions. For example, dihydrolipoamide acetyltransferase 2 (DLA2) is a subunit of the plastidial pyruvate dehydrogenase complex and is involved in the conversion of pyruvate to acetyl-CoA as well as in the translation of *psbA* mRNA, which encodes a reaction center protein of photosystem II (PSII) (Bohne et al., 2013). DLA2 carries in total eight acK sites, including one (K197) that is significantly upregulated under heterotrophic and mixotrophic compared to photoautotrophic conditions, while the DLA2 protein level is unaltered under

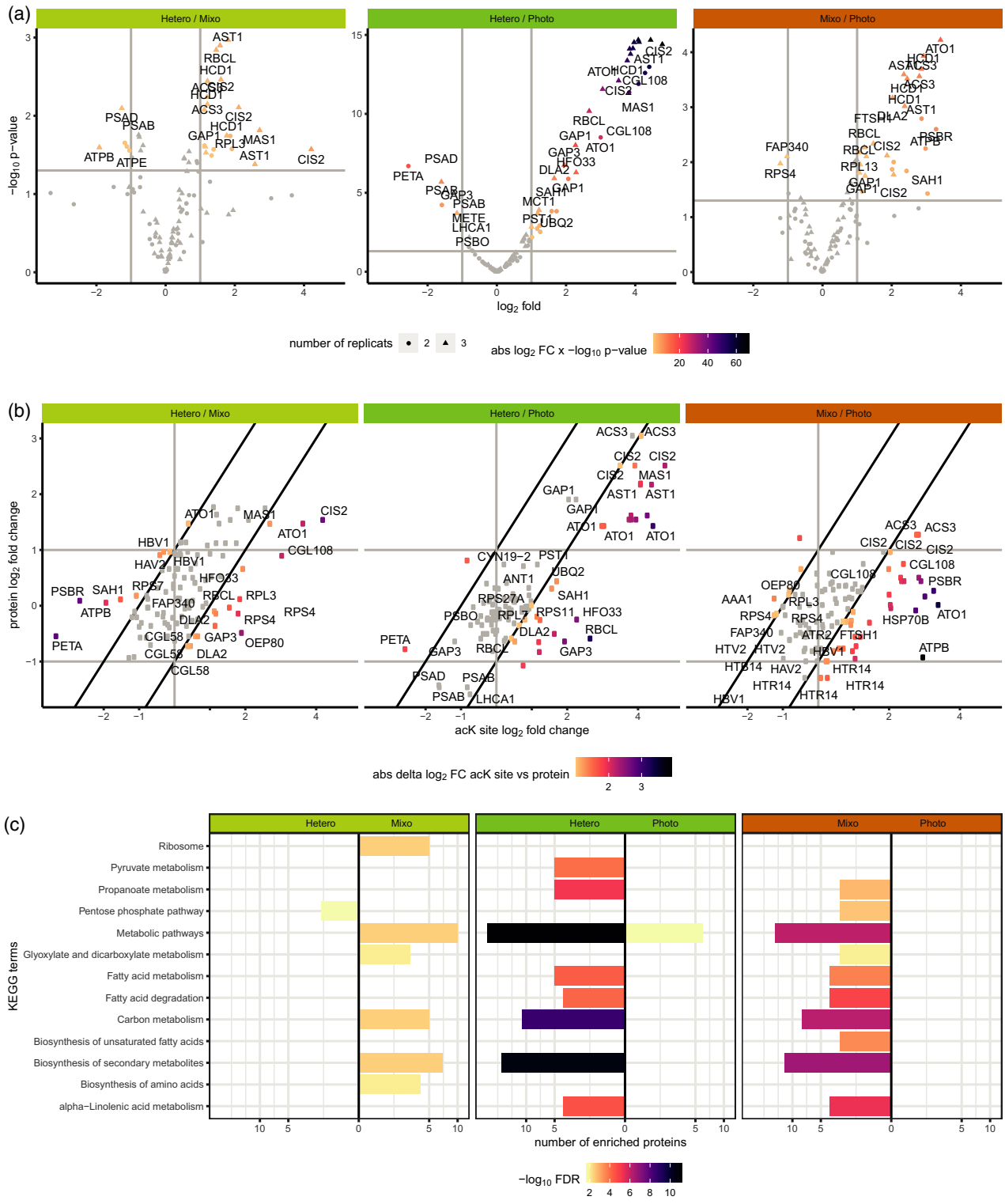
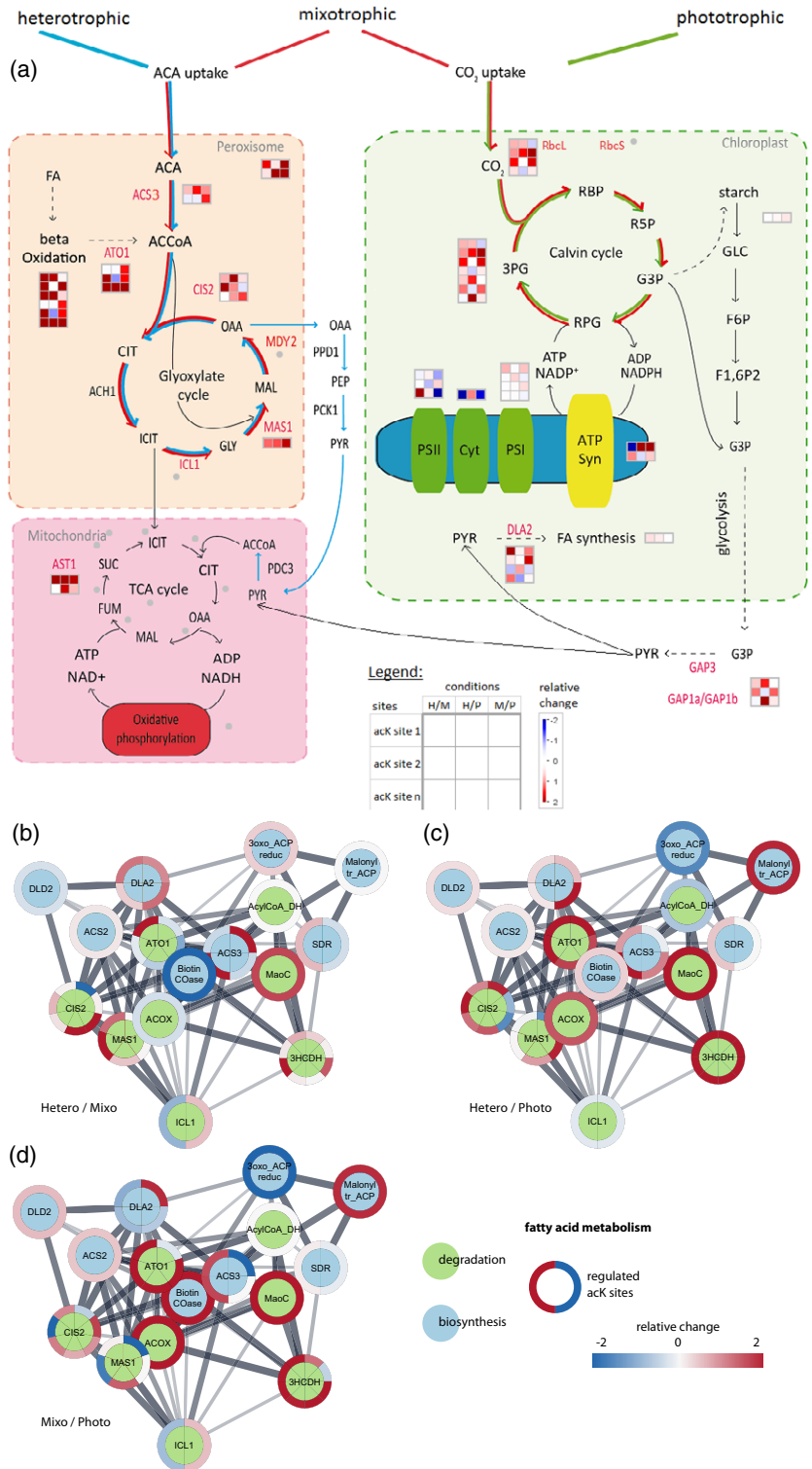


**Figure 4.** Quantitative profiling of regulated acetylation sites depending on growth conditions in *Chlamydomonas*. (a) Volcano plots correlating the  $\log_2(FC)$  values of acK sites and the respective  $-\log_{10}(p\text{-values})$  from LIMMA statistical analyses for the comparison of different growth conditions. Only sites quantified in at least two replicates are shown. A color gradient indicates the absolute value of the product of the  $\log_2(FC)$  and  $-\log_{10}(p\text{-values})$ . (b) Scatter plots correlating the acK and protein FC values for different growth conditions. The color gradient indicates the difference in  $\log_2(FC)$  values for proteins and acK sites. The vertical reference line indicates  $\log(FC) = 0$  for acK site changes, the horizontal reference lines indicate  $\log_2(FC) = \pm 1$  for proteins, and diagonal reference lines with slope = 1 and intercept =  $\pm 1$  represent the difference between acK and protein FC values. (c) Functional enrichment analysis performed with StringDB on differentially acetylated proteins. Box plots correlate the number of acetylated proteins per KEGG term enriched in either growth condition. The number of proteins per term is depicted on the x-axis and the respective  $-\log_{10}(FDR)$  are shown as fill color of the respective bar.

**Figure 5.** Effect of lysine acetylation on *Chlamydomonas* metabolism. (a) Metabolic map of carbon metabolism showing enzymes, protein complexes, and pathways in different compartments. (b–d) Protein–protein interaction (PPI) networks of proteins associated with fatty acid metabolism. (a–d)  $\text{Log}_2(\text{FC})$  values of acK sites normalized to protein levels between different growth conditions. Down-regulated sites are shown in blue and upregulated sites in red. Each box in (a) represents a protein, protein complex, or pathway as indicated. Each row of three squares represents one acK site. The three columns represent the  $\text{log}_2(\text{FC})$  values of an acK site in the binary comparison of the growth conditions: heterotrophic and mixotrophic (H/M), heterotrophic and photoautotrophic (H/P), and mixotrophic and photoautotrophic (M/P). In the PPI networks in (b–d), the changes in normalized acK status are given as rings surrounding the proteins. Rings are split if more than one acK site was detected for a protein. The inner circle is colored depending on whether a protein is involved in fatty acid degradation (green) or biosynthesis (blue). Visualization for (a) was performed with MapMan (Thimm *et al.*, 2004) while (b–d) were created using Cytoscape (Shannon *et al.*, 2003).



these conditions (Figure 4b) (Bohne *et al.*, 2013). Fifteen acK sites were identified on the large subunit of RuBisCO (RbcL), of which six could be quantified. Again, K175 of RbcL showed a strong and significant upregulation in acetylation under heterotrophic conditions.

*Mixotrophic versus photoautotrophic growth conditions.* When comparing mixotrophic and photoautotrophic growth conditions, acetate is the main factor which influences lysine acetylation. In total, 45 acK sites from 32 unique proteins were significantly differentially

regulated in the comparison of the two conditions. Again, eight of these 32 proteins, which showed a strong increase in acetylation, were peroxisomal proteins involved in lipid breakdown. Remarkably, the lysine-acetylated proteins showed only minor changes in their total protein abundance (Figure 4b, right,  $|\log_2(\text{FC})| \leq 1$ , Figure 5), indicating that the protein expression of the enzymes from the glyoxylate cycle is mainly controlled by light/dark acclimation, but not by acetate. Increased acetylation under mixotrophic growth conditions was identified on ADH1, which is a key enzyme in fermentative metabolism (Magneschi et al., 2012). Under these conditions also Calvin–Benson cycle enzymes and proteins involved in the light reaction showed an increase in acetylation in the presence of acetate in the light. Among the photosynthetic proteins, the PSBR protein from PSII showed a more than eightfold and significant upregulation in lysine acetylation on K38 in the presence of acetate and light (Figure 4a,b, right column). PSBR is required for efficient binding of the light-harvesting complex (LHC) protein LHCS3 to PSII in *Chlamydomonas*, and hence PSBR acetylation could be important for PSII–LHCII\_LHC3 supercomplex formation and thermal dissipation in the light (Xue et al., 2015).

#### Lysine acetylation on enzymes involved in carbon and fatty acid metabolism

We performed a functional enrichment analysis with StringDB to evaluate to which pathways the proteins belong for which the acK status was altered (Figure 4c). When comparing the proteins with altered acetylation levels between algae grown under phototrophic conditions and those grown in the presence of acetate in the medium, it becomes clear that proteins responsible for carbon and fatty acid metabolism were affected (Figure 4c, middle and right panels). When directly comparing proteins with altered acK status between the mixo- and heterotrophic states, proteins connected to the ribosome and amino acid biosynthesis show increased acetylation when light was available (Figure 4c, left).

We went on to evaluate the effect of lysine acetylation on fatty acid metabolism in more detail (Table S4). We found 16 proteins with differentially acetylated lysines under the different growth conditions that also form a highly connected interaction network (Figure 5b–d). Six of those proteins play a role in fatty acid biosynthesis (blue circles), while the other 10 are associated with fatty acid degradation (green). Both catabolic and anabolic enzymes show a high degree of acetylation. Especially 3-hydroxyacyl-CoA dehydrogenase (3HCDH), involved in fatty acid degradation, carries eight acK sites, which show stronger acetylation in the presence of acetate and with no light available (Figure 5c,d). The biotin carboxylase subunit (biotin COase) of the polymeric acetyl-CoA carboxylase complex is acetylated to a higher extent when comparing photo-

mixotrophic or to heterotrophic growth. Ketoacyl-ACP reductase shows a strong decrease in acetylation when comparing phototrophic growth to the other two conditions.

#### The large subunit of RuBisCO and citrate synthase show a strong increase in lysine acetylation occupancies under heterotrophic conditions

To get an impression of lysine acetylation occupancies on *Chlamydomonas* proteins, we selected the highly regulated acK site K175 of RbcL, since increased lysine acetylation was reported previously for RuBisCO during the night in Arabidopsis, which resulted in a significant downregulation in RuBisCO activity (Finkemeier et al., 2011; Gao et al., 2016). The concept of site occupancy calculation for PTMs was initially presented by Olsen and co-workers for phosphorylated peptides (Olsen et al., 2010). It assumes that in different conditions modified peptides should have their abundance changed inversely proportional to their non-modified counterpart. In the case of acK sites this is not easily possible, since the acetylation is masking the positive charge of the side chain, which would lead to a tryptic cleavage. Hence, the modified and unmodified peptides are of very different lengths and the unmodified peptides might contain too few amino acids for an unambiguous identification. However, in case both peptides can be detected, the increase in abundance of the acetylated peptides between two conditions can be calculated relative to the decrease in their non-modified counterparts carrying a missed cleavage at the site of interest (Nakayasu et al., 2014). We made use of this fact in our calculations. Figure 6(a) shows that the peptide GLLGCTIKPK was detected in its acetylated form on position K8 in all three dimethyl labeling states. The peptide was also detected with one missed cleavage in its unmodified form, probably due to the presence of proline. Hence, we were able to calculate the occupancy for this particular site of K175 of RbcL using the ratios for the acetylated and the corresponding unmodified peptide that has not been cleaved at K175. The occupancy was the highest (35%) in the algae grown heterotrophically without light. This site shows the lowest occupancy (only 6%) in the phototrophically grown *Chlamydomonas* cultures, indicating active deacetylation (Figure 6a). In addition to RbcL, we also evaluated the occupancy of two acK sites (K99 and K340) on the peroxisomal citrate synthase CIS2, where corresponding unmodified peptides were detected. In the case of CIS2 we calculated the occupancies based on dimethyl ratios for acetylated and unmodified peptides not cleaved at the respective positions as outline before. For another strongly acetylated site (K446) on CIS2 no unmodified counterpart was detected, and hence no occupancy could be calculated. CIS2 is a key enzyme of the glyoxylate cycle and catalyzes the conversion of acetyl-CoA to citrate. The enzyme

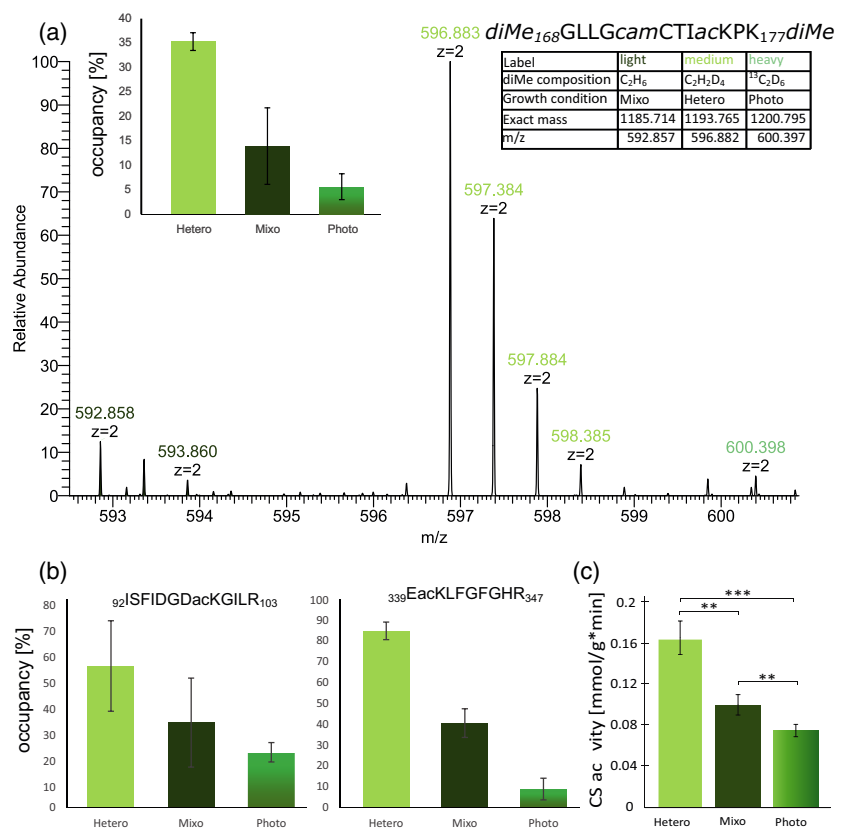
showed a strong increase in acetylation that was dependent on acetate in the growth medium (Figures 4 and 5). The occupancy calculation revealed that K99 is acetylated to about 50% under heterotrophic conditions. A lower occupancy was observed under mixo- (33%) and phototrophic (21%) growth conditions (Figure 6b). In a sequence alignment, this amino acid position turns out to be conserved in algae; however, in land plants such as *A. thaliana*, this position is exchanged to a negatively charged glutamic acid (Figure S3a). The acK site K340 of CIS2 was almost fully acetylated when the algae were grown without any light (heterotrophically). The occupancy level was reduced to 41% under mixo- and to 9% under phototrophic conditions, again indicating active deacetylation. The lysine residue K340 is highly conserved amongst plants in general. To investigate whether the acetylation occupancy correlated with the activity of citrate synthase, we determined the total citrate synthase activity in protein extracts from all three growth conditions (Figure 6c). It must be noted that next to the peroxisomal CIS2, a mitochondrial CS isoenzyme (CIS1) exists in *Chlamydomonas*, which however showed no significant change in protein abundance under the investigated conditions (Table S1). The total citrate synthase activity was increased more than 2.2-fold under heterotrophic compared to photoautotrophic growth conditions, which corresponds with the strong

increase in protein abundance (5.6-fold) as well as an even stronger increase in lysine acetylation (11- to 25-fold) of CIS2 (Figure 4b, Table S1).

## DISCUSSION

In recent years, several global acetylome characterizations have been reported both in prokaryotes and eukaryotes (Choudhary et al., 2014). The present study presents the *Chlamydomonas* acetylome in combination with a stable dimethyl-labeling technique to compare heterotrophic, photoautotrophic, and mixotrophic growth conditions. Mixotrophic growth conditions promote optimal lipid formation, which is important for large-scale generation of algal-based biofuels (Sager and Granick, 1953; Work et al., 2010). It is known that the addition of acetate to the growth medium boosts metabolism and leads to a higher growth rate in several green algae (Lauersen et al., 2016; Rai et al., 2013; Smith et al., 2015). In *Euglena gracilis* the number of microbodies increased in the presence of acetate (Graves et al., 1971). This is in accordance with the finding that the total volume of peroxisomal microbodies and the transcript levels of enzymes involved in the glyoxylate cycle increased when *Chlamydomonas* cells were grown on acetate-containing medium (Hayashi et al., 2015). Strikingly, genes belonging to the GPR1/FUN34/YaaH (GFY) superfamily also showed increased expression upon

**Figure 6.** acK site occupancies and enzyme activity. (a) acK site occupancy of K175 of RbcL (detected in a peptide spanning G168–K177 of RbcL). The table indicates mass details and the labeling scheme of the detected dimethyl-labeled acK peptide of RbcL, as shown in the zoomed-in panel of the labeled triplet in the MS<sup>1</sup> spectrum. The bar graph shows average site occupancies  $\pm$  standard deviation (SD) ( $n = 3$ ). (b) Bar graph of acK site (K99 left [I92–R103], K340 right [E339–R347]) occupancies for the peroxisomal citrate synthase CIS2. The respective numbers of the first and last amino acids are also given in the figure. Replicate values are shown in Table EV3. (c) Total enzymatic activity of citrate synthase (CS) in *Chlamydomonas* protein extracts from different growth conditions  $\pm$  SD ( $n = 3$ ). Significant differences are indicated with asterisks (Student's *t*-test,  $p$ -value  $< 0.05$ ).



acetate addition. CrGFY1–5 show structural similarity to bacterial succinate-acetate channels and specifically localize to microbodies. GFY3–5 expression was strongly upregulated in the presence of acetate, and they were found to be co-expressed with genes participating in acetate metabolism especially with those involved in the glyoxylate cycle (Durante et al., 2019). Also in this study, we observed a strong increase in abundances of proteins involved in the glyoxylate cycle, as well as of the GFY3–5 proteins, particularly under heterotrophic conditions. Thus, these results provide further confirmation that peroxisomal microbodies play a key role in acetate assimilation (Lauersen et al., 2016). A recent metabolomic and proteomic study in *Isochrysis galbana* showed that fatty acids accumulated when the algae were fed with acetate. The enzymes acting in the glyoxylate cycle accumulated when the medium was supplemented with acetate and nitrogen but not under nitrogen starvation conditions. Hence, the acetate-dependent regulation relies on nitrogen availability (Kaur et al., 2021). To further improve biofuel production, it is of great interest to understand the underlying principles of metabolic pathway regulation in *Chlamydomonas*. The acetylome data which we present here provide new possible regulatory mechanisms based on this PTM. However, it is important to note that a change in acetylation status does not necessarily mean that the activity or function of this protein is also regulated by this modification. This depends on whether the site of modification is essential for protein function, which needs to be confirmed in a case-by-case manner for every protein and modification site (Hosp et al., 2017). By using an MS-based approach, we identified an overall number of 5863 protein groups with 1376 acK sites (Table 1). Our data indicate that lysine acetylation occurs on proteins involved in diverse metabolic pathways in *Chlamydomonas*, which is in accordance with observations from several other organisms (Cobbold et al., 2016; Fang et al., 2015; Finkemeier et al., 2011; Hartl et al., 2017; Henriksen et al., 2012; Liu et al., 2014; Uhrig et al., 2019; Wu et al., 2011; Zhou et al., 2018). The widespread distribution recapitulates the vital biological function of this PTM, and includes metabolic enzymes involved in protein biosynthesis and photosynthesis, as well as several important carbon utilization pathways, such as glycolysis, the TCA cycle, and the glyoxylate cycle. Here we investigated the influence of acetate and inorganic carbon, as well as light availability on lysine acetylation of proteins in *Chlamydomonas*, thereby allowing to uncover the possible regulatory function of this modification. Our data show that acetate as carbon source has a major influence on lysine acetylation of selected nuclear, peroxisomal, and plastid proteins, as indicated by the large changes in lysine acetylation, when comparing either heterotrophic or mixotrophic with photoautotrophic conditions (Figure 4). Since acetate can be converted to acetyl-CoA via ACS and ACK in

*Chlamydomonas*, it can be speculated that lysine acetylation plays a major role in causing changes in the activity of metabolic enzymes, which direct the metabolic flux to produce energy from acetate (Yang et al., 2014). Especially the enzymes of the glyoxylate cycle showed a strong increase in the total proteome and an even stronger increase in their acetylation levels. This supports previous findings that acetate enters the glyoxylate cycle pathway in peroxisomal microbodies of *Chlamydomonas*, which is the preferred carbon utilization pathway especially for heterotrophically grown cells (Plancke et al., 2014; Lauersen et al., 2016). In addition, the strong upregulation of enzymes involved in the glyoxylate cycle under heterotrophic conditions could be necessary because during longer periods of darkness plants start degrading their endomembrane system and depend on fatty acid beta-oxidation (Kunze et al., 2006). Additionally, the number of peroxisomal microbodies increases with acetate in the media (Hayashi et al., 2015). In Arabidopsis peroxisomal proliferation is regulated by an increased abundance of PEX11 proteins (Lingard and Trelease, 2006). Here we observed an increase in acetylation of PEX11a under heterotrophic conditions (Table S2), which could be important for regulation of PEX11 function. The link between acetate metabolism and lysine acetylation is well studied and is mainly established because of the known activity regulation of ACS by lysine acetylation in several organisms (Crosby et al., 2010; Gardner et al., 2006; Starai et al., 2002). While in *Salmonella enterica* Lys609 is actively acetylated by the acetyltransferase Pat and thereby inactivated (Starai and Escalante-Semerena, 2004), this lysine site, although it is conserved in *Chlamydomonas*, was not affected in our study (Figure S3b). Thus, it remains to be discovered whether the highly increased acetylation on ACS3, as well as on many other enzymes of the glyoxylate cycle, which we observed when acetate is present resulted from active acetylation via an acetyltransferase or from chemical acetylation as a by-product from acetyl-P production via ACK as in *E. coli* (Castano-Cerezo et al., 2014). While acetylation of metabolic enzymes is more often reported in the context of inhibition of enzyme activity, activation of an enzyme by this PTM was reported for the glycolytic activity of the *E. coli* glyceraldehyde-3-phosphate dehydrogenase, enoyl-coenzyme A hydratase/3-hydroxyacyl-coenzyme A dehydrogenase in fatty acid beta-oxidation, the TCA cycle enzymes aconitase and malate dehydrogenase in human liver and heart tissue, respectively, and malate dehydrogenase from Arabidopsis and *Physcomitrella* (Balparda et al., 2021; Fernandes et al., 2015; Finkemeier et al., 2011; Wang et al., 2010; Zhao et al., 2010). Hence, it cannot be easily predicted whether acetylation has a positive or negative effect on enzyme function, because the effect on activity or function is highly dependent on the position of the acetylation site within the protein structure (Hartl et al., 2017; Hosp et al., 2017; Schmidt

et al., 2017). In addition, the site stoichiometry of acetylation on a given enzyme within a cellular context can be important, and generally lysine acetylation was reported to occur only at sub-stoichiometric levels on most sites under the analyzed conditions (Hansen et al., 2019; Weinert et al., 2017). However, site stoichiometry analyses in an *E. coli* deacetylase mutant revealed that metabolic enzymes which either utilize or generate acetyl-CoA show occupancy rates of up to 98% on selected enzymes (Baeza et al., 2014), and acetyl-phosphate-dependent acetylations were responsive to changes in carbon flux (Schilling et al., 2015). Here we identified particularly high acetylation site occupancies for RuBisCO and peroxisomal citrate synthase under heterotrophic conditions (Figure 6). A strong negative impact of lysine acetylation on RuBisCO initial activities has previously been observed in *A. thaliana* (Finkemeier et al., 2011), and since K175 is a catalytically active site and responsible for protonation of the acid carboxylate, acetylation of K175 would inactivate RuBisCO activity (Knight et al., 1990). It will be interesting to investigate whether K175 acetylation is an evolutionarily conserved mechanism that inhibits RuBisCO in cells grown under heterotrophic growth conditions and whether this modification also prevents the degradation of the enzyme under these conditions. Especially for site stoichiometry analyses, single-cell algae will be particularly useful since they can be grown in a highly synchronized manner under standardized growth conditions. In addition to RuBisCO, the peroxisomal citrate synthase CIS2 showed occupancy levels of up to 85%, which correlated with high activities of total cellular citrate synthase (Figure 6). In future studies, it would be interesting to perform site-directed mutagenesis on the different acK sites of CIS2 and to identify the putative acetyltransferases and deacetylases in peroxisomal microbodies and chloroplasts of *Chlamydomonas*.

In conclusion, *Chlamydomonas* proved to be an excellent organism to study PTM-mediated regulation of proteins, which might be important for engineering algal and plant metabolism via genetic manipulations of their acK sites.

## EXPERIMENTAL PROCEDURES

### Algal strain and culture conditions

For *Chlamydomonas*, we used the cell wall-deficient strain CC-3491 cw15 *mt-* (Chlamydomonas Resource Center), which showed a reduced abundance of acetylated tubulin due to a high proportion of non-flagellated cells. The strain was maintained on 0.8% agar-solidified Tris/acetate/phosphate (TAP) medium (Harris, 1989) at 25°C under constant light (30  $\mu\text{mol m}^{-2} \text{sec}^{-1}$ ). Liquid cultures were incubated under agitation at 25°C. For analysis, a pre-culture was grown in 2 L of TAP medium containing 1% sorbitol (TAPS) to a density of approximately  $5 \times 10^6$  cells/ml. Cells were harvested by centrifugation (5 min, room temperature, 1000 g), washed once with 200 ml high-salt minimal medium (HSM), and resuspended in 120 ml HSM (approximately  $8 \times 10^7$  cells  $\text{ml}^{-1}$ ) (Sager and Granick, 1953). Considering different doubling times of *Chlamydomonas* cells under the selected growth conditions we used adjusted cell

numbers for inoculation to reach a final cell number of approximately  $2 \times 10^9$  cells after 30 h of growth per replicate. The suspension was used to inoculate the following cultures. For heterotrophic growth,  $3 \times 10$  ml resuspended culture was used to inoculate  $3 \times 300$  ml TAPS; for mixotrophic growth,  $3 \times 8$  ml was used to inoculate  $3 \times 300$  ml TAPS; and for growth under photoautotrophic conditions,  $3 \times 15$  ml was used to inoculate  $3 \times 500$  ml HSM to compensate for different growth rates under the applied conditions and to reach approximately the same final cell densities after 30 h. For mixotrophic and photoautotrophic growth, cells were then incubated in the light (100  $\mu\text{mol m}^{-2} \text{sec}^{-1}$ ), and cells were kept in complete darkness for heterotrophic growth. Cells were harvested by centrifugation, immediately frozen in liquid nitrogen, and stored at  $-80^\circ\text{C}$  until further use.

### Immunoenrichment and Western blot analysis

Cells were harvested by centrifugation and lysed by resuspending them in 2 ml basic extraction buffer (BEB) containing 50 mM Tris pH 7.5, 150 mM NaCl, 10% (v/v) glycerol, 2 mM EDTA, 0.5% (w/v) Triton X-100, and 5 mM dithiothreitol and protease inhibitor cocktail (cOMplete Tablets, Roche, Mannheim, Germany) by continuous pipetting. Additionally, to avoid deacetylation of proteins, 3  $\mu\text{M}$  apicidin and 1 mM nicotinamide were added to the extraction buffer. For immunoenrichment of lysine-acetylated proteins, 200  $\mu\text{g}$  protein extract was incubated with 20  $\mu\text{l}$  anti-acetyl lysine antibody immobilized on agarose beads (ImmuneChem Pharmaceuticals, Burnaby, BC, Canada) for 3 h at 4°C. Immunoprecipitates were washed three times with extraction buffer and eluted by boiling in gel loading buffer for 5 min. For Western blot analysis, proteins were separated by SDS-PAGE, transferred to a nitrocellulose membrane, and probed using an acetyl lysine antibody in a 1:1000 (v/v) dilution (ImmuneChem Pharmaceuticals, Burnaby, BC, Canada). Horseradish peroxidase-conjugated secondary antibody (Bio-Rad, Feldkirchen, Germany) was used in a 1:10 000 dilution.

### Protein extraction and peptide preparation

Protein pellets from *Chlamydomonas* were extracted in 10 ml heated SDT lysis buffer containing 4% (w/v) SDS, 100 mM Tris/HCl pH 7.6, and 10 mM DTT for 10 min at 95°C with occasional mixing followed by 15 min of sonication. Protein extracts were cleared by centrifugation and the protein amount was determined using the 660 nm Pierce protein assay with compatibility reagent (Pierce, Rockford, IL, USA) as previously described (Hartl et al., 2015).

To remove excess SDS and to prepare samples for tryptic digestion, the FASP method with Amicon Ultra-15 centrifugal filter units (Millipore, Darmstadt, Germany) was used (Wisniewski et al., 2009). Briefly, 10 mg of the protein extract was diluted with 8 M urea in 100 mM Tris/HCl pH 8 until an SDS concentration of <0.5% was reached. After SDS removal, the extract was alkylated using 50 mM iodoacetamide for 30 min in the dark, excess reagent was washed through a filter, and the buffer was replaced with 50 mM  $\text{NH}_4\text{HCO}_3$ . The reduced and alkylated proteins were digested using MS-grade trypsin (T6567, Sigma-Aldrich, Darmstadt, Germany) in an enzyme-to-protein ratio of 1:100. Eluted peptides were quantified at 280 nm. Digested peptides were dimethyl-labeled on  $\text{C}_{18}$  Sep-Pak plus short columns (Waters, Eschborn, Germany) as previously described (Lassowskat et al., 2017). Equal amounts of light, medium, and heavy dimethyl-labeled peptides were pooled for each replicate and the solvent was evaporated in a vacuum centrifuge. The dried peptides were dissolved in 1 ml TBS buffer (50 mM Tris-HCl, 150 mM NaCl, pH 7.6) and pH was checked and adjusted if required. Peptides (15  $\mu\text{g}$ ) were stored for whole proteome analysis. About 10 mg of the pooled labeled peptides were

resuspended in 2 ml 95% solvent A (95% acetonitrile, 5 mM ammonium acetate) and 5% buffer B (5 mM ammonium acetate) and fractionated with a flow rate of 500  $\mu\text{l min}^{-1}$  on a Sequant ZIC-HILIC column (3.5  $\mu\text{m}$ , Merck, Darmstadt, Germany) using a segmented linear gradient of 0–60% solvent B (5 mM ammonium acetate). The fractions were combined to seven final fractions and dried in a vacuum centrifuge. Peptides were resuspended in IP buffer (50 mM Tris/HCl pH 7.6, 150 mM NaCl) and the concentration was determined on a spectrophotometer at 280 nm. Lysine-acetylated peptide enrichment was performed as previously described with 1 mg peptide per fraction (Lassowskat et al., 2017). After enrichment, the eluted peptides were desalted using  $\text{C}_{18}$  Stagetips and dried in a vacuum centrifuge.

### Mass spectrometry

Dried peptides were redissolved in 2% acetonitrile (ACN), 0.1% trifluoroacetic acid for analysis. Total proteome samples were adjusted to a final concentration of 0.2  $\mu\text{g } \mu\text{l}^{-1}$ . Samples were analyzed using an EASY-nLC 1000 (Thermo Fisher Scientific) coupled to a Q Exactive Plus mass spectrometer (Thermo Fisher). Peptides were separated on 16-cm frit-less silica emitters (New Objective, Littleton, MA, USA, 0.75  $\mu\text{m}$  inner diameter), packed in-house with reversed-phase ReproSil-Pur  $\text{C}_{18}$  AQ 3  $\mu\text{m}$  resin (Dr. Maisch, Ammerbuch, Germany). Peptides (5  $\mu\text{l}$ ) were loaded on the column and eluted for 120 min using a segmented linear gradient of 0–5% solvent B (solvent A 5% ACN, 0.5% formic acid [FA]; solvent B 100% ACN, 0.5% FA) at a flow rate of 250  $\text{nl min}^{-1}$ . Mass spectra were acquired in data-dependent acquisition mode with a top 15 method. MS spectra were acquired in the Orbitrap analyzer with a mass range of 300–1750  $m/z$  at a resolution of 70 000 full width at half maximum (FWHM) and a target value of  $3 \times 10^6$  ions. Precursors were selected with an isolation window of 1.3  $m/z$ . HCD fragmentation was performed at a normalized collision energy of 25. MS/MS spectra were acquired with a target value of  $10^5$  ions and an intensity threshold of  $7.3 \times 10^5$  (acetylated peptides) or  $1.1 \times 10^5$  (total proteome samples) at a resolution of 17 500 FWHM and a fixed first mass of  $m/z = 100$ . Peptides with a charge of +1, a charge of  $> +6$ , or an unassigned charge state were excluded from fragmentation for MS<sup>2</sup>. Dynamic exclusion for 30 sec prevented repeated selection of precursors.

### MS/MS data analysis

Raw data were processed using MaxQuant software (version 1.6.14.0, <http://www.maxquant.org/>) (Cox and Mann, 2008) with standard settings and the match-between run and re-quantification option enabled (Cox et al., 2014). The MS ratio count was set to a minimum of two and only unmodified peptides were used for protein quantification. MS/MS spectra were searched by the Andromeda search engine (integrated in MaxQuant) against the Phytozome 13 database for genomically encoded proteins (Creinhardtii\_281\_v5.6) supplemented with organelle-specific FASTA files for mitochondrial and plastidial sequences obtained from the NCBI GenBank (Goodstein et al., 2012; Merchant et al., 2007). Sequences of 248 common contaminant proteins and decoy sequences were automatically added during the search. Data of the total proteome and acetyl lysine-enriched samples were separated into two parameter groups to permit combined analysis. Dimethylation of peptide N-termini and lysine residues were set as light ( $\text{H}_4\text{C}_2$ ), medium ( $\text{D}_4\text{C}_2$ ), and heavy ( $-\text{H}_2 + \text{D}_6^{13}\text{C}_2$ ) labels. Trypsin specificity was required and a maximum of two or four missed cleavages was allowed for total proteome and acetyl lysine-enriched samples, respectively. Minimal peptide length was set to seven amino acids. Carbamidomethylation of cysteine residues was set as fixed, with oxidation of methionine

and protein N-terminal acetylation as variable modifications. Acetylation of lysine was added as a variable modification for the antibody-enriched samples. Allowed mass deviation was 4.5 ppm for peptides and 20 ppm for fragments. The minimum score and delta score for modified peptides were filtered for a minimum Andromeda score of 35 and 6, respectively. Peptide-spectrum matches and corresponding proteins were retained if they were below a false discovery rate of 1% as estimated using a target-decoy approach from a reversed sequence database. Localization probabilities of acetylated peptides are given in Table S2. Subsequent data analyses were performed in R. The LIMMA 3.42.2 package was used to determine differentially regulated proteins and acetylation sites (Ritchie et al., 2015) in R 3.6.2 (R Core Team, 2016). Volcano plots were generated with ggplot2 3.3.0, plotting the ( $-\log_{10}$ -transformed) non-adjusted  $p$ -values versus the  $\log_2(\text{FC})$  values. The iceLogo web server was used for sequence logo creation (Colaert et al., 2009). A local blast was used in order to map the protein entries from Phytozome and the NCBI GenBank to String identifiers. String's 'Proteins with Values/Ranks - Functional Enrichment Analysis' was used to analyze the  $\log(\text{FC})$  values from full proteome experiments, while pre-filtered lists were used for functional enrichment and protein-protein interaction network analysis for acetylation sites. Mercator4 was used for functional annotation and classification of the significantly differentially regulated acK sites (Schwacke et al., 2019). The protein sequence information used for identification was uploaded to the website for annotation and the resulting mapping was used for downstream analysis and visualization in MapMan 3.6 (Lohse et al., 2014; Thimm et al., 2004).

### Citrate synthase activity

Protein extraction was carried out in BEB followed by desalting with PD-10 columns (GE Healthcare, Solingen, Germany). The protein extract was treated with deacetylase inhibitors (3  $\mu\text{M}$  apicidin [Darkin-Ratray et al., 1996] and 1 mM nicotinamide [Schmidt et al., 2004]). Citrate synthase activity was measured spectrophotometrically as described previously (Schmidtman et al., 2014). The assay was based on the absorbance of DTNB after reaction with CoA at 412 nm. Prepared protein extract (100  $\mu\text{g}$ ) was incubated with 0.5 mM acetyl-CoA (AppliChem, Darmsatdt, Germany) in 1 mM DTNB (in 100 mM Tris-HCl pH 8.0) and the reaction was started after addition of 10 mM oxaloacetate.

### Experimental design and statistical rationale

To work with the same starting material, a pre-culture of *Chlamydomonas* cells was split into three sub-cultures per condition (heterotroph, mixotroph, photoautotroph). Samples were randomly numbered 1–3 and every first, second, or third replicate sample from each condition was selected for differential dimethyl labeling to end with a light, medium, and heavy dimethyl-labeled peptide sample, which were pooled for subsequent MS analysis. The light, medium, and heavy isotopes were swapped in the third replicate to prevent any labeling bias in the data analysis. Statistical tests used to analyze data are indicated in the respective figure legends.

### ACKNOWLEDGMENTS

This work was supported by the Max-Planck Society and the University of Muenster. Open Access funding enabled and organized by Projekt DEAL.

### AUTHOR CONTRIBUTIONS

MF, A-CK, MH, LK, AH, A-VB, and KK performed research; A-CK, MH, A-VB, JN, and IF designed research; A-CK, MF,

MH, KK, and JE analyzed data; MF, A-CK, JE, DL, and IF wrote the paper.

### CONFLICTS OF INTEREST

The authors declare that they have no conflict of interest.

### DATA AVAILABILITY STATEMENT

The raw MS data and MaxQuant output files have been deposited to the ProteomeXchange Consortium (<http://proteomecentral.proteomexchange.org>) via the JPOST partner repository (Vizcaino et al., 2014) with the dataset identifiers PXD025168 and JPST001115.

### SUPPORTING INFORMATION

Additional Supporting Information may be found in the online version of this article.

**Figure S1.** Stitch DB network of proteins associated with acetate.

**Figure S2.** Stitch DB network of proteins associated with carbon dioxide.

**Figure S3.** Protein sequence alignments.

**Table S1.** Quantitative proteome analysis.

**Table S2.** Quantitative acetylome data analysis.

**Table S3.** Acetylation site occupancies.

**Table S4.** AcK fold changes of proteins involved in fatty acid metabolism.

### REFERENCES

- Attea, A., Adrait, A., Brugiére, S., Tardif, M., van Lis, R., Deusch, O. *et al.* (2009) A proteomic survey of *Chlamydomonas reinhardtii* mitochondria sheds new light on the metabolic plasticity of the organelle and on the nature of the alpha-proteobacterial mitochondrial ancestor. *Molecular Biology and Evolution*, **26**, 1533–1548.
- Baeza, J., Dowell, J.A., Smallegan, M.J., Fan, J., Amador-Noguez, D., Khan, Z. *et al.* (2014) Stoichiometry of site-specific lysine acetylation in an entire proteome. *Journal of Biological Chemistry*, **289**, 21326–21338.
- Balparda, M., Elsässer, M., Badia, M. B., Giese, J., Bovdilova, A. & Hüdig, M., *et al.* (2021) Acetylation of conserved lysines fine-tunes mitochondrial malate dehydrogenase activity in land plants. *The Plant Journal*. <https://doi.org/10.1111/tpj.15556>
- Bogaert, K.A., Perez, E., Rumin, J., Giltay, A., Carone, M., Coosemans, N. *et al.* (2019) Metabolic, physiological, and transcriptomics analysis of batch cultures of the green microalga *Chlamydomonas* grown on different acetate concentrations. *Cells*, **8**, 1367.
- Bohne, A.V., Schwarz, C., Schottkowski, M., Lidschreiber, M., Piotrowski, M., Zerges, W. *et al.* (2013) Reciprocal regulation of protein synthesis and carbon metabolism for thylakoid membrane biogenesis. *PLoS Biology*, **11**, e1001482.
- Boyle, N.R. & Morgan, J.A. (2009) Flux balance analysis of primary metabolism in *Chlamydomonas reinhardtii*. *BMC Systems Biology*, **3**, 4.
- Boyle, N.R., Sengupta, N. & Morgan, J.A. (2017) Metabolic flux analysis of heterotrophic growth in *Chlamydomonas reinhardtii*. *PLoS One*, **12**, e0177292.
- Castano-Cerezo, S., Bernal, V., Post, H., Fuhrer, T., Cappadona, S., Sanchez-Diaz, N.C. *et al.* (2014) Protein acetylation affects acetate metabolism, motility and acid stress response in *Escherichia coli*. *Molecular Systems Biology*, **10**, 762.
- Choudhary, C., Weinert, B.T., Nishida, Y., Verdin, E. & Mann, M. (2014) The growing landscape of lysine acetylation links metabolism and cell signalling. *Nature Reviews Molecular Cell Biology*, **15**, 536–550.
- Cobbold, S.A., Santos, J.M., Ochoa, A., Perlman, D.H. & Llinas, M. (2016) Proteome-wide analysis reveals widespread lysine acetylation of major protein complexes in the malaria parasite. *Scientific Reports*, **6**, 19722.
- Colaert, N., Helsens, K., Martens, L., Vandekerckhove, J. & Gevaert, K. (2009) Improved visualization of protein consensus sequences by ice-Logo. *Nature Methods*, **6**, 786–787.
- Cox, J., Hein, M.Y., Luber, C.A., Paron, I., Nagaraj, N. & Mann, M. (2014) Accurate proteome-wide label-free quantification by delayed normalization and maximal peptide ratio extraction, termed MaxLFQ. *Molecular & Cellular Proteomics*, **13**, 2513–2526.
- Cox, J. & Mann, M. (2008) MaxQuant enables high peptide identification rates, individualized p.p.b.-range mass accuracies and proteome-wide protein quantification. *Nature Biotechnology*, **26**, 1367–1372.
- Crosby, H.A., Heiniger, E.K., Harwood, C.S. & Escalante-Semerena, J.C. (2010) Reversible N epsilon-lysine acetylation regulates the activity of acyl-CoA synthetases involved in anaerobic benzoate catabolism in *Rhodospseudomonas palustris*. *Molecular Microbiology*, **76**, 874–888.
- Darkin-Rattray, S.J., Gurnett, A.M., Myers, R.W., Dulski, P.M., Crumley, T.M., Allocco, J.J. *et al.* (1996) Apicidin: a novel antiprotozoal agent that inhibits parasite histone deacetylase. *Proceedings of the National Academy of Sciences of the United States of America*, **93**, 13143–13147.
- Durante, L., Hubner, W., Lauersen, K.J. & Remacle, C. (2019) Characterization of the GPR1/FUN34/YaaH protein family in the green microalga *Chlamydomonas* suggests their role as intracellular membrane acetate channels. *Plant Direct*, **3**, e00148.
- Erickson, E., Wakao, S. & Niyogi, K.K. (2015) Light stress and photoprotection in *Chlamydomonas reinhardtii*. *The Plant Journal*, **82**, 449–465.
- Fang, X., Chen, W., Zhao, Y., Ruan, S., Zhang, H., Yan, C. *et al.* (2015) Global analysis of lysine acetylation in strawberry leaves. *Frontiers in Plant Science*, **6**, 739.
- Fernandes, J., Weddle, A., Kinter, C.S., Humphries, K.M., Mather, T., Szweida, L.I. *et al.* (2015) Lysine Acetylation Activates Mitochondrial Aconitase in the Heart. *Biochemistry*, **54**, 4008–4018.
- Finkemeier, I., Laxa, M., Miguet, L., Howden, A.J. & Sweetlove, L.J. (2011) Proteins of diverse function and subcellular location are lysine acetylated in *Arabidopsis*. *Plant Physiology*, **155**, 1779–1790.
- Gao, X., Hong, H., Li, W.C., Yang, L., Huang, J., Xiao, Y.L. *et al.* (2016) Downregulation of rubisco activity by non-enzymatic acetylation of RbcL. *Molecular Plant*, **9**, 1018–1027.
- Gardner, J.G., Grundy, F.J., Henkin, T.M. & Escalante-Semerena, J.C. (2006) Control of acetyl-coenzyme A synthetase (AcsA) activity by acetylation/deacetylation without NAD(+) involvement in *Bacillus subtilis*. *Journal of Bacteriology*, **188**, 5460–5468.
- Giese, J., Lassowskat, I. & Finkemeier, I. (2020) High-resolution lysine acetylome profiling by offline fractionation and immunoprecipitation. *Methods in Molecular Biology*, **2139**, 241–256.
- Goodenough, U., Blaby, I., Casero, D., Gallaher, S.D., Goodson, C., Johnson, S. *et al.* (2014) The path to triacylglyceride obesity in the sta6 strain of *Chlamydomonas reinhardtii*. *Eukaryotic Cell*, **13**, 591–613.
- Goodstein, D.M., Shu, S., Howson, R., Neupane, R., Hayes, R.D., Fazo, J. *et al.* (2012) Phytozome: a comparative platform for green plant genomics. *Nucleic Acids Research*, **40**, D1178–1186.
- Gorman, D.S. & Levine, R.P. (1965) Cytochrome f and plastocyanin: their sequence in the photosynthetic electron transport chain of *Chlamydomonas reinhardtii*. *Proceedings of the National Academy of Sciences of the United States of America*, **54**, 1665–1669.
- Graves, L.B. Jr, Hanzely, L. & Trelease, R.N. (1971) The occurrence and fine structural characterization of microbodies in *Euglena gracilis*. *Protoplasma*, **72**, 141–152.
- Hallmann, A. (2011) Evolution of reproductive development in the volvocine algae. *Sexual Plant Reproduction*, **24**, 97–112.
- Hansen, B.K., Gupta, R., Baldus, L., Lyon, D., Narita, T., Lammers, M. *et al.* (2019) Analysis of human acetylation stoichiometry defines mechanistic constraints on protein regulation. *Nature Communications*, **10**, 1055.
- Harris, E.H. (1989) 2 - Culture and Storage Methods. In: Harris, E.H. (Ed.) *The Chlamydomonas sourcebook*. Academic Press, pp. 25–63. Available at: <https://www.sciencedirect.com/science/article/pii/B9780123268808500079>
- Harti, M., Füssl, M., Boersema, P.J., Jost, J.O., Kramer, K., Bakirbas, A. *et al.* (2017) Lysine acetylome profiling uncovers novel histone deacetylase substrate proteins in *Arabidopsis*. *Molecular Systems Biology*, **13**, 949.
- Harti, M., König, A.C. & Finkemeier, I. (2015) Identification of lysine-acetylated mitochondrial proteins and their acetylation sites. *Methods in Molecular Biology*, **1305**, 107–121.

- Hayashi, Y., Sato, N., Shinozaki, A. & Watanabe, M. (2015) Increase in peroxisome number and the gene expression of putative glyoxysomal enzymes in *Chlamydomonas* cells supplemented with acetate. *Journal of Plant Research*, **128**, 177–185.
- Henriksen, P., Wagner, S.A., Weinert, B.T., Sharma, S., Bacinskaja, G., Rehman, M. et al. (2012) Proteome-wide analysis of lysine acetylation suggests its broad regulatory scope in *Saccharomyces cerevisiae*. *Molecular & Cellular Proteomics*, **11**, 1510–1522.
- Hooper, J.K. (1989) The *Chlamydomonas* Sourcebook. A Comprehensive Guide to Biology and Laboratory Use. Elizabeth H. Harris. Academic Press, San Diego, CA, 1989. xiv, 780 pp., illus. \$145. *Science*, **246**, 1503–1504.
- Hosp, F., Lassowskat, I., Santoro, V., De Vleeschauwer, D., Flegner, D., Redestig, H. et al. (2017) Lysine acetylation in mitochondria: from inventory to function. *Mitochondrion*, **33**, 58–71.
- Jing, E., O'Neill, B.T., Rardin, M.J., Kleinriders, A., Ilkeyeva, O.R., Ussar, S. et al. (2013) Sirt3 regulates metabolic flexibility of skeletal muscle through reversible enzymatic deacetylation. *Diabetes*, **62**, 3404–3417.
- Kato, J., Yamahara, T., Tanaka, K., Takio, S. & Satoh, T. (1997) Characterization of catalase from green algae *Chlamydomonas reinhardtii*. *Journal of Plant Physiology*, **151**, 262–268.
- Kaur, S., Héroult, J., Caruso, A., Pencréac'h, G., Come, M., Gauvry, L. et al. (2021) Proteomics and expression studies on lipids and fatty acids metabolic genes in *Isochrysis galbana* under the combined influence of nitrogen starvation and sodium acetate supplementation. *Bioresource Technology Reports*, **15**, 100714.
- Knight, S., Andersson, I. & Brändén, C.-I. (1990) Crystallographic analysis of ribulose 1,5-bisphosphate carboxylase from spinach at 2.4 Å resolution: subunit interactions and active site. *Journal of Molecular Biology*, **215**, 113–160.
- König, A.-C., Hartl, M., Boersema, P.J., Mann, M. & Finkemeier, I. (2014) The mitochondrial lysine acetylome of *Arabidopsis*. *Mitochondrion*, **19**, 252–260.
- Koskela, M.M., Brünje, A., Ivanauskaitė, A., Lopez, L.S., Schneider, D., DeTar, R.A. et al. (2020) Comparative analysis of thylakoid protein complexes in state transition mutants *nsi* and *stn7*: focus on PSI and LHClI. *Photosynthesis Research*, **145**, 15–30.
- Kunze, M., Pracharoenwattana, I., Smith, S.M. & Hartig, A. (2006) A central role for the peroxisomal membrane in glyoxylate cycle function. *Biochimica Et Biophysica Acta (BBA) - Molecular Cell Research*, **1763**, 1441–1452.
- Lassowskat, I., Hartl, M., Hosp, F., Boersema, P.J., Mann, M. & Finkemeier, I. (2017) Dimethyl-labeling-based quantification of the lysine acetylome and proteome of plants. In: Fernie, A.R., Bauwe, H. & Weber, A.P.M. (Eds.) *Photorespiration*. New York, NY: Springer New York, pp. 65–81
- Lauersen, K.J., Willamme, R., Coosemans, N., Joris, M., Kruse, O. & Remacle, C. (2016) Peroxisomal microbodies are at the crossroads of acetate assimilation in the green microalga *Chlamydomonas reinhardtii*. *Algal Research*, **16**, 266–274. <https://doi.org/10.1016/j.algal.2016.03.026>
- Ledford, H.K., Chin, B.L. & Niyogi, K.K. (2007) Acclimation to singlet oxygen stress in *Chlamydomonas reinhardtii*. *Eukaryotic Cell*, **6**, 919–930.
- Leite, G.B., Abdelaziz, A.E. & Hallenbeck, P.C. (2013) Algal biofuels: challenges and opportunities. *Bioresource Technology*, **145**, 134–141.
- L'Hernault, S.W. & Rosenbaum, J.L. (1983) *Chlamydomonas* alpha-tubulin is posttranslationally modified in the flagella during flagellar assembly. *Journal of Cell Biology*, **97**, 258–263.
- L'Hernault, S.W. & Rosenbaum, J.L. (1985) *Chlamydomonas* alpha-tubulin is posttranslationally modified by acetylation on the epsilon-amino group of a lysine. *Biochemistry*, **24**, 473–478.
- Lingard, M.J. & Trelease, R.N. (2006) Five *Arabidopsis* peroxin 11 homologs individually promote peroxisome elongation, duplication or aggregation. *Journal of Cell Science*, **119**, 1961–1972.
- Liu, F., Yang, M., Wang, X., Yang, S., Gu, J., Zhou, J. et al. (2014) Acetylome analysis reveals diverse functions of lysine acetylation in *Mycobacterium tuberculosis*. *Molecular & Cellular Proteomics*, **13**, 3352–3366.
- Liu, Z., Song, J., Miao, W., Yang, B., Zhang, Z., Chen, W. et al. (2021) Comprehensive proteome and lysine acetylome analysis reveals the widespread involvement of acetylation in cold resistance of pepper (*Capsicum annuum* L.). *Frontiers in Plant Science*, **12**, 730489.
- Lohse, M., Nagel, A., Herter, T., May, P., Schroda, M., Zrenner, R. et al. (2014) Mercator: a fast and simple web server for genome scale functional annotation of plant sequence data. *Plant, Cell and Environment*, **37**, 1250–1258.
- Magneschi, L., Catalanotti, C., Subramanian, V., Dubini, A., Yang, W., Mus, F. et al. (2012) A mutant in the ADH1 gene of *Chlamydomonas reinhardtii* elicits metabolic restructuring during anaerobiosis. *Plant Physiology*, **158**, 1293–1305.
- Merchant, S.S., Kropat, J., Liu, B.S., Shaw, J. & Warakanont, J. (2012) TAG, You're it! *Chlamydomonas* as a reference organism for understanding algal triacylglycerol accumulation. *Current Opinion in Biotechnology*, **23**, 352–363.
- Merchant, S.S., Prochnik, S.E., Vallon, O., Harris, E.H., Karpowicz, S.J., Witman, G.B. et al. (2007) The *Chlamydomonas* genome reveals the evolution of key animal and plant functions. *Science*, **318**, 245–250.
- Nakayasu, E.S., Wu, S., Sydor, M.A., Shukla, A.K., Weitz, K.K., Moore, R.J. et al. (2014) A method to determine lysine acetylation stoichiometries. *International Journal of Proteomics*, **2014**, 730725.
- Narita, T., Weinert, B.T. & Choudhary C. (2019) Functions and mechanisms of non-histone protein acetylation. *Nature Reviews Molecular Cell Biology*, **20**, 156–174.
- Olsen, J.V., Vermeulen, M., Santamaria, A., Kumar, C., Miller, M.L., Jensen, L.J. et al. (2010) Quantitative phosphoproteomics reveals widespread full phosphorylation site occupancy during mitosis. *Science Signalling*, **3**, ra3.
- Plancke, C., Vigeolas, H., Hohner, R., Roberty, S., Emonds-Ait, B., Larosa, V. et al. (2014) Lack of isocitrate lyase in *Chlamydomonas* leads to changes in carbon metabolism and in the response to oxidative stress under mixotrophic growth. *The Plant Journal*, **77**, 404–417.
- R Core Team. (2016) *R: A language and environment for statistical computing*. Vienna: R Foundation for Statistical Computing. Available at: <https://www.R-project.org/>
- Rai, M.P., Nigam, S. & Sharma, R. (2013) Response of growth and fatty acid compositions of *Chlorella pyrenoidosa* under mixotrophic cultivation with acetate and glycerol for bioenergy application. *Biomass and Bioenergy*, **58**, 251–257.
- Ritchie, M.E., Phipson, B., Wu, D., Hu, Y., Law, C.W., Shi, W. et al. (2015) Limma powers differential expression analyses for RNA-sequencing and microarray studies. *Nucleic Acids Research*, **43**, e47.
- Roach, T., Sedoud, A. & Krieger-Liszak, A. (2013) Acetate in mixotrophic growth medium affects photosystem II in *Chlamydomonas reinhardtii* and protects against photoinhibition. *Biochimica Et Biophysica Acta*, **1827**, 1183–1190.
- Sager, R. & Granick, S. (1953) Nutritional studies with *Chlamydomonas reinhardtii*. *Annals of the New York Academy of Sciences*, **56**, 831–838.
- Schilling, B., Christensen, D., Davis, R., Sahu, A.K., Hu, L.L., Walker-Peddakotla, A. et al. (2015) Protein acetylation dynamics in response to carbon overflow in *Escherichia coli*. *Molecular Microbiology*, **98**, 847–863.
- Schmidt, C., Beilstein-Edmands, V., Mohammed, S. & Robinson, C.V. (2017) Acetylation and phosphorylation control both local and global stability of the chloroplast F1 ATP synthase. *Scientific Reports*, **7**, 44068.
- Schmidt, M.T., Smith, B.C., Jackson, M.D. & Denu, J.M. (2004) Coenzyme specificity of Sir2 protein deacetylases: implications for physiological regulation. *Journal of Biological Chemistry*, **279**, 40122–40129.
- Schmidtman, E., König, A.C., Orwat, A., Leister, D., Hartl, M. & Finkemeier, I. (2014) Redox regulation of *Arabidopsis* mitochondrial citrate synthase. *Molecular Plant*, **7**, 156–169.
- Schwacke, R., Ponce-Soto, G.Y., Krause, K., Bolger, A.M., Arsova, B., Hallab, A. et al. (2019) MapMan4: a refined protein classification and annotation framework applicable to multi-omics data analysis. *Molecular Plant*, **12**, 879–892.
- Scranton, M.A., Ostrand, J.T., Fields, F.J. & Mayfield, S.P. (2015) *Chlamydomonas* as a model for biofuels and bio-products production. *The Plant Journal*, **82**, 523–531.
- Shannon, P., Markiel, A., Ozier, O., Baliga, N.S., Wang, J.T., Ramage, D. et al. (2003) Cytoscape: a software environment for integrated models of biomolecular interaction networks. *Genome Research*, **13**, 2498–2504.
- Smith, R.T., Bangert, K., Wilkinson, S.J. & Gilmour, D.J. (2015) Synergistic carbon metabolism in a fast growing mixotrophic freshwater microalgal species *Micractinium inermum*. *Biomass and Bioenergy*, **82**, 73–86.
- Stabenau, H. (1974) Localization of enzymes of glycolate metabolism in the alga *Chlorogonium elongatum*. *Plant Physiology*, **54**, 921–924.

- Stabenau, H., Winkler, U. & Säftel, W. (1993) Localization of glycolate dehydrogenase in two species of *Dunaliella*. *Planta*, **191**, 362–364.
- Starai, V.J., Celic, I., Cole, R.N., Boeke, J.D. & Escalante-Semerena, J.C. (2002) Sir2-dependent activation of acetyl-CoA synthetase by deacetylation of active lysine. *Science*, **298**, 2390–2392.
- Starai, V.J. & Escalante-Semerena, J.C. (2004) Identification of the protein acetyltransferase (Pat) enzyme that acetylates acetyl-CoA synthetase in *Salmonella enterica*. *Journal of Molecular Biology*, **340**, 1005–1012.
- Sterner, D.E. & Berger, S.L. (2000) Acetylation of histones and transcription-related factors. *Microbiology and Molecular Biology Reviews*, **64**, 435–459.
- Szklarczyk, D., Santos, A., von Mering, C., Jensen, L.J., Bork, P. & Kuhn, M. (2016) STITCH 5: augmenting protein-chemical interaction networks with tissue and affinity data. *Nucleic Acids Research*, **44**, D380–D384.
- Thimm, O., Blasing, O., Gibon, Y., Nagel, A., Meyer, S., Kruger, P. *et al.* (2004) MAPMAN: a user-driven tool to display genomics data sets onto diagrams of metabolic pathways and other biological processes. *The Plant Journal*, **37**, 914–939.
- Tirumani, S., Kokkanti, M., Chaudhari, V., Shukla, M. & Rao, B.J. (2014) Regulation of CCM genes in *Chlamydomonas reinhardtii* during conditions of light-dark cycles in synchronous cultures. *Plant Molecular Biology*, **85**, 277–286.
- Tyanova, S., Temu, T. & Cox, J. (2016) The MaxQuant computational platform for mass spectrometry-based shotgun proteomics. *Nature Protocols*, **11**, 2301–2319.
- Uhrig, R.G., Schlapfer, P., Roschitzki, B., Hirsch-Hoffmann, M. & Gruissem, W. (2019) Diurnal changes in concerted plant protein phosphorylation and acetylation in *Arabidopsis* organs and seedlings. *The Plant Journal*, **99**, 176–194.
- Vizcaino, J.A., Deutsch, E.W., Wang, R., Csordas, A., Reisinger, F., Rios, D. *et al.* (2014) ProteomeXchange provides globally coordinated proteomics data submission and dissemination. *Nature Biotechnology*, **32**, 223–226.
- Wagner, G.R. & Payne, R.M. (2013) Widespread and enzyme-independent Nepsilon-acetylation and Nepsilon-succinylation of proteins in the chemical conditions of the mitochondrial matrix. *Journal of Biological Chemistry*, **288**, 29036–29045.
- Wang, Q., Zhang, Y., Yang, C., Xiong, H., Lin, Y., Yao, J. *et al.* (2010) Acetylation of metabolic enzymes coordinates carbon source utilization and metabolic flux. *Science*, **327**, 1004–1007.
- Weinert, B.T., Satpathy, S., Hansen, B.K., Lyon, D., Jensen, L.J. & Choudhary, C. (2017) Accurate quantification of site-specific acetylation stoichiometry reveals the impact of sirtuin deacetylase CobB on the *E. coli* acetylome. *Molecular & Cellular Proteomics*, **16**, 759–769.
- Wisniewski, J.R., Zougman, A., Nagaraj, N. & Mann, M. (2009) Universal sample preparation method for proteome analysis. *Nature Methods*, **6**, 359–362.
- Work, V.H., Radakovits, R., Jinkerson, R.E., Meuser, J.E., Elliott, L.G., Vinyard, D.J. *et al.* (2010) Increased lipid accumulation in the *Chlamydomonas reinhardtii* sta7-10 starchless isoamylase mutant and increased carbohydrate synthesis in complemented strains. *Eukaryotic Cell*, **9**, 1251–1261.
- Wu, X., Oh, M.H., Schwarz, E.M., Larue, C.T., Sivaguru, M., Imai, B.S. *et al.* (2011) Lysine acetylation is a widespread protein modification for diverse proteins in *Arabidopsis*. *Plant Physiology*, **155**, 1769–1778.
- Xue, H., Tokutsu, R., Bergner, S.V., Scholz, M., Minagawa, J. & Hippler, M. (2015) PHOTOSYSTEM II SUBUNIT R is required for efficient binding of LIGHT-HARVESTING COMPLEX STRESS-RELATED PROTEIN3 to photosystem II-light-harvesting supercomplexes in *Chlamydomonas reinhardtii*. *Plant Physiology*, **167**, 1566–1578.
- Yang, W., Catalanotti, C., D'Adamo, S., Wittkopp, T.M., Ingram-Smith, C.J., Mackinder, L. *et al.* (2014) Alternative acetate production pathways in *Chlamydomonas reinhardtii* during dark anoxia and the dominant role of chloroplasts in fermentative acetate production. *The Plant Cell*, **26**, 4499–4518.
- Ynalvez, R.A., Xiao, Y., Ward, A.S., Cunnusamy, K. & Moroney, J.V. (2008) Identification and characterization of two closely related beta-carbonic anhydrases from *Chlamydomonas reinhardtii*. *Physiologia Plantarum*, **133**, 15–26.
- Zhao, S., Xu, W., Jiang, W., Yu, W., Lin, Y., Zhang, T. *et al.* (2010) Regulation of cellular metabolism by protein lysine acetylation. *Science*, **327**, 1000–1004.
- Zhou, H., Finkemeier, I., Guan, W., Tossounian, M.A., Wei, B., Young, D. *et al.* (2018) Oxidative stress-triggered interactions between the succinyl- and acetyl-proteomes of rice leaves. *Plant, Cell and Environment*, **41**, 1139–1153.

Publication 2

**Beyond Histones: New Substrate Proteins of  
Lysine Deacetylases in *Arabidopsis* Nuclei.**

**Füßl M**, Lassowski I, Née G, Koskela M, Brünje A, Tilak P, Giese J,  
Leister D, Mulo P, Schwarzer D, Finkemeier I.  
(2018)

*Frontiers in Plant Science* (10;9:461)



# Beyond Histones: New Substrate Proteins of Lysine Deacetylases in Arabidopsis Nuclei

Magdalena Füßl<sup>1,2</sup>, Ines Lassowskat<sup>1</sup>, Guillaume Née<sup>1</sup>, Minna M. Koskela<sup>3</sup>, Annika Brünje<sup>1</sup>, Priyadarshini Tilak<sup>1</sup>, Jonas Giese<sup>1</sup>, Dario Leister<sup>2</sup>, Paula Mulo<sup>3</sup>, Dirk Schwarzer<sup>4</sup> and Iris Finkemeier<sup>1\*</sup>

<sup>1</sup> Plant Physiology, Institute of Plant Biology and Biotechnology, University of Münster, Münster, Germany, <sup>2</sup> Plant Molecular Biology, Department Biology I, Ludwig-Maximilians-University Munich, Munich, Germany, <sup>3</sup> Molecular Plant Biology, Department of Biochemistry, University of Turku, Turku, Finland, <sup>4</sup> Interfaculty Institute of Biochemistry, University of Tübingen, Tübingen, Germany

## OPEN ACCESS

### Edited by:

Stéphane Bourque,  
Université de Bourgogne, France

### Reviewed by:

Serena Varotto,  
Università degli Studi di Padova, Italy  
Valentin Hammoudi,  
Freie Universität Berlin, Germany

### \*Correspondence:

Iris Finkemeier  
iris.finkemeier@uni-muenster.de

### Specialty section:

This article was submitted to  
Plant Physiology,  
a section of the journal  
Frontiers in Plant Science

**Received:** 11 February 2018

**Accepted:** 23 March 2018

**Published:** 10 April 2018

### Citation:

Füßl M, Lassowskat I, Née G, Koskela MM, Brünje A, Tilak P, Giese J, Leister D, Mulo P, Schwarzer D and Finkemeier I (2018) Beyond Histones: New Substrate Proteins of Lysine Deacetylases in Arabidopsis Nuclei. *Front. Plant Sci.* 9:461. doi: 10.3389/fpls.2018.00461

The reversible acetylation of lysine residues is catalyzed by the antagonistic action of lysine acetyltransferases and deacetylases, which can be considered as master regulators of their substrate proteins. Lysine deacetylases, historically referred to as histone deacetylases, have profound functions in regulating stress defenses and development in plants. Lysine acetylation of the N-terminal histone tails promotes gene transcription and decondensation of chromatin, rendering the DNA more accessible to the transcription machinery. In plants, the classical lysine deacetylases from the RPD3/HDA1-family have thus far mainly been studied in the context of their deacetylating activities on histones, and their versatility in molecular activities is still largely unexplored. Here we discuss the potential impact of lysine acetylation on the recently identified nuclear substrate proteins of lysine deacetylases from the Arabidopsis RPD3/HDA1-family. Among the deacetylase substrate proteins, many interesting candidates involved in nuclear protein import, transcriptional regulation, and chromatin remodeling have been identified. These candidate proteins represent key starting points for unraveling new molecular functions of the Arabidopsis lysine deacetylases. Site-directed engineering of lysine acetylation sites on these target proteins might even represent a new approach for optimizing plant growth under climate change conditions.

**Keywords:** lysine acetylation, histone deacetylase, acetyltransferase, Arabidopsis, histones, transcription factors

## INTRODUCTION

Lysine acetylation was first discovered on histones (Allfrey et al., 1964); and the deacetylases and acetyltransferases were originally named accordingly (Brownell et al., 1996; Taunton et al., 1996). Lysine deacetylases (KDACs), formerly referred to as histone deacetylases (HDACs), have profound functions in plant development and acclimation toward abiotic and biotic stresses (reviewed in Luo et al., 2017). KDACs catalyze the removal of the acetyl group on lysine residues, and therefore antagonize lysine acetyltransferases (KATs). While inactivation of some plant KDACs can improve abiotic stress tolerance, the inactivation of others decreases stress resistance and induces developmental defects (Kim et al., 2017; Ueda et al., 2017). The different roles of KDACs

partially correlate with their classification into three families: (1) Reduced Potassium Dependency 3/Histone Deacetylase 1 (RPD3/HDA1)-like, (2) the plant-specific type 2 Histone Deacetylases (HD-tuins), and (3) Silent Information Regulator 2-like (sirtuins). The RPD3/HDA1-family, which is referred to as the 'classical' KDAC family (De Ruijter et al., 2003), can be further subdivided into three classes: class I (RPD3-like), class II (HDA1-like), and class IV KDACs. Members of the classical KDAC family are Zn<sup>2+</sup>-dependent enzymes, which cleave the acetyl-group of modified lysine residues hydrolytically. Based on sequence homology, the Arabidopsis genome encodes four class I (HDA 6, 7, 9, 19), five class II (HDA 5, 8, 15, 14, 18), and one class IV (HDA 2) KDAC proteins (Ueda et al., 2017). In addition, two potential class I KDAC proteins (HDA10, 17) lacking an intact catalytic domain are encoded in the Arabidopsis genome. For only a few Arabidopsis KDAC proteins, such as HDA6 and HDA14, specific acetylated target proteins, other than histones, have been identified thus far (Tran et al., 2012; Hao et al., 2016; Hartl et al., 2017). Inhibitors have been successfully used to study KDAC functions in various organisms. The fungal antibiotic trichostatin A (TSA) was the first identified and potent inhibitor of all classical KDAC enzymes. Apicidin, another fungal KDAC inhibitor, has a much higher potency for class I KDACs than for class II KDACs, and is thus regarded as a class I specific inhibitor (Bradner et al., 2010). Both inhibitors have recently been used in two different proteomic approaches to elucidate potential *in vivo* substrates of the classical KDACs in Arabidopsis leaf tissue and human cell culture (Schölz et al., 2015; Hartl et al., 2017). Furthermore, KDAC inhibitors can enhance the resistance to salinity in plants, and in humans they are used in cancer therapy (Gallinari et al., 2007; Ueda et al., 2017). Hence, understanding the molecular function of these inhibitors will be fundamental for therapeutic applications, as well as genetic engineering of crops.

## NUCLEAR SUBSTRATE PROTEINS OF THE CLASSICAL KDACs IN ARABIDOPSIS

Under physiological conditions, lysine residues of proteins are usually positively charged. Loss of the positive charge, as well as the increased length of the lysine side chain upon acetylation, can affect the biological function of proteins, such as enzyme activities, protein-protein, and protein-DNA interactions (Yang and Seto, 2008). For example, lysine acetylation regulates the charge of a basic interface on SUMO proteins, which then controls SUMO-mediated interactions (Ullmann et al., 2012). Hartl et al. (2017) identified 77 putatively nuclear KDAC substrate proteins with increased abundance in lysine acetylation after application of TSA or apicidin to Arabidopsis leaves. While acetylation sites on 25 of those proteins were up-regulated by both inhibitors, 39 and 13 proteins were regulated by either apicidin or TSA, respectively. This indicates that different classes of classical KDACs are active in the nucleus of Arabidopsis leaves. However, further studies will be required to match the protein targets with the respective KDAC. In the following, we will discuss the possible implications of lysine acetylation on

the functions of selected nuclear protein substrates important in plant stress physiology and development, which might be either direct or indirect targets of the classical Arabidopsis KDACs (Hartl et al., 2017).

## HISTONES

Histone octamers are responsible for packaging DNA into chromatin. The histone octamers consist of two copies of each H2A-, H2B-, H3-, and H4-type histones (Kornberg, 1974; Luger et al., 1997). The unstructured lysine-rich N-terminal tails of histones (**Figure 1**) are largely conserved in higher eukaryotes (Fuchs et al., 2006; Postberg et al., 2010). At least 20 of these lysine residues of mammalian histones can be acetylated, which is known to stimulate transcriptional activation (Jenuwein and Allis, 2001; Robyr et al., 2004). While the acetylation sites on the H3- and H4- tails are highly conserved between Arabidopsis and human, the sequences of the H2A and H2B-tails are much more diverse (**Figure 1**) (Kawashima et al., 2015). Lysine acetylation sites on all four core-histones were found strongly up-regulated upon KDAC inhibition in plant and human cells (**Figure 1**) (Schölz et al., 2015; Hartl et al., 2017). Acetylation of the histone tails generally results in an open chromatin structure, which makes the DNA more accessible to transcriptional regulators. Acetylated lysine residues are recognized by bromodomains, which serve as acetyl-lysine binding modules (Taverna et al., 2007). Furthermore, lysine acetylation antagonizes other regulatory lysine modifications such as methylation, which modulates transcription by recruiting chromodomain-containing chromatin factors to the DNA template. While several lysine acetylation sites on H3- and H4-type histones have been identified as targets of specific Arabidopsis KDACs previously (reviewed in Luo et al., 2017), the KDAC target sites on H2A- and H2B-type histones were only recently discovered (**Figure 1**) (Hartl et al., 2017). Different H2 variants have important roles in environmental stress acclimation in plants, such as in DNA-strand break repair (Talbert and Henikoff, 2014). Hence, in this context it will be interesting to investigate the specific role of the H2A- and H2B- acetylation sites, and whether all of them are targets of Arabidopsis HDA6 (Earley et al., 2006), or whether other KDACs are also involved in the regulation of H2 acetylation.

## TRANSCRIPTION FACTORS AND CHROMATIN REMODELING COMPLEXES

Next to histones, at least 20 different proteins involved in transcriptional regulation have been identified as putative target proteins of the Arabidopsis KDACs (Hartl et al., 2017). It can be expected that these newly identified acetylation sites might have important roles for transcriptional regulation (**Figure 2A**). The zinc finger transcription factor Yin Yang 1 (YY1, At4g06634) becomes hyper-acetylated upon KDAC inhibition (Hartl et al., 2017). YY1 plays important roles in

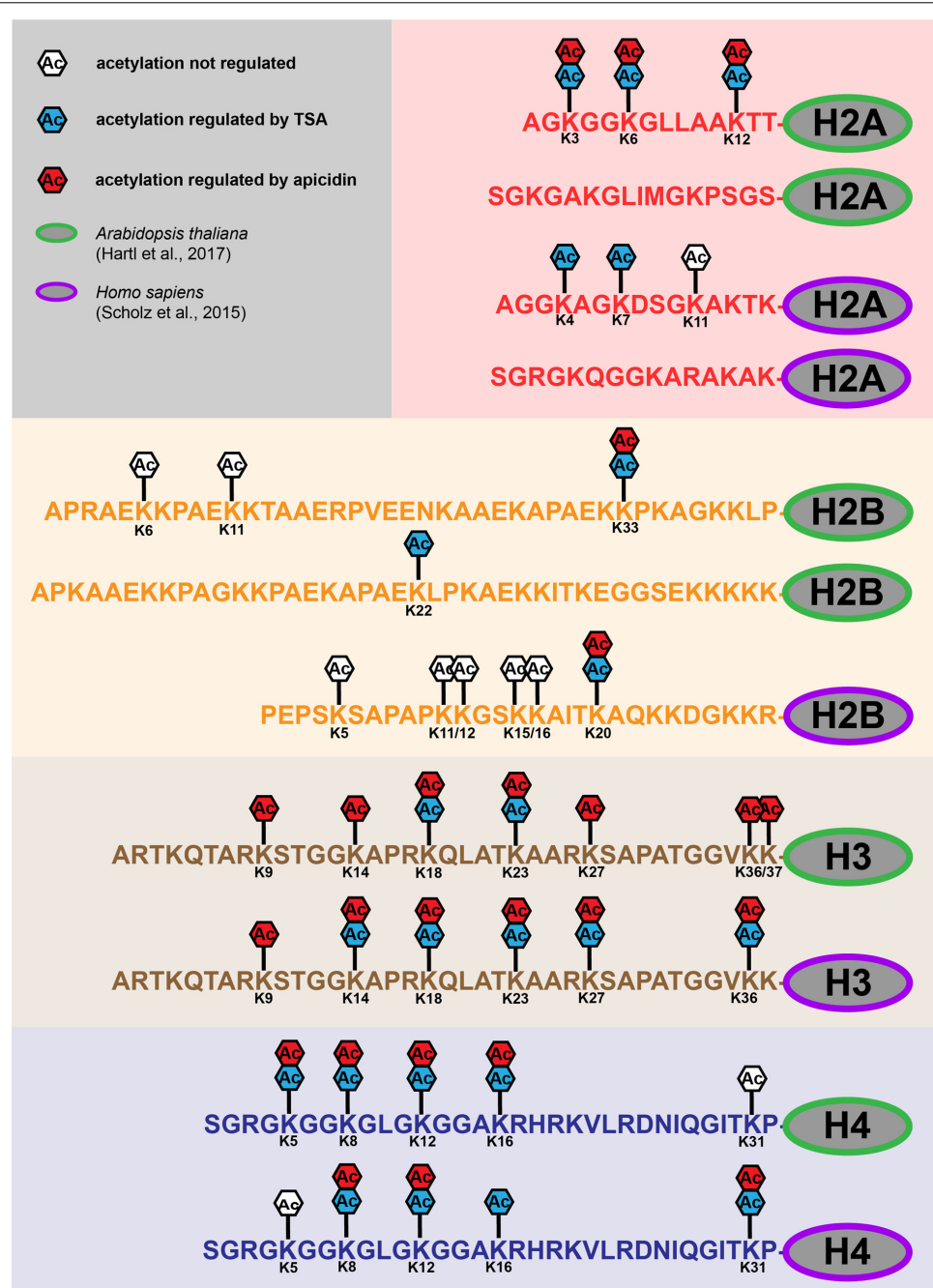
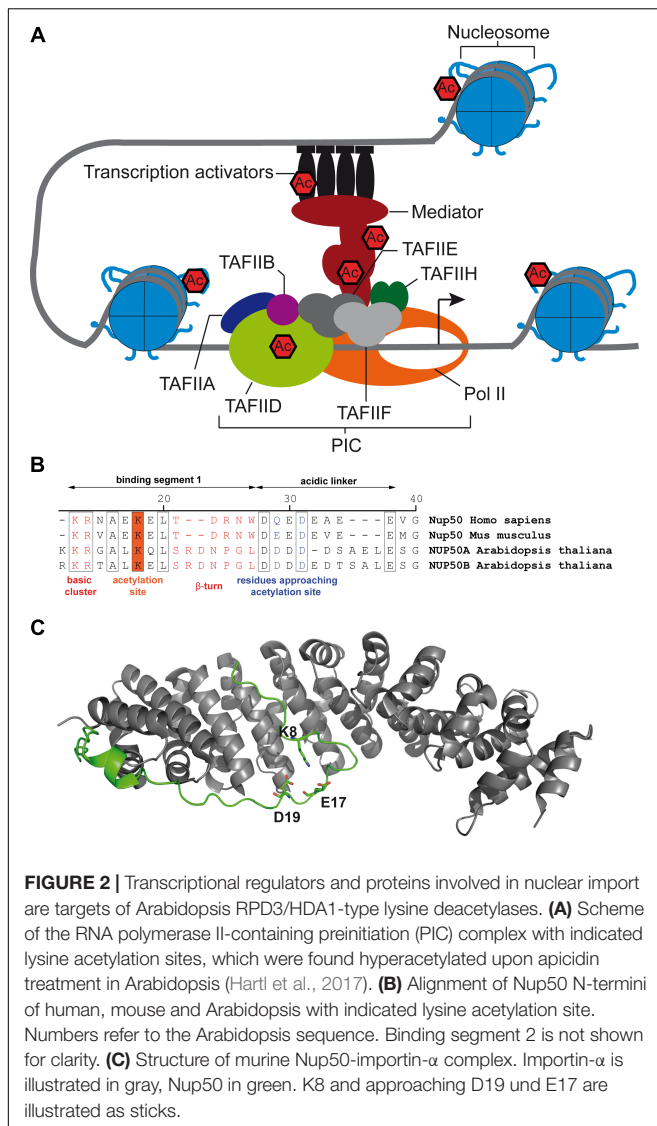


**FIGURE 1 |** Regulation of lysine acetylation sites of core histones in *Arabidopsis thaliana* and *Homo sapiens*. Up-regulation of lysine acetylation sites (Ac) on histone tails (H2A, H2B, H3 and H4) of *Arabidopsis* (green) and human (purple) upon TSA (blue) and apicidin (red) treatment. White boxes (Ac) indicate acetylation sites, which were not regulated in abundance upon inhibitor treatments. For details on identifications, see Table EV1a and Table EV2a (Hartl et al., 2017) and Supplementary Table S2 (Schölz et al., 2015). Human histone H2B lysine acetylation sites where derived from multiple proteins differing only a few amino acids in their histone tails (Q93079, B4DLA9, P62807, P33778, P58876, Q8N257, Q99880). Human and *Arabidopsis* histone H2As and *Arabidopsis* histone H2B variants exhibit two distinct tails shown here separately. Lysine acetylation sites in structured domains of histones are not depicted.

the abscisic acid (ABA) response and was recently identified as regulated by phosphorylation (Wu et al., 2012; Wu and Li, 2017). Hence, it will be interesting to investigate the interplay between phosphorylation and acetylation on YY1. YY1 shows structural similarities with the mammalian YY1 protein, which contains

four conserved C2H2 zinc fingers domains. The human YY1 protein is part of the INOSITOL AUXOTROPHY80 (INO80) chromatin-remodeling complex, which enables YY1 to bind its target genes (Cai et al., 2007). Although INO80 is conserved in *Arabidopsis*, it is still unknown if YY1 is also part of this complex



in plants. YY1 can simultaneously act as transcriptional activator and repressor. While it is a negative regulator of ABA-responsive gene expression in plants, it enhances the expression of the ABA REPRESSOR 1 gene and thereby tunes the ABA signaling pathway (Li et al., 2016). In Arabidopsis, YY1 was shown to interact with the protein Mediator 18 (MED18) to suppress the expression of certain disease susceptibility genes, thereby enhancing fungal resistance (Lai et al., 2014). The identified lysine acetylation site (K210) is present in the interaction domain of YY1 and MED18. Hence, the interaction between MED18 and YY1 might be regulated by KDACs to induce the plant resistance against fungal infection. Overexpression of Arabidopsis HDA19, for example, enhanced the resistance against *Alternaria brassicicola* (Zhou et al., 2005).

In addition to YY1, the transcription factor WRKY1 was identified as potential target of class I KDACs (Hartl et al., 2017). WRKY1, also known as Zinc-dependent Activator Protein-1 (ZAP1), is strongly induced by salicylic acid, and it regulates

the plant's response to pathogen attack (Duan et al., 2007). In addition, it acts as a negative regulator of ABA signaling in guard cells (Qiao et al., 2016). This is especially interesting in the context of HDA6-deficient mutants showing increased drought resistance (Kim et al., 2017). Hence, it will be of great interest to investigate whether drought resistance is mediated via acetylation of WRKY1. The acetylation site within the WRKY 1 (K421) protein lies downstream of the second WRKY domain (AS 301-366) in a unique domain of WRKY1-like proteins.

Another interesting putative KDAC target protein is TIME FOR COFFEE (TIC; AT3G22380). TIC is a nuclear protein required for the light-dependent regulation of the circadian clock in plants (Hall et al., 2003). TIC has been shown to play a role in multiple clock-regulated processes including iron homeostasis (Duc et al., 2009), jasmonic acid signaling (Shin et al., 2012), auxin transport (Hong et al., 2014), and metabolic signaling through SnRK1 to the circadian clock (Shin et al., 2017). Hence, TIC seems to play an important role in synchronizing environmental signals and cellular homeostasis with the circadian clock. TIC encodes a nuclear protein without conserved functional domains, rendering sequence-based predictions challenging. TIC potentially contains A-motifs (Ding et al., 2007), typically found in ATP/GTP binding proteins, but this remains to be experimentally verified. Despite its connection to the light-dependent control of circadian rhythm, the expression of TIC and the abundance of the protein remain unaltered throughout the day-night cycle (Ding et al., 2007). This implies that TIC function could be mediated either via PTMs or by interactions with other components. Recently, a lysine acetylation site (K340) was discovered on TIC after TSA treatment (Hartl et al., 2017). Whether this modification bears a significance to the protein-protein interactions and function of TIC needs to be investigated. In this context it is tempting to speculate that acetylation, via the abundance of acetyl-CoA, would function as a signal from cellular metabolism to the circadian clock.

In eukaryotes, transcription starts with the binding of specific transcription factors and chromatin remodelers at gene promoters, which enables the assembly of the preinitiation complex at the core promoter (Figure 2A). The preinitiation complex includes RNA polymerase II, as well as the general transcription factors [transcription initiation factor II A (TFIIA), TFIIB, TFIID, TFIIE, TFIIIF, and TFIIH], in addition to the Mediator complex. The Mediator complex, composed of at least 25 subunits, is essential for transcription in all higher eukaryotes, and it acts as a transcriptional co-regulator (reviewed in Soutourina, 2017). The Mediator complex directly interacts with various transcription factors, and in plants expression of its subunits is strongly regulated by environmental conditions (Samanta and Thakur, 2015). So far, it is elusive how the protein-protein interactions between Mediator and the different transcription factors, as well as interactions between Mediator subunits, are regulated, but PTMs are thought to play a key role in this (Soutourina, 2017). In Arabidopsis, three subunits of the Mediator complex, MED12 (K930, At4g00450), MED13 (K1676, At1g55325) and MED19a (K210, At5g12230), are hyperacetylated after KDAC inhibition (Hartl et al., 2017).

Interestingly, the orthologs of MED12 and MED13 were also identified as KDAC targets in human cell lines (Schölz et al., 2015). In plants, both MED12 and MED13 are known as global regulators of development during germination, vegetative phase change and flowering (Gillmor et al., 2014). Hence, it will be of great interest to investigate whether the developmental defects observed in various KDAC mutants of Arabidopsis are, apart from changes in histone acetylation, also due to altered activities of the Mediator complex (Wang et al., 2014). Additionally, some Mediator subunits, such as MED19a, are also important for abiotic and biotic stress signaling (Seo et al., 2017).

As antagonists of KDACs, KATs are critical for the regulation of gene expression. Reminiscent of kinase activation by auto-phosphorylation, KATs are often activated by auto-acetylation (Karanam et al., 2006). While several KATs were identified as de-acetylation targets of Arabidopsis KDACs, it is interesting to note that KDACs were not identified among the lysine-acetylated proteins. This might indicate that KDACs are regulated by other PTMs, such as nitrosylation (Mengel et al., 2017). Two paralogous acetyltransferases, HAC1 (AT1G79000) and HAC5 (AT3G12980) from the CBP-type family, were identified among the nuclear KDAC substrate proteins in Arabidopsis (Hartl et al., 2017). HAC1 and HAC5 are orthologs of the human p300 and CBP acetyltransferases, respectively, and they have roles in the regulation of flowering time and ethylene signaling (Li et al., 2014). In addition, HAC1 is necessary for resistance against bacteria (Li et al., 2014; Singh et al., 2014). HAC1 and HAC5 showed a marked increase of acetylation on three (HAC1: K1354, K1355, K1359) and four (HAC5: K1330, K1334, K1335, K1339) lysine residues, respectively, after apicidin treatment. All four lysine residues are conserved between both HAC1 and HAC5 and two sites (HAC5: K1330 and K1334) are conserved and found acetylated in the human p300 (K1546 and K1560) and CBP proteins, respectively (Thompson et al., 2004; Schölz et al., 2015). In p300, these sites belong to an auto-inhibitory loop (K1520–1560) that is regulated by auto-acetylation. Removal of this loop constantly activated the acetyltransferase domain (Thompson et al., 2004). A p300 K1560R mutant was defective in acetylation-based enzyme activation. In addition, acetylation of the loop was shown to be under control of KDACs in human cell extracts. Hence, due to the high conservation of the enzyme functions and acetylation sites in the activation loop, it can be expected that the activity of Arabidopsis HAC1 and HAC5 is negatively regulated by KDACs as well. Upon TSA treatment, two additional lysine acetylation sites were identified on HAC1 (K770, K819). The motif and lysine acetylation of K819 is again conserved in human p300 (K1024) and regulated by the sirtuin-type lysine deacetylase SIRT1 (Bouras et al., 2005). In p300, K1024 is part of the cell cycle regulatory domain 1, and is also target of sumoylation. SIRT1 stimulates p300 sumoylation by deacetylating K1024 to suppress p300 activity. Although sumoylation sites have been identified on Arabidopsis KATs (Miller et al., 2013), it is yet unclear whether sumoylation also negatively regulates the activity of HAC1 in Arabidopsis.

GCN5 is the catalytic acetyltransferase subunit of the SAGA (Spt-Ada-Gcn5) complex, which is conserved in eukaryotes and

acts as a transcriptional activator at many target loci. In this complex, the subunit Ada2 serves as an anchor to incorporate the GCN5-KAT module into the structure of SAGA (Kassem et al., 2017). In Arabidopsis, three acetylated lysine residues of ADA2a (AT3G07740) were found increased in abundance upon inhibition with apicidin and TSA (Hartl et al., 2017). The three lysine residues, K214, K229 and K230, are located in a protein region of Ada2a, which is involved in binding GCN5 (Mao et al., 2006). Hence, it can be assumed that acetylation of these lysine residues could be a prerequisite for the association of ADA2a with GCN5 (Srivastava et al., 2015). In addition, the TATA-binding protein associated factor 5 (TAF5) becomes hyperacetylated at four consecutive lysine residues (K274, 280, 286, 293) after apicidin treatment. TAF5 is a scaffold protein connecting different structural domains in both SAGA and transcription factor II D (TFIID) complexes (Figure 2A). The stretch of acetylated lysine residues in Arabidopsis TAF5 lies within a linker region between two conserved functional domains: the TAF5 N-terminal domain 2 domain (aa 60–200), which defines the homodimer interface and contains a Ca<sup>2+</sup>-binding site, and six WD40 repeat domains (from aa 320–669). WD-repeat domains form a beta-propeller architecture for protein interactions and the WD40 domains of TAF5 were shown to be important for incorporating TAF5 into both TFIID and the SAGA complex in yeast (Durso et al., 2001).

Interestingly, two additional proteins, AtSWC4 (At2g47210) and AtEAF1 (At3g24870), which are thought to be involved in the formation of a nuclear KAT complex NuA4 (Bieluszewski et al., 2015), were identified as putative targets of Arabidopsis KDACs (Hartl et al., 2017). The yeast homolog of SWC4 is part of both the NuA4 complex (and important for histone H4 acetylation) and the chromatin remodeling complex SWR1-C, in which SWC4 is involved in the incorporation of the histone variant H2AZ into nucleosomes (Kobor et al., 2004).

## NUCLEAR PROTEIN IMPORT: Nup50

Nuclear import of proteins exceeding a mass of 40 kD requires specific carrier proteins (Stewart, 2007). The regulation of nuclear protein import and export is particularly important for the regulation of gene expression during developmental and acclimation responses in all eukaryotes. Different PTMs play key roles in regulating protein import (Christie et al., 2016), and lysine acetylation can modulate the nuclear localization sequences (NLS) of proteins by modulating the residue charge thus altering the interaction with the transport machinery. The most common translocation pathway employs basic NLSs on cargo proteins, importin- $\beta$  enabling passage through the nuclear pore, and importin- $\alpha$  serving as an adapter between cargo and importin- $\beta$ . The small GTPase Ran, in its GTP-bound state, disassembles the import complex after transport to the nucleoplasm. In mammals, the cargo release is further facilitated by the Nup50 protein, which binds to the C-terminal region of importin- $\alpha$  and competes for the NLS binding groove (Matsuura and Stewart, 2005). The Arabidopsis genome encodes

two nucleoplasm-localized Nup50 homologues, At1g52380 (Nup50a) and At3g52380 (Nup50b), which show significant similarity to mammalian Nup50 (Tamura et al., 2010). Structural analysis of murine Nup50 has revealed that Nup50 interacts with importin- $\alpha$  via two binding segments (Matsuura and Stewart, 2005). Binding segment 2 binds to the C-terminal armadillo repeats of importin- $\alpha$  allowing segment 1 to interact with the NLS binding groove thereby supporting cargo release. Binding segment 1 contains a basic cluster (K3 and R4) that binds to the minor NLS binding site and a  $\beta$ -turn (T11 to W15) that overlaps in part with the major NLS binding site of importin- $\alpha$  (Figure 2B). An 8-residue-comprising acidic linker connects both binding segments. Interestingly, binding segment 1 contains a conserved lysine residue (K18), which has been identified as acetylation site (similarly to murine K8) regulated by the KDAC inhibitors apicidin and TSA (Hartl et al., 2017). The crystal structure of the murine importin- $\alpha$ /Nup50 complex shows that K8 approaches an aspartic and a glutamic acid residue in the acidic linker (Figure 2C). Acetylation of K18 (AtNup50) or K8 (MmNup50) might hinder the formation of the  $\beta$ -turn that packs against the major NLS binding site of importin- $\alpha$  thereby decelerating the import complex disassembly. A potential modulation of import complex disassembly by lysine acetylation might add a new layer of complexity to the regulation of nuclear transport processes, which might be worthy to investigate.

## FUTURE DIRECTIONS

The regulation of protein functions by lysine acetylation is evolutionary conserved and has the potential to be highly important for cell signaling and regulation (just like protein phosphorylation). The identification of new substrate proteins of Arabidopsis KDACs now allows to uncover detailed molecular processes in plant development and stress responses, in which the individual classical KDACs are involved in, apart from their deacetylase function on histones. Additionally, further interesting target proteins of other KDAC families such as sirtuins might exist among the lysine-acetylated nuclear proteins that have been recently identified in Arabidopsis (Hartl et al., 2017). One of such

## REFERENCES

- Allfrey, V. G., Faulkner, R., and Mirsky, A. E. (1964). Acetylation and methylation of histones and their possible role in regulation of RNA synthesis. *Proc. Natl. Acad. Sci. U.S.A.* 51, 786–794. doi: 10.1073/pnas.51.5.786
- Bieluszewski, T., Galganski, L., Sura, W., Bieluszewska, A., Abram, M., Ludwikow, A., et al. (2015). AtEAF1 is a potential platform protein for Arabidopsis NuA4 acetyltransferase complex. *BMC Plant Biol.* 15:75. doi: 10.1186/s12870-015-0461-1
- Bouras, T., Fu, M. F., Sauve, A. A., Wang, F., Quong, A. A., Perkins, N. D., et al. (2005). SIRT1 deacetylation and repression of p300 involves lysine residues 1020/1024 within the cell cycle regulatory domain 1. *J. Biol. Chem.* 280, 10264–10276. doi: 10.1074/jbc.M408748200
- Bradner, J. E., West, N., Grachan, M. L., Greenberg, E. F., Haggarty, S. J., Warnow, T., et al. (2010). Chemical phylogenetics of histone deacetylases. *Nat. Chem. Biol.* 6, 238–243. doi: 10.1038/nchembio.313

example is the lysine acetylation site (K146) on the Arabidopsis cMyc-Binding Protein 1 (AtMBP-1, AT2G36530). It was recently discovered that the stability of AtMBP-1 is regulated by lysine acetylation through the action of the sirtuin-1 deacetylase (Liu et al., 2017). The identified acetylated lysine residues by Hartl et al. (2017) lies in a domain that has previously been shown to be required for MBP1 repressor activity (Subramanian and Miller, 2000). Interestingly, this residue has also been found to be acetylated in human (Choudhary et al., 2009). By investigating the conservation of acetylation sites and regulatory patterns, important key lysine residues can be selected for site-directed mutagenesis in plants. With advances in CRISPR/CAS technologies, these sites are now accessible to study via targeted genome editing. Modifying these lysine residues to constitute acetylated or non-acetylated mimics, might allow a switching of metabolic activities and outputs that can enhance plant yields.

## AUTHOR CONTRIBUTIONS

MF, IL, GN, MK, AB, PT, JG, DL, PM, DS, and IF performed the data mining, literature mining, sequence analyses, and alignments, and prepared the manuscript. IL, DS, and IF prepared the figures.

## FUNDING

This work was supported by the Deutsche Forschungsgemeinschaft (Emmy Noether Program FI-1655/1, ERA-CAPS KatNat FI-1655/4, FI-1655/6), Germany, and Academy of Finland (307335 “Centre of Excellence in Molecular Biology of Primary Producers” for PM and MK). We acknowledge the support by Open Access Publication Fund of University of Münster.

## ACKNOWLEDGMENTS

We apologize to all colleagues whose work could not be cited due to space restrictions.

- Brownell, J. E., Zhou, J. X., Ranalli, T., Kobayashi, R., Edmondson, D. G., Roth, S. Y., et al. (1996). Tetrahymena histone acetyltransferase A: a homolog to yeast Gcn5p linking histone acetylation to gene activation. *Cell* 84, 843–851. doi: 10.1016/S0092-8674(00)81063-6
- Cai, Y., Jin, J., Yao, T., Gottschalk, A. J., Swanson, S. K., Wu, S., et al. (2007). YY1 functions with INO80 to activate transcription. *Nat. Struct. Mol. Biol.* 14, 872–874. doi: 10.1038/nsmb1276
- Choudhary, C., Kumar, C., Gnäd, F., Nielsen, M. L., Rehman, M., Walther, T. C., et al. (2009). Lysine acetylation targets protein complexes and co-regulates major cellular functions. *Science* 325, 834–840. doi: 10.1126/science.1175371
- Christie, M., Chang, C. W., Rona, G., Smith, K. M., Stewart, A. G., Takeda, A. A. S., et al. (2016). Structural biology and regulation of protein import into the nucleus. *J. Mol. Biol.* 428, 2060–2090. doi: 10.1016/j.jmb.2015.10.023
- De Ruijter, A. J. M., Van Gennip, A. H., Caron, H. N., Kemp, S., and Van Kuilenburg, A. B. P. (2003). Histone deacetylases (HDACs): characterization of the classical HDAC family. *Biochem. J.* 370, 737–749. doi: 10.1042/bj20021321

- Ding, Z., Millar, A. J., Davis, A. M., and Davis, S. J. (2007). TIME FOR COFFEE encodes a nuclear regulator in the Arabidopsis thaliana circadian clock. *Plant Cell* 19, 1522–1536. doi: 10.1105/tpc.106.047241
- Duan, M. R., Nan, J., Liang, Y. H., Mao, P., Lu, L., Li, L. F., et al. (2007). DNA binding mechanism revealed by high resolution crystal structure of Arabidopsis thaliana WRKY1 protein. *Nucleic Acids Res.* 35, 1145–1154. doi: 10.1093/nar/gkm001
- Duc, C., Cellier, F., Lobreaux, S., Briat, J. F., and Gaymard, F. (2009). Regulation of iron homeostasis in *Arabidopsis thaliana* by the Clock Regulator Time for Coffee. *J. Biol. Chem.* 284, 36271–36281. doi: 10.1074/jbc.M109.059873
- Durso, R. J., Fisher, A. K., Albright-Frey, T. J., and Reese, J. C. (2001). Analysis of TAF90 mutants displaying allele-specific and broad defects in transcription. *Mol. Cell. Biol.* 21, 7331–7344. doi: 10.1128/MCB.21.21.7331-7344.2001
- Earley, K., Lawrence, R. J., Pontes, O., Reuther, R., Enciso, A. J., Silva, M., et al. (2006). Erasure of histone acetylation by *Arabidopsis* HDA6 mediates large-scale gene silencing in nucleolar dominance. *Genes Dev.* 20, 1283–1293. doi: 10.1101/gad.1417706
- Fuchs, J., Demidov, D., Houben, A., and Schubert, I. (2006). Chromosomal histone modification patterns - from conservation to diversity (vol 11, pg 199, 2006). *Trends Plant Sci.* 11, 212–212. doi: 10.1016/j.tplants.2006.02.008
- Gallinari, P., Di Marco, S., Jones, P., Pallaoro, M., and Steinkuhler, C. (2007). HDACs, histone deacetylation and gene transcription: from molecular biology to cancer therapeutics. *Cell Res.* 17, 195–211. doi: 10.1038/sj.7310149
- Gillmor, C. S., Silva-Ortega, C. O., Willmann, M. R., Buendia-Monreal, M., and Poethig, R. S. (2014). The *Arabidopsis* mediator CDK8 module genes *CCT (MED12)* and *GCT (MED13)* are global regulators of developmental phase transitions. *Development* 141, 4580–4589. doi: 10.1242/dev.111229
- Hall, A., Bastow, R. M., Davis, S. J., Hanano, S., Mcwatters, H. G., Hibberd, V., et al. (2003). The TIME FOR COFFEE gene maintains the amplitude and timing of Arabidopsis circadian clocks. *Plant Cell* 15, 2719–2729. doi: 10.1105/tpc.013730
- Hao, Y. H., Wang, H. J., Qiao, S. L., Leng, L. N., and Wang, X. L. (2016). Histone deacetylase HDA6 enhances brassinosteroid signaling by inhibiting the BIN2 kinase. *Proc. Natl. Acad. Sci. U.S.A.* 113, 10418–10423. doi: 10.1073/pnas.1521363113
- Hartl, M., Füßl, M., Boersema, P. J., Jost, J. O., Kramer, K., Bakirbas, A., et al. (2017). Lysine acetylome profiling uncovers novel histone deacetylase substrate proteins in *Arabidopsis*. *Mol. Syst. Biol.* 13:949. doi: 10.15252/msb.20177819
- Hong, L. W., Yan, D. W., Liu, W. C., Chen, H. G., and Lu, Y. T. (2014). TIME FOR COFFEE controls root meristem size by changes in auxin accumulation in *Arabidopsis*. *J. Exp. Bot.* 65, 275–286. doi: 10.1093/jxb/ert374
- Jenuwein, T., and Allis, C. D. (2001). Translating the histone code. *Science* 293, 1074–1080. doi: 10.1126/science.1063127
- Karanam, B., Jiang, L. H., Wang, L., Kelleher, N. L., and Cole, P. A. (2006). Kinetic and mass spectrometric analysis of p300 histone acetyltransferase domain autoacetylation. *J. Biol. Chem.* 281, 40292–40301. doi: 10.1074/jbc.M608813200
- Kassem, S., Villanyi, Z., and Collart, M. A. (2017). Not5-dependent co-translational assembly of Ada2 and Spt20 is essential for functional integrity of SAGA. *Nucleic Acids Res.* 45, 1186–1199. doi: 10.1093/nar/gkw1059
- Kawashima, T., Lorkovic, Z. J., Nishihama, R., Ishizaki, K., Axelsson, E., Yelagandula, R., et al. (2015). Diversification of histone H2A variants during plant evolution. *Trends Plant Sci.* 20, 419–425. doi: 10.1016/j.tplants.2015.04.005
- Kim, J. M., To, T. K., Matsui, A., Tanoi, K., Kobayashi, N. I., Matsuda, F., et al. (2017). Acetate-mediated novel survival strategy against drought in plants. *Nat. Plants* 3:17097. doi: 10.1038/nplants.2017.97
- Kobor, M. S., Venkatasubrahmanyam, S., Meneghini, M. D., Gin, J. W., Jennings, J. L., Link, A. J., et al. (2004). A protein complex containing the conserved Swi2/Snf2-related ATPase Swr1p deposits histone variant H2A.Z into euchromatin. *PLoS Biol.* 2:587–599.
- Kornberg, R. D. (1974). Chromatin structure - repeating unit of histones and DNA. *Science* 184, 868–871. doi: 10.1126/science.184.4139.868
- Lai, Z. B., Schluttenhofer, C. M., Bhide, K., Shreve, J., Thimmapuram, J., Lee, S. Y., et al. (2014). MED18 interaction with distinct transcription factors regulates multiple plant functions. *Nat. Commun.* 5:3064. doi: 10.1038/ncomms4064
- Li, C., Xu, J., Li, J., Li, Q., and Yang, H. (2014). Involvement of Arabidopsis HAC family genes in pleiotropic developmental processes. *Plant Signal. Behav.* 9:e28173.
- Li, T., Wu, X. Y., Li, H., Song, J. H., and Liu, J. Y. (2016). A dual-function transcription factor, AtYY1, is a novel negative regulator of the Arabidopsis ABA response network. *Mol. Plant* 9, 650–661. doi: 10.1016/j.molp.2016.02.010
- Liu, X. Y., Wei, W., Zhu, W. J., Su, L. F., Xiong, Z. Y., Zhou, M., et al. (2017). Histone deacetylase AtSRT1 links metabolic flux and stress response in *Arabidopsis*. *Mol. Plant* 10, 1510–1522. doi: 10.1016/j.molp.2017.10.010
- Luger, K., Mader, A. W., Richmond, R. K., Sargent, D. F., and Richmond, T. J. (1997). Crystal structure of the nucleosome core particle at 2.8 angstrom resolution. *Nature* 389, 251–260. doi: 10.1038/38444
- Luo, M., Cheng, K., Xu, Y. C., Yang, S. G., and Wu, K. Q. (2017). Plant responses to abiotic stress regulated by histone deacetylases. *Front. Plant Sci.* 8:2147. doi: 10.3389/fpls.2017.02147
- Mao, Y. P., Pavangadkar, K. A., Thomashow, M. F., and Triezenberg, S. J. (2006). Physical and functional interactions of Arabidopsis ADA2 transcriptional coactivator proteins with the acetyltransferase GCN5 and with the cold-induced transcription factor CBF1. *Biochim. Biophys. Acta* 1759, 69–79. doi: 10.1016/j.bbaexp.2006.02.006
- Matsuura, Y., and Stewart, M. (2005). Nup50/Npap60 function in nuclear protein import complex disassembly and importin recycling. *EMBO J.* 24, 3681–3689. doi: 10.1038/sj.emboj.7600843
- Mengel, A., Ageeva, A., Georgii, E., Bernhardt, J., Wu, K. Q., Durner, J., et al. (2017). Nitric oxide modulates histone acetylation at stress genes by inhibition of histone deacetylases. *Plant Physiol.* 173, 1434–1452. doi: 10.1104/pp.16.01734
- Miller, M. J., Scaif, M., Rytz, T. C., Hubler, S. L., Smith, L. M., and Vierstra, R. D. (2013). Quantitative proteomics reveals factors regulating RNA biology as dynamic targets of stress-induced SUMOylation in *Arabidopsis*. *Mol. Cell. Proteomics* 12, 449–463. doi: 10.1074/mcp.M112.025056
- Postberg, J., Forcob, S., Chang, W. J., and Lipps, H. J. (2010). The evolutionary history of histone H3 suggests a deep eukaryotic root of chromatin modifying mechanisms. *BMC Evol. Biol.* 10:259. doi: 10.1186/1471-2148-10-259
- Qiao, Z., Li, C. L., and Zhang, W. (2016). WRKY1 regulates stomatal movement in drought-stressed *Arabidopsis thaliana*. *Plant Mol. Biol.* 91, 53–65. doi: 10.1007/s11103-016-0441-3
- Robyr, D., Kurdistani, S. K., and Grunstein, M. (2004). Analysis of genome-wide histone acetylation state and enzyme binding using DNA microarrays. *Methods Enzymol.* 376, 289–304. doi: 10.1016/S0076-6879(03)76019-4
- Samanta, S., and Thakur, J. K. (2015). Importance of Mediator complex in the regulation and integration of diverse signaling pathways in plants. *Front. Plant Sci.* 6:757. doi: 10.3389/fpls.2015.00757
- Schölz, C., Weinert, B. T., Wagner, S. A., Beli, P., Miyake, Y., Qi, J., et al. (2015). Acetylation site specificities of lysine deacetylase inhibitors in human cells. *Nat. Biotechnol.* 33, 415–423. doi: 10.1038/nbt.3130
- Seo, J. S., Sun, H. X., Park, B. S., Huang, C. H., Yeh, S. D., Jung, C., et al. (2017). ELF18-INDUCED LONG-NONCODING RNA associates with mediator to enhance expression of innate immune response genes in *Arabidopsis*. *Plant Cell* 29, 1024–1038. doi: 10.1105/tpc.16.00886
- Shin, J., Heidrich, K., Sanchez-Villarreal, A., Parker, J. E., and Davis, S. J. (2012). TIME FOR COFFEE represses accumulation of the MYC2 transcription factor to provide time-of-day regulation of jasmonate signaling in *Arabidopsis*. *Plant Cell* 24, 2470–2482. doi: 10.1105/tpc.111.095430
- Shin, J., Sanchez-Villarreal, A., Davis, A. M., Du, S. X., Berendzen, K. W., Koncz, C., et al. (2017). The metabolic sensor AKIN10 modulates the Arabidopsis circadian clock in a light-dependent manner. *Plant Cell Environ.* 40, 997–1008. doi: 10.1111/pce.12903
- Singh, P., Yekondi, S., Chen, P. W., Tsai, C. H., Yu, C. W., Wu, K., et al. (2014). Environmental history modulates *Arabidopsis* pattern-triggered immunity in a HISTONE ACETYLTRANSFERASE1-Dependent Manner. *Plant Cell* 26, 2676–2688. doi: 10.1105/tpc.114.123356
- Soutourina, J. (2017). Transcription regulation by the Mediator complex. *Nat. Rev. Mol. Cell Biol.* 19, 262–274. doi: 10.1038/nrm.2017.115
- Srivastava, R., Rai, K. M., Pandey, B., Singh, S. P., and Sawant, S. V. (2015). Spt-Ada-Gcn5-acetyltransferase (SAGA) complex in plants: genome wide identification, evolutionary conservation and functional determination. *PLoS One* 10:e0134709. doi: 10.1371/journal.pone.0134709
- Stewart, M. (2007). Molecular mechanism of the nuclear protein import cycle. *Nat. Rev. Mol. Cell Biol.* 8, 195–208. doi: 10.1038/nrm2114

- Subramanian, A., and Miller, D. M. (2000). Structural analysis of alpha-enolase - Mapping the functional domains involved in down-regulation of the c-myc protooncogene. *J. Biol. Chem.* 275, 5958–5965. doi: 10.1074/jbc.275.8.5958
- Talbert, P. B., and Henikoff, S. (2014). Environmental responses mediated by histone variants. *Trends Cell Biol.* 24, 642–650. doi: 10.1016/j.tcb.2014.07.006
- Tamura, K., Fukao, Y., Iwamoto, M., Haraguchi, T., and Hara-Nishimura, I. (2010). Identification and characterization of nuclear pore complex components in *Arabidopsis thaliana*. *Plant Cell* 22, 4084–4097. doi: 10.1105/tpc.110.079947
- Taunton, J., Hassig, C. A., and Schreiber, S. L. (1996). A mammalian histone deacetylase related to the yeast transcriptional regulator Rpd3p. *Science* 272, 408–411. doi: 10.1126/science.272.5260.408
- Taverna, S. D., Li, H., Ruthenburg, A. J., Allis, C. D., and Patel, D. J. (2007). How chromatin-binding modules interpret histone modifications: lessons from professional pocket pickers. *Nat. Struct. Mol. Biol.* 14, 1025–1040. doi: 10.1038/nsmb1338
- Thompson, P. R., Wang, D., Wang, L., Fulco, M., Pediconi, N., Zhang, D., et al. (2004). Regulation of the p300 HAT domain via a novel activation loop. *Nat. Struct. Mol. Biol.* 11, 308–315. doi: 10.1038/nsmb740
- Tran, H. T., Nimick, M., Uhrig, R. G., Templeton, G., Morrice, N., Gourlay, R., et al. (2012). *Arabidopsis thaliana* histone deacetylase 14 (HDA14) is an alpha-tubulin deacetylase that associates with PP2A and enriches in the microtubule fraction with the putative histone acetyltransferase ELP3. *Plant J.* 71, 263–272. doi: 10.1111/j.1365-313X.2012.04984.x
- Ueda, M., Matsui, A., Tanaka, M., Nakamura, T., Abe, T., Sako, K., et al. (2017). The distinct roles of class I and II RPD3-like histone deacetylases in salinity stress response. *Plant Physiol.* 175, 1760–1773. doi: 10.1104/pp.17.01332
- Ullmann, R., Chien, C. D., Avantaggiati, M. L., and Muller, S. (2012). An acetylation switch regulates SUMO-dependent protein interaction networks. *Mol. Cell* 46, 759–770. doi: 10.1016/j.molcel.2012.04.006
- Wang, Z., Cao, H., Chen, F. Y., and Liu, Y. X. (2014). The roles of histone acetylation in seed performance and plant development. *Plant Physiol. Biochem.* 84, 125–133. doi: 10.1016/j.plaphy.2014.09.010
- Wu, X. P., Cheng, Y. S., Li, T., Wang, Z., and Liu, J. Y. (2012). In vitro identification of DNA-binding motif for the new zinc finger protein AtYY1. *Acta Biochim. Biophys. Sin.* 44, 483–489. doi: 10.1093/abbs/gms020
- Wu, X. Y., and Li, T. (2017). A casein kinase II phosphorylation site in AtYY1 affects its activity, stability, and function in the ABA response. *Front. Plant Sci.* 8:323. doi: 10.3389/fpls.2017.00323
- Yang, X. J., and Seto, E. (2008). Lysine acetylation: codified crosstalk with other posttranslational modifications. *Mol. Cell* 31, 449–461. doi: 10.1016/j.molcel.2008.07.002
- Zhou, C. H., Zhang, L., Duan, J., Miki, B., and Wu, K. Q. (2005). *HISTONE DEACETYLASE19* is involved in jasmonic acid and ethylene signaling of pathogen response in *Arabidopsis*. *Plant Cell* 17, 1196–1204. doi: 10.1105/tpc.104.028514

**Conflict of Interest Statement:** The authors declare that the research was conducted in the absence of any commercial or financial relationships that could be construed as a potential conflict of interest.

Copyright © 2018 Füßl, Lassowskat, Née, Koskela, Brünje, Tilak, Giese, Leister, Mulo, Schwarzer and Finkemeier. This is an open-access article distributed under the terms of the Creative Commons Attribution License (CC BY). The use, distribution or reproduction in other forums is permitted, provided the original author(s) and the copyright owner are credited and that the original publication in this journal is cited, in accordance with accepted academic practice. No use, distribution or reproduction is permitted which does not comply with these terms.

Publication 3

**Lysine acetylome profiling uncovers novel  
histone deacetylase substrate proteins in *Arabidopsis*.**

Hartl M, **Füßl M**, Boersema PJ, Jost JO, Kramer K, Bakirbas A,  
Sindlinger J, Plöchinger M, Leister D, Uhrig G, Moorhead GB, Cox J,  
Salvucci ME, Schwarzer D, Mann M, Finkemeier I.

(2017)

*Molecular Systems Biology* (13:949)

# Lysine acetylome profiling uncovers novel histone deacetylase substrate proteins in *Arabidopsis*

Markus Hartl<sup>1,2,3,§</sup> , Magdalena Füßl<sup>1,2,4,§</sup>, Paul J Boersema<sup>5,†</sup>, Jan-Oliver Jost<sup>6,‡</sup>, Katharina Kramer<sup>1</sup>, Ahmet Bakirbas<sup>1,4,¶</sup>, Julia Sindlinger<sup>6</sup> , Magdalena Plöching<sup>2</sup>, Dario Leister<sup>2</sup>, Glen Uhrig<sup>7</sup>, Greg BG Moorhead<sup>7</sup> , Jürgen Cox<sup>5</sup>, Michael E Salvucci<sup>8</sup>, Dirk Schwarzer<sup>6</sup> , Matthias Mann<sup>5</sup>  & Iris Finkemeier<sup>1,2,4,\*</sup> 

## Abstract

Histone deacetylases have central functions in regulating stress defenses and development in plants. However, the knowledge about the deacetylase functions is largely limited to histones, although these enzymes were found in diverse subcellular compartments. In this study, we determined the proteome-wide signatures of the RPD3/HDA1 class of histone deacetylases in *Arabidopsis*. Relative quantification of the changes in the lysine acetylation levels was determined on a proteome-wide scale after treatment of *Arabidopsis* leaves with deacetylase inhibitors apicidin and trichostatin A. We identified 91 new acetylated candidate proteins other than histones, which are potential substrates of the RPD3/HDA1-like histone deacetylases in *Arabidopsis*, of which at least 30 of these proteins function in nucleic acid binding. Furthermore, our analysis revealed that histone deacetylase 14 (HDA14) is the first organellar-localized RPD3/HDA1 class protein found to reside in the chloroplasts and that the majority of its protein targets have functions in photosynthesis. Finally, the analysis of HDA14 loss-of-function mutants revealed that the activation state of RuBisCO is controlled by lysine acetylation of RuBisCO activase under low-light conditions.

**Keywords** *Arabidopsis*; histone deacetylases; lysine acetylation; photosynthesis; RuBisCO activase

**Subject Categories** Methods & Resources; Plant Biology; Post-translational Modifications, Proteolysis & Proteomics

**DOI** 10.15252/msb.20177819 | Received 16 June 2017 | Revised 22 September 2017 | Accepted 25 September 2017

**Mol Syst Biol.** (2017) **13**: 949

## Introduction

Optimal plant growth and development are dependent on fine-regulation of the cellular metabolism in response to environmental conditions (Nunes-Nesi *et al*, 2010). During a day or a season, plants often face rapidly changing environmental conditions such as changes in temperature, light intensity, and water and nutrient availability (Calfapietra *et al*, 2015). Due to their sessile life style, plants cannot escape from environmental perturbations. Instead, plants activate a variety of cellular response mechanisms that allow them to acclimate their metabolism to the environment. Cellular signaling networks are activated within seconds when metabolic homeostasis is perturbed, and these networks regulate the plant's physiology (Dietz, 2015; Mignolet-Spruyt *et al*, 2016). Such signaling networks regulate gene expression, translation, protein activity, and turnover. Post-translational modifications (PTMs) of proteins like phosphorylation, ubiquitination, methylation, and acetylation play a pivotal role in all of these regulatory processes (Hartl & Finkemeier, 2012; Johnova *et al*, 2016). Except for phosphorylation, most of the cellular protein targets and the regulating enzymes of these PTMs are largely unexplored in plants (Huber, 2007). Here, we study the regulation of lysine acetylation.

Lysine acetylation is a post-translational modification (PTM), which was first discovered on histone tails where it is now known to regulate chromatin structure and gene expression (Allfrey *et al*, 1964). The transfer of the acetyl group to lysine neutralizes the positive charge of the amino group, which can affect the biological function of proteins such as enzyme activities, protein–protein, and protein–DNA interactions (Yang & Seto, 2008). Acetyl-CoA serves as

1 Plant Proteomics, Max Planck Institute for Plant Breeding Research, Cologne, Germany

2 Plant Molecular Biology, Department Biology I, Ludwig-Maximilians-University Munich, Martinsried, Germany

3 Mass Spectrometry Facility, Max F. Perutz Laboratories (MFPL), Vienna Biocenter (VBC), University of Vienna, Vienna, Austria

4 Plant Physiology, Institute of Plant Biology and Biotechnology, University of Muenster, Muenster, Germany

5 Proteomics and Signal Transduction, Max-Planck Institute of Biochemistry, Martinsried, Germany

6 Interfaculty Institute of Biochemistry, University of Tübingen, Tübingen, Germany

7 Department of Biological Sciences, University of Calgary, Calgary, AB, Canada

8 US Department of Agriculture, Agricultural Research Service, Arid-Land Agricultural Research Center, Maricopa, AZ, USA

\*Corresponding author. Tel: +49 251 8323805; E-mail: iris.finkemeier@uni-muenster.de

§These authors contributed equally to this work

†Present address: Department of Biology, Institute of Biochemistry, ETH Zurich, Zurich, Switzerland

‡Present address: Leibniz-Forschungsinstitut für Molekulare Pharmakologie im Forschungsverbund Berlin e.V. (FMP), Berlin, Germany

¶Present address: Plant Biology Graduate Program, University of Massachusetts Amherst, Amherst, USA

[Correction added on 7 November 2017 after first online publication: current address affiliation has been added.]

substrate for lysine acetylation in an enzymatic process catalyzed by different types of lysine acetyltransferases (KATs) (Kleff *et al*, 1995; Parthun *et al*, 1996; Yuan & Marmorstein, 2013; Drazic *et al*, 2016). However, lysine acetylation can also occur non-enzymatically especially at a cellular pH higher than eight (Wagner & Payne, 2013; König *et al*, 2014a); a level that can be reached during active respiration in the mitochondrial matrix, as well as in the chloroplast stroma during photosynthesis (Hosp *et al*, 2016). Non-enzymatic acetylation is of particular abundance in bacteria, which additionally contain the highly reactive acetyl-phosphate as metabolite (Weinert *et al*, 2013). In plants, many organellar proteins from mitochondria and chloroplasts were previously identified as lysine-acetylated (Finkemeier *et al*, 2011; Wu *et al*, 2011; König *et al*, 2014a; Nallamilli *et al*, 2014; Smith-Hammond *et al*, 2014; Fang *et al*, 2015; He *et al*, 2016; Hosp *et al*, 2016; Xiong *et al*, 2016; Zhang *et al*, 2016; Zhen *et al*, 2016).

Lysine acetylation can be reversed by lysine deacetylases (KDACs), which were named histone deacetylases (HDA/HDAC) before the more recent discovery of non-histone protein acetylation. KDACs can be grouped into three different families: (i) reduced potassium dependency 3/histone deacetylase 1 (RPD3/HDA1)-like, (ii) HD-tuins (HDT), and (iii) silent information regulator 2 (Sir2) (Pandey *et al*, 2002; Alinsug *et al*, 2009; Shen *et al*, 2015). While the RPD3/HDA1 family has primarily been found in eukaryotes, the Sir2-type deacetylases also occur in bacteria, and the HDT-type deacetylases only occur in plants. The *Arabidopsis* genome encodes 18 KDACs from the three different families. The largest family comprises the RPD3/HDA1-like with 12 genes, four genes belong to the HDTs and two to the Sir2 family. The RPD3/HDA1 family can be further subdivided into class I (RPD3-like), class II (HDA1-like), and class IV KDACs, of which *Arabidopsis* possesses 6, 5, and 1 putative members, respectively (Pandey *et al*, 2002; Alinsug *et al*, 2009; Shen *et al*, 2015). Numerous studies have characterized different genes from the *Arabidopsis* KDAC families over the last two decades (Shen *et al*, 2015). In particular, HDA6, HDA9, and HDA19 from class I are the most well studied *Arabidopsis* KDACs and they have been implicated in many important developmental processes such as seed germination, flowering time, as well as plant hormone-related stress responses (Zhou *et al*, 2005; Benhamed *et al*, 2006; Chen *et al*, 2010; Choi *et al*, 2012; Cigliano *et al*, 2013; Zheng *et al*, 2016; Mengel *et al*, 2017). In terms of protein targets for deacetylation, very little is known about the preferences and targets of the different plant KDACs. While *Arabidopsis* sirtuin 2 deacetylates selected mitochondrial proteins such as the ATP/ADP carrier (König *et al*, 2014b), mainly histone H3 and H4 deacetylation has been studied for the other two families of KDACs (Shen *et al*, 2015).

Here, we report the first comprehensive profiling of putative *Arabidopsis* KDAC targets by using two different inhibitors of the RPD3/HDA1 family. By this approach, we identify several heretofore-unknown potential targets of the *Arabidopsis* KDACs in the nucleus and other subcellular localizations including plastids. Additionally, by the use of a peptide-based KDAC-probe, we were able to identify the first KDAC of the RPD3/HDA1 family, which is active in organelles and regulates the activity and activation state of ribulose-1,5-bisphosphate-carboxylase/oxygenase, the key enzyme in photosynthetic CO<sub>2</sub> fixation, and the most abundant protein on earth.

## Results

### The *Arabidopsis* leaf lysine acetylome 2.0

The first two lysine acetylomes of *Arabidopsis* leaves were reported in 2011, with only around 100 lysine acetylation sites identified (Finkemeier *et al*, 2011; Wu *et al*, 2011). Tremendous advances in mass spectrometry, improvements in antibody reagents, and the optimization of the overall protocol now allows a more in-depth profiling of the *Arabidopsis* lysine acetylome. To be able to quantify acetylome changes upon KDAC inhibitor treatment, we applied an isotopic dimethyl-labeling approach to differentially label two different protein samples (e.g., treatment and control), combined with an enrichment strategy for lysine-acetylated peptides (Fig 1A). For this procedure, proteins extracted from leaves were processed and trypsin-digested via filter-assisted sample preparation. Peptides were isotopically dimethyl-labeled, and samples for comparison were pooled. For proteome quantifications, samples were collected at this step and the rest of the sample was further processed by hydrophilic interaction liquid chromatography fractionation to reduce the peptide complexity. Six to seven fractions were collected and used for immuno-affinity enrichment using anti-acetyllysine agarose beads. Peptides were further processed for high-resolution mass spectrometry, and MaxQuant was used for the data analysis.

Altogether the datasets presented here comprise 2,152 lysine acetylation sites (localization probability > 0.75) on 1,022 protein groups (6,672 identified protein groups in total, Table 1, Datasets EV1–EV5)—this corresponds to 959 novel acetylated proteins and 2,057 novel acetylation sites when compared to the previously published datasets for *Arabidopsis* (Finkemeier *et al*, 2011; Wu *et al*, 2011; König *et al*, 2014a). A MapMan functional annotation analysis (Thimm *et al*, 2004) was used for the classification of the lysine-acetylated proteins, applying the TAIR mapping and selecting all identified proteins of the proteome analysis as background population. From the different cellular processes, the functional categories photosynthesis, tetrapyrrole synthesis, gluconeogenesis, redox, TCA cycle, as well as DNA and RNA regulation of transcription were identified as overrepresented as determined by a Fisher's exact test, while processes such as hormone metabolism, cell wall, and secondary metabolism were underrepresented (Fig 1B, at 5% FDR and a 1.5-fold enrichment/depletion cut-off). Based on the classification of localization of proteins using SUBA consensus (Heazlewood *et al*, 2007), proteins from plastids and nucleus were clearly overrepresented, while proteins from endoplasmic reticulum, vacuole, mitochondrion, plasma membrane, and extracellular space were significantly underrepresented in our dataset (Fig 1C).

Additionally, we analyzed the local sequence context around the acetylation sites using iceLogo (Maddelein *et al*, 2015) in combination with the *Arabidopsis* TAIR10 database with all identified proteins as background reference (Fig 1D). Overall, negatively charged amino acids, such as glutamate and aspartate, were significantly enriched in the -1, -2, -3 as well as +1 positions surrounding the lysine acetylation site. In more distant positions, lysine residues were the most strongly enriched on either side of the lysine acetylation site. The sequence motif surrounding the lysine acetylation site appeared different depending on the subcellular localization of the respective proteins. For example, the negatively charged amino acids were more prominent on cytosolic and plastidial

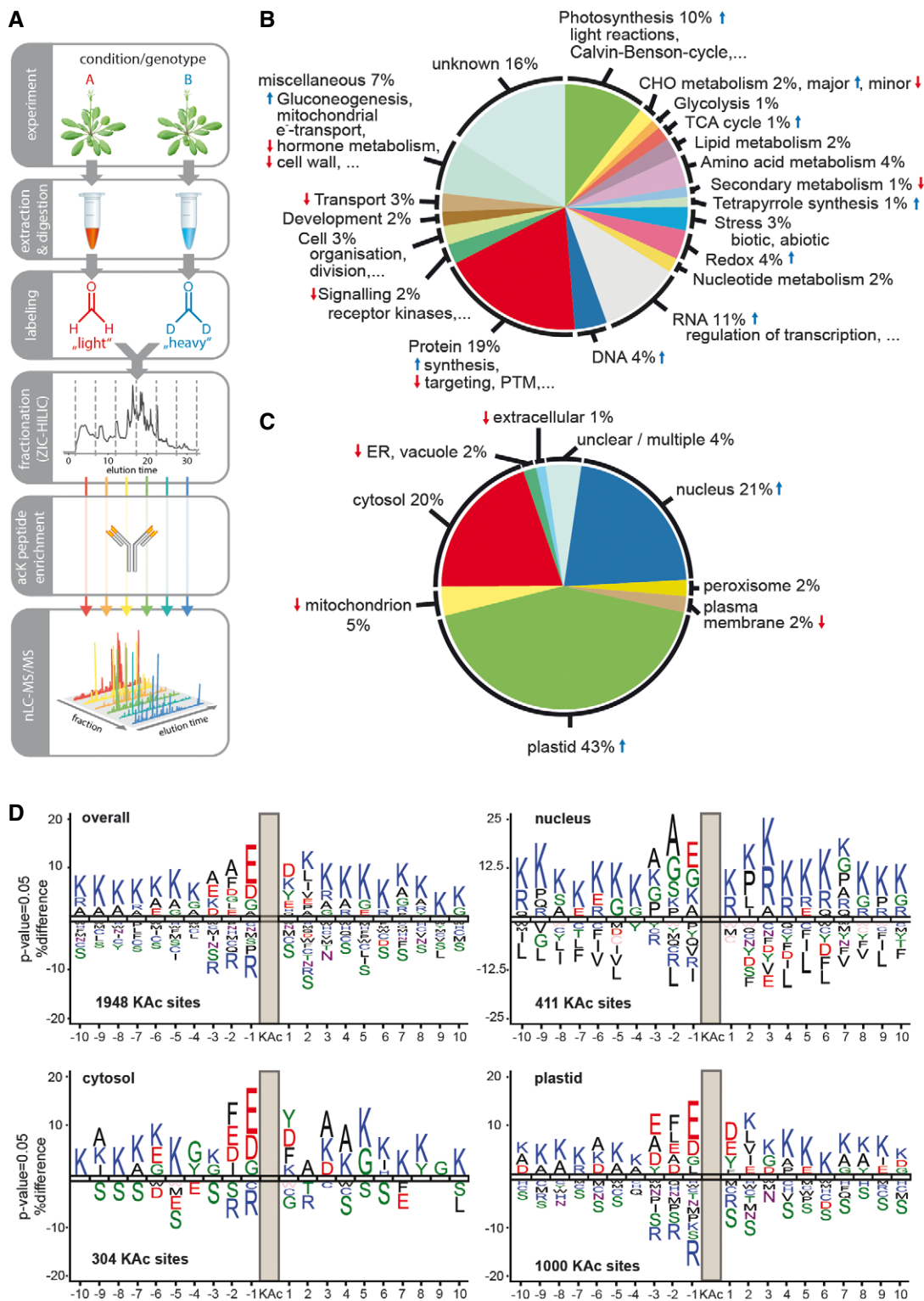


**Figure 1. Proteome-wide identification and classification of the *Arabidopsis thaliana* lysine acetylome.**

- A Experimental overview.
- B, C Functional classification and subcellular localization of identified lysine-acetylated proteins. Lysine-acetylated proteins identified over all experiments were classified according to MapMan categories and SUBA4 localization information, respectively. Over- or underrepresentation of categories was determined using a Fisher's exact test with all proteins identified at 1% FDR as background population. Blue and red arrows mark categories significantly enriched at 5% FDR (Benjamini–Hochberg) and a 1.5-fold-change cut-off.
- D Sequence logos for all lysine acetylation sites with all proteins identified as background population (sequence logos were generated using iceLogo, Maddelein et al, 2015).

Table 1. Summary of identified features.

Experiment	Description	Whole proteome analysis		Acetyllysine-containing		
		Protein groups	Peptides	Protein groups	Peptides	Sites
1	Apicidin versus Ctrl	2,384	11,188	538	1,064	1,041
2	TSA versus Ctrl	5,107	32,809	493	1,002	930
3	<i>hda14</i> versus WT	2,889	13,755	545	1,133	920
4	<i>hda14</i> versus WT low-light	4,138	27,835	367	756	700
5	<i>hda14</i> versus WT thylakoids	2,904	15,064	237	592	546
Total		6,672	47,338	1,022	2,405	2,152

Filters applied: 1% FDR at PSM and protein level, score for modified peptides  $\geq 35$ , delta score for modified peptides  $\geq 6$ , acetyllysine site localization probability  $\geq 0.75$ ; contaminants removed.

proteins in comparison with nuclear proteins, as well as the presence of a phenylalanine at position  $-2$ . Tyrosine at position  $+1$  was found on cytosolic and plastid proteins, while phenylalanine at position  $+1$  was only found enriched on cytosolic proteins. Interestingly, on the nuclear sequence motifs only positively charged amino acids were found at position  $+1$  as well as generally more neutral amino acids such as glycine and alanine at positions  $-1$  to  $-3$ , which are dominating on histone sequence motifs (Fig 1D).

Since 43% of all identified lysine-acetylated proteins are putative plastid proteins, we further analyzed the distribution of those proteins and number of acetylation sites in photosynthesis (Fig 2). About 24% of the proteins from the photosynthetic light reactions were acetylated on at least four lysine residues (Fig 2A). Proteins from the light harvesting complexes (LHC) of both PSII and PSI were heavily acetylated with 29 lysine acetylation sites on LHCII and 16 on LHCI proteins (Fig 2A). All enzyme complexes involved in the carbon fixing reactions (Calvin–Benson cycle) as well as RuBisCO activase (RCA) contained four or more lysine acetylation sites. With 18 lysine acetylation sites, the large subunit of RuBisCO was the most heavily modified of all the proteins (Fig 2B).

#### Identification of novel lysine acetylation sites targeted by *Arabidopsis* RPD3/HDA1-type KDACs

Different types of lysine deacetylase inhibitors have been developed in the past decade, which are widely used to modulate the activities of human KDACs in diseases (Newkirk et al, 2009). Here, we selected two commonly used KDAC inhibitors, apicidin and trichostatin A (TSA), to target the RPD3/HDA1-type family of KDACs and to profile their potential protein substrates. While apicidin was shown to specifically inhibit class I KDACs, TSA was described as a general inhibitor of class I and class II KDACs in HeLa cells (Scholz et al, 2015). For inhibitor treatment, *Arabidopsis* leaf strips were infiltrated either with a mock control or with 5  $\mu\text{M}$  apicidin and 5  $\mu\text{M}$  trichostatin A (TSA), respectively. Experiments were performed in three independent biological replicates, and the leaf strips were incubated for 4 h in the light before harvest. The protein intensities of the biological replicates had a Pearson correlation coefficient of  $> 0.87$ – $0.98$  (Appendix Fig S1), which indicates the robustness of the approach. Site-specific acetylation changes were quantified (Fig 3A and B) in addition to changes on total proteome level as control (Fig 3C and D). No significant changes in the regulation of protein abundances were observed after the inhibitor

treatments, which covered about 67–88% of proteins carrying the identified acetylated sites (Appendix Fig S2). However, the whole proteome analysis did not cover very low abundant proteins without enrichment. Therefore, we cannot exclude that the other sites, for which we were not able to quantify protein ratios, were not regulated due to bona fide stoichiometry differences from inhibited KDAC activity. However, we restricted inhibitor treatment to 4-h incubation time in order to minimize potential changes in protein abundances that might result from KDAC-dependent alterations in gene expression.

For apicidin treatment, 832 lysine acetylation sites were quantified, of which 148 were significantly regulated according to a LIMMA statistical analysis with a FDR cut-off  $< 5\%$  (Fig 3A; Dataset EV1). As expected for a KDAC inhibitor treatment, most of the lysine acetylation sites (136 in total) were up-regulated ( $\log_2\text{-FC}$  0.4–7.4) after apicidin treatment. The 12 down-regulated lysine acetylation sites comprise mainly multiply acetylated peptides for which peptide variants of lower acetylation status show a down-regulation of particular sites, whereas the corresponding peptide with higher acetylation status shows up-regulation in comparison. Interestingly, while the overall 832 lysine acetylation sites were detected on proteins from various subcellular compartments, 139 of the regulated lysine acetylation sites were found on proteins exclusively localized to the nucleus, such as histones, HATs, proteins involved in the regulation of transcription and signaling (G-protein and light signaling), DNA-repair and cell cycle, as revealed from a SUBAcon analysis (Dataset EV1). Three up-regulated lysine acetylation sites were detected on plastidial proteins including proteins involved in the light reactions (K99, PSAH-1; PSAH-2  $\log_2\text{-FC}$  0.43) as well as in the Calvin–Benson cycle (K305, SBPase,  $\log_2\text{-FC}$  0.61). Looking at a less stringent  $P$ -value cut-off  $< 0.05$  (Fig 1B), 182 lysine acetylation sites were found up-regulated of which 29 were found on organellar proteins. While most of these 29 lysine acetylation sites occur on proteins from the plastids, they only show a rather small increase in acetylation level ( $\log_2\text{-FC}$  0.2–0.8) (Dataset EV1).

After TSA treatment, only 37 sites of the 385 quantified lysine acetylation sites were significantly up-regulated with an FDR  $< 5\%$  ( $\log_2\text{-FC}$  1.4–6.1) (Fig 3B, Dataset EV2). This low number of regulated sites, compared to apicidin treatment, was mainly due to a higher variability in the biological replicates of the TSA treatment. Of the 37 up-regulated lysine acetylation sites, only one was detected on a protein with a plastidial localization (K165,

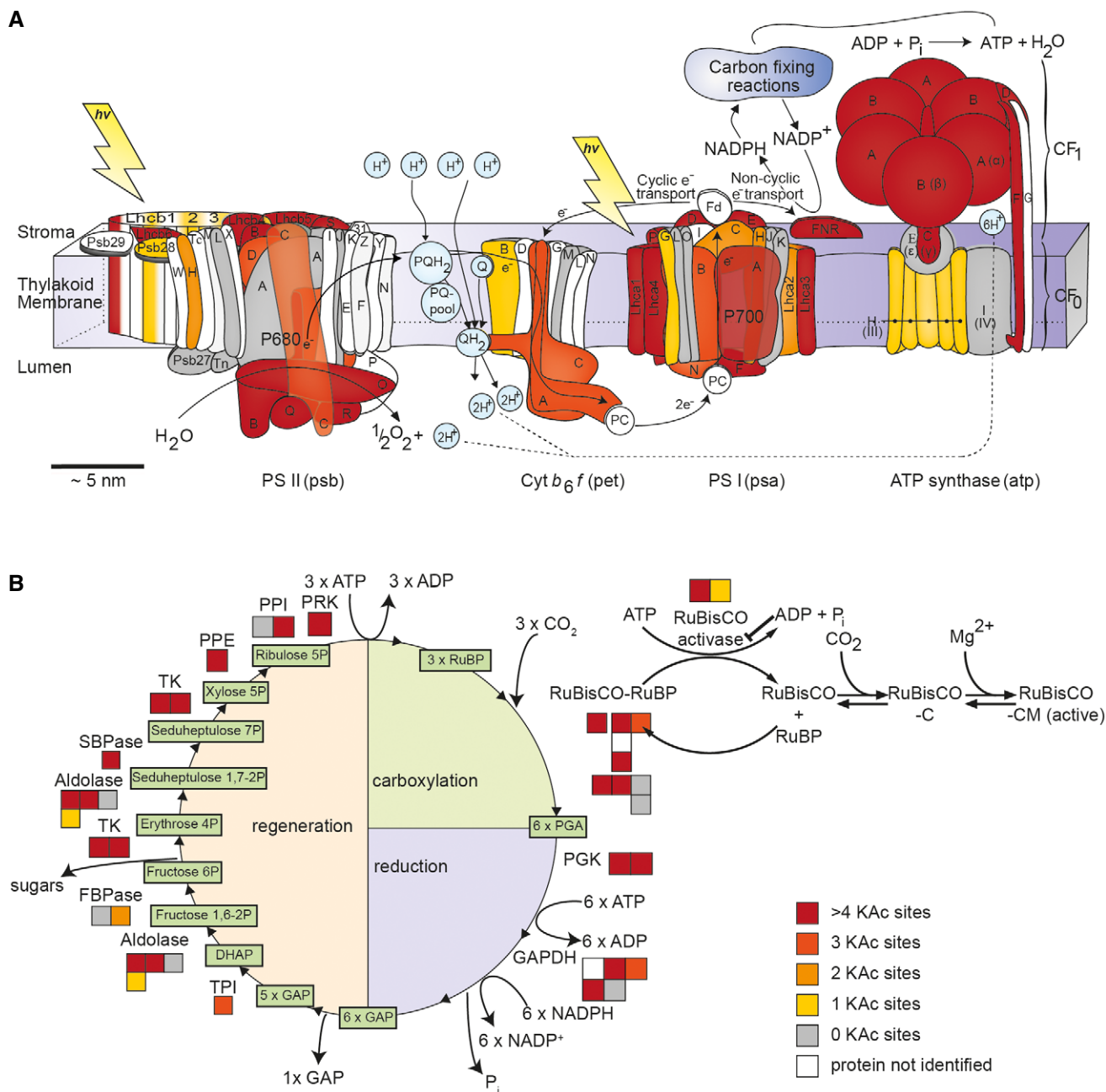


**Figure 2. Overview of lysine-acetylated proteins in the light reactions (A) and the Calvin–Benson cycle (B) identified in this study in *Arabidopsis*.**

A, B The classification of proteins into functional bins was performed using MapMan (Thimm *et al*, 2004). Color code: proteins not identified in the LC-MS/MS analyses (white), proteins without identified lysine-acetylated sites (gray), and proteins with one (yellow), two (orange), three (dark orange), or four or more acetylation sites (red). For the Calvin–Benson cycle, each box indicates a separate *Arabidopsis* AGI identifier as indicated in Dataset EV6. *Cyt<sub>b6/f</sub>*, cytochrome *b<sub>6/f</sub>*; *FBPase*, fructose-1,6-bisphosphatase; *GAPDH*, glyceraldehyde-3-phosphate dehydrogenase; *PGK*, phosphoglycerate kinase; *PPE*, phosphopentose epimerase; *PPI*, phosphopentose isomerase; *PRK*, phosphoribulokinase; *PSII*, photosystem II; *PSI*, photosystem I; *RuBisCO*, ribulose-1,5-bisphosphate-carboxylase/oxygenase; *SBPase*, seduheptulose-1,7-bisphosphatase; *TPI*, triose phosphate isomerase; *TK*, transketolase. A template of the light-reaction schematic was kindly provided by Jon Nield and modified.

At3g17930,  $\log_2$ -FC 3.6). Analyzing the data with a less stringent *P*-value cut-off ( $P < 0.05$ ) resulted in 72 up-regulated lysine acetylation sites with an average  $\log_2$ -FC of 0.8–6. Among those were two more plastidial proteins, the RCA  $\beta$ 1-isoform (K438,  $\log_2$ -FC 1.37) and PSAD-1/2 (K187/K191,  $\log_2$ -FC 1.77). Among the common nuclear targets of apicidin and TSA were several histone proteins. In

total, 19 regulated lysine acetylation sites were found on histone 2A (H2A) and histone 2B (H2B) proteins. On HTB1 two different lysine acetylation sites were specifically and strongly ( $\log_2$ -FC at least 2) up-regulated either upon apicidin (K39, K40) or TSA (K28, K33) inhibition (Appendix Fig S3, Dataset EV1A, Dataset EV2A). The same was true for other histones of the H2B family (HTB9, HTB2),

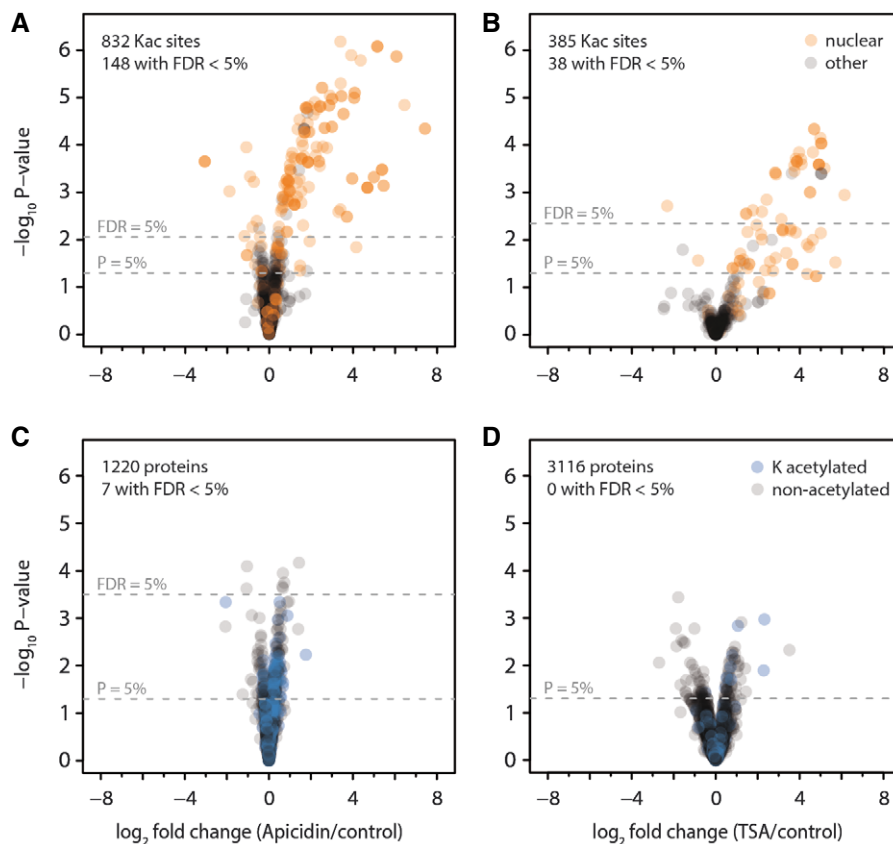


**Figure 3. Differential lysine acetylation and protein expression in *Arabidopsis* leaves after inhibitor treatment.**

A–D Vacuum infiltration of leaf strips with solutions containing either of the two deacetylase inhibitors apicidin (A, C) or trichostatin A (B, D) versus a buffer control for 4 h leads to differential accumulation of lysine acetylation sites. Volcano plots depict lysine acetylation site ratios (A, B) or protein ratios (C, D) for inhibitor treatment versus control, with  $P$ -values determined using the LIMMA package. Orange, protein with nuclear localization according to SUBA4 database. Blue, proteins with lysine acetylation sites identified. Dashed lines indicate significance thresholds of either uncorrected  $P$ -values  $< 5\%$  or Benjamini–Hochberg corrected  $FDR < 5\%$ . A missing line indicates that the significance threshold was not reached by any of the data points.

which also showed unique up-regulated sites depending on the inhibitor used. Interestingly, histones of the H2A family showed the same up-regulated lysine acetylation sites upon apicidin and TSA treatment. Overall, between apicidin and TSA treatment, there was an overlap of 25 protein groups ( $P$ -value  $< 0.05$ ), which showed enhanced lysine acetylation sites after both treatments (Dataset EV1A, Dataset EV2A). The KDAC inhibitor study revealed that most of the RPD3/HDA1 classes KDACs of *Arabidopsis* have their potential substrate proteins in the nucleus, but that some members also seem to have their targets in other subcellular compartments, such as the plastids.

#### HDA14 is the first member of a RPD3/HDA1-family protein to be localized in organelles

Members of the RPD3/HDA1 family are usually localized in the nucleus and/or in the cytosol. Here, we had clear indications that proteins targeted to the chloroplast were found hyper-acetylated upon inhibitor treatment. However, it was not clear whether the hyper-acetylation already occurred due to KDAC inhibition in the cytosol during transit of the proteins to the plastid or whether there exists a plastid-localized member of the RPD3/HDA1-class. Since

KDACs are low abundant proteins, they are usually not detected in leaf proteomes and therefore need to be enriched before detection. Here, we used a recently developed peptide-based KDAC-probe, mini-AsuHd (Dose *et al*, 2016), to pull-down active RPD3/HDA1-class KDACs from leaf extracts and isolated chloroplasts, respectively, in comparison with the mini-Lys probe as background control (Table 2). The mini-AsuHd probe contains a hydroxamate moiety spaced with five carbon atoms to the peptide backbone, which chelates the catalytic  $Zn^{2+}$  ion of RPD3/HDA1 family-HDACs with nanomolar affinities (Dose *et al*, 2016). The mini-Lys probe contains a lysine residue instead. Three different *Arabidopsis* KDACs were identified in total leaf extracts (HDA5, 14, 15), while in isolated chloroplasts, only HDA14 was identified (Table 2). Although HDA14 contains a predicted target sequence for plastids, it was reported to be localized in the cytosol in a previous study (Tran *et al*, 2012). To confirm the plastid localization of HDA14, we fused GFP to the C-terminus of the HDA14 protein, instead of the N-terminus as in the previous study. Protoplasts of the stable transformed 35S:HDA14:GFP plants showed that the signal of the HDA14:GFP fusion protein was overlapping with the autofluorescence of the chlorophyll, as well as with a TMRM signal which visualizes

**Table 2. KDAC pull-down with mini-AsuHd probe.**

Majority protein IDs	Name	Peptides	MS/MS count	Log2-LFQ CP AsuHd	Log2-LFQ CP Lys	Log2 enrichment CP	Log2-LFQ LF AsuHd	Log2-LFQ LF Lys	Log2 enrichment LF
AT5G61060.1/2	HDA5	6	11	n.d.	n.d.	n.d.	24.50 ± 0.12	n.d.	> 7 <sup>a</sup>
AT4G33470.1	HDA14	7	22	24.74 ± 1.83	19.54 ± 0.05	5.2	26.20 ± 0.2	21.12 ± 0.49	5.1
AT3G18520.1/2	HDA15	2	2	n.d.	n.d.	n.d.	20.84 ± 0.08	n.d.	> 3 <sup>a</sup>
ATCG00490.1	RBCL	28	545	33.65 ± 0.36	33.73 ± 0.13	-0.1	33.91 ± 0.09	33.75 ± 0.03	0.2

Selected proteins identified and quantified in pull-downs by LC-MS/MS analysis. Protein abundances are expressed as label free quantification (LFQ) values. Numbers indicate mean log2-transformed LFQ values from two biological replicates of *Arabidopsis* leaves (LF) and isolated chloroplasts (CP). Mini-Lys probes were used as pull-down controls to calculate relative enrichments of proteins. LFQ values for RuBisCO are indicated in all samples as background control.  
<sup>a</sup>Estimated enrichment factor assuming a minimum Log2-LFQ threshold of 17.

mitochondria (Fig 4A). Hence, these results indicate a dual localization of HDA14 in mitochondria and chloroplasts. To further confirm the results, we performed a Western blot analysis with HDA14 antiserum on proteins from isolated chloroplasts and mitochondria from WT and stably expressing 35S:HDA14:GFP seedlings and detected the endogenous HDA14 as well as the HDA14-GFP fusion protein in the chloroplast stroma as well as in mitochondria (Appendix Fig S4).

#### HDA14 is a functional lysine deacetylase and is mainly inhibited by TSA *in vitro*

We produced a recombinant N-terminally His-tagged HDA14 protein, which lacks the first 45 amino acids of the predicted N-terminal signal peptide (Appendix Fig S5), to investigate the predicted KDAC activity of HDA14. The activity of the purified protein was tested in a colorimetric assay based on the deacetylation of a synthetic acetylated p53 peptide coupled to a chromophore (Dose *et al.*, 2012). Using this assay, a deacetylase rate of 0.05/s (± 0.0032) was calculated for His-HDA14 at 100 μM substrate, which is active with both Zn<sup>2+</sup> or Co<sup>2+</sup> as cofactors (Fig 4B). Recent publications have shown that recombinant human HDAC8 is more active when the catalytic Zn<sup>2+</sup> is replaced by Co<sup>2+</sup> (Gantt *et al.*, 2006). However, this is not the case for HDA14, but the enzyme is also active with Co<sup>2+</sup>. Interestingly, apicidin acted only as a weak inhibitor for HDA14 even at concentrations of 100 μM. In contrast, TSA inhibited its activity by 80% at a concentration of 5 μM, the same concentration used in the leaf strip inhibitor experiments.

#### HDA14 regulates lysine acetylation levels of plastid proteins related to photosynthesis

To analyze the *in vivo* function of HDA14, a knock-out line (*hda14*) was obtained (Appendix Fig S6) and changes in lysine acetylation site and protein abundances between *hda14* and WT leaves were compared (Fig 5A–F). In total, 832 lysine acetylation sites were identified and quantified from leaves under normal light conditions (Fig 5A; Dataset EV3), and a further 425 lysine acetylation sites were identified from isolated thylakoids (Fig 5B, Dataset EV4), presumably associated with photosynthetic membrane proteins. While no major changes in protein abundances and plant growth were detected for *hda14* in comparison with WT (Fig 5D–F, Appendix Fig S6), 26 lysine acetylation sites on 26 protein groups

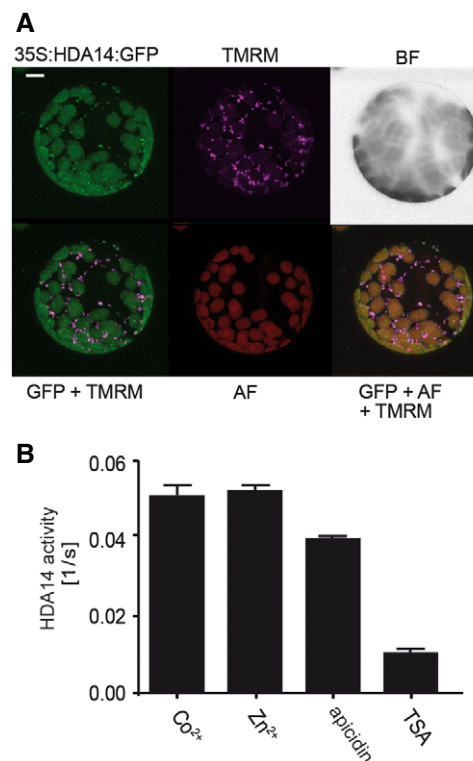


**Figure 4. HDA14 protein localizes to the chloroplasts and mitochondria in *Arabidopsis*, and its activity is dependent on cofactors and can be inhibited by deacetylase inhibitors.**

A GFP localization (green) of the HDA14-GFP fusion constructs in *Arabidopsis* protoplasts (35S:HDA14:GFP) from stable transformants. The mitochondrial marker TMRM is depicted in purple. GFP+TMRM shows the overlay image of 35S:HDA14:GFP and TMRM, AF indicates the chlorophyll autofluorescence and BF the bright-field image of the protoplast. GFP+AF+TMRM represents the overlay image of the three fluorescence channels. Scale bar: 10 μm.

B Deacetylase activity of the recombinant 6xHis-HDA14 protein using a colorimetric assay. Co<sup>2+</sup> and Zn<sup>2+</sup> were used as cofactors, apicidin (100 μM) and trichostatin A (5 μM) as deacetylase inhibitors (*n* = 5, ± SD).

were increased in between twofold and 80-fold in abundance in the mutant with a FDR < 5%. All of these lysine acetylation sites were detected on proteins localized in the plastid. Another 137 lysine acetylation sites from 122 protein groups were found significantly up-regulated in the mutant but with a lower confidence level

( $P < 0.05$ ). Of these 137 up-regulated lysine acetylation sites, 35 were uniquely identified in the thylakoid fraction and 13 sites were detected in both pull-downs. More than 90% of these proteins are annotated as plastid-localized and are involved in several biochemical processes according to a MapMan analysis (Thimm *et al.*, 2004). While around 30% of the proteins have unknown functions, 24% are involved in photosynthesis, 12% in protein synthesis, degradation, and assembly, and around 5% each in lipid metabolism, redox regulation, regulation of transcription, and tetrapyrrole synthesis, as well as 1–3% each are involved in nucleotide metabolism, cell division, ABC transport, secondary metabolism, signaling, organic acid transformation, and amino acid metabolism. Eight of the HDA14 potential target proteins are encoded in the plastome, which further indicates that the deacetylation reaction is occurring within the chloroplast stroma. Among the eight plastome-encoded proteins affected in their acetylation status by the absence of HDA14, the alpha and beta-subunit of the ATP-synthase as well as several photosystem proteins, including the PSII reaction center protein D

and the PSI PsaA/PsaB protein, were identified. These results provide a further indication that HDA14 has a regulatory role in photosynthesis.

The regulation of photosynthesis by post-translational modifications such as phosphorylation and redox regulation is known to be of major importance at low light intensities, for example, during dawn and sunset, when the Calvin–Benson cycle becomes gradually activated or inactivated, respectively, due to changes in stromal pH, ATP, and NADPH levels (Carmo-Silva & Salvucci, 2013; Buchanan, 2016). Hence, we analyzed the acetylation status of the *hda14* plants in comparison with WT after the plants were transferred from normal light (100  $\mu\text{mol quanta m}^{-2}\text{s}^{-1}$ ) to low light (20  $\mu\text{mol quanta m}^{-2}\text{s}^{-1}$ ) intensities for 2 h. Under these conditions, 36 lysine acetylation sites on 32 protein groups showed a significant increase ( $P < 0.05$ , 2 to 100-fold), while the total protein abundances of these proteins were unchanged (Fig 5C and F, Dataset EV5). Twenty-six of these proteins are predicted to be localized in plastids. The MapMan analysis revealed that the biological process

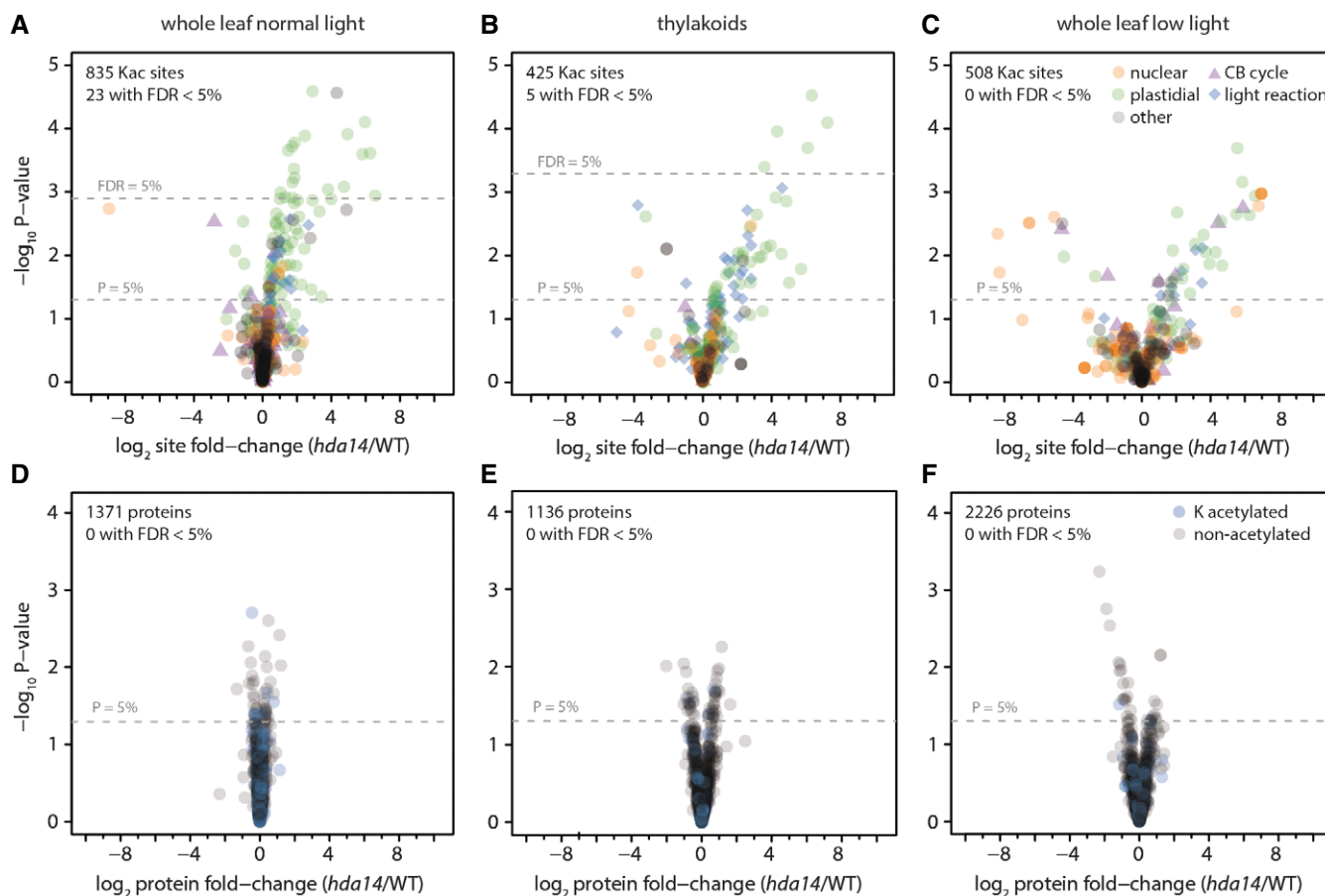


**Figure 5. Differential lysine acetylation and protein expression in *hda14* versus wild-type leaves under normal light (A, D), in isolated thylakoids (B, E), and under low-light conditions (C, F).**

A–F Volcano plots depict lysine acetylation site ratios (A–C, top row) or protein ratios (D–F, bottom row) for mutant versus control, with  $P$ -values determined using the LIMMA package. Orange, protein with nuclear localization; green, protein with plastidial localization; purple triangles, proteins of the Calvin–Benson (CB) cycle; blue diamonds (top row), proteins of the light reaction; localization information according to SUBA4 database. Blue circles (bottom row), proteins with lysine acetylation sites identified. Dashed lines indicate significance thresholds of either uncorrected  $P$ -values  $< 5\%$  or Benjamini–Hochberg corrected FDR  $< 5\%$ . A missing FDR line indicates that the 5% threshold was not reached by any of the data points.

photosynthesis is significantly enriched among those regulated proteins, including RCA (K368/K438, log<sub>2</sub>-FC 5.89/4.85) as a master regulator of Calvin–Benson cycle activity and RuBisCO large subunit (K474, log<sub>2</sub>-FC 1.96) itself. RuBisCO catalyzes the carboxylation or alternatively oxygenation of ribulose-1,5-bisphosphate as the first step in either the Calvin–Benson cycle or photorespiration, and thereby enables the photoautotrophic lifestyle of plants. The RuBisCO enzyme is activated by carbamylation of the active site, a process that is dependent on pH, Mg<sup>2+</sup>-ions and requires the removal of sugar-phosphate inhibitors that otherwise block the active site (Portis *et al*, 2008). The removal of these inhibitors requires specific conformational changes to RuBisCO that are induced by RCA, a AAA<sup>+</sup>-ATPase enzyme. RCA is composed of redox-active alpha isoforms as well as redox-inactive beta-isoforms in *Arabidopsis* (Carmo-Silva & Salvucci, 2013). The RCA activity itself is inhibited under low light by rising ADP concentrations and remains inactive until the photosynthetic electron transport chain again raises the ATP/ADP ratio in response to higher irradiance. The RuBisCO activation state or initial activity, that is, the percentage of active sites free to perform catalysis, as well as total potential activity can be measured by rapid leaf protein extractions (Carmo-Silva *et al*, 2012). Hence, we determined the RuBisCO activity as well as the RuBisCO activation state of the *hda14* plants compared to WT. The results clearly demonstrate that the RuBisCO initial as well as total activity is significantly increased in the *hda14* mutant compared to WT (Fig 6A). While the total activity was increased on average by around 30%, the initial activity was more than doubled in *hda14* compared to WT (Fig 6A), leading to a significantly 90% increased RuBisCO activation state in the mutant under low light (Fig 6B).

Since the lysine acetylation site K438 of the RCA β1-isoform was also found increased after TSA treatment (but not K368), we performed a site-directed mutagenesis on this site in a N-terminally His-tagged RCA-β1 protein. Lysine 438 was exchanged to glutamine (K438Q) and arginine (K438R) to mimic and abolish the lysine acetylation status, respectively. The ATPase activities of the purified mutant RCA proteins were compared to the unmodified WT-like RCA-β1 protein (Fig 6C). Strikingly, the total activity of the K438Q mutant was not affected by this mutation, while the replacement of lysine to arginine led to a strongly diminished enzyme activity. Under low-light conditions, the increase in plastid ADP level plays an important role in the regulation of the RCA activity. Hence, we tested the level of ADP inhibition on the three RCA variants. While the WT-like isoform was inhibited by nearly 19% at an ATP:ADP ratio of 0.11, the activity of the K438Q mutant was only inhibited by about 8%. The K438R mutant, which mimics the non-acetylated state, showed an even stronger ADP inhibition of about 30% under these conditions (Fig 6C). Taken together, the results from this experiment further support that lysine acetylation at K438 leads to a higher RCA and thus RuBisCO activity under low light as observed in the *hda14* mutant.

## Discussion

KDACs have important functions in plant development and acclimation of plants to environmental stresses (Shen *et al*, 2015). So far, these enzymes have mainly been studied with respect to their deacetylase function on histones in plants, despite the large number of different types of lysine-acetylated proteins detected in

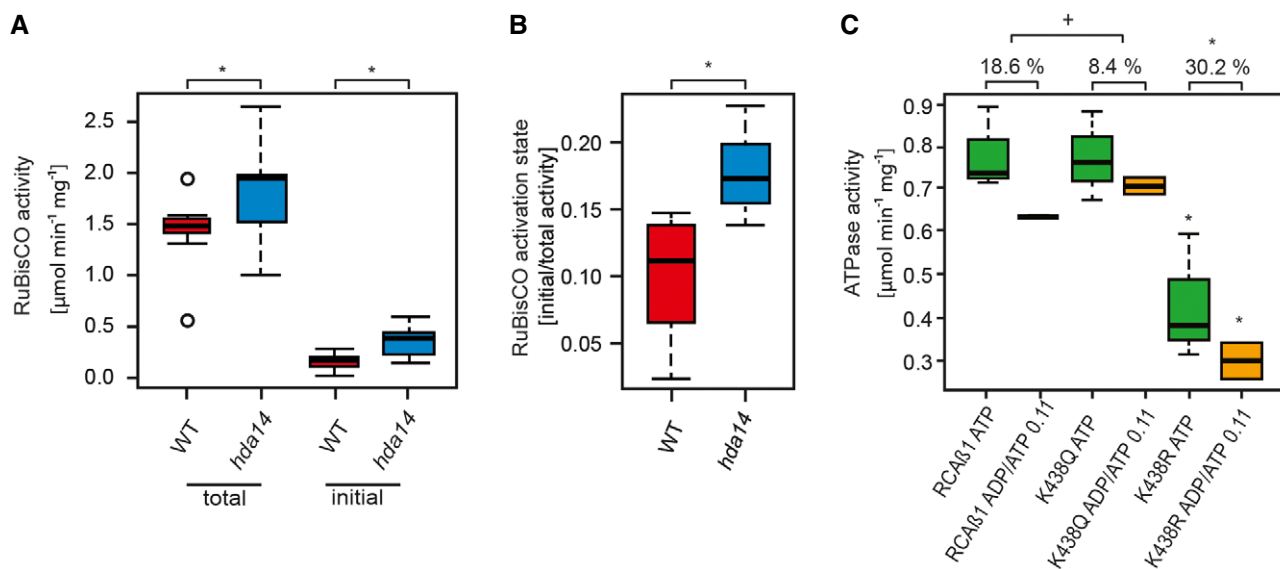


**Figure 6. RuBisCO activity and RuBisCO activation state are increased in the *hda14* mutant under low-light conditions.**

A RuBisCO initial and total activity in WT and *hda14* in low-light-treated plants. Initial activity was measured directly upon extraction. For the total activity, samples were incubated with H<sub>2</sub>CO<sub>3</sub> for 3 min to fully carbamylate the active site of RuBisCO ( $n = 10$ ,  $*P < 0.05$ ,  $t$ -test).

B RuBisCO activation state ( $P < 0.05$ ,  $t$ -test).

C ATPase activity of recombinant 6x-HisRCAβ1 WT, K438Q and K438R with ATP and ADP/ATP = 0.11, respectively ( $n = 3$ ,  $*P < 0.05$ ,  $^+P < 0.1$ ,  $t$ -test). Percentage values on top indicate percent ADP inhibition.

Data information: Boxes indicate lower and upper quartiles of data and whiskers indicate highest and lowest values. Small circles represent outliers. The bars across boxes indicate median values.

recent years (Hosp *et al*, 2016). In this work, we studied the proteome-wide putative targets of the RPD3/HDA1 class of lysine deacetylases in *Arabidopsis* by relative quantification of the changes in the lysine acetylome after inhibitor treatment of *Arabidopsis* leaves with apicidin and TSA. In total, we detected 2,152 lysine acetylation sites in 4-week-old *Arabidopsis* leaves when combining all experiments included in this study. The lysine acetylation sites were found on 1,022 protein groups from all different subcellular compartments and compartment-specific amino acid motifs surrounding the lysine acetylation sites were detected. Similar to human and *Drosophila* sequence motifs, glutamic acid and glycine can be frequently found at position  $-1$  next to the lysine acetylation site also in *Arabidopsis*, while tyrosine, phenylalanine, but not proline, are also enriched in the *Arabidopsis* motifs at position  $+1$ , but with a lower frequency (Choudhary *et al*, 2009; Weinert *et al*, 2011). Generally, the acetylated lysines also occur in lysine-rich regions in *Arabidopsis* similar to those described for human and fly (Weinert *et al*, 2011).

In HeLa cells, apicidin was identified as an inhibitor of mainly the RPD3-like KDACs, while TSA inhibits enzymes from both RPD3/HDA1 classes (Scholz *et al*, 2015). Although we cannot exclude that apicidin and TSA have different specificities for *Arabidopsis* KDACs compared to humans, we observed that recombinant *Arabidopsis* HDA14, which is a HDA1-like KDAC, is not efficiently inhibited by apicidin but by TSA. This supports the notion that similar specificities of both inhibitors exist for the *Arabidopsis* KDACs as well. In *Arabidopsis*, four KDACs belong to the RPD3-like group, including HDA1/19, HDA6, HDA7, and HDA9 (Hollender & Liu, 2008). Two additional KDAC genes, *HDA10* and *HDA17*, are closely related to *HDA9*, but the predicted proteins lack a catalytic domain and therefore are probably inactive. Lysine acetylation sites on 91 protein groups were significantly ( $P < 0.05$ ) up-regulated after apicidin treatment and are therefore most likely substrates of at least one of these four KDACs. The dominant nuclear localization among these proteins fits to the observed localizations of the RPD3-like KDACs in the nucleus. While HDA1/19, HDA6, and HDA9 were detected mainly in the nucleus, the localization of HDA7 has yet to be determined. Although the predicted HDA7 protein contains both a nuclear localization sequence as well as a nuclear export signal, it is unclear to what extent this protein is active due to its low expression level in most tissues.

From the 91 target protein groups identified upon inhibition with apicidin, only 14 are histone-like proteins. Hence, we identified 77 new candidate protein groups, which are potential substrates of the RPD3-like KDACs in *Arabidopsis*. This list of potential target proteins with the exact information on their acetylation sites can be regarded as valuable resource for future studies on the KDAC functions in plant stress response and development. Interestingly, a high mobility group box protein with ARID/BRIGHT DNA-binding domain (At1g76110) was identified as one of the substrate proteins, which was also regulated upon TSA treatment. These types of proteins have been identified as interaction partners of human HDAC1/2 (Joshi *et al*, 2013). Furthermore, a physical interaction was previously detected between *Arabidopsis* HDA6 and the histone H3.3 (At4g40030) (Earley *et al*, 2006). We identified several peptides of histone H3-like proteins that were up-regulated by more than 2-fold at the positions K9, 14, 18, 23, 27, 36, and 37 after apicidin treatment, but less so after treatment with TSA. Several of

these lysine acetylation sites on histone H3 are of great importance for chromatin regulation and remodeling [e.g., (Mahrez *et al*, 2016)]. For example, H3K9 acetylation was found to be associated with actively transcribed genes and has a strong impact on various developmental processes in plants (e.g., Ausin *et al*, 2004; Benhamed *et al*, 2006). Differences in the strength of TSA and apicidin inhibition could be explained by differences in the uptake of the inhibitors into the *Arabidopsis* cells, as well as by differences in the  $K_i$  values of the different *Arabidopsis* KDACs for these chemicals. Furthermore, our data indicate that TSA might not be effectively taken up into plastids, since the recombinant HDA14 protein was strongly inhibited by TSA, but only few plastid proteins were affected by TSA treatment of *Arabidopsis* leaves.

In addition to the many new KDAC inhibitor target proteins in the nucleus, there were also several interesting candidate proteins identified in the cytosol, such as the FRIENDLY protein (At3g52140), which is required for correct distribution of mitochondria within the cell. In a previous study, we already demonstrated that two lysine sites, which can be acetylated, regulate FRIENDLY function (El Zawily *et al*, 2014).

After TSA treatment, lysine acetylation sites from unique protein groups were regulated, which were not affected by apicidin treatment, indicating that those sites are specifically regulated by HDA1-type HDACs. These proteins included RCA- $\beta$ 1, photosystem I subunit D-2, ribosomal L6 family protein, S-adenosyl-L-methionine-dependent methyltransferases superfamily protein, the telomere repeat binding factor 1, and a histone H2B protein (Dataset EV2). Candidates of KDAC proteins from the HDA1-type group that might be responsible for the regulation of the lysine acetylation sites of these proteins include HDA5, 8, 14, 15, and 18, which cluster together with the human class 2 KDACs (Alinsug *et al*, 2009). By using a hydroxamate-based KDAC-probe, which allows the enrichment of active RPD3/HDA1-class KDACs from protein extracts, we were able to detect HDA5, 14, and 15 in total leaf extracts of 4-week-old *Arabidopsis* leaves. By using the same probe, we previously enriched all class 1 and class 2b KDACs from HeLa cells, indicating that the probe is able to bind all types of RPD3/HDA1-class KDACs (Dose *et al*, 2016). Hence, we conclude that HDA5, 14, and 15 are the most abundant KDACs in *Arabidopsis* leaves. Strikingly, both TSA and apicidin treatment resulted in an increased acetylation of plastid proteins involved in photosynthesis. Here, we identified HDA14 as the first organellar-localized RPD3/HDA1 class protein which is active as a KDAC and which has the majority of its candidate target proteins in the plastid stroma. At the concentration of apicidin used in our study, HDA14 was not significantly inhibited in its activity, which further supports the observation that apicidin mainly inhibits RPD3-like KDACs. Hence, the plastid target proteins, which showed mildly increased lysine acetylation after apicidin treatment, might be regulated by an unknown RPD3-like deacetylase. For example, we identified six lysine acetylation sites on the TROL protein, which is required for anchoring the ferredoxin-NADP reductase (FNR) to the thylakoid membranes and to sustain efficient linear electron flow in the light reactions of photosynthesis. While K328 and K348 of TROL were more than twofold increased in their acetylation level in the *hda14* loss-of-function mutant, only K337 showed a 1.2-fold increased acetylation after apicidin treatment. Lysine acetylation sites on FNR itself were not significantly regulated upon KDAC inhibition. Here, we identified four lysine

acetylation sites on both FNR1 (K287, 290, 321, 325) and FNR2 (K90, 243, 299, 330) isoforms, of which only two have been previously reported (Lehtimäki *et al.*, 2014).

By analyzing the acetylome of *hda14* mutants, we were able to identify the unique substrate proteins of HDA14. HDA14 was previously identified as a nuclear/cytosolic protein based on enrichment in the microtubule fraction of a red fluorescent-tagged version of the protein (Tran *et al.*, 2012). However, the N-terminal location of this tag would hinder the protein from entering the chloroplast. Moreover, the authentic N-terminus of HDA14 contains a clear signal sequence for the plastids as predicted by bioinformatical analysis (Alinsug *et al.*, 2009). By using the Asu-Hd probe on isolated plastid fractions as well as by using C-terminal GFP-tagged fusion proteins, we were able to confirm the predicted plastid localization of HDA14. Furthermore, most of the candidate HDA14 substrate proteins identified reside in the plastids and are involved in metabolism and photosynthesis.

With the analysis of the HDA14-dependent acetylome, we found that the RCA- $\beta$ 1 site K438 is a substrate site of HDA14. Increased acetylation of this site reduced the ADP sensitivity of the RCA protein, which plays an important role for the Calvin–Benson cycle activation under low light intensities when the ADP/ATP ratio in plastids is still high (Carmo-Silva & Salvucci, 2013). Since the alpha-isoform of RCA in *Arabidopsis* is considerably more sensitive to inhibition by ADP than the beta-isoform (Carmo-Silva & Salvucci, 2013), the effect of acetylation of K438 of RCA- $\beta$ 1 in relieving ADP inhibition might be mediated by RCA- $\alpha$  through an effect of acetylation on subunit (i.e., alpha–beta) interaction.

Lysine acetylation on *Arabidopsis* RCA was detected in a previous study (Finkemeier *et al.*, 2011), but on a different lysine residue and the functional consequences were not studied so far. In addition to increased acetylation, we also observed increased RuBisCO activity under low-light conditions in the *hda14* mutant, which co-occurred with increased acetylation at K474 on the RuBisCO large subunit next to the strongly increased acetylation of K368 and K438 on RCA and on carbonic anhydrase (K269, At3g01500). Acetylation on all of these proteins might play an important role in fine-tuning of RuBisCO activity. In contrast to our results obtained in the *hda14* mutant, two independent previous studies revealed that a decrease in RuBisCO acetylation resulted in a higher activity of the enzyme (Finkemeier *et al.*, 2011; Gao *et al.*, 2016). However, K474 on the RuBisCO large subunit (RBCL) was not detected in either of these studies, and hence, this site could have a different role than acetylation on any of the other 18 acetylation sites detected here and elsewhere.

In conclusion, in this study, we were able to define the heretofore-unknown acetylation candidate target proteins of RPD3/HDA1 class HDACs in *Arabidopsis* and specifically those of HDA14, as the first identified RPD3/HDA1 KDACs in organelles. Furthermore, our study revealed that about 10% of the detected lysine acetylation sites can be regulated by these types of KDACs in *Arabidopsis* leaves. Many sites might be specifically regulated under certain environmental or developmental conditions due to changes in KDAC activities, as we observed for low-light conditions for example. The activity of KDAC themselves might be regulated via post-translational modifications (Mengel *et al.*, 2017) or by change in interaction partners that lead to the formation of different KDAC complexes (Dose *et al.*, 2016). Future studies, with more detailed

analyses of individual lysine sites in proteins and the analysis of further KDAC mutants and environmental conditions, will allow unraveling this complex network of fine-tuning of protein functions and interactions by lysine acetylation. Since lysine acetylation sites can act as molecular switches, they could be engineered in plant proteins to regulate cell-signaling cascades, the expression of certain genes, or to modulate the activities of metabolic enzymes. Furthermore, due to recent advances in advances in CRISPR/CAS technologies, lysine acetylation sites can be used for site-directed mutagenesis also in crop plants. Modifying these lysine residues to constitute acetylated or non-acetylated mimics ideally will allow a switching of metabolic activities and outputs that have the potential to enhance plant yields or direct metabolism in a way to enhance the accumulation of metabolic intermediates to increase the nutritional values of crops and thereby indirectly promote human health.

## Materials and Methods

### Plant material and growth conditions

*Arabidopsis thaliana* (Col-0) plants were grown for 4 weeks in a climate chamber using a 12-h light/12-h dark (21°C) photoperiod with a light intensity of 100  $\mu\text{mol quanta m}^2/\text{s}$  and 50% relative humidity. For low-light treatments, plants were transferred to 20  $\mu\text{mol quanta m}^2/\text{s}$  for 2 h before harvest. For growth on plates, *Arabidopsis* seeds were sterilized and transferred to half-strength Murashige–Skoog medium supplemented with 0.8% phytoagar. The *hda14* line (SALK\_144995C) was obtained from the Nottingham *Arabidopsis* stock center (NASC) and PCR screened according to Salk Institute Genomic Analysis Laboratory instructions (O'Malley *et al.*, 2007) using the following primers: HDA14\_LP 5'-GAAAC ATGTCACGCAAAAATG-3', HDA14\_RP 5'-TTTGTGGTTGCTTC TTCC-3', and the TDNA primer SALK-Lb1.3 5'-ATTTTGCCGA TTTCGGAAC-3'. PCR products were run on 1% agarose Tris–acetate (TAE: 40 mM Tris, 20 mM acetate, 1 mM EDTA, pH 8.0) and visualized by UV illumination upon ethidium bromide staining.

### Trichostatin A and apicidin treatment

About 20 fully expanded leaves from 4-week-old *Arabidopsis* plants were pooled and cut into 2-mm-diameter leaf slices (for each biological replicate). After vacuum infiltration in effector solutions (three times for 5 min), the leaf slices were incubated at 100  $\mu\text{mol quanta m}^2/\text{s}$  for 4 h. All solutions used for infiltrations were made in 1 mM MES pH 5.5 (KOH). All chemicals were purchased from Sigma-Aldrich (Gillingham, Dorset, UK). All stock solutions were dissolved in DMSO. Control experiments were then performed with DMSO added in same concentrations without effectors. Leaf material was briefly dried on tissues for harvest and flash-frozen in liquid nitrogen.

### GFP fusion and plant transformation

Entry clones for Gateway cloning were generated with the pENTR/SD/TOPO vector (Invitrogen™). The open reading frame of HDA14 (At4g33470) without stop codon from *Arabidopsis* (Col-0) was amplified from cDNA using the following primers: 5'-CACCATGTC CATGGCGCTAATTGT-3' and 5'-TAAGCAATGAATGCTTTGGCTC

TC-3'. LR reactions were performed for recombination into the pK7GW2 vector (Karimi *et al.*, 2007). The vector construct was verified by sequencing and transformed into *Agrobacterium tumefaciens* strain C58 followed by floral dip transformation of *Arabidopsis* (Col-0) plants (Clough & Bent, 1998). Transformants were selected by germination of seeds on MS-agar plates containing kanamycin (50 µg/ml). Resistant plants were transferred to soil and propagated.

#### RNA isolation and RT-PCR

Total RNA of *Arabidopsis* leaves was extracted using Trizol<sup>®</sup> (Invitrogen<sup>™</sup>) followed by chloroform extraction, and precipitation with isopropanol and subsequently LiCl<sub>2</sub>. The quality and quantity of the RNA were confirmed on agarose gels and a UV-spectrometer. Complementary DNA (cDNA) was synthesized from DNase-treated RNA with SuperScriptIII reverse transcriptase (Invitrogen<sup>™</sup>) following the manufacturer's instruction and using dT<sub>20</sub>. Real-time qPCR was carried out in triplicate in an iQ<sup>™</sup>5 Multicolor Real-Time PCR Detection System (Bio-Rad) using iQ<sup>™</sup>5 SYBR Green Super Mix (Bio-Rad) and gene-specific primers: HDA14-F 5'-ATCTGTGGCAGACTCGTTTCG-3', HDA14-R 5'-TCGCACCTTCTCATTGGTTC-3'. Levels of selected transcripts in each sample were calculated using a standard curve method (Finkemeier *et al.*, 2013). Expression levels of the HDA14 transcript were normalized to *ACTIN2* (At3g18780) transcript as housekeeping gene using the following primers: actin2-F 5'-CTGTACGGTAACATTGTGCTCAG-3' and actin2-R 5'-CCGATCCAGACTGTACTTCC-3'.

#### Protoplast isolation and confocal laser scanning microscopy

Protoplast isolation was performed from 4-week-old *Arabidopsis* leaves after the tape-sandwich method (Wu *et al.*, 2009). Staining with 20 nM TMRM (Sigma) was performed according to the manufacturer's protocol. Imaging was performed with a spectral TCS SP5 MP confocal laser scanning microscope (Leica Microsystems, Mannheim, Germany) using an argon and DPSS-Laser laser, respectively, at an excitation wavelength of 488 nm (eGFP) and 543 nm (TMRM). The water immersion objective lens HCX PL APO 20.0× 0.70 IMM UV was used for imaging in multitrack mode with line switching. eGFP fluorescence and TMRM fluorescence were measured at 500–530 and 565–615 nm, respectively.

#### Heterologous expression and purification of recombinant HDA14 protein

cDNAs were amplified by PCR excluding the coding region for the 45aa signal peptide using the following primers: HDA14p-F: 5'-TTTAGTACAGAGAAGAATCCTCTATTACCATCT-3' and 5'-TCAAA CAAATTCACCTTATAAGCAATG-3'. The PCR product was cloned into pEXP-5-NT/TOPO<sup>®</sup> TA (Invitrogen<sup>™</sup>), which allows expression and purification of the recombinant, N-terminally 6× His-tagged protein. Vector constructs were verified by sequencing. After transforming *E. coli* BL21(DE3) (Invitrogen<sup>™</sup>) with the expression vector, the recombinant protein was expressed using the EnPresso system (BioSilta, Germany) as described before (Jost *et al.*, 2015): 500 ml of EnPresso medium was mixed with 12.5 µl ZnCl<sub>2</sub> (1 mM) solution and 25 µl of the "EnZ I'm" mix. Freshly prepared medium was

inoculated 1:100 with a 6-h-cultivated pre-culture at 37°C under gentle shaking (160 rpm) and incubated overnight. Subsequently, the temperature was reduced to 25°C and a "booster tablet" and 50 µl "EnZ I'm" mix were added to the culture medium followed by 500 µM IPTG. The culture was incubated for 24 h at 250 rpm. The cells were harvested by centrifugation (10 min at 3,000 × g), and the pellet was resuspended in PBS buffer (pH 8.0) and lysed with a homogenizer (EmulsiFlex-C5, Avestin) at 4°C. The cleared lysate (centrifugation for 20 min at 30,000 × g) was incubated with 1 ml of Ni-NTA Agarose slurry (Qiagen) for 2 h at 4°C. The resin was washed with 50 ml PBS, pH 8.0, 4°C, and the protein was eluted with 300 mM imidazole in HDAC buffer (8 mM KCl, 100 mM NaCl, 10 mM HEPES, pH 8.0). Pure fractions were combined and dialyzed against HDAC buffer containing 10 mM EDTA and subsequently against HDAC buffer supplied with 0.5 mM EDTA. The sample was concentrated with a centrifugation filter device with 10 kD MWCO (Amicon Ultra, Merck Millipore), supplied with 20% (v/v) glycerol and stored at –80°C until usage.

#### HDA14 activity assay

The deacetylation assays were performed with a previously described p53-derived peptide substrate containing the chromophore 5-amino-2-nitrobenzoic acid (p53-5,2-ANB) (Dose *et al.*, 2012). To produce the apoenzyme, the purified HDA14 protein was first dialyzed against 10 mM EDTA and 1 mM DTT and in a second step against 0.5 mM EDTA to remove bound metal ions. For the enzyme assay, HDA14 was supplied with either Zn<sup>2+</sup> or Co<sup>2+</sup> ions by incubating the enzyme solution with 1 mM of ZnCl<sub>2</sub> or CoCl<sub>2</sub> on ice for 30 min. Deacetylation assays were performed by incubating 1 µM of either Zn<sup>2+</sup> or Co<sup>2+</sup> supplied HDA14 with 100 µM p53-5,2-ANB substrate in HDAC reaction buffer (10 mM HEPES, 100 mM NaCl, 8 mM KCl, 10 µM BSA, pH 8.0) in a total volume of 50 µl at RT. The reaction was stopped after 10 min by adding 10 µl quenching solution (6.25 µM TSA in 0.1% (v/v) TFA) and developed by adding 10 µl of trypsin solution (6 mg/ml). After 30 min of trypsinization, the reaction mixture was supplied with 70 µl of HDAC reaction buffer, transferred into a 100-µl quartz cuvette, and the absorbance was monitored at 405 nm in a photometer (Helma, Germany). Studies with inhibitors apicidin (5 and 100 µM) and TSA (5 µM) were performed by adding these compounds to the assay before the reactions were started. All rates were normalized to the concentration of HDA14.

#### Western blot analyses

Proteins were separated on 12% SDS-polyacrylamide gels, blotted onto nitrocellulose membrane, and incubated overnight with the primary antibodies. The secondary IRDye 800CW antibody (LI-COR) was used in a 1:10,000 dilution and detected with the Odyssey reader (LI-COR).

#### RuBisCO activity measurements for activation state determination

For determination of the RubisCO activation state under low-light conditions, plants were transferred to low irradiation (20 µmol quanta m<sup>2</sup>/s) for 5 h at 21°C, then harvested, and frozen in liquid

nitrogen. RuBisCO initial and total activity were assayed by incorporation of  $^{14}\text{CO}_2$  into acid-stable products (Salvucci, 1992). The leaves were homogenized in extraction medium [100 mM Tricine–NaOH pH 8.0, 1 mM EDTA, 5% polyvinylpyrrolidone (PVP-40), 5% polyethylene glycol 3350 (PEG3350), 5 mM (DTT), and protease inhibitor cocktail (Roche)]. Initial activities were measured immediately upon extraction, whereas total activities were measured after 3-min incubation in assays without RuBP to fully carbamylate the enzyme (Carmo-Silva *et al*, 2012). For each sample, assays were conducted in duplicate. Initial and total activities were used to calculate RuBisCO activation state, that is, (initial/total activity  $\times$  100) = % activation.

### Purification and assay of RCA

The coding sequence of the RCA $\beta$ 1 spliceform (At2g39730.2) was amplified from *Arabidopsis* cDNA using the following primers: 5'-CTCCGATATCTTACTTGCTGGGCTCCTTT-3' and 5'-TTTTGATATCTCAAACCTCTGTTTACC-3' introducing *SacI* and *EcoRV* restriction sites for cloning into pCDFDuet-1 (Novagen<sup>®</sup>). Site-directed mutants of RCA K438R and K438Q were introduced with the Quik-Change Site-Directed Mutagenesis Kit (Agilent Technologies) using the following primers: RCA $\beta$ 2-K438R 5'-GAACTTCTACGGTAGAA CAGAGGAAAAGG-3' and RCA $\beta$ 2-K438Q 5'-GAACTTCTACGGTCAA ACAGAGGAAAAGG-3'. The N-terminally 6-His-tagged protein was expressed and purified from Rosetta-gami cells (Novagen<sup>®</sup>) as described detail in (Barta *et al*, 2011). ATPase activity of 5  $\mu\text{g}$  recombinant RCA was measured for 1 min at 23°C in 50  $\mu\text{l}$  reaction buffer (100 mM HEPES-KOH (pH 8.0), 20 mM  $\text{MgCl}_2$ ) containing 500  $\mu\text{M}$  ATP and 500  $\mu\text{M}$  ATP and 55  $\mu\text{M}$  ADP, respectively. The reaction was heat inactivated at 95°C. The ATP consumption was determined using the KinaseGlo Max Luminescent Assay Kit (Promega) according to the manufacturer's protocol.

### Isolation of intact chloroplasts and mitochondria

Chloroplasts were isolated from dark incubated (12 h) 5-week-old rosette leaves of *Arabidopsis*. Leaves were homogenized in ice-cold HB-buffer (0.45 M sorbitol, 20 mM Tricine-KOH pH 8.45, 10 mM EDTA, 10 mM  $\text{NaHCO}_3$ , 0.1% BSA, and 2 mM sodium ascorbate). Chloroplasts were purified on a Percoll gradient (40–80%) and resuspended in sorbitol buffer (0.3 M sorbitol, 20 mM Tricine-KOH pH 8.45, 2.5 mM EDTA, and 5 mM  $\text{MgCl}_2$ , 2 mM sodium ascorbate). Mitochondria were isolated as described previously (König *et al*, 2014a).

### Isolation of thylakoids

Chloroplasts were lysed in 2 ml TMK buffer (50 mM HEPES/KOH pH 7.5, 0.1 M sorbitol, 5 mM  $\text{MgCl}_2$ , 10 mM NaF), and thylakoid membranes were sedimented at 14,000  $\times$  g.

### Preparation of cell extracts and enrichment of active histone deacetylases

Leaves from 5-week-old *Arabidopsis* plants were homogenized in extraction buffer (50 mM Tris–KOH (pH 7.5), 150 mM NaCl, 10% [v/v] glycerol, 5 mM dithiothreitol (DTT), 1% [v/v] Triton X-100,

and protease inhibitor cocktail (Sigma-Aldrich). Homogenates were centrifuged at 14,000  $\times$  g, and protein concentration of the supernatant was determined with the Pierce 660 nm Protein Assay (Thermo Fisher Scientific). All protein extracts were desalted on PD-10 Desalting Columns (GE Life Sciences), and the samples were eluted with immunoprecipitation buffer (50 mM Tris, pH 7.5, 150 mM NaCl, 10% [v/v] glycerol).

The immobilized peptide probes, mini-AsuHd, and mini-Lys (Dose *et al*, 2016) were equilibrated with immunoprecipitation buffer two times and incubated with the protein extracts overnight at 4°C, under constant rotation. The next day, the beads were gently pelleted by centrifugation. The beads were transferred onto micro-centrifugal filter system (Amchro GmbH) and washed five times with 1 ml immunoprecipitation buffer. Proteins bound on beads were subjected to on-bead digestion. Proteins were denatured in 6 M urea prepared in 0.1 M Tris–HCl (pH 8.0), 1 mM  $\text{CaCl}_2$  and reduced with 5 mM DTT. Reduced cysteines were alkylated with 14 mM chloroacetamide for 30 min. Excess chloroacetamide was quenched with DTT. Proteins were trypsinated at a urea concentration of 1 M and a trypsin (Sigma-Aldrich) to protein ratio of 1:100 at 37°C. Resulting peptides were desalted on SDB-RPS and C18 Stage-Tips, respectively (Rappsilber *et al*, 2007; Kulak *et al*, 2014).

### Protein extraction, peptide dimethyl labeling, and lysine-acetylated peptide enrichment

Frozen leaf material was ground to fine powder in liquid nitrogen and extracted using a modified filter-assisted sample preparation (FASP) protocol with 30k MWCO Amicon filters (Merck Millipore) as described in detail in Lassowskat *et al* (2017). Digested peptides were dimethyl-labeled on C18 Sep-Pak plus short columns (Waters) as described previously (Boersema *et al*, 2009; Lassowskat *et al*, 2017). Equal amounts of light and medium-labeled peptides (3–5 mg) were pooled for each replicate and the solvent evaporated in a vacuum centrifuge. The dried peptides were dissolved in 1 ml TBS buffer (50 mM Tris–HCl, 150 mM NaCl, pH 7.6), and pH was checked and adjusted where required. 15  $\mu\text{g}$  peptide mixture was stored for whole proteome analysis. About 10 mg of the pooled labeled peptides was resuspended in 2 ml 95% solvent A (95% acetonitrile, 5 mM ammonium acetate) and 5% buffer B (5 mM ammonium acetate) and fractionated with a flow rate of 500  $\mu\text{l}/\text{min}$  on a Sequant ZIC<sup>®</sup>-HILIC column (3.5  $\mu\text{m}$ , Merck) using a segmented linear gradient of 0–60%. The fractions were combined to seven final fractions and dried in a vacuum centrifuge. Peptides were resuspended in IP buffer (50 mM Tris–HCl pH 7.6, 150 mM NaCl), and the concentration was determined on the spectrophotometer at 280 nm. Lysine-acetylated peptide enrichment was performed as previously described with 1 mg peptide per fraction (Hartl *et al*, 2015; Lassowskat *et al*, 2017). After enrichment, the eluted peptides were desalted using C18 StageTips and dried in a vacuum centrifuge.

### LC-MS/MS

Dried peptides were redissolved in 2% ACN, 0.1% TFA for analysis. Total proteome samples were adjusted to a final concentration of 0.2  $\mu\text{g}/\mu\text{l}$ . Samples were analyzed using an EASY-nLC 1000 (Thermo Fisher) coupled to a Q Exactive, Q Exactive Plus, and an Orbitrap Elite mass spectrometer (Thermo Fisher), respectively. Peptides

were separated on 16 cm frit-less silica emitters (New Objective, 0.75  $\mu\text{m}$  inner diameter), packed in-house with reversed-phase ReproSil-Pur C18 AQ 3  $\mu\text{m}$  resin (Dr. Maisch). Peptides (5  $\mu\text{l}$ ) were loaded on the column and eluted for 120 min using a segmented linear gradient of 0% to 95% solvent B (solvent A 5% ACN, 0.5% FA; solvent B 100% ACN, 0.5% FA) at a flow rate of 250 nl/min. Parameters for the different machines are listed in Dataset EV1.

### MS data analysis

Raw data were processed using MaxQuant software version 1.5.2.8 (<http://www.maxquant.org/>) (Cox & Mann, 2008). MS/MS spectra were searched with the Andromeda search engine against the TAIR10 database (TAIR10\_pep\_20101214; [ftp://ftp.arabidopsis.org/home/tair/Proteins/TAIR10\\_protein\\_lists/](ftp://ftp.arabidopsis.org/home/tair/Proteins/TAIR10_protein_lists/)). Sequences of 248 common contaminant proteins and decoy sequences were automatically added during the search. Trypsin specificity was required, and a maximum of two (proteome) or four missed cleavages (acetylome) were allowed. Minimal peptide length was set to seven amino acids. Carbamidomethylation of cysteine residues was set as fixed, oxidation of methionine, and protein N-terminal acetylation as variable modifications. Acetylation of lysines was set as variable modification only for the antibody-enriched samples. Light and medium dimethylation of lysines and peptide N-termini were set as labels. Peptide-spectrum matches and proteins were retained if they were below a false discovery rate of 1%, modified peptides were filtered for a score  $\geq 35$  and a delta score of  $\geq 6$ . Match between runs and requantify options were enabled. Downstream data analysis was performed using Perseus version 1.5.5.3 (Tyanova et al, 2016). For proteome and acetylome, reverse hits and contaminants were removed, the site ratios log<sub>2</sub>-transformed, and flip-label ratios inverted. For quantitative lysine acetylome analyses, sites were filtered for a localization probability of  $\geq 0.75$ . The “expand site table” feature of Perseus was used to allow separate analysis of site ratios for multiply acetylated peptides occurring in different acetylation states. Technical replicates were averaged, and proteins or sites displaying less than two out of three ratios were removed. The resulting matrices for proteome and acetylome, respectively, were exported and significantly differentially abundant protein groups and lysine acetylation sites were determined using the LIMMA package (Ritchie et al, 2015) in R 3.3.1 (R Core Team, 2016). Volcano plots were generated with R base graphics, plotting the non-adjusted *P*-values versus the log<sub>2</sub> fold-change and marking data points below 5% FDR (i.e., adjusted *P*-values, Benjamini–Hochberg) when present.

### Data availability

The raw data, MaxQuant output files, and annotated MS2 spectra for all acetylated peptides have been deposited to the ProteomeX-change Consortium (<http://proteomecentral.proteomexchange.org>) via the PRIDE partner repository with the dataset identifiers PXD006651, PXD006652, PXD006695, PXD006696.

**Expanded View** for this article is available online.

### Acknowledgements

We would like to thank Jon Nield (Queen Mary, University of London) for the light-reaction figure template, Julia Kimmel for cloning of 35S:HDA14-GFP

constructs, and Anne Harzen and Gintaute Dailydaite (MPIPZ) as well as Anne Orwat (LMU Munich) for technical assistance. This work was supported by the Deutsche Forschungsgemeinschaft, Germany (Emmy Noether Programme FI-1655/1-1), and the Max Planck Gesellschaft.

### Author contributions

MF, MH, IF, AB, MP, KK, MS, PJB, J-OJ, and JS performed research; JC performed computational analysis; MH, MS, and IF designed research; DS, DL, GU, GBGM, and MM provided reagents and analytical equipment; MF, MH, J-OJ, KK, and IF analyzed data; IF drafted the manuscript with input from MH, KK, DL, DS, and MES.

### Conflict of interest

The authors declare that they have no conflict of interest.

## References

- Alinsug MV, Yu CW, Wu K (2009) Phylogenetic analysis, subcellular localization, and expression patterns of RPD3/HDA1 family histone deacetylases in plants. *BMC Plant Biol* 9: 37
- Alfrey VG, Faulkner R, Mirsky AE (1964) Acetylation and methylation of histones and their possible role in regulation of Rna synthesis. *Proc Natl Acad Sci USA* 51: 786–794
- Ausín I, Alonso-Blanco C, Jarillo JA, Ruiz-García L, Martínez-Zapater JM (2004) Regulation of flowering time by FVE, a retinoblastoma-associated protein. *Nat Genet* 3: 162–166
- Barta C, Carmo-Silva AE, Salvucci ME (2011) Purification of rubisco activase from leaves or after expression in *Escherichia coli*. In *Photosynthesis research protocols*, Carpentier R (ed.), pp 363–374. Totowa, NJ: Humana Press
- Benhamed M, Bertrand C, Servet C, Zhou DX (2006) *Arabidopsis* GCN5, HD1, and TAF1/HAF2 interact to regulate histone acetylation required for light-responsive gene expression. *Plant Cell* 18: 2893–2903
- Boersema PJ, Raijmakers R, Lemeer S, Mohammed S, Heck AJR (2009) Multiplex peptide stable isotope dimethyl labeling for quantitative proteomics. *Nat Protoc* 4: 484–494
- Buchanan BB (2016) The carbon (formerly dark) reactions of photosynthesis. *Photosynth Res* 128: 215–217
- Calfapietra C, Penuelas J, Niinemets U (2015) Urban plant physiology: adaptation-mitigation strategies under permanent stress. *Trends Plant Sci* 20: 72–75
- Carmo-Silva AE, Gore MA, Andrade-Sanchez P, French AN, Hunsaker DJ, Salvucci ME (2012) Decreased CO<sub>2</sub> availability and inactivation of Rubisco limit photosynthesis in cotton plants under heat and drought stress in the field. *Environ Exp Bot* 83: 1–11
- Carmo-Silva AE, Salvucci ME (2013) The regulatory properties of rubisco activase differ among species and affect photosynthetic induction during light transitions. *Plant Physiol* 161: 1645–1655
- Chen LT, Luo M, Wang YY, Wu K (2010) Involvement of *Arabidopsis* histone deacetylase HDA6 in ABA and salt stress response. *J Exp Bot* 61: 3345–3353
- Choi SM, Song HR, Han SK, Han M, Kim CY, Park J, Lee YH, Jeon JS, Noh YS, Noh B (2012) HDA19 is required for the repression of salicylic acid biosynthesis and salicylic acid-mediated defense responses in *Arabidopsis*. *Plant J* 71: 135–146
- Choudhary C, Kumar C, Gnäd F, Nielsen ML, Rehman M, Walther TC, Olsen JV, Mann M (2009) Lysine acetylation targets protein complexes and co-regulates major cellular functions. *Science* 325: 834–840

- Cigliano RA, Cremona G, Paparo R, Termolino P, Perrella G, Gutzat R, Consiglio MF, Conicella C (2013) Histone deacetylase AtHDA7 is required for female gametophyte and embryo development in *Arabidopsis*. *Plant Physiol* 163: 431–440
- Clough SJ, Bent AF (1998) Floral dip: a simplified method for *Agrobacterium*-mediated transformation of *Arabidopsis thaliana*. *Plant J* 16: 735–743
- Cox J, Mann M (2008) MaxQuant enables high peptide identification rates, individualized p.p.b.-range mass accuracies and proteome-wide protein quantification. *Nat Biotechnol* 26: 1367–1372
- Dietz KJ (2015) Efficient high light acclimation involves rapid processes at multiple mechanistic levels. *J Exp Bot* 66: 2401–2414
- Dose A, Jost JO, Spiess AC, Henklein P, Beyersmann M, Schwarzer D (2012) Facile synthesis of colorimetric histone deacetylase substrates. *Chem Commun* 48: 9525–9527
- Dose A, Sindlinger J, Bierlmeier J, Bakirbas A, Schulze-Osthoff K, Einsele-Scholz S, Hartl M, Essmann F, Finkemeier I, Schwarzer D (2016) Interrogating substrate selectivity and composition of endogenous histone deacetylase complexes with chemical probes. *Angew Chem Int Ed Engl* 55: 1192–1195
- Drazic A, Myklebust LM, Ree R, Arnesen T (2016) The world of protein acetylation. *Bba-Proteins Proteom* 1864: 1372–1401
- Earley K, Lawrence RJ, Pontes O, Reuther R, Enciso AJ, Silva M, Neves N, Gross M, Viegas W, Pikaard CS (2006) Erasure of histone acetylation by *Arabidopsis* HDA6 mediates large-scale gene silencing in nucleolar dominance. *Gene Dev* 20: 1283–1293
- El Zawily AM, Schwarzlander M, Finkemeier I, Johnston IG, Benamar A, Cao Y, Gissot C, Meyer AJ, Wilson K, Datla R, Macherel D, Jones NS, Logan DC (2014) FRIENDLY regulates mitochondrial distribution, fusion, and quality control in *Arabidopsis*. *Plant Physiol* 166: 808–828
- Fang XP, Chen WY, Zhao Y, Ruan SL, Zhang HM, Yan CQ, Jin L, Cao LL, Zhu J, Ma HS, Cheng ZY (2015) Global analysis of lysine acetylation in strawberry leaves. *Front Plant Sci* 6: 739
- Finkemeier I, Laxa M, Miguet L, Howden AJ, Sweetlove LJ (2011) Proteins of diverse function and subcellular location are lysine acetylated in *Arabidopsis*. *Plant Physiol* 155: 1779–1790
- Finkemeier I, König AC, Heard W, Nunes-Nesi A, Pham PA, Leister D, Fernie AR, Sweetlove LJ (2013) Transcriptomic analysis of the role of carboxylic acids in metabolite signaling in *Arabidopsis* leaves. *Plant Physiol* 162: 239–253
- Gantt SL, Gattis SG, Fierke CA (2006) Catalytic activity and inhibition of human histone deacetylase 8 is dependent on the identity of the active site metal ion. *Biochemistry* 45: 6170–6178
- Gao X, Hong H, Li WC, Yang L, Huang J, Xiao YL, Chen XY, Chen GY (2016) Downregulation of rubisco activity by non-enzymatic acetylation of RbcL. *Mol Plant* 9: 1018–1027
- Hartl M, Finkemeier I (2012) Plant mitochondrial retrograde signaling: post-translational modifications enter the stage. *Front Plant Sci* 3: 253
- Hartl M, König A-C, Finkemeier I (2015) Identification of lysine-acetylated mitochondrial proteins and their acetylation sites. In *Plant mitochondria: methods and protocols*, Whelan J, Murcha MW (eds), pp 107–121. New York, NY: Springer New York
- He DL, Wang Q, Li M, Damaris RN, Yi XL, Cheng ZY, Yang PF (2016) Global proteome analyses of lysine acetylation and succinylation reveal the widespread involvement of both modification in metabolism in the embryo of germinating rice seed. *J Proteome Res* 15: 879–890
- Heazlewood JL, Verboom RE, Tonti-Filippini J, Small I, Millar AH (2007) SUBA: the *Arabidopsis* subcellular database. *Nucleic Acids Res* 35: D213–D218
- Hollender C, Liu ZC (2008) Histone deacetylase genes in *Arabidopsis* development. *J Integr Plant Biol* 50: 875–885
- Hosp F, Lassowskat I, Santoro V, De Vleeschauwer D, Fliegner D, Redestig H, Mann M, Christian S, Hannah MA, Finkemeier I (2016) Lysine acetylation in mitochondria: from inventory to function. *Mitochondrion* 33: 58–71
- Huber SC (2007) Exploring the role of protein phosphorylation in plants: from signalling to metabolism. *Biochem Soc Trans* 35: 28–32
- Johnova P, Skalak J, Saiz-Fernandez I, Brzobohaty B (2016) Plant responses to ambient temperature fluctuations and water-limiting conditions: a proteome-wide perspective. *Bba-Proteins Proteom* 1864: 916–931
- Joshi P, Greco TM, Guise AJ, Luo Y, Yu F, Nesvizhskii AI, Cristea IM (2013) The functional interactome landscape of the human histone deacetylase family. *Mol Syst Biol* 9: 672
- Jost JO, Hanswillemenke A, Schwarzer D (2015) A miniaturized readout strategy for endogenous histone deacetylase activity. *Mol BioSyst* 11: 1820–1823
- Karimi M, Depicker A, Hilson P (2007) Recombinational cloning with plant gateway vectors. *Plant Physiol* 145: 1144–1154
- Kleff S, Andrulis ED, Anderson CW, Sternglanz R (1995) Identification of a gene encoding a yeast histone H4 acetyltransferase. *J Biol Chem* 270: 24674–24677
- König AC, Hartl M, Boersema PJ, Mann M, Finkemeier I (2014a) The mitochondrial lysine acetylome of *Arabidopsis*. *Mitochondrion* 19(Pt B): 252–260.
- König AC, Hartl M, Pham PA, Laxa M, Boersema PJ, Orwat A, Kalitventseva I, Plöschinger M, Braun HP, Leister D, Mann M, Wachter A, Fernie AR, Finkemeier I (2014b) The *Arabidopsis* class II sirtuin is a lysine deacetylase and interacts with mitochondrial energy metabolism. *Plant Physiol* 164: 1401–1414
- Kulak NA, Pichler G, Paron I, Nagaraj N, Mann M (2014) Minimal, encapsulated proteomic-sample processing applied to copy-number estimation in eukaryotic cells. *Nat Methods* 11: 319–U300
- Lassowskat I, Hartl M, Hosp F, Boersema PJ, Mann M, Finkemeier I (2017) Dimethyl-labeling based quantification of the lysine acetylome and proteome of plants. *Methods Mol Biol*, photorespiration, AFeeE (ed), 1653: 65–81
- Lehtimäki N, Koskela MM, Dahlstrom KM, Pakula E, Lintala M, Scholz M, Hippler M, Hanke GT, Rokka A, Battchikova N, Salminen TA, Mulo P (2014) Posttranslational modifications of FERREDOXIN-NADP(+) OXIDOREDUCTASE in *Arabidopsis* chloroplasts. *Plant Physiol* 166: 1764–U1917
- Maddelein D, Colaert N, Buchanan I, Hulstaert N, Gevaert K, Martens L (2015) The iceLogo web server and SOAP service for determining protein consensus sequences. *Nucleic Acids Res* 43: W543–W546
- Mahrez W, Arellano MST, Moreno-Romero J, Nakamura M, Shu H, Nanni P, Kohler C, Gruissem W, Hennig L (2016) H3K36ac is an evolutionary conserved plant histone modification that marks active genes. *Plant Physiol* 170: 1566–1577
- Mengel A, Ageeva A, Georgii E, Bernhardt J, Wu K, Durner J, Lindermayr C (2017) Nitric oxide modulates histone acetylation at stress genes by inhibition of histone deacetylases. *Plant Physiol* 173: 1434–1452
- Mignolet-Spruyt L, Xu EJ, Idanheimo N, Hoeberichts FA, Muhlenbock P, Brosche M, Van Breusegem F, Kangasjarvi J (2016) Spreading the news: subcellular and organellar reactive oxygen species production and signalling. *J Exp Bot* 67: 3831–3844
- Nallamilli BRR, Edelmann MJ, Zhong XX, Tan F, Mujahid H, Zhang J, Nanduri B, Peng ZH (2014) Global analysis of lysine acetylation suggests the involvement of protein acetylation in diverse biological processes in rice (*Oryza sativa*). *PLoS ONE* 9: e89283

- Newkirk TL, Bowers AA, Williams RM (2009) Discovery, biological activity, synthesis and potential therapeutic utility of naturally occurring histone deacetylase inhibitors. *Nat Prod Rep* 26: 1293–1320
- Nunes-Nesi A, Fernie AR, Stitt M (2010) Metabolic and signaling aspects underpinning the regulation of plant carbon nitrogen interactions. *Mol Plant* 3: 973–996
- O'Malley RC, Alonso JM, Kim CJ, Leisse TJ, Ecker JR (2007) An adapter ligation-mediated PCR method for high-throughput mapping of T-DNA inserts in the *Arabidopsis* genome. *Nat Protoc* 2: 2910–2917
- Pandey R, Muller A, Napoli CA, Selinger DA, Pikaard CS, Richards EJ, Bender J, Mount DW, Jorgensen RA (2002) Analysis of histone acetyltransferase and histone deacetylase families of *Arabidopsis thaliana* suggests functional diversification of chromatin modification among multicellular eukaryotes. *Nucleic Acids Res* 30: 5036–5055
- Parthun MR, Widom J, Gottschling DE (1996) The major cytoplasmic histone acetyltransferase in yeast: Links to chromatin replication and histone metabolism. *Cell* 87: 85–94
- Portis AR Jr, Li C, Wang D, Salvucci ME (2008) Regulation of Rubisco activase and its interaction with Rubisco. *J Exp Bot* 59: 1597–1604
- R Core Team (2016) *R: A language and environment for statistical computing*. Vienna, Austria: R Foundation for Statistical Computing. <https://www.R-project.org/>
- Rappsilber J, Mann M, Ishihama Y (2007) Protocol for micro-purification, enrichment, pre-fractionation and storage of peptides for proteomics using StageTips. *Nat Protoc* 2: 1896–1906
- Ritchie ME, Phipson B, Wu D, Hu YF, Law CW, Shi W, Smyth GK (2015) limma powers differential expression analyses for RNA-sequencing and microarray studies. *Nucleic Acids Res* 43: e47
- Salvucci ME (1992) Subunit Interactions of Rubisco Activase - Polyethylene-Glycol Promotes Self-Association, Stimulates ATPase and Activation Activities, and Enhances Interactions with Rubisco. *Arch Biochem Biophys* 298: 688–696
- Scholz C, Weinert BT, Wagner SA, Beli P, Miyake Y, Qi J, Jensen LJ, Streicher W, McCarthy AR, Westwood NJ, Lain S, Cox J, Matthias P, Mann M, Bradner JE, Choudhary C (2015) Acetylation site specificities of lysine deacetylase inhibitors in human cells. *Nat Biotechnol* 33: 415–423
- Shen Y, Wei W, Zhou DX (2015) Histone acetylation enzymes coordinate metabolism and gene expression. *Trends Plant Sci* 20: 614–621
- Smith-Hammond CL, Hoyos E, Miernyk JA (2014) The pea seedling mitochondrial N-epsilon-lysine acetylome. *Mitochondrion* 19: 154–165
- Thimm O, Blasing O, Gibon Y, Nagel A, Meyer S, Kruger P, Selbig J, Muller LA, Rhee SY, Stitt M (2004) MAPMAN: a user-driven tool to display genomics data sets onto diagrams of metabolic pathways and other biological processes. *Plant J* 37: 914–939
- Tran HT, Nimick M, Uhrig RG, Templeton G, Morrice N, Gourlay R, DeLong A, Moorhead GBG (2012) *Arabidopsis thaliana* histone deacetylase 14 (HDA14) is an alpha-tubulin deacetylase that associates with PP2A and enriches in the microtubule fraction with the putative histone acetyltransferase ELP3. *Plant J* 71: 263–272
- Tyanova S, Temu T, Sinitcyn P, Carlson A, Hein MY, Geiger T, Mann M, Cox J (2016) The Perseus computational platform for comprehensive analysis of (prote)omics data. *Nat Methods* 13: 731–740
- Wagner GR, Payne RM (2013) Widespread and enzyme-independent N-is an element of-acetylation and N-is an element of-succinylation of proteins in the chemical conditions of the mitochondrial matrix. *J Biol Chem* 288: 29036–29045
- Weinert BT, Wagner SA, Horn H, Henriksen P, Liu WSR, Olsen JV, Jensen LJ, Choudhary C (2011) Proteome-wide mapping of the *Drosophila* acetylome demonstrates a high degree of conservation of lysine acetylation. *Sci Signal* 4: ra48
- Weinert BT, Iesmantavicius V, Wagner SA, Scholz C, Gummesson B, Beli P, Nystrom T, Choudhary C (2013) Acetyl-phosphate is a critical determinant of lysine acetylation in *E. coli*. *Mol Cell* 51: 265–272
- Wu FH, Shen SC, Lee LY, Lee SH, Chan MT, Lin CS (2009) Tape-*Arabidopsis* Sandwich - a simpler *Arabidopsis* protoplast isolation method. *Plant Methods* 5: 16
- Wu X, Oh MH, Schwarz EM, Larue CT, Sivaguru M, Imai BS, Yau PM, Ort DR, Huber SC (2011) Lysine acetylation is a widespread protein modification for diverse proteins in *Arabidopsis*. *Plant Physiol* 155: 1769–1778
- Xiong YH, Peng XJ, Cheng ZY, Liu WD, Wang GL (2016) A comprehensive catalog of the lysine-acetylation targets in rice (*Oryza sativa*) based on proteomic analyses. *J Proteomics* 138: 20–29
- Yang XJ, Seto E (2008) Lysine acetylation: codified crosstalk with other posttranslational modifications. *Mol Cell* 31: 449–461
- Yuan H, Marmorstein R (2013) Histone acetyltransferases: rising ancient counterparts to protein kinases. *Biopolymers* 99: 98–111
- Zhang YM, Song LM, Liang WX, Mu P, Wang S, Lin Q (2016) Comprehensive profiling of lysine acetylproteome analysis reveals diverse functions of lysine acetylation in common wheat. *Sci Rep* 6: 21069
- Zhen SM, Deng X, Wang J, Zhu GR, Cao H, Yuan LL, Yan YM (2016) First comprehensive proteome analyses of lysine acetylation and succinylation in seedling leaves of *Brachypodium distachyon* L. *Sci Rep* 6: 31576
- Zheng Y, Ding Y, Sun X, Xie SS, Wang D, Liu XY, Su LF, Wei W, Pan L, Zhou DX (2016) Histone deacetylase HDA9 negatively regulates salt and drought stress responsiveness in *Arabidopsis*. *J Exp Bot* 67: 1703–1713
- Zhou CH, Zhang L, Duan J, Miki B, Wu KQ (2005) HISTONE DEACETYLASE19 is involved in jasmonic acid and ethylene signaling of pathogen response in *Arabidopsis*. *Plant Cell* 17: 1196–1204



**License:** This is an open access article under the terms of the Creative Commons Attribution 4.0 License, which permits use, distribution and reproduction in any medium, provided the original work is properly cited.